Host Cell modulation by Brucella effectors

Jean-Baptiste Luizet

N°d'ordre NNT : xxx

THESE de DOCTORAT DE L'UNIVERSITE DE LYON
opérée au sein de
l'Université Claude Bernard Lyon 1

Ecole Doctorale N° 205
Ecole Doctorale Interdisciplinaire Sciences Santé

Spécialité de doctorat :
Discipline : **Infectiologie Fondamentale**

Soutenue publiquement le 27/09/2019, par :
Jean-Baptiste Luizet

Host cell modulation by *Brucella abortus* effectors

Devant le jury composé de :

Doublet Patricia Professeure des Universités Université Lyon 1	Présidente
Buchrieser Carmen Directrice de Recherche Institut Pasteur Paris	Rapporteure
Celli Jean Professeur Associé Washington State University	Rapporteur
Méresse Stéphane Directeur de Recherche Université Aix-Marseille	Rapporteur
Salcedo Suzana Chargée de Recherche Université Lyon 1	Directrice de thèse

Remerciements

Tout d'abord je tiens à remercier l'ensemble des membres de mon jury de thèse pour avoir accepté d'évaluer mon travail. Je remercie la Professeure Patricia Doublet présidente de mon jury et mes 3 rapporteurs la docteure Carmen Buchrieser, le docteur Jean Celli et le docteur Stéphane Méresse.

Je remercie la Région Auvergne-Rhône-Alpes et l'Agence Nationale de la Recherche pour leurs financements.

Je remercie également mon comité de suivi de thèse composé des docteurs Christophe Grangeasse et Matteo Bonazzi pour leurs écoutes et leurs conseils afin de mener au mieux ce projet de thèse.

Je souhaite remercier les membres des plateaux techniques avec qui j'ai eu la chance de travailler à savoir la plateforme de microscopie PLATIM, merci à Christophe Claire et Elodie. Je remercie la plateforme de biochimie PSF, un grand merci à Virginie pour ses conseils techniques et son écoute.

Je souhaite remercier également tous les membres de l'IBCP qui m'ont aidé à avancer dans mon projet de thèse en me donnant des conseils ou qui ont pris le temps de me former. Merci à Fabien, Charlotte M et Aurore.

Ensuite la personne que j'aimerai remercier c'est toi Suzana, « chef » comme j'aime t'appeler au quotidien. Je ne te remercierai jamais assez de m'avoir accueilli dans ton équipe pour mes stages et ces années de thèse. Au cours de ces années à tes côtés, j'ai énormément appris que ce soit sur un point de vue scientifique et professionnel mais aussi sur un point de vue humain. Merci d'avoir pris tout ce temps pour moi, de m'avoir transmis ta passion, ton savoir-faire et ta vision de la vie que j'emmènerai avec moi lorsque je quitterai le labo. Pour moi travailler dans ton labo a été une très belle expérience et sur un plan plus personnel. Tu es vraiment une super chef Suz, j'aurai rêvé de pouvoir continuer avec toi pendant des années à travailler sur ces charmantes bactéries mais bon je repars d'ici avec une super amie avec qui travailler tous les jours est vraiment un plaisir. J'espère que nous arriverons à continuer dans le futur à travailler ensemble.

Ensuite j'aimerai remercier Catherine (Cat') mon ancienne professeure de SVT de terminale. C'est grâce à toi que j'ai aimé la biologie, car tu as su transmettre cette passion de la science du vivant. Tu restes pour moi un modèle de par la façon dont tu t'investis avec tes élèves, tes « enfants » comme tu dis. Tu es mon premier mentor dans le domaine de la biologie c'est pourquoi j'espère que tu prendras plaisir à lire cette thèse. Vraiment merci j'espère plus tard arriver à susciter des vocations avec d'autres jeunes comme tu as su le faire avec moi.

Ensuite j'aimerai remercier tous mes collègues de labo qui ont rendu ces années des plus agréables et épanouissantes

A Magali qui aura été une stagiaire en or tant par la qualité de son travail mais aussi de sa personnalité qui font que j'ai eu beaucoup de plaisir à te superviser pendant tes 2 stages de master

A Julien mon deuxième stagiaire de master que je remercie pour toute l'aide apportée.

A Arthur (Monsieur Louche) pour ton humour, ta plus grande qualité pour tous tes conseils pour nos soirées jeux, ninkasi, au labo jusqu'à pas d'heures. C'était vraiment un plaisir de passer toutes ces années avec toi monsieur louche et je te souhaite bon courage car tu es le prochain ☺.

A Amandine (Blondie). Pour ta bonne humeur ta joie de vivre et ta gentillesse. C'était vraiment un plaisir de travailler avec toi en rigolant de nos maladresses respectives (Dicton « un geste, une connerie »). Merci aussi de m'avoir soutenu pour les périodes critiques comme la préparation au concours, la soutenance du master2, mais aussi pour ton écoute par sur un plan plus personnel.

A Julie (Juju) pour toute l'aide apportée au cours de cette thèse que ce soit sur un plan professionnel ou personnel. Merci pour tout ce que tu as fait surtout dans les derniers moments rush de la thèse, tu as tenu bon et je t'en suis très reconnaissant. Tu es une fille vraiment super et je suis content que tu fasses partie de mes amies proches en dehors du labo.

Merci à Morgane (Momo) la conseillère mode du labo et la meilleure pâtissière de Meyzieux. J'ai vraiment apprécié de travailler avec toi avec nos moqueries légères des tenues vestimentaires de certains. Je te souhaite le meilleur pour ta fin de thèse qui je suis sûr sera belle.

Merci aux deux précédents thésards du labo Paul et Stéphanie, vous avez ouvert la voie et je suis sûr qu'avec nous 3 la chef sera rodé pour les thésards suivants. J'ai également apprécié de travailler avec vous par la solidarité qu'il y avait entre nous dans les moments de galères et nos sorties extra-labo. J'espère vous rejoindre bientôt dans le cercle des jeunes docteurs

Merci à Tristan et Orane les deux derniers arrivés dans le labo pour votre fraîcheur et votre peps au quotidien. Même si nous n'avons pas eu la chance de travailler longtemps ensemble, c'était super chouette de partager votre bureau et d'avoir eu l'opportunité d'apprendre à vous connaître. Je vous souhaite à vous deux le meilleur pour la suite avec un super post doc pour Tristan et une belle maternité à toi Rano.

Je tiens à remercier Guillermo ancien post-doc du labo et qui a été mon premier maître de stage en laboratoire. Merci de m'avoir donné le goût de ma recherche et une approche expérimentale que j'ai toujours gardé, même si je n'aurai jamais ton don pour la Biologie Moléculaire. J'espère arriver comme toi à transmettre cette passion et cette façon de voir les choses à d'autres par la suite.

A ma soeur (Maouh) qui m'a toujours soutenu, qui a cru en moi et m'a beaucoup encouragé. Je t'aime très fort et merci d'avoir été là tout au long de cette thèse.

A ma filleule Estelle dont l'affection et le soutien m'ont aussi porté tout au long de cette thèse. J'espère que tu seras fière de ton parrain, en tout cas sache que moi je suis déjà très fier de la jeune femme que tu es déjà.

A mon frère (Philou) pour tout ce que tu m'as apporté tout du long de la thèse j'espère qu'on pourra fêter l'occasion autour d'une bonne bouteille car entre nous toutes les occasions sont bonnes pour boire un bon verre de vin rouge. Merci mon parrain.

A mes parents que je remercie de m'avoir poussé à aller le plus loin possible et à me dépasser. Maman je sais que tu aurais aimé faire des études de Biologie plus jeune et j'espère que tu seras fière de moi en lisant ce manuscrit ainsi que le jour de la soutenance orale. Papa je sais que tu étais fier le jour où tu as appris que j'avais une bourse doctorale et je suis vraiment content que tu puisses lire ce manuscrit et assister à ma soutenance. Je ne serai peut-être pas un docteur qui soigne les gens comme toi mais je préfère des patients comme *Brucella* ou *Acinetobacter*. Merci de m'avoir donné cette chance de faire ces études dans de bonnes conditions. Je vous aime fort

Sophie S Un gros merci à toi pour ton soutien et ton affection indéfectible. Une belle rencontre faite grâce à notre passion commune une belle amitié, merci d'avoir été là à la fin et de m'avoir soutenu par tes petits cœurs récurrents qui touchent et toucheront toujours ton doudou.

Nadège merci à toi Nadège pour ton écoute et tous tes conseils sages et avisés tu as su me tempérer quand il fallait maintenir le cap et je t'en serai toujours reconnaissant. Tu es une personne formidable n'en doute jamais et merci encore pour tout ce que tu m'as apporté.

A tous mes amis du volley, de la fac et du lycée. Merci d'avoir été là pour me soutenir m'encourager me changer les idées. Vous m'avez rendu ce marathon de thèse beaucoup plus léger et facile.

A tous les copains de labo (Célia, Gina, Morgane B, Halima, Charlotte M, Marine M, Josuha, Ben, Alexandre B, Aurore, Julie et à tous ceux que j'ai oublié) pour tous les bons moments passés ensemble, les G-SWITCH endiablés, les soirées au Ninkasi, les pauses ragots dans les couloirs et les soirées jeux de société qui font que tous les jours on est aussi content d'aller au boulot.

Enfin je finirai par toi mon ourson ou mon nounours comme j'aime t'appelere (Lucas) qui a été là quasiment tout du long de cette thèse. Tu m'auras vraiment beaucoup apporté au cours de cette thèse, ton soutien ton affection et la chance de pouvoir vivre avec une personne qui compte beaucoup pour moi. J'espère que tu seras fier de moi en voyant le travail abouti. Merci de m'avoir soutenu quand j'ai arrêté la cigarette en plein milieu de la thèse et de m'avoir aidé à maintenir le cap. En effet c'est grâce à toi si j'ai pu persister dans cette

démarche tout en continuant ce long marathon qu'est la thèse. Je tiens très fort à toi et merci encore pour tout.

Table des matières

Résumé de la thèse

Brucella abortus, est une bactérie pathogène appartenant au genre *Brucella* et responsable d'une zoonose ré-émergente appelée brucellose. Cette bactérie est capable d'infecter de nombreux types cellulaires. A l'intérieur de la cellule, *Brucella* est retrouvée dans une vacuole appelée *Brucella*-containing vacuole (BCV). Cette vacuole interagit partiellement avec les différents compartiments endosomaux et lysosomaux jusqu'à atteindre le réticulum endoplasmique où la bactérie va établir sa niche réplicative. Une fois sa réplication achevée, *Brucella* va alors modifier sa BCV afin de sortir de la cellule et amorcer son processus de réinfection. Il a été démontré qu'un des acteurs clé dans la virulence de *B. abortus* est le système de sécrétion de type IV (SST4). Ce sont les protéines injectées (ou effecteurs) par ce système de sécrétion qui permettent à *Brucella* de contrôler les différentes voies cellulaires de son hôte. Mon projet de thèse a consisté à caractériser un nouvel effecteur de ce système de sécrétion appelé « *Brucella* secreted protein L » (BspL). Nous avons observé la localisation de cet effecteur au sein du réticulum endoplasmique et l'induction de stress par celui-ci dans la cellule. En parallèle nous avons identifié la protéine « Homocysteine-responsive endoplasmic reticulum-resident ubiquitin-like domain member 1 » (Herp) comme cible de BspL. Herp est impliquée dans de nombreux processus de régulations physiologiques du réticulum comme la dégradation associée au réticulum (ERAD). Nous avons démontré que BspL stimule cette capacité d'action de l'ERAD au sein de la cellule. Par la suite nous avons découvert que l'ERAD et BspL sont impliqués dans la formation des vésicules de sortie de *Brucella*. En effet nous avons pu voir que BspL ralentissait la formation de ces vacuoles de sortie et dépendamment de Herp. Ces résultats sont synthétisés dans un manuscrit en cours de soumission dans lequel je suis le premier auteur.

En parallèle, nous avons observé que BspL fragmentait les mitochondries en réduisant leur connectivité dans différentes lignées cellulaires. Nous avons néanmoins vu que ce processus de fragmentation des mitochondries était indépendant du stress induit par BspL dans le réticulum et de Herp ce qui suggèrerait que BspL cible les mitochondries indépendamment du réticulum. Ces phénotypes nécessitent une caractérisation plus approfondie afin d'élucider les conséquences de cette fragmentation.

En conclusion, nous avons identifié un nouvel effecteur de *Brucella* qui participe à la formation des vésicules de sortie aBCVs en modulant l'ERAD. Par ailleurs BspL cible également les mitochondries ce qui indique que l'effecteur pourrait avoir un rôle différentiel au cours du temps pendant l'infection.

Objectives

The objective of this thesis was to characterize a novel *Brucella* effector called BspL by combining different experimental approaches. We aimed mainly at determining the role of BspL in the virulence of *Brucella abortus*, identify its cellular target and its impact on the infected eukaryotic cell. We have found that this effector impacts endoplasmic reticulum functions as well as mitochondrial integrity. Therefore, to introduce the context of this work the introduction is composed of 3 chapters. The first chapter describes in great detail the functions of the endoplasmic reticulum particularly regarding ER stress and quality control; the second chapter is focused on mitochondria and the last chapter summarizes the most important information regarding *Brucella abortus* pathogenesis. The manuscript then has 2 results chapters, describing all the data that I have obtained during my thesis. The first chapter of results deals with the impact of BspL on the endoplasmic reticulum and the second one its impact on mitochondria. A general conclusion about my work is included at the end to explain how it contributes to improve our knowledge on the virulence mechanisms of *Brucella*. Finally, I included a final chapter that sums up my contributions in other collaborative projects, on *Pseudomonas aeruginosa* and *Acinetobacter baumannii*.

Abbreviations

Ab: *Acinetobacter baumannii*
Alex3: Armadillo repeat-containing X-linked protein 3
ATF 6: Activating Transcription Factor 6
ADP: Adénosine DiPhosphate
AMP: Adénosine Monophosphate
APC : Antigen Presented Cell
AR : Aspect Ratio
ATP: Adénosine TriPhosphate
BCV: *Brucella*-Containing Vacuole
BH3: BCL2 homology 3
BiP: Binding immunoglobulin protein
Bsp: *Brucella* secreted protein
BMDM: Bone-Marrow Derived Macrophages
Ca^{2+}: Calcium
CagA : Cytotoxin-Associated Gene A
CCCP: carbonyl cyanide m-chlorophenyl hydrazone
CFU : Colony Forming Unit
CNX: Calnexin
CRT : Calréticulin
Co-IP : Co-immunoprecipitation
COP: Coat Protein
DC: Dendritic Cell
DISC: Death-Inducing Signaling Complex
Dnm: Dynamin
Drp1: Dynamin-related like protein 1
EEA1: Early Endosomal Antigen 1
eIF2A: Eukaryotic translation initiation factor 2A
Eeya: Eeyarestatin
ER: Endoplasmic Reticulum
EDEM: ER degradation-enhancing α-mannosidase-like
ERAD: Endoplasmic Reticulum Associated Degradation
ERES: Endoplasmic Reticulum Exit Sites
ERdj: ER-localized DnaJ
ERGIC: Endoplasmic Reticulum Golgi Intermediate Compartment
ERQC: Endoplasmic Reticulum Quality Control
FACL4: Fatty Acid CoA Ligase 4
FADD: Fas-Associated Death Domain
FRET: Fluorescence Resonance Energy Transfer
Glc: Glucose
Gly: Glycine
Grp78: Glucose regulated protein 78
GTP: Guanosine TriPhosphate
Herp: homocysteine-inducible endoplasmic reticulum protein
Hrd1: Hydroxymethyl glutaryl-coenzyme A reductase degradation protein 1
Hsp: Heat-shock protein
iBMDM: immortalized Bone-Marrow Derived Macrophages
IC: Intracellular Cytosol

ÌL: Interleukin
IMM: Inner Mitochondrial Membrane
Insp3: inositol-1,4,5-trisphosphate
IRE: Inositol-Requiring Enzym
KD: Knock-Down
KO: Knock-Out
LAMP1: Lysosomal-associated membrane protein 1
LCR: Lir-containign Region
LLO: Listeriolysin O
MAMs: mitochondria-associated membranes
Man: Mannose
MDR: Multi-Drug Resistant
Mfn: Mitofusin
mRNA: messenger RNA
NBD: Nucleotide Binding Domain
NEF: Nucleotide Exchange Factor
NLR: Nod-Like Receptor
OMM: Outer Mitochondrial Membrane
Opa-1: Optic atrophy 1
OXPHOS: OXydative PHOSphorylation
PACS 2: phosphofurin acidic cluster sorting protein-2
PAMP: Pathogen associated molecular pattern
PBS: Phosphate Buffer Salt
PDI: Protein Disulfide Isomerase
Phe: Phenylalanine
Pi: post-infection
PERK: PKR-like ER protein kinase
PM: Plasma membrane
PPP: Pentose Phosphatase Pathway
PRR: Pattern Recognition Receptor
PTEN: Phosphatase and TEnsin Homolog
RER: Rough Endoplasmic Reticulum
RIDD: regulated-IRE1 dependent decay
ROS: Reactive Oxygen Species
SBD: Substrate Binding Domain
SEAP: Secreted Enzyme Alkaline Phosphatase
SER: Smooth Endoplasmic Reticulum
SMAC: Second Mitochondria-derived Activators of Caspases
SS: Sec Signal
TCR: T Cell Receptor
TLR: Toll-like Receptor
TGN: Trans-Golgi Network
TNF: Tumor Necrosis Factors
TRADD: TNF1R-Associated Death Domain
TSS: Type Secretion System
TUDCA: Tauroursodeoxycholic acid
TUNAK: Tunicamycin
Ub: Ubiquitin
Ubqln: Ubiquilin
UPR: Unfolded Protein Response

VDAC1: Voltage-Dependent Anion Channel isoform 1
WHO: World Health Organization
WT: Wild Type
XBP1: X-Box binding Protein 1
Y2H: Yeast two hybrid

Chapter 1 Endoplasmic reticulum

I-) Endoplasmic reticulum: structure, functions and the secretory pathway.

The endoplasmic reticulum (ER) is a dynamic organelle, a specialized membranous network of elongated tubules and flattened discs which covers a huge surface of the cytoplasm [1]. The ER is classically divided into rough ER (RER) and smooth ER (SER), depending on the presence or absence of ribosomes on the cytosolic face of the membrane respectively. The SER and RER can be found as spatially distinct compartments or highly interconnected and each of them is specialized in specific biological processes [2]. The RER is contiguous to the nuclear membrane and specializes mostly in protein synthesis whereas the more tubular SER is production and metabolism of lipids and associated molecules. The ER spans a large area of the cell ensuring many contacts with other cellular organelles as the Golgi apparatus. Together with other organelles, the ER can sense intrinsic and extrinsic perturbations enabling its central role as a coordinator of cellular homeostasis. Another important organelle association is the ER-mitochondria interconnectivity. This forms physical contact sites between the ER and mitochondria, named mitochondria-associated membranes (MAMs), which play a pivotal role in several cellular processes such as the control of calcium (Ca^{2+}) homeostasis and metabolic processes [3].

One of the most well-known functions of the ER is maintaining cellular homeostasis by controlling protein biosynthesis. Indeed, a significant proportion of the mammalian genome encodes for proteins that will be synthesized by ER membrane-bound ribosomes and translocated into the ER for further processing [4]. Therefore, the ER represents the entry point of the secretory pathway which is highly conserved in the eukaryotic kingdom. The secretory pathway is composed of different membrane-bound compartments notably the ER and Golgi that control the export of mature proteins from the lumen or the membrane of the ER to the Golgi apparatus and subsequently to either the plasma membrane, the extracellular medium or other organelles.

The ER in fact provides a specialized environment for folding, assembly and maturation of newly synthesized proteins. Protein folding and assembly are discussed in more detail in this introduction (**Part II-1**) as their regulation is essential for maintaining cellular homeostasis. Once synthesized, proteins undergo a process of maturation including signal sequence

cleavage, glycosylation, isomerization of proline or lipid conjugation and formation, isomerization or reduction of disulfide bonds catalyzed by protein disulfide isomerases (PDIs). All these modifications ultimately allow proteins to achieve a properly folded conformation for ternary or quaternary structures [5,6]. After maturation, proteins can then be exported from the ER in coat protein complex II (COP II)-coated transport vesicles in specialized region of the ER: the ER exit sites (ERES). The COP II machinery mediates the budding event to initiate vesicle formation and traffic for subsequent steps of the secretory pathway [7], the ER-Golgi intermediate compartment (ERGIC) and the Golgi complex to finalize their maturation and traffic to their final destination [8,9]. And, it is important to precise that the organization and functionality of ERES are regulated by the activity of the small GTPase Sar1, which controls the assembly of COPII complexes on ER membranes. Indeed, we will discuss their importance for *Brucella* in the **Chapter 3**. This secretory pathway is represented in the **Figure 1- (**extracted from [10]), and **Figure 2-,** with other important ER steps as folding or protein degradation, essential for ER homeostasis and further described later in this chapter [11].

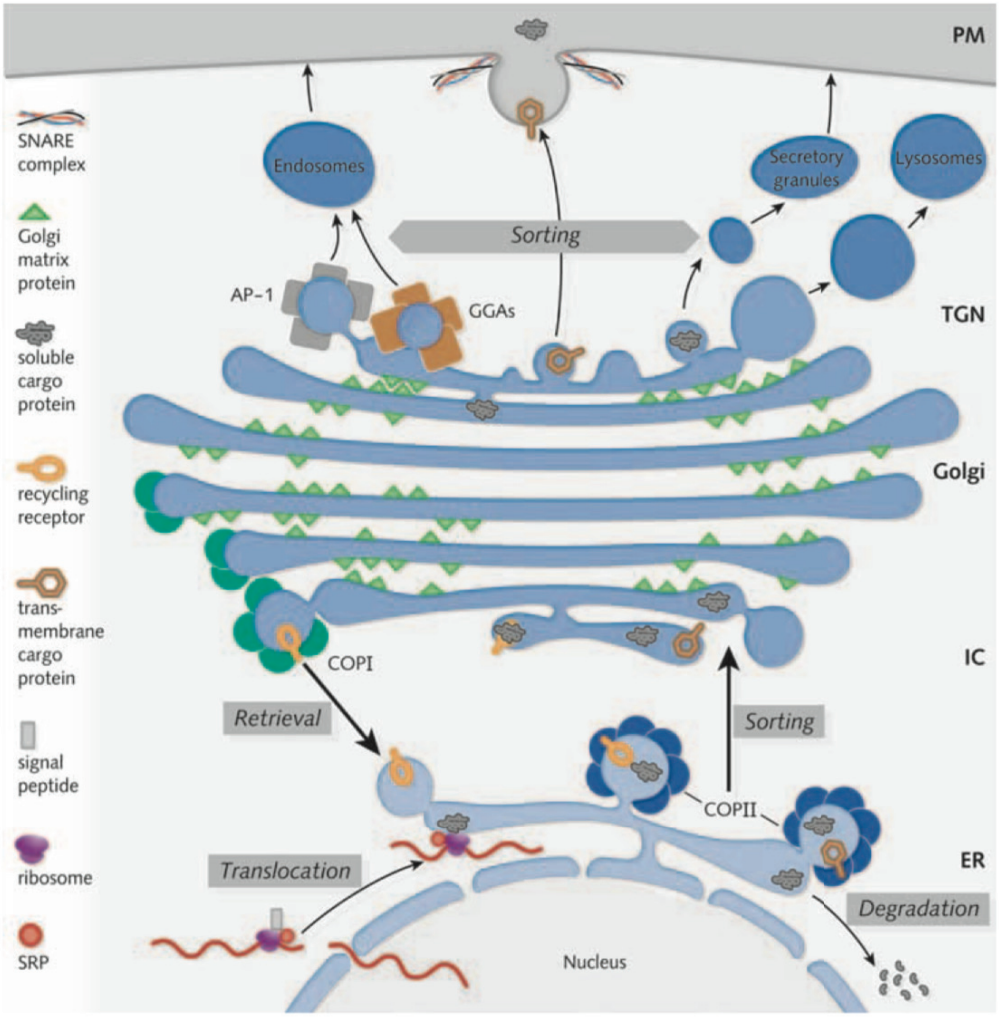

Figure 1- Schematic representation of the secretory pathway, highlighting some of the components discussed during the conference newly synthesized proteins enter the pathway at the ER and are subejcted to repeated sorting and transport between membrane organelles until they arrive at their designated destination. Figures and legends extracted from [10].

Indeed, correct folding and maturation of proteins to prevent aggregation and transport of dysfunctional proteins to the rest of the cell makes the ER a central point for protein quality control, a process termed ER quality control (ERQC).

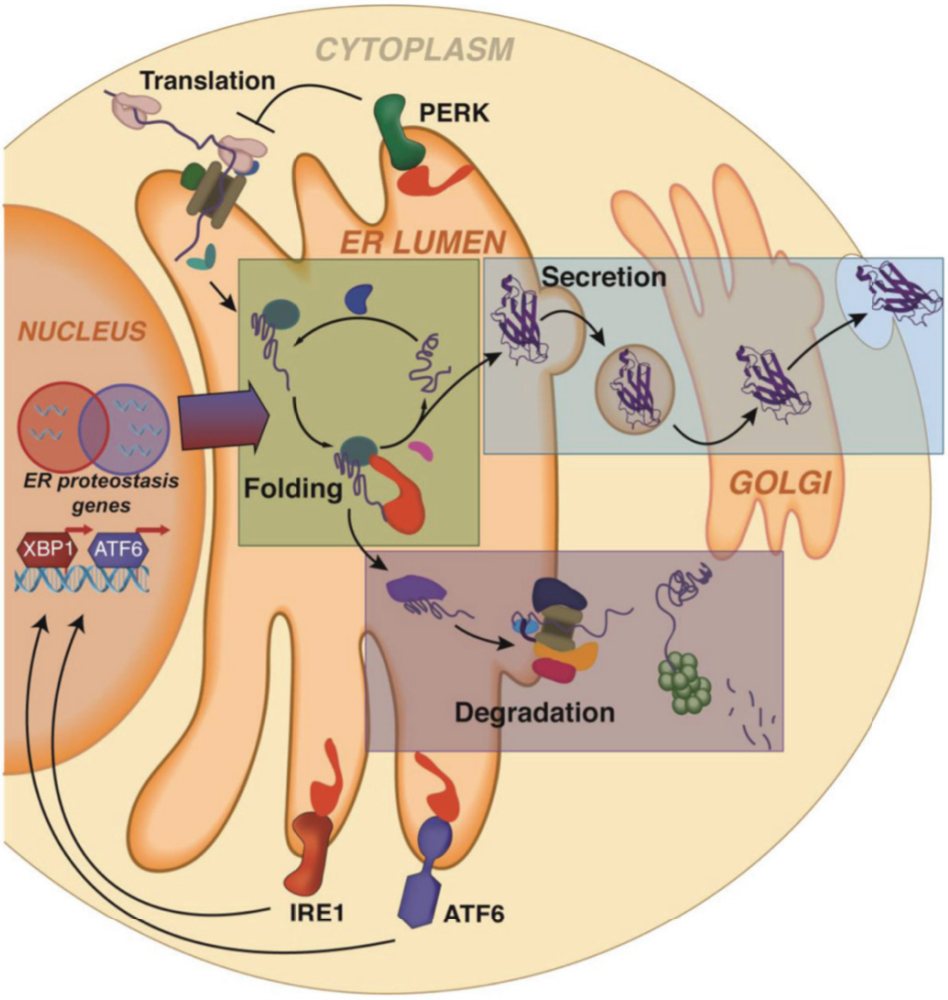

Figure 2- Protein Secretion Through the Secretory Pathway is Regulated by the Activity of ER Protein Folding, Trafficking and Degradation Pathways. Proteins co-translationally entering into the ER in non-native conformations engage ER- localized chaperones (e.g., BiP, GRP94, CNX, CRT) and folding factors (e.g., PDIs, PPIases) that facilitate their folding into their proper three-dimensional conformation (green box). These proteins are then packaged into vesicles for trafficking to downstream secretory environments such as the extracellular space (blue box). However, proteins unable to fold in the ER are directed towards degradation pathways such as ER-associated degradation where they are retrotranslocated from the ER to the cytosol and degraded by the ubiquitin- proteasome pathway (purple box). This partitioning of proteins between ER protein folding/ trafficking or degradation pathways is referred to as ER quality control and functions to limit secretion of non-native protein conformations to downstream secretory environments. The primary impact of activating each UPR signaling arm on ER quality control is also depicted. PERK-dependent translation attenuation decreases the import of newly-synthesized proteins entering the ER, reducing ER protein folding load (top). Alternatively, IRE1/XBP1s and ATF6 activation induces transcriptional remodeling of ER proteostasis pathways involved in protein import, folding, degradation and trafficking. Figures and legends extracted from [11].

II-) Endoplasmic Reticulum Stress and Endoplasmic Reticulum Quality Control

Any conditions that disrupt ER homeostasis create a state commonly referred to as "ER stress" [12]. A few examples of these conditions provoking ER stress are loss of calcium homeostasis, point mutations in secreted proteins that stabilize intermediate folding forms or cause aggregation, nutrient deprivation, hypoxia and microbial infections [13]. In order to overcome ER stress the cell activates multiple adaptive mechanisms. However, when the stress is too high to be counteracted it can also lead to programmed cell-death, also known as apoptosis. The specific response elicited to restore homeostasis is dependent on the perturbing agent (bacteria, virus), conditions (drugs as tunicamycin) and the intensity or duration of the stress (chronic or transient). Eukaryotic cells have many regulatory checkpoints to manage and to control this stress which can be divided in 4 major mechanisms: (i) increase or acceleration of adequate protein folding, (ii) induction of protein clearance via ER-associated degradation (ERAD), (iii) activation of the unfolded protein response (UPR), (iv) or a specific autophagy also called ER-phagy [14]. It is important to keep in mind that all these pathways are intimately connected inside the cell. For example, the same ER resident protein chaperone can participate in different mechanisms. Moreover, these different regulatory mechanisms can occur simultaneously if necessary.

For the sake of clarity, I have decided to split the description of these processes in four different parts even if they are intimately connected.

1-) Chaperons and Protein Folding Process

The accumulation of misfolded proteins is one of the main causes of ER stress. Although protein misfolding takes place continually, it can be enhanced because of intrinsic and/or extrinsic perturbations. This is why the ER requires a robust system for protein folding. Indeed, the simultaneous presence in the ER of misfolded proteins, nascent proteins, and proteins at intermediate stages of folding may expose hydrophobic patches, making them available and vulnerable to aggregation with other misfolded or nascent proteins [15]. Fortunately, this exposure of hydrophobic patches to the environment is also recognized by protein chaperones in the ER which will ensure that exposed hydrophobic patches on such proteins are concealed, inhibiting protein aggregation. ER chaperones and their co-factors are therefore essential actors for ensuring ERQC.

The most common and abundant type of molecular chaperones are the heat-shock proteins (Hsps) which were firstly identified in *Drosophila melanogaster* [16]. These chaperones have been classified into families according to their molecular weights, including Hsp40, Hsp60, Hsp70, Hsp90. As interest in these proteins grew, it was discovered that Hsps play a role in elicitation of proper protein folding, assembly, secretion and degradation and, as we will see later in this chapter, also in the UPR. There are two major chaperone families in the ER the Hsp70s and the lectin-chaperones such as the type I membrane protein calnexin that resides in the ER membrane and its soluble homolog calreticulin that resides in the ER lumen.

The Hsp70 family can interact with both glycosylated and non-glycosylated proteins in contrast to lectin-chaperones which generally recognize incompletely folded glycosylated proteins. More recently, the Hsp40 proteins also called Endoplasmic Reticulum DNA J domain containing proteins (ERdjs)1-7 have been implicated in the ERQC. Indeed, several studies have since highlighted their connection with the Hsp70 family and their implication in several ER-related functions including protein folding (discussed just below, **section II-1-b**) but also in ERAD (**section II-2**).

a-) BiP

Of the Hsp70 family members the most famous chaperon is BiP (also called Grp78). Nascent polypeptide chains, both in the cytosol and in the ER, bind primarily to the Hsp70 family proteins and especially BiP [17,18]. BiP has structural features that are common to all proteins of the Hsp70 family, such as a highly conserved N-terminal nucleotide-binding domain (NBD) that interacts with various nucleotide exchange factors (NEFs) and a C-terminal substrate-binding domain (SBD) composed of eight β-strands with a helical lid. There is also a linker between these 2 domains that controls their allosteric interaction [18]

While hydrolysis of ATP to ADP allows stable interactions between BiP and its substrates, exchange of ADP to ATP causes substrate dissociation by inducing conformational changes in the substrate-binding domain of BiP. At the structural level, when BiP is in its ATP-bound form, the SBD maintains its lid open and is docked on the NBD. ATP hydrolysis causes a conformational change that results in undocking of the two domains and the closing of the lid over the SBD providing a high-affinity state. Nucleotide-exchange factors then release ADP allowing ATP to rebind and the new protein to be released and folded or targeted

for degradation. This process is illustrated in the **Figure 3-** extracted from the study of Pobre *et al*[4].

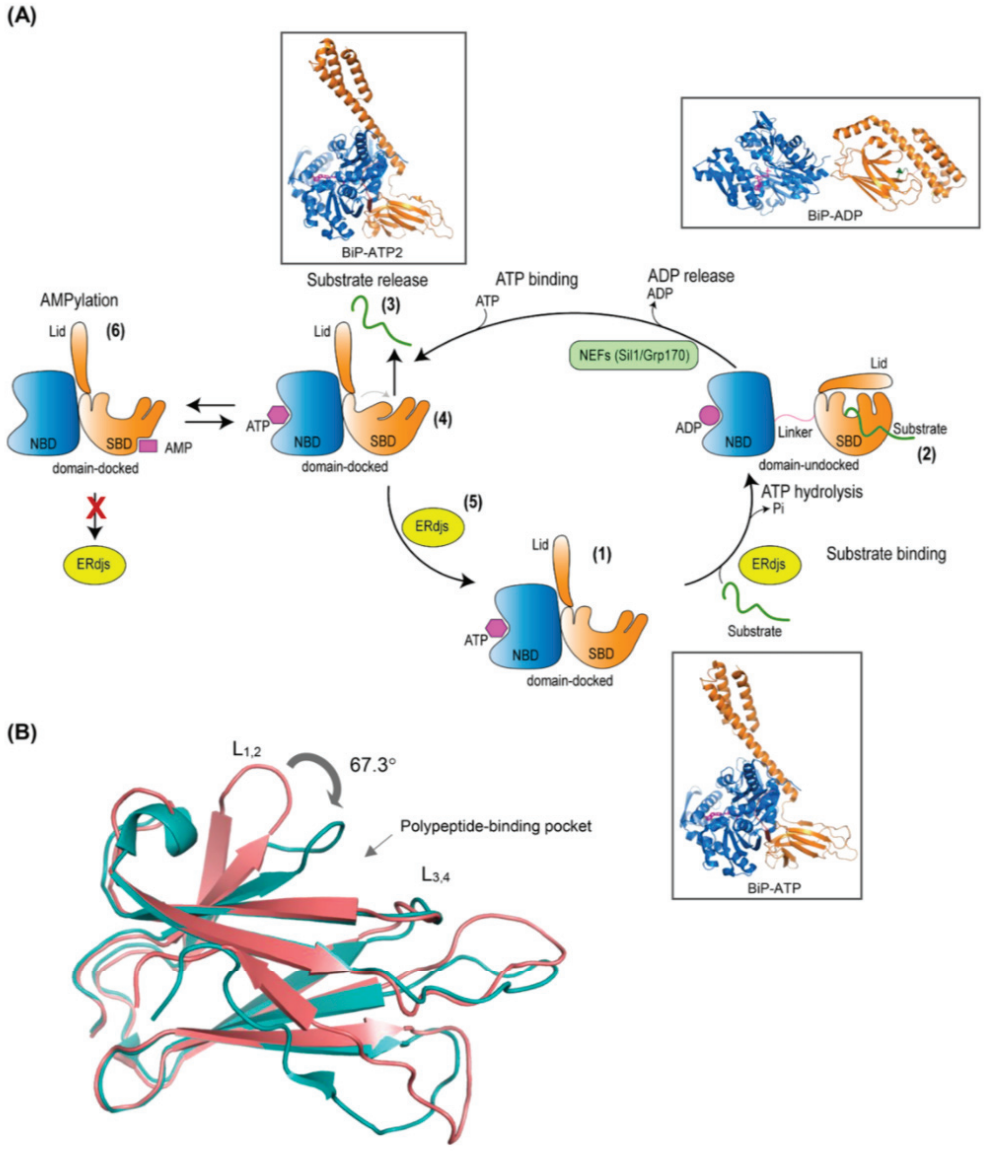

Figure 3- BiP ATPase cycle. *Step 1,* in the ATP-bound form, the nucleotide-binding domain (NBD) (*blue*) and the substrate-binding domain (SBD) (*orange*), with its lid open, are docked to each other resulting to a form with high-substrate binding and release kinetics and low-substrate affinity. *Step 2,* upon ATP hydrolysis, the NBD and SBD become undocked, and the lid of the SBD closes providing a form that has high-substrate affinity but slow binding and release rates. This cycle is regulated by ER-localized DnaJ cofactors (ERdjs) that interact with unfolded proteins and transfer them to the ATP-bound form of BiP, while simultaneously triggering ATP hydrolysis. *Step 3,* substrate is released with the help of nucleotide-exchange factors (NEFs) that stimulate the release of ADP. *Step 4,* binding of ATP causes a conformational change in the SBD resulting in a more tightly compacted conformation that is thought to "squeeze" the substrate out. *Step 5,* interaction with ERdjs reorders the polypeptide-binding pocket of the BiP–ATP2 SBD, readying it to interact with another substrate. *Step 6,* BiP

is post-translationally modified through AMPylation, and this causes the protein to be inactive. AMPylated BiP adopts a "domain-docked" structure similar to that of the ATP-bound state even in the apo- or ADP-bound state and is unable to interact productively with ERdjs. Ribbon representations of the structures (*insets*): ATP-bound BiP with the polypeptide-binding pocket open (BiP-ATP). Figures and legends extracted from [4]

b-) ERdj proteins

The ERdj family is composed of seven ERdj1-7 proteins that contribute to diverse cellular functions. ERdj3-6 can directly interact with proteins which need to be folded. This family is divided in 3 different types [19,20]:

- Type I (DNAJA) with an N-Terminal J domain, followed by a Gly/Phe-rich region which can serve as a flexible linker. This linker is necessary for the substrate binding domain which often includes a cysteine-rich zinc-binding motif and which terminates with a dimerization domain. This structural conformation is similar to BiP structure. This subgroup only has ERdj3.
- Type II (DNAJB) proteins possess all the same domains and in the same order as type I proteins, except that the cysteine-rich domain is missing. As the type I we only find one protein, Erdj4, in this subtype. However, it is important to note that both type I and II DnaJ family members can bind directly substrates for folding processes.
- Type III (DNAJC) proteins is the largest group of ERdjs with ERdj1,2,5,6,7. This subgroup only contains the J domain in their sequences, anywhere in the protein. Some of the type III DnaJ proteins bind unfolded proteins directly, whereas others do not seem to be able to.

The domains of all ERdjs are presented in the **Figure 4-**

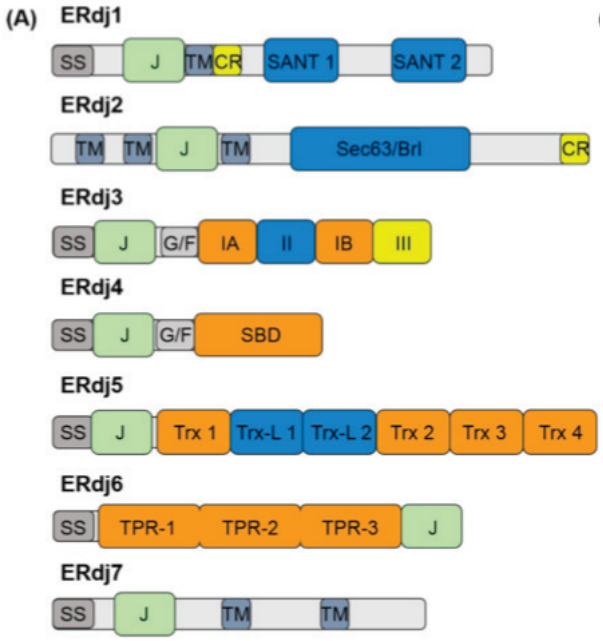

Figure 4- Domain structure of ERdj family members. *A*, domain arrangements of primary sequences of each of the known ERdj proteins. Abbreviations used are as follows: *SS*, signal sequence; *J*, J domain; *TM*, transmembrane region; *CR*, charged amino acid region; *SANT*, SANT domain; *Sec63/Brl*, Sec63/Brl domain; *G/F*, glycine/phenylalanine-rich flexible linker region; *IA* and *IB*, bifurcated substrate-binding domain; *II*, cysteine-rich domain; *III*, dimerization domain; *SBD*, substrate-binding domain; *Trx*, thioredoxin domains; *Trx-L*, thioredoxin-like, enzymatically inactive domain; *TPR*, tetratricopeptide repeat domain (each con- taining three subdomains). Figures and legends extracted from [4]

ERdjs are well described for having a role in folding, in particular they are involved in the BiP-dependent folding processes. In some cases, ERdjs can interact directly with unfolded proteins in the ER and transfer them to the ATP-bound form of BiP, while simultaneously triggering ATP hydrolysis and closing the lid on the substrate [21,22]. All ERdjs can also directly interact with Hsp70 proteins or *via* a ribosome-associated complex in order to increase folding of nascent proteins. Taken together, the available data suggests a role of ERdjs in substrate recruitment and modulation of BiP function [23,24]. A recent example nicely illustrating the importance of these interactions is ERdj1, a transmembrane protein with a cytosolic domain that associates with ribosomes on the ER membrane while its luminal domain associates with BiP. It was demonstrated that this ERDj protein, in the absence of BiP, inhibits nascent polypeptide translocation into the ER, thus ensuring BiP association to nascent proteins [24].

ERdj3 directly interacts with the substrate via highly conserved hydrophobic residues in the substrate-binding domain[23]. As these substrates fold rapidly in cells, the binding

appears to be very transient and terminated by transfer of the substrate to BiP, which depends on the interaction of the conserved QPD motif located in its J domain.

ERdj5, considered in the field as the lonely ERdj, has the property of also belonging to the PDI family of enzymes that form, isomerize or reduce disulfide bonds, processes that are also critical for assigning a protein its final structure [25]. Not surprisingly, ERdj5 is shown to bind peptides lacking cysteines *in vivo* [26]. One example of the role of ERdj5 is its implication in the maturation of the low-density lipoprotein receptor, which requires the reduction of non-native disulfide bonds that are part of its normal folding trajectory [27].

Finally, ERdj6 was shown to selectively bind misfolded vesicular stomatitis virus G proteins. After the folding process, ERdj6 is released. Furthermore, it was demonstrated that the function of ERdj6 depends of its interaction with BiP. Indeed, in some studies it was indicated that overexpression of the ER form of ERdj6 enhanced the proper maturation of some substrates, arguing for a possible role as a pro-folding co-chaperone [23]. Evidence that ERdj directly participates in folding process is still lacking, but it is clear that ERdj6 is a cofactor that helps BiP activity.

Recent advances have provided a better understanding of the regulation of BiP and more generally of folding processes with the characterization of the ERdj protein family. Nonetheless, it is clear that more studies are needed to understand whether ERdjs that bind unfolded proteins play dedicated roles in folding versus Endoplasmic-Reticulum Associated Degradation (ERAD, process that is described just below) or whether this outcome is protein-specific. It is also unclear whether the substrate binding ERdjs have distinct specificities. The finding that some proteins can associate with multiple ERdjs raises the questions of how common this is, whether there is an order to these interactions, and how transfer from one type of ERdj protein to another is carried out.

In the next section we will learn about another system which allows reduction of the amount of misfolded proteins if the normal folding process is not sufficient: ERAD.

2-) ERAD

Despite the presence of a sophisticated system for protein folding with the involvement of several chaperones to help regulate the process, some misfolded proteins can persist in the ER [28]. Fortunately, these misfolded or unfolded proteins are quickly identified by the ER, retrotranslocated to the cytosol to be ubiquitinated, and then degraded via the 26S

subunit of the proteasome [29]. This succession of events is called ERAD and is an important part of ERQC. The ERAD was first investigated in the model organism *Saccharomyces cerevisiae* where several studies identified 3 main different ERAD pathways depending on the localization of the misfolded protein or more precisely the localization of the misfolded domain.

a-) Overview of different ERADs

ERAD substrates have molecular degradation signals which are called degrons [28] and whi[30,31]. Thus, ERAD-C is associated with membrane proteins that have their misfolded domains or degrons in the cytosol. On the contrary, ERAD-M substrates have their degrons in the membrane. ERAD-L is associated with substrates which have their misfolded domains located in the ER lumen. Then they are retrotranslocated into the cytosol to be uquitinated and degraded. However, there is one exception described for soluble ERAD-C substrates which do not require retrotranslocation for proteasome-mediated degradation [31].

In addition to the canonical ERAD-L, -C, and -M pathways, recent studies have provided evidence of more specialized ERAD pathways mediating protein quality control at the ER. One of these newly characterized pathways involves the degradation of ribosome-associated polypeptide chains at the ER membrane, which has been called ERAD of ribosome-associated proteins (ERAD-RA). In budding yeast, ER-targeted polypeptides within stalled ribosome complexes are marked for proteasomal degradation by the E3 ligase Ltn1 [32]. Ltn1 interacts with ribosomes and has a general role in mediating ribosome-associated protein quality control [33]. The ERAD-RA pathway seems to be conserved in higher eukaryotes as the Ltn1 mammalian ortholog called Listerin also appears to mediate ERAD-RA [34].

The second pathway recently described is ERAD-T for translocon-associated proteins. This ERAD pathway mediates the degradation of Sec proteins associated with the translocation complex (also called translocon), induced by aberrant interactions or abnormalities in the translocation process [35].

ERAD-RA and ERAD-T are two examples of newly identified ERAD pathways where the molecular mechanisms remain poorly characterized. Therefore, for the rest of the discussion I decided to focus only on ERAD-L, -M and -C summarized in the **Figure 5-**.

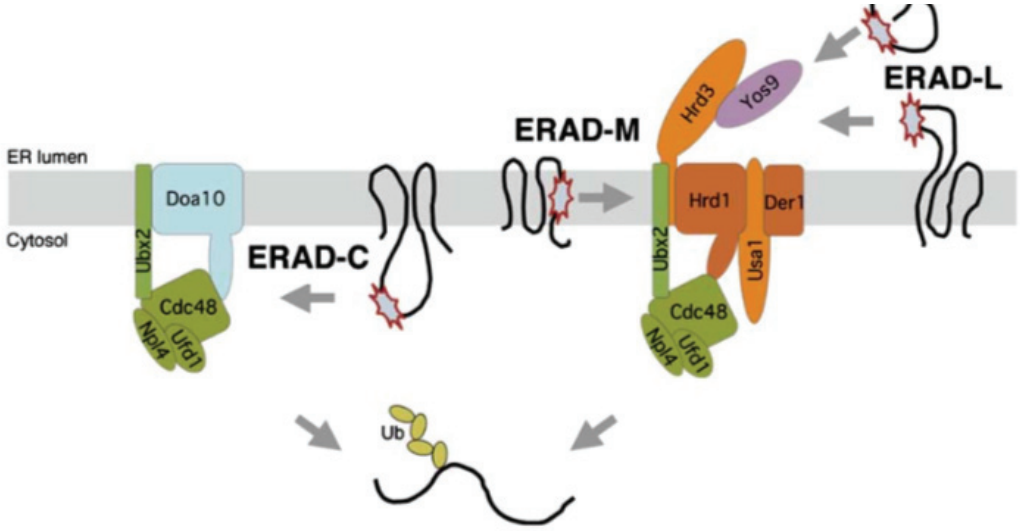

Figure 5- The scheme shows the ubiquitin-ligase complexes involved in the ERAD-L, -M, and -C pathways. Components in orange and green belong to the Hrd1p core and Cdc48p ATPase complexes, respectively. Stars show the location of the misfolded domain of a substrate. Ub is ubiquitin. Figures and legends extracted from [36].

b-) Recognition and retrotranslocation of misfolded proteins

As mentioned above, ERAD begins with the recognition of misfolded protein domains. This step is primordial and needs to be tightly controlled because inefficient detection of misfolded proteins will lead to their accumulation [31]. On the other hand, overactive ERAD would come at a very expensive energy cost for the cell, with the degradation of folding intermediates. In ERAD the main recognition actors are the E3 ligase complexes. E3 ligase complexes are best characterized in yeast where Doa10 (mammalian TEB4/MARCH) and Hrd1 (mammalian HRD1/Gp78) complexes were shown to assemble in the ER. These complexes are responsible for specific classes of ERAD substrates. Indeed, depending on the nature of the ERAD substrate a specific E3 ligase complex takes charge of the protein for degradation. ERAD-L and -M substrates are taken by the Hrd1 complex while ERAD-C substrates by the Doa10 complex [28]. For a summary of the equivalence between identified proteins in yeast and in mammals please see **Table 1**.

	Saccharomyces cerevisiae	Mammals	Functions
Hrd1 complex			
	Hrd1	Hrd1; gp78	E3 ligase activity; retrotranslocation; substrate recognition
	Hrd3	Sel1	Substrate recognition
	Usa1	Herp	Hrd1 and Der1 oligomerization
	Kar2	BiP	Chaperone activity, substrate recognition
	Yos9	Os9 XTP3-B	Substrate recognition
	Der1	Derlin-1, -2, -3	Recognition; transfer of substrate to Hrd1; retrotranslocation
Doa10 complex			
	Doa10	Teb4; March	E3 ligase activity; retrotranslocation; substrate recognition
	Ubc6	Ubc6, Ubc6e	E2 ubiquitin-conjugating activity
Common to Hrd1 and Doa 10 complexes			
	Cdc48	p97; VCP	Substrate retrotranslocation and memebrane extraction
	Ubx2	Ubxd8	Membrane-recruiting factor for Cdc48
	Npl4	Npl4	Cdc48 cofactor
	Ufd1	Ufd1	Cdc48 cofactor
	Ubc7	UBE2G1; UBE2G2	E2 ligase
	Cue1	Cue1	susbstrate membrane anchor and activator of Ubc 7 for ubiquitylation
	Saccharomyces cerevisiae	mammals	Functions
Hrd1 complex			
	Hrd1	Hrd1; gp78	E3 ligase activity; retrotranslocation; substrate recognition
	Hrd3	Sel1	Substrate recognition
	Usa1	Herp	Hrd1 and Der1 oligomerization

Table 1

α-) Hrd1 complex

The Hrd1 complex will process all of ERAD-L and -M substrates with the help of several other important proteins: Hrd3, Kar 2, Der1 and Yos9 as represented in **Figure 5-**. Briefly, Hrd1 is the main component of the complex with its ligase activity involved in the retrotranslocation of the substrates. Hrd3 also plays an important role because it is involved in the recognition of a large panel of ERAD-L substrates helped by lectin chaperons specialized in recognition of glycoproteins, as for example Yos9 in yeast and OS9 in mammals [37,38]. However, certain ERAD-M substrates appear to be recognized directly by the E3 ligase Hrd1 without the help of Hrd3 or other chaperons [39]. In yeast, the membrane protein Der1 is also involved in the recognition of the substrates and allows membrane insertion of the misfolded protein in the Hrd1 complex [40]. Finally, Kar2, the last component of this complex, has a chaperone activity besides its ability to transfer and insert substrates in the membrane channel formed by the Hrd1 ligase [36]. It is the synergy of all these actors that ensures the high efficiency of the Hrd1 complex in the recognition process which is an essential first step of ERAD.

One particular exception worth mentioning is the case of misfolded glycoproteins and ERAD-L. This process is well described in *Saccharomyces cerevisiae*, nicely illustrating how ERAD can coexist with the protein folding process in the same compartment, often with the involvement of the same protein complexes. For this reason, I have decided to present this process in more detail.

When glycoproteins enter the ER lumen, they are often modified at asparagine (N) residues with a fixed glycan chain moiety composed of three glucose, nine mannose, and two N-acetylglucosamine residues, Glc3–Man9–GlcNAc2 [41]. The N-linked glycan or N-glycoprotein is then trimmed by several enzymes which will determine their fate in the secretory pathway. Indeed, early glycan-processing enzymes such as glucosidases lead to the binding of lectin chaperons that facilitate the folding of the newly synthesized N-glycoproteins [42]. In contrast, late acting enzymes, such as the mannosidase Htm1, trigger the binding of a different lectin that engages the protein in ERAD [43]. This difference in the kinetics of the glycan-trimming enzymes provides an opportunity for newly synthesized proteins to acquire the native conformation and traffic beyond the secretory pathway. When

these glycoproteins stay too long in the ER, the N-linked glycan is truncated to generate a terminal α-1,6-linked mannose residue with the mannosidase Htm1. This protein extremity can then be recognized by the lectin Yos9 which in turn is bound to the luminal domain of Hrd3 of the Hrd1 complex directing the target towards degradation [40,44]. Both the yeast Htm1 and its mammalian counterpart EDEM are in complex with oxidoreductases (Pdi1 in yeast and Erdj5 in mammals), required for the stability of Htm1 and also for reducing disulfide bonds in misfolded proteins, which impacts specific ERAD steps [45]. However, the binding of Yos9 to the α1,6-linked mannose is not sufficient to trigger the degradation of the misfolded protein, which must be unstructured to bind Hrd3, with the help of the luminal chaperone Kar2 (BiP) [44]. The dual recognition of a specific N-linked glycan by Yos9 and an unstructured segment by Hrd3 likely enhances the specificity of ERAD substrate recognition and clearly facilitates its insertion in Hrd1 hub [46].

The recognition mechanism of misfolded luminal N-linked glycoproteins is very similar in mammalian cells because the yeast components are largely conserved in eukaryotes, but with an added level of complexity. OS-9 and XTP3-B, the mammalian homologues of Yos9, interact with glycans in the misfolded protein but also with Sel1, the mammalian version of Hrd3, which is itself a glycoprotein. In either case, using the same domain to interact with a component and a substrate offers OS-9/XTP3-B an additional mechanism to regulate recognition of N-glycosylated ERAD substrates [47].

Finally, additional work in yeast suggests that a different type of glycosylation, O-mannosylation, is important for removal of certain luminal proteins from unsuccessful folding cycles to favour their degradation by ERAD. The enzymes involved in O-mannosylation directly interact with the ERAD machinery. However, how ERAD components capture O-mannosylated proteins is still unknown. Interestingly, N-glycan trimming and O-mannosylating enzymes both appear to mediate relatively slow processes, in which substrates have to be retained for prolonged periods in the ER. In contrast, newly synthesized proteins seem to be protected from degradation for an initial period of time, even when conditions are suitable for inducing misfolding [48]

β-) Doa10 complex

The main component of the Doa10 complex is Doa10, a large E3 ubiquitin ligase with 14 transmembrane segments and an N-terminal RING domain [49]. The Doa10 complex is

also conserved in eukaryotes and the human Doa10 ortholog TEB4/MARCH6 appears to contain a similar membrane topology and localization. Initially it was thought Doa10 primarily targets ERAD-C substrates with degrons exposed to the cytoplasm or nucleoplasm. However, it was recently demonstrated Doa10 can also recognize specific ERAD-M substrates [50,51]. The first evidence suggesting Doa10 could target intramembrane degrons came from studies showing that the Doa10 cofactor Ubc6 is a short-lived protein and that its C-terminal membrane anchor is likely to be part of the relevant degron [52,53]. The identification of Doa10 substrates containing ERAD-M degrons suggests Doa10 can recognize a broader spectrum of substrates than previously thought. While cytosolic and membrane degrons are placed into separate categories, it is possible these degrons share certain features that remain to be identified.

Although shared characteristics of Doa10-dependent degrons have been described, it remains unclear if Doa10 directly interacts with substrates. It is possible that Doa10 interacts with substrates through its transmembrane segments, forming an internal channel [49], similar to what has been suggested for the E3 ligase Hrd1 [54]. The conserved regions of Doa10 that might have a role in substrate recognition include the TEB4-Doa10 domain, which includes three transmembrane segments, and the highly conserved 16-residue C-terminal element [55]. Another possibility is that Doa10 substrate recognition is mediated through adaptor proteins, such as molecular chaperones as for Hrd1 recognition process. Indeed, it has been shown that degradation of several Doa10 substrates requires Hsp40 and Hsp70 molecular chaperones [56,57], highlighting the interconnexion between folding and ERAD.

To conclude it appears that these E3 ligases Hrd1 or Doa10 are quite specific for each ERAD branch even if some downstream actors are common. In mammalian cells the best studied E3 ligases are the homonymous Hrd1 and Gp78. These 2 mammalian ligases are homologous to yeast Hrd1 E3 ligase. Nevertheless, they have differential affinities according to the substrate class. The molecular mechanisms of ERAD in mammalian cells still require further elucidating as new E3 ligases participating in ERAD are still being identified but whose functions remains mostly unknown. It remains to be determined for example whether there is a substrate affinity difference between these E3 ligases.

All these studies described in this section of the introduction, highlight how challenging it is to clearly separate ERAD pathways due to such high level of cross-interactions of E3 ligases and their protein complexes.

Finally, it is important to keep in mind that recognition of misfolded proteins can be divided in 2 processes one slow and one faster. Not surprisingly it is the slowest recognition process which is associated to ERAD more likely to allow for extra time for folding intermediates to be taken by folding chaperons. The molecular mechanisms that allow a cell to co-regulate folding kinetics and ERAD in the same compartment remain to be elucidated.

c-) Retrotranslocation and Ubiquitylation

Nascent protein translocation involves the insertion of integral membrane proteins into the ER membrane or the transport of luminal and secretory proteins to the ER lumen [58]. Consequently, translocation does not concern all the proteins. Nevertheless, this step is essential in the protein biogenesis process. At the molecular level, translocation occurs through a protein-conducting channel that is formed by a heterotrimeric membrane protein complex, the Sec61 or SecY complex. In the previous section relating to ERAD we mentioned retrotranslocation as means for elimination of membrane or luminal proteins [58,59]. At cellular level, retrotranslocation consists of transport of the substrate across the ER lipid bilayer back into the cytoplasm.

Once at the cytosolic side of the ER membrane, the substrate is ubiquitylated [36]. Briefly, ubiquitin is a small protein of 8.5 kDa that can be attached to substrates in a variety of ways. It is the attached ubiquitin which is recognized by the proteasome for degradation. The general process of ubiquitination is represented in Figure **6-.** E1, E2 and E3 are ligases that will pass the ubiquitin group between them to finally bind to the substrate. Attachment of a single ubiquitin (mono-ubiquitination) to a protein is not usually sufficient for recognition by the proteasome and is typically involved in other regulatory processes as it can inhibit interaction of the ubiquitinated protein with other partners [60] ; however, ubiquitination at multiple sites within a protein can target it for proteasomal degradation. More commonly, ubiquitin is attached to proteins in the form of ubiquitin chains, which are formed when the C-terminus of a donor ubiquitin (G76) is attached to one of the seven lysine side chains or the α-amino group of the first methionine of an acceptor ubiquitin. Poly-ubiquitin chains can be homotypic or heterotypic: the former is composed of a single linkage type while the latter contains multiple types of linkage and is characterized by a branched topology [61].

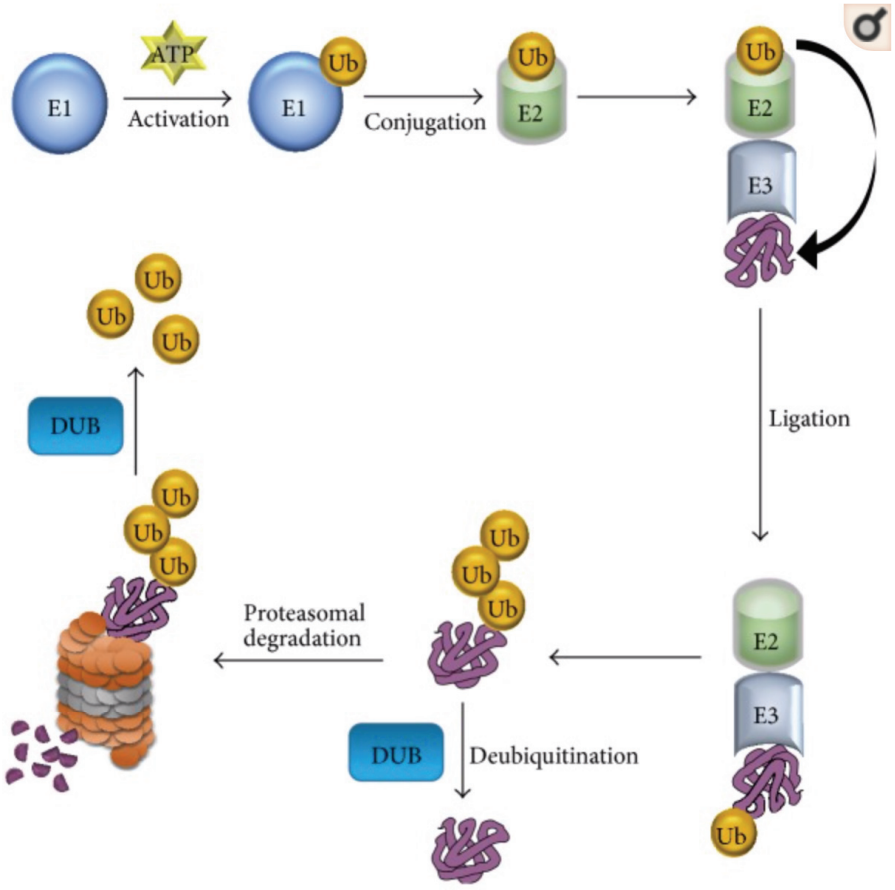

Figure 6- The ubiquitin proteasome system. The process of ubiquitination is catalyzed by an organized milieu of E1, E2, and E3 enzymes, which promote the ligation of a ubiquitin molecule to the lysine residues in the protein substrates. Lysine-48-linked polyubiquitination chain attached proteins are targeted to the 26S proteasome for protein degradation. DUB enzymes are involved in reversing ubiquitin conjugation and in the recycling of ubiquitin molecules through the ubiquitin proteasome pathway. Figures and legends extracted from [62].

Ubiquitination is an ATP-dependent mechanism. It is the RING domain of E3 ligases that is responsible for the ligase activity in the cytoplasm [63]. We have mentioned E3 ligases Doa10 and Hrd1, previously, but E2 ligases are also well characterized: Ubc6 and Ubc7. Ubc6 is specific for the Doa10 complex whereas Ubc7 is associated with all 3 previously described ERAD and thus the Hrd1 complex. They both have mammalian orthologs Ubc6 and Ube2G1/Ube2G2 [31].

It is difficult to dissociate retrotranslocation from ubiquitination because these 2 processes are closely connected. After the recognition of ERAD substrates, these are inserted in Hrd1 or Doa complexes. The precise mechanism still remains unclear because to date it is not yet known how the misfolded proteins enter in the Hrd1 channel with even the possibility

that the entry would occur via the lipid phase.

Once the substrate is in the cytoplasmic side, the next step is its ubiquitination by Ubc6 and 7 proteins. Ubc7 cooperates with Cue1, which serves as a membrane anchor and activator [64,65]. Its CUE domain promotes K48 ubiquitin chain formation which is required for the degradation of ERAD substrates [66]. In human cells, the Ubc7 ortholog, UBE2G2, associates with TEB4 to promote K48 (Lysine 48) chain formation *in vitro*.

Until recently, Doa10 and Hrd1 were thought to be the only ER resident E3 ligases participating in ERAD in yeast; however, recent studies have identified the transmembrane Asi complex as part of a previously uncharacterized ERAD pathway operating exclusively at the inner membrane of the nuclear envelope which is a subdomain of the ER [67]. This specialized complex highlights again the high complexity of ERAD even in a simple organism as the yeast. Asi complex is composed of 3 proteins Asi1-3 and is specialized in the degradation of misfolded proteins from the inner nuclear membrane. This spatial segregation of different ERADs strongly suggests the importance of this process for ERQC [67]. I mention this particular ERAD because the E2 ligase Ubc6 is also involved. Ubc6, is an integral component of the Doa10 pathway and in Asi pathway Ubc6 was shown to take part at this process. Ubc6 and Ubc7 are both required for efficient degradation of most Doa10 substrates. This raises the question of why these ERAD pathways should require multiple E2 ligases while Hrd1 complex in yeast only has Ubc7. The answer could be that Ubc6 and Ubc7 ligases have distinct catalytic properties which would explain their specificity [67] but this remains to be investigated.

Before reaching the proteasome for degradation there is the involvement of the cytosolic Cdc48 ATPase complex (p97 or Valosin-containing protein VCP in mammals) that separates polypeptides from protein complexes or from membranes, in our case Doa 10 or Hrd1 complexes [68]. Cdc48 is recruited to the membrane by an interaction between the polyubiquitin chain with the cofactors Ufd1/Npl4/Ubx2 and is thus involved in the late stages of the retrotranslocation process but also in ubiquitination [69]. The ATPase activity of Cdc48 is used to drive the unfolding of the substrate, [70]. Then the factor Ufd2 intervenes, possibly following substrate release from Cdc48 to increase substrate affinity for the proteasome or the proteasome shuttle factors Rad23 and Dsk2 [71]. Once the substrate is fully removed from the ER, Cdc48 probably dissociates from the Ubx2 anchor, diffusing away from the membrane with its associated substrate. The substrate is then released from Cdc48 in a process that

requires trimming of the polyubiquitin chain by a deubiquitinase. Finally, the substrate is passed on to the proteasome for degradation.

Another recent Cdc48 cofactor was identified in yeast, the deubiquitylating enzyme Otu1, is required for substrate release following substrate unfolding and initial polypeptide transfer through the Cdc48 pore [72]. This illustrates that much remains to be discovered, constantly increasing the complexity of ERAD-associated pathways, especially in mammals. Even if *Saccharomyces* is a model organism that allowed researchers to establish the basics of our knowledge of ERAD, it is now crucial to increase the number of studies using mammalian models. It seems clear that mammalian system is more sophisticated than yeast because there is a higher diversity of molecular actors as shown by the increasing number of identified E3 ligases. In addition, although I tried to separate the different kinds of ERAD-L-M and –C, even in yeast there are exceptions or cross-interactions so only future studies will lead to a better and total comprehension of ERAD processes in humans. Moreover, the identification of orthologs does not mean that proteins have exactly the same functions. This is why this research area is still very exciting and, in addition, dysregulations of this pathway can lead to severe diseases. Understanding the molecular mechanisms implicated could pave the way for developing new therapeutic approaches to counter these dysfunctions and help restore ER homeostasis in a disease context.

In the next section we will focus on the molecular mechanisms of the proteasome which ends the ERAD process and how this macromolecular machine is tightly regulated.

d-) Proteasomal degradation

The 26S proteasome is the principal macromolecular machinery responsible for protein degradation in eukaryotes. It is composed of a 20S subunit which is the proteasome capped core particle and a second 19S subunit which is the regulatory particle (**Figure 7-**). It degrades proteins to peptides by a multistep process and is essential for ensuring protein recycling in the cell [73].

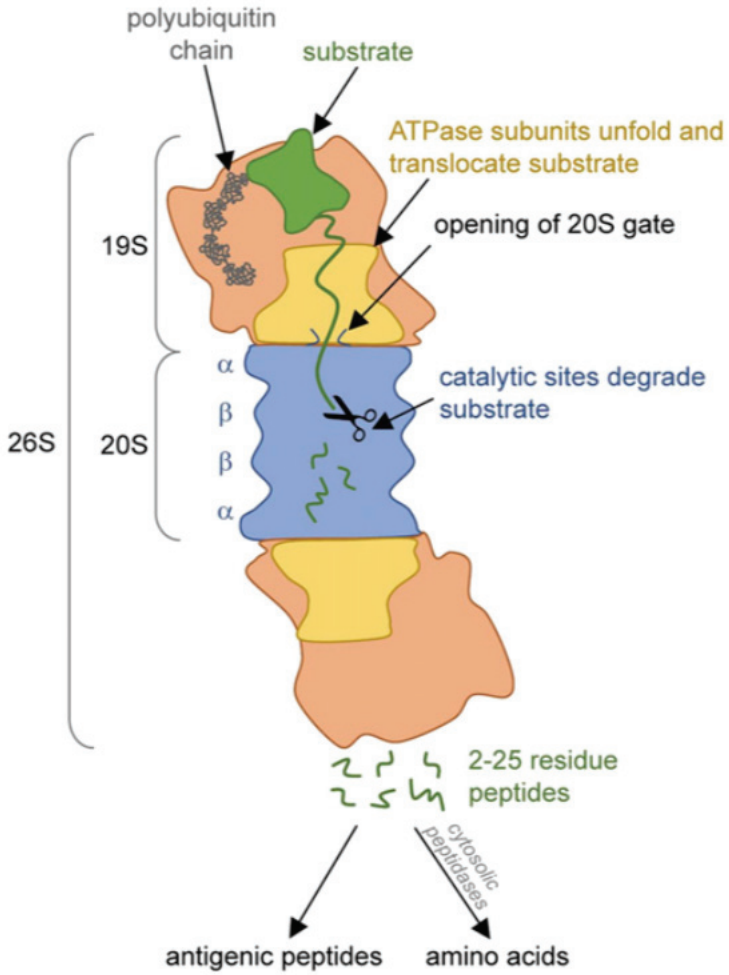

Figure 7- Structure of the proteasome. Figures extracted from [74]

Regulation of gate opening in the 20S proteasome is essential for proteasome function. The cell has evolved many different proteasomal regulators that control 20S gate opening with the 19S subunit [75]. The 26S proteasome is a structurally dynamic complex. Indeed, many conformational changes take place around the central axis during the ATP-dependent processing of substrates. These conformational changes are necessary for substrate protein unfolding and injection into the 20S core particle [76]. Ubiquitin-dependent proteasomal degradation requires several steps: (i) substrate binding, (ii) 20S gate opening, (iii) substrate unfolding and translocation, and (iv) deubiquitination.

α-) Substrate binding

First, the 19S regulatory particle has three integral subunits that serve as substrate receptors: Rpn1, Rpn10, and Rpn13. These substrate receptors reversibly associate with ubiquitin and have only low affinity for mono-ubiquitin this is why substrates destined for

degradation require poly-ubiquitination [77]. The multiplicity of ubiquitin receptors coupled with a variety of shuttling factors, such as proteins that have a ubiquitin-like (UBL) domain and a ubiquitin-associating domain (UBA), allows the 26S proteasome to recognize and degrade many types of ubiquitin conjugates [78]. Substrate binding to the ubiquitin receptors induces a conformational change aligning the 19S ATPase translocation channel directly over the 20S gate [79], induces gate opening, and stimulates ATP hydrolysis [80].

β-) 20s gate opening

Substrate insertion requires a poorly folded region of the protein and particularly an unstructured initiation site. Substrate is then inserted into the ATPase ring in an ATP-dependent manner [81]; the six ATPase subunits (Rpt1–6) form a ring at the bottom of the 19S complex with their C termini inserting into the 20S inter-subunit pockets, likely inducing a conformational change in the subunits, opening the gate [82].

χ-) substrate unfolding

Tyrosine pore loops inside the ATPases tightly associate with the substrate enabling substrate unfolding and translocation into the 20S core [78]. The six ATPase subunits ensure processive unfolding and translocation of substrates into the 20S core coupled with ATP hydrolysis [29].

δ-) Deubiquitination

Rpn11 is a proteasome-associated deubiquitinase enzyme of the 19S complex that is positioned directly above the translocation channel. When the substrate is committed for degradation, Rpn11 removes the entire ubiquitin chain as the protein is translocated. Two other deubiquitinases are transiently associated with proteasomes (Usp14 and Uch37) and can trim substrate ubiquitin chains prior to the commitment step, rescuing the substrate from degradation which constitutes an important regulatory checkpoint [77].

In addition to the general process of proteasomal degradation described above, other proteasome gate activator families exist, 11S and PA200/Blm10, neither of which contains unfoldase activity or require ATP. These other proteasome activators are specific of some other cellular processes [74]. Indeed, the proteasome gate PA200 was demonstrated to play a crucial role in spermatogenesis [83] to thus form the spermatoproteasome crucial for sperm maturation and viability [84]. The existence of interchangeable proteasome subunits allowing

for different proteasome "combinations" highlights the flexible cell repertoire of proteasome complexes tailored for specific cellular roles.

Proteasome is the last component in the ERAD. Because of its dominant role in the degradation of proteins, any inhibition would lead to an accumulation of misfolded proteins. The ERAD is initiated when the folding process does not succeed to properly fold proteins as it is presented in the **Figure 8-.** If the protein is properly folded after the involvement of different chaperones the protein will be exported (pathway c.). Otherwise it is the ERAD pathway that will be activated, and the protein will go from the step b. to d. Consequently, if both folding and ERAD are not enough to fulfill ERQC by drastically reducing the load of misfolded proteins, the cell will enter in a stress state which will activate a particular pathway known as the UPR as it is summarized in the **figure 9-**.

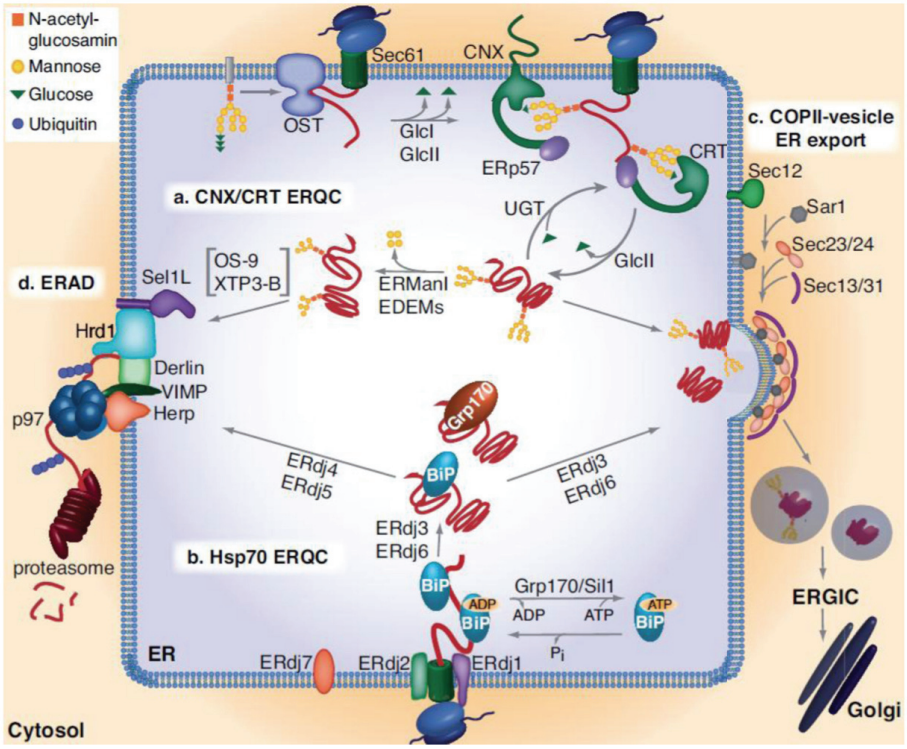

Figure 8- The ER Quality Control (ERQC) Machinery. Two main chaperone systems, the lectins CNX/CRT (a) and the Hsp70 chaperone BiP (b), aid the folding proteins for secretion (c) or if folding fails, target them for ERAD (d). (a) The oligosaccharyl transfer (OST) complex attaches a core oligosaccharide from a dolichol donor to the Asn of the Asn-X-Ser/Thr motif on nascent proteins during their translocation into the ER. GlcI and II remove the outer two glucose residues of the oligosaccharide, allowing the remaining glucose to be recognized by CNX/CRT. CNX/CRT assists protein folding in concert with further co-chaperones such as the protein-disulfide isomerase ERp57. Proteins exit the CNX/CRT cycle once the last glucose residue is removed by GlcII. If folded properly, the protein is released from the lectin chaperone cycle and is transported further

along the secretory pathway. Incompletely folded intermediates can re-enter the CNX/CRT cycle if a single glucose is re-attached by the folding sensor UGT. If folding ultimately fails, proteins are further trimmed by ERManI and/or an EDEM resulting in removal of 4 mannose residues and recognition by OS-9 and XTP3-B, which then transfer the trimmed glycoprotein to the ERAD machinery for disposal. (b) The Hsp70 chaperone. BiP binds hydrophobic patches exposed on nascent or incompletely folded proteins that are often non-glycosylated. BiP possesses low substrate binding affinity in the ATP-bound state and high affinity upon hydrolysis of ATP to ADP. Grp170 and Sil1 facilitate substrate release from BiP by stimulating the release of ADP and allowing ATP to rebind and open the lid on the substrate binding domain. Seven ERdj co-factors have been identified that interact with BiP *via* their J-domain and assist BiP in its functions during protein translocation (ERdj2), protein folding (ERdj3 and 6) and ERAD (ERdj4 and 5). The functions of ERdj1 and ERdj7 are not well understood, nor is the role of the large Hsp70, Grp170, that also binds to some incompletely folded BiP client proteins. (c) Once the threshold of folding set by the ERQC is met, proteins exit the ER in COPII-coated vesicles, a process that is initiated by Sec12 and driven by a GTPase, Sar1, and four major coat proteins, Sec23, Sec24, Sec13 and Sec31. (d) Once proteins that are clients of either chaperone system are delivered to the ERAD machinery, their retrotranslocation into the cytosol is facilitated by a complex of several transmembrane proteins including Sel1, Derlins, VIMP, Herp and Hrd1, which connect the machinery in the ER lumen to the protein ubiquitination machinery in the cytosol, allowing the ERAD client to be recognized by the p97 hexameric ATPase in the cytosol that provides the energy for extracting a protein from the ER for degradation by the 26S proteasome. Figures and legends extracted from [24].

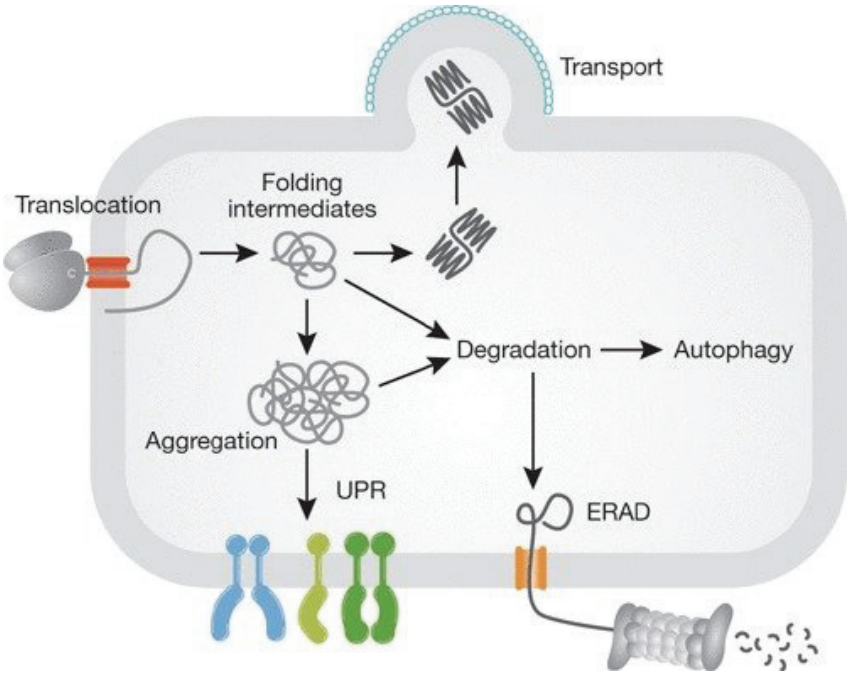

Figure 9- The general ERAD pathway for degradation of misfolded ER proteins. ERAD is initiated on the recognition of non-native proteins as aberrant molecules by quality control receptors. These terminally misfolded or unassembled proteins are then sorted to an ER-membrane-associated dislocation/ubiquitination complex containing adaptor proteins that recognize the quality control receptor and/or the ERAD substrate directly. A translocon then acts as a conduit for the retrotranslocation of the protein to the

cytosol, and this process is often coupled with ubiquitination by an ER-associated E3 ubiquitin ligase. Cytosolic components are also recruited to the retrotranslocation complexes to aid in the extraction of the ERAD substrate from the ER and prepare the substrate for proteasomal degradation. Figures and legends extracted from [85]

3-) Unfolded Protein Response

As mentioned above, the ER tries to ensure efficient quality control of protein biogenesis coordinating the action of its several chaperones and the ubiquitin-proteasome system in order to properly fold proteins or to degrade misfolded proteins. In order to restore homeostasis and to fight against "protein-toxic" stress or more generally ER stress, cells can activate a signaling pathway called UPR that results in the reprogramming of a series of events that can be either pro-survival or pro-death, depending on the extent of the damage or the length of the stress [13,86].

In yeast, ER stress results in the upregulation of a large cluster of genes involved in protein folding, quality control, and secretion. While in mammals, the UPR has evolved a complex network of interconnected signaling pathways initiated by the stimulation of three signal transducers located in the ER known as Inositol-REquiring protein 1 (IRE1) (α and β), activating transcription factor- 6 (ATF6) (α and β) and protein kinase RNA (PKR)-like ER kinase (PERK) [87]. Activation of the UPR will play on two temporally distinct cellular events to fight against protein misfolding: an initial reaction to reduce protein synthesis and enhance degradation of misfolded proteins and a second wave of transcriptional upregulation of hundreds of target genes involved in ERQC, including those implicated in protein folding and ERAD. The ER chaperone BiP/Grp78 previously introduced in the folding process is also fundamental for the activation of the three main sensors. Upon ER stress, BiP binds to misfolded proteins through its substrate binding domain, operating as an allosteric regulator to release the sensors IRE1, ATF6 and PERK [88]. Under basal conditions, BiP associates with the ER luminal domain of PERK and IRE1α via its ATPase domain, maintaining them in an inactive monomeric state [88]. When stress is induced, the ER relies on its three distinct UPR branches to first attempt to overcome this stress and restore homeostasis. However, when the stress conditions are too intense and cannot be controlled, the UPR activates a cell death pathway, generally via intrinsic apoptosis involving the mitochondria [89,90]. In fact, ER stress is primarily a pro-survival adaptive response against different types of cellular troubles.

a-) UPR for homeostasis: the adaptive UPR

α-) IRE1

IRE1 was the first pathway characterized genetically in *S. cerevisiae*, leading to the identification of a signaling pathway between the ER and the nucleus in cells witnessing the stress of unfolded protein accumulation [91]. This pathway is involved in ERAD enhancement, regulation of lipid synthesis and protein secretion.

IRE1 is the most conserved UPR signaling branch. It is a transmembrane protein with an N-terminal ER luminal sensing domain and a cytosolic C-terminal domain containing a serine/threonine kinase and an endoribonuclease (RNase) [92,93]. There are two IRE isoforms, IRE1α and IRE1β; the first one is expressed ubiquitously on ER membranes, while the second one is found only on epithelial cells of the gastrointestinal tract [90]. In the context of this introduction we will focus only on IRE1α.

In response to unfolded protein accumulation in the ER, IRE1 dissociates from BiP, its luminal domain self-associates, causing its own dimerization and trans-autophosphorylation. This in turn induces a conformational change that activates its RNase domain to catalyze excision of a 26-nucleotide intron within the X-Box Protein 1 (XBP1) gene [92,93]. The spliced form of XBP1 controls the expression of genes encoding factors that modulate protein folding, secretion, ERAD, protein translocation into the ER and lipid synthesis [94].

The efficiency of XBP1 mRNA splicing is regulated at different levels. For example, the delivery of its mRNA to the ER membrane is mediated by the transient expression of the unspliced form of XBP1 (XBP1u). Although XBP1u is very unstable and rapidly degraded by the 26S proteasome, during its translation, the nascent chain docks the ribosome to the ER membrane allowing the efficient processing of XBP1 mRNA in the cytosol [95,96]. In addition, the selective targeting of the XBP1u mRNA to the ER membrane is mediated by a direct interaction of IRE1α with the Sec61 translocon [97]. Interestingly, the XBP1u mRNA is delivered to the IRE1/Sec61 complex by docking of its nascent protein to the classical signal-recognition particle pathway through the hydrophobic domain. After cleavage of XBP1 mRNA, the tRNA ligase RtcB completes the cytosolic splicing event, leading to the expression of XBP1s [98], a hallmark of activation of the IRE1 UPR pathway.

β-) PERK

As IRE1, PERK is also transmembrane protein kinase associated with BiP in its inactive form that gets activated after BiP dissociation. The role of this UPR pathway is to

inhibit general protein translation through the phosphorylation of eukaryotic translation initiator factor-2 (eIF2α) [12]. which blocks the recycling of eIF2α in its active GTP-bound state, needed for starting polypeptide chain synthesis. This event thus reduces the overload of ER translocating proteins in a stressed cell but also allows the selective translation of the mRNA encoding the transcription factor ATF4, contributing to reinforcement of an antioxidant response, enhancement of the folding capacity of the ER, upregulation the transcription of growth arrest and upregulation of autophagy [99-101]

χ-) ATF6

ATF6α is also an ER transmembrane protein that contains a bZIP transcription factor on its cytosolic domain, a member of the leucine zipper family. As IRE 1, ATF6 also has 2 isoformes ATF6 α and β.

Following UPR activation, ATF6 translocates to the Golgi apparatus, where it is cleaved by the proteases S1P and S2P in a cytosolic fragment cleaved ATF6 α [102]. In this active form, it translocates to the nucleus and acts as a transcription factor. It will cause upregulation of a select set of UPR genes presenting ATF/cAMP response elements or ER stress response elements (ERSE) within their promoter. Upregulated genes include those that enhance the ERAD pathway such as BiP, and protein disulfide isomerase [103]. Unlike ATF6α, ATF6β is not crucial in responding to UPR or regulating ER chaperones. Moreover, ATF6β has been shown to inhibit ATF6α-mediated activity during UPR [104].

ATF6α was also shown to regulate the transcription of ERAD components. Levels of ERAD components, including EDEM, HRD1 and Herp. Herp is also a very important player in ERQC and will be further described below. All these critical regulators were found to be lower in ER stress-induced ATF6α–/– mouse embryonic fibroblasts (MEFs) compared to ATF6α+/+ MEFs (Hirsch 2013 Apoptosis).

Finally, it has also been shown that ATF6 can associate with XBP1s by forming heterodimers, which may drive specific gene expression programs [105]. This final example perfectly illustrates the interconnexion between the different UPR pathways (**Figure 10-**).

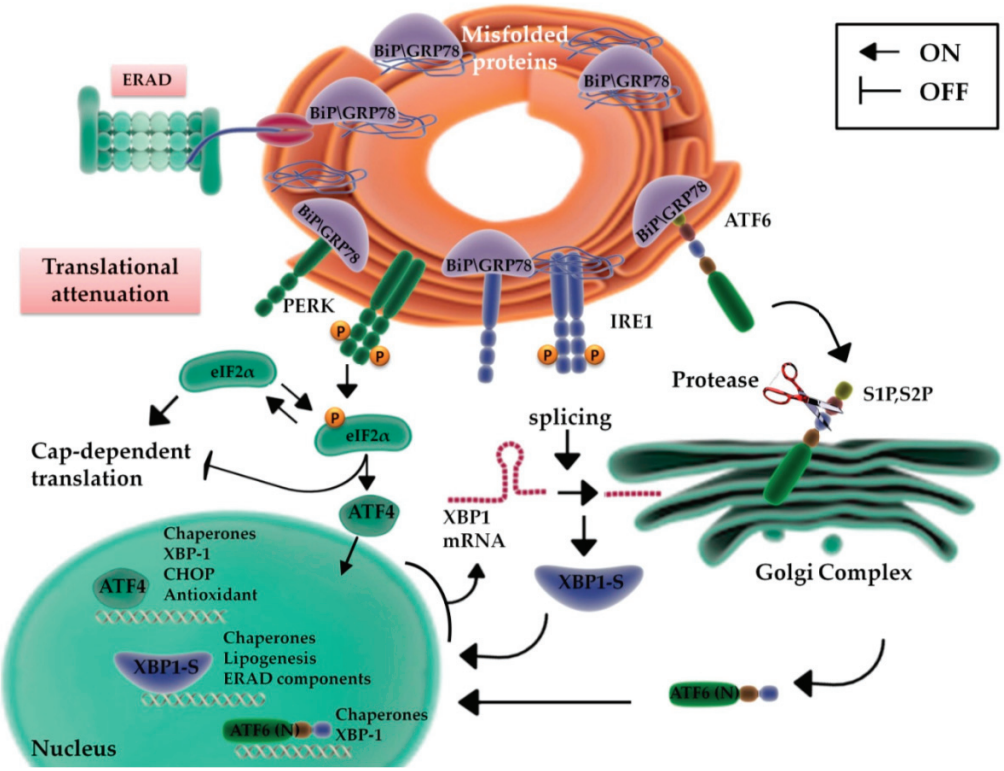

Figure 10- Unfolded protein response activation during Endoplasmic Reticulum (ER) stress conditions. Accumulation of misfolded proteins in endoplasmic reticulum induces the activation of three ER stress sensors. Figures and legends extracted from [106].

b-) UPR for cell death: the terminal UPR

If the adaptive responses fail to restore protein-folding homeostasis, UPR signaling continues to persist and can progress into a signaling program called the "terminal UPR" that promotes apoptosis (see **Figure 11-**) [107]. Strong evidence supports that the two UPR kinases, PERK and IRE1α, engage a distinct set of pro-apoptotic genes that contribute to cell degeneration and death if ER stress cannot be resolved. For example, while a temporary pause in protein translation due to eIF2α phosphorylation can be beneficial by reducing secretory load, a prolonged block in translation from sustained PERK signaling is incompatible with survival [108].

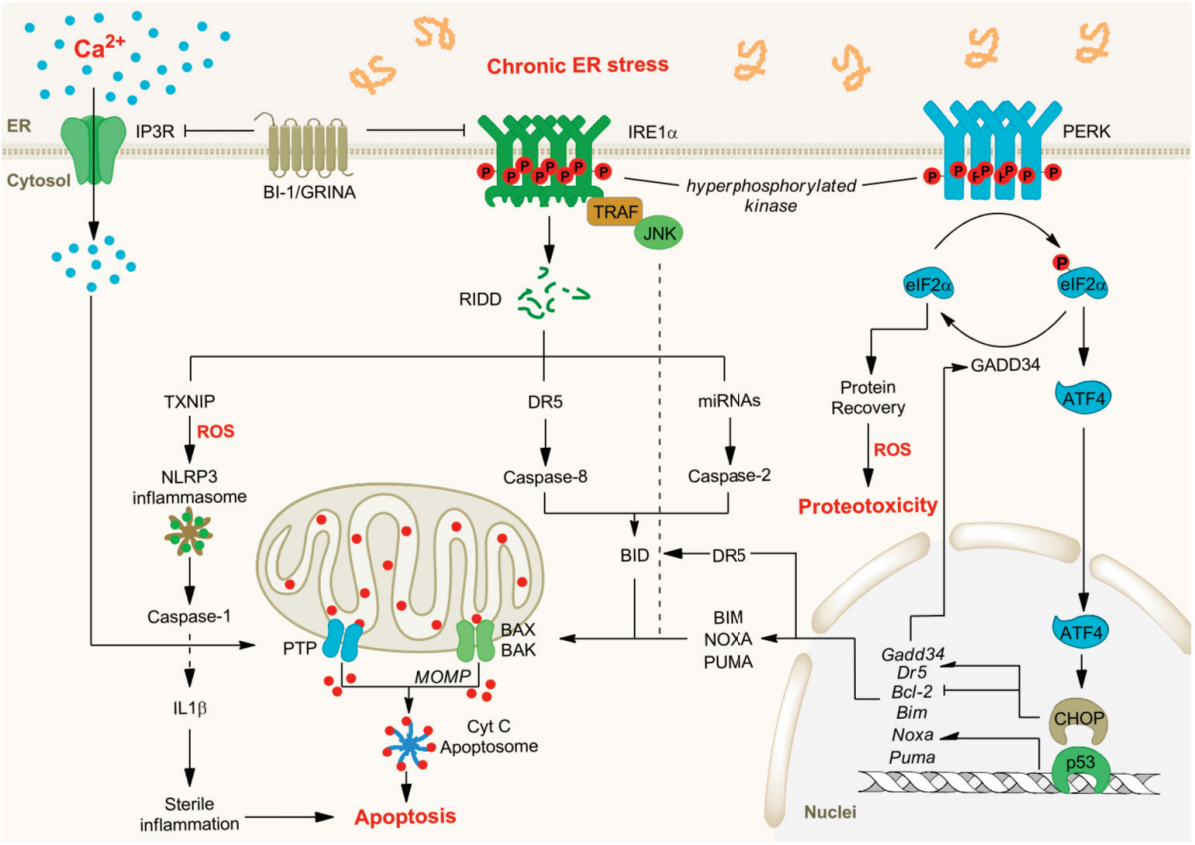

Figure 11- ER Stress-Induced Apoptosis Pathways. When exposed to chronically high levels of ER stress, PERK and IRE1 both drive multiple signaling outputs that lead to cell dysfunction, activation of the inflammasome, and apoptosis. A key step in the regulation of apoptosis is the crosstalk between the ER and mitochondria through transcriptional and post- translational modifications of members of the BCL-2 family of proteins. In addition, calcium release from the ER and exacerbated protein synthesis and ROS production may influence the induction of apoptosis. Figures and legends extracted from [13]

α-) IRE1

As described above, IRE1 RNase is involved in the splicing of XBP1. But its RNase activity also regulates the stability of multiple RNAs through a direct endonucleolytic cleavage reaction in a process known as regulated IRE1-dependent decay (RIDD). When hyperactivated by chronic ER stress, phosphorylated IRE1α assembles into high-order oligomers. These associations allow the RNase domain to acquire affinity for RIDD substrates, causing massive endonucleolytic decay of hundreds of these ER-localized mRNAs. Consequently, it will lead to degradation of ER and protein-folding components that will further worsen ER stress [109]. RNA substrates include mRNAs, ribosomal RNA and microRNAs which have important biological functions in the control of glucose metabolism, inflammation and apoptosis [110].

IRE1α oligomerization under irremediably high levels of ER stress also induces activation or upregulation of a number of pro-inflammatory and pro-apoptotic proteins. For example, when hyperactivated, IRE1 RNase reduces the levels of select microRNAs that normally repress pro-apoptotic targets, such as thioredoxin-interacting protein (TXNIP), leading to their rapid upregulation. Increased TXNIP protein levels then activate the NLRP3 inflammasome and its caspase-1-dependent pro-death pathway, leading to sterile inflammation and pyroptotic cell death [111].

Sustained IRE1α activity may serve as an activation platform. It can associate with many different proteins, in which the nature of the associated proteins will engage different cellular responses. For instance, association with apoptosis signal-regulating kinase 1 (ASK1) and its downstream target c-Jun NH2-terminal kinase (JNK) may regulate apoptosis under chronic stress [112,113]. Another example, ABL kinase family members hyperactivate IRE1α RNase at the ER membrane to promote apoptosis. While other interactions with the adaptor proteins Nck engages nuclear factor κB (NF-κB) [114,115].

Fortunately for the cell, the kinetics and amplitude of IRE1α signaling are also controlled by the binding of positive and negative regulators including several proteins previously linked to apoptosis, including members of the BCL-2 family or BH3-only proteins [116,117]. The BCL-2 family (Bak, Bax, Bim, Puma, and Noxa) is a large class of both pro- and anti-death proteins whereas BH3-only proteins are another class of exclusive pro-apoptotic proteins with Bim and Puma. These 2 proteins were shown to selectively enhance the sustained signaling of IRE1α [118].

In contrast, the ER-located protein BAX inhibitor-1 (BI-1) interacts with the cytosolic domain of IRE1α accelerating its attenuation after prolonged ER stress [119]. Other proteins, such as Fortilin, were recently shown to inhibit IRE1α signaling through a direct interaction, increasing cell death resistance under ER stress [120]. In addition, another study suggested that IRE1α levels are also controlled by the ERAD pathway, a process that unexpectedly depends again on BiP. It was proposed that, under ER stress, BiP is released and IRE1α is stabilized [121]. Thus, multiple checkpoints regulate IRE1 signaling through distinct protein-protein interactions, defining the precise threshold of stress necessary for its activation.

β-) PERK and ATF6

PERK under chronic ER stress and sustained ATF4 expression contribute to induction of apoptosis with the activation of downstream genes such as CHOP and HERP [122,123]. This latter protein will be discussed in the next part.

Upregulation of the CHOP transcription factor inhibits the expression of the gene encoding anti-apoptotic BCL-2 to hasten cell death. CHOP represents a crucial player in ER stress-mediated cell death and all three branches of UPR can affect CHOP expression [124]. Nevertheless, PERK and ATF6 are the most involved branches that can sustain CHOP upregulation. During persisting ER stress, ATF4 and CHOP promote cell death by activating genes involved in protein synthesis, such as GADD34 and endoplasmic reticulum oxireductin1α (ERO1α) [125]. GADD34 induces the dephosphorylation of eIF2α and thus restores protein synthesis. If the protein synthesis is over-regulated, it saturates the system with accumulation of high amount of proteins that worsen the ER stress. ERO1α, which is involved in the oxidation of PDI, leads to a condition of hyper-oxidation in ER which is deleterious for cell [126]. Moreover, by augmenting ERO1α expression, CHOP also promotes Ca^{2+} release via channel inositol 1,4,5-triphosphate receptor (IP3R) from ER to the cytoplasm. The increase of Ca^{2+} in the cytoplasm activates the calcium/calmodulin-dependent protein kinase II (CaMKII), which acts as an upstream molecule regulating apoptosis (Ozcan 2010 Cell Cycle).

CHOP can also directly induce apoptosis by inducing both extrinsic and intrinsic apoptotic pathways. CHOP up-regulates death receptor 5 together with caspase-8, which in turn generates the truncated form of Bid (tBid) and transports it into the mitochondria [127], activating the intrinsic apoptotic pathway. On the other hand, CHOP can also trigger the intrinsic pathway by decreasing the expression of anti–apoptotic Bcl-2 and Bcl-xL proteins, while increasing the expression of pro-apoptotic proteins such as Bak, Bax, Puma, and Noxa [128]. Finally, it can also enhance the expression of pro-apoptotic BCL-2 members such as Bim, as well as improving protein synthesis and oxidative stress [108].

c-) General conclusions on UPR

In mammals, the activation of ER stress sensors involves the chaperone BiP, in addition to the binding of misfolded proteins to engage an optimal UPR response. It is important to keep in mind that other ER chaperones were also implicated in modulation of the UPR. For example, the disulfide isomerase PDIA6 binds and controls the attenuation of

IRE1α and PERK signaling, but not ATF6 [129]. In contrast, another disulfide isomerase (PDIA5) selectively regulates ATF6 activation [130] with the fact that luminal disulfide bonds in ATF6 modulate its translocation to the Golgi apparatus.

The control of the temporal behavior of UPR signaling is fundamental in determining the fate of a cell under ER stress, although the mechanisms explaining the transition from adaptive to a terminal pro-apoptotic UPR are not completely established yet [13,131]. Under conditions of mild ER stress, activation of XBP1 mRNA splicing is transient, leading to its attenuation after prolonged stimulation, which may sensitize cells to undergo apoptosis [132]. In contrast, the activity of RIDD under increased IRE1α oligomerization is sustained over longer periods of time [133].

Initially, studies viewed UPR signaling as a direct and linear transduction of ER stress levels. However, recent findings have indicated that the three major UPR sensors are tightly regulated through post-translational modifications and the binding of cofactors. A new concept has recently been described: the UPRosome. This term was mainly associated to IRE1, considered as a scaffold where many components assemble dynamically to regulate different signaling outputs. The UPRosome may also serve as a platform to enable the crosstalk between UPR and other signaling pathways [13]. Indeed, the nature of the components which associate to IRE1 will engage different cellular responses. Although less explored, PERK and ATF6 are important for ER even if PERK is more associated to terminal UPR. There are also subject to complex regulation that is not totally characterized and understood [13,134]. Overall, these selected findings illustrate the dynamic and complex nature of UPR signaling, where several checkpoints are established to determine downstream signaling responses.

d-) UPR and immunity

Recently, UPR was shown to be interconnected at different levels with innate immune response pathways. Briefly, in the innate immune response, pathogen-associated molecular patterns (PAMPs), for example, lipopolysaccharides or nucleic acids such as CpG DNA or dsRNA, are recognized by pattern recognition receptors (PRRs), such as Toll-like receptors (TLRs), nucleotide-binding oligomerization domain (NOD)-like receptors or retinoic acid-inducible gene I (RIG-I) receptors. PRRs activate signaling pathways leading to the expression of genes involved in inflammation, immune cell regulation, survival and

proliferation. TLRs are amongst the most characterized PRRs [135,136]. UPR signaling was shown to be connected to TLR2 and TLR4. These 2 TLRs specifically activate the IRE1-XBP1 branch of the UPR, promoting the production of inflammatory mediators (i.e., IL-6) [137]. Interestingly, this activation occurs in the absence of a full ER stress response, demonstrating that a specific arm of the UPR can be activated independently of the others. Recently, researchers of Tsolis lab demonstrated that NOD1 and NOD2, two members of the NOD-like receptor family of PRRs, which are traditionally considered as sensors of bacterial peptidoglycan, have a major role in inducing inflammation during ER stress [138]. This study is further discussed in the **Chapter 3** on *Brucella* (**section IV3-)**).

The activation of NF-κB, a key regulator for immune and inflammatory responses, has being also linked to UPR [139]. NF-κB activation may be dependent on the intensity of UPR. These new data are very exciting because they changed our perception that UPR is only activated for ER stress with a negative connotation. In the case of NF-κB, preconditioning with low dose of ER stress inducers was shown to attenuate NF-κB activation in endothelial cells. However, additional studies have shown that ER stress can influence NF-κB activity positively or negatively making it difficult to make a general statement regarding the outcome of UPR activation on NF-κB activation. It has been proposed that NF-κB activation by ER stress occurs in the early adaptive phase, whereas its inhibition occurs in the terminal phase; the inhibition of signaling mediated by NF-κB was shown to be dependent on induction of CHOP by UPR [140].

Finally, the UPR has been implicated in additional cellular functions not described in this introduction as for example in the production of reactive oxygen species (ROS) that have an anti-microbial role [135], consistent with an overall critical impact of UPR pathways on cellular responses.

4-) ER-phagy

Before describing ER-phagy, I have to briefly introduce the general concept of autophagy. This a cellular process which allows degradation and recycling of cellular components. There are three major types of autophagy: macro, micro and chaperone mediated-autophagy (all represented **Figure 12-**) [141]. Macro-autophagy more commonly referred to as autophagy is the best-studied type, a catabolic process that gathers all degradation pathways. The component to be degraded, called cargo, is engulfed by a double-

membrane organelle termed phagophore, which eventually closes to form a vesicle called the autophagosome. The cargo is then delivered for degradation in the lysosome (vacuole in yeast), a major recycling cellular compartment [142]. However, autophagy can also selectively target distinct organelles and cellular structures that are damaged and/or need to be turned over [143].

The 2 other types of autophagy, micro-autophagy and chaperone-mediated autophagy do not require autophagosome formation. During micro-autophagy invagination of the lysosome/vacuole membrane directly engulfs small cytosolic components [144]. In contrast, in chaperone-mediated autophagy, cytosolic proteins containing a KFERQ motif are recognized by the chaperone protein Hsp70 and directly translocate across the lysosomal membrane [145].

Typical substrates and receptors of selective autophagy have LC3-interacting regions (LIRs) that bind to autophagosomal protein light chain 3 LC3 and γ-aminobutyric acid receptor-associated protein (GABARAP) family proteins. Selective substrates are directly or indirectly recognized by Atg8 or its homologs present on autophagic membranes [143,146]. Alternatively, autophagy adaptors or receptors that have LC3-interacting regions (LIRs) or GABARAP interaction motifs (GIMs) mediate recognition of selective substrates, often in a ubiquitination-dependent manner [147,148].

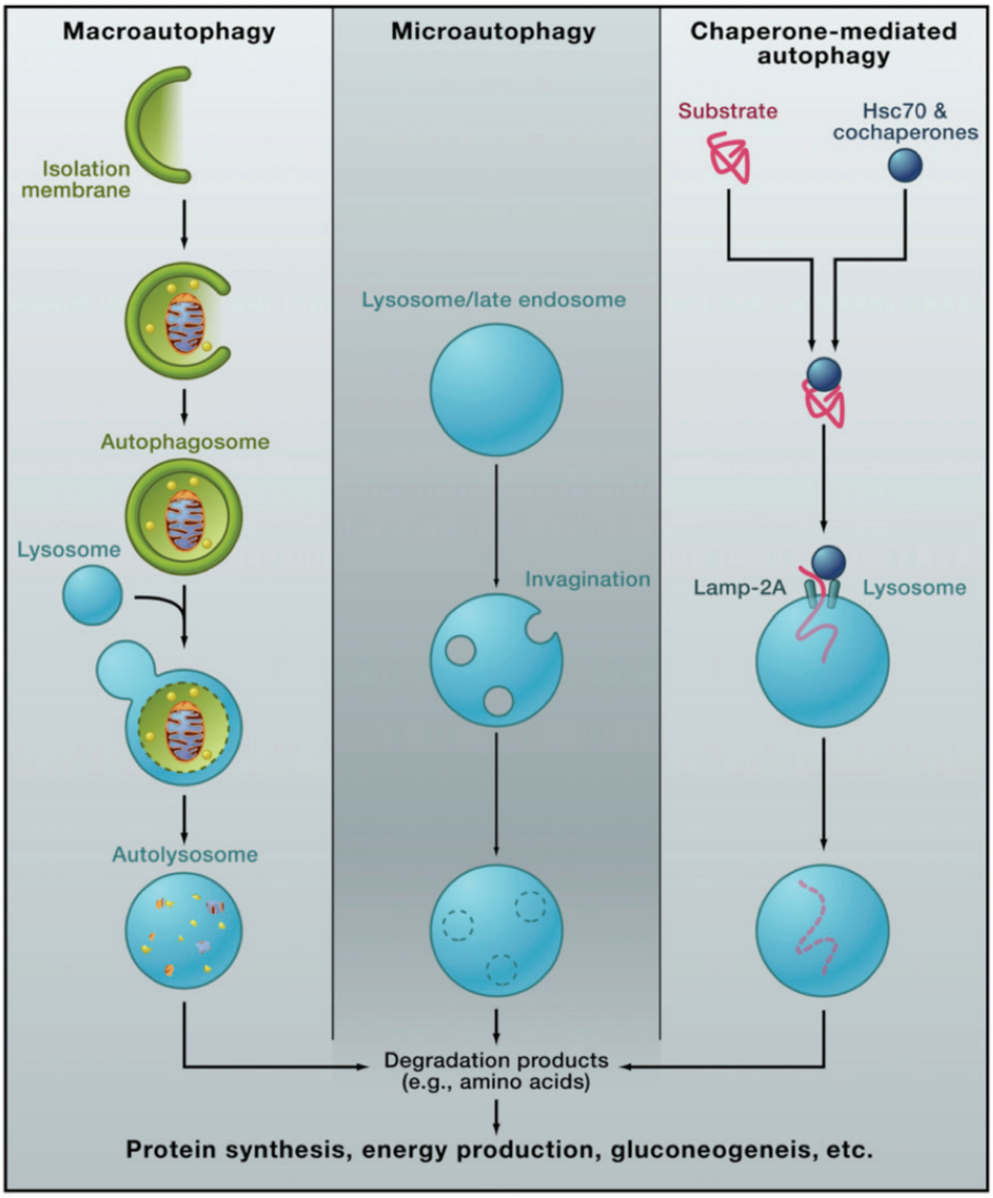

Figure12- Different Types of Autophagy. Macroautophagy: A portion of cytoplasm, including organelles, is enclosed by an isolation membrane (also called phagophore) to form an autophagosome. The outer membrane of the autophagosome fuses with the lysosome, and the internal material is degraded in the autolysosome. Microautophagy: Small pieces of the cytoplasm are directly engulfed by inward invagination of the lysosomal or late endosomal membrane. Chaperone-mediated autophagy: Substrate proteins containing a KFERQ-like pentapeptide sequence are first recognized by cytosolic Hsc70 and cochaperones. Then they are translocated into the lysosomal lumen after binding with lysosomal Lamp-2A.

After all three types of autophagy, the resultant degradation products can be used for different purposes, such as new protein synthesis, energy production, and gluconeogenesis. Figures and legends extracted from [149]

a-) ER-Phagy in yeast

The first studies on ER-phagy were performed in yeast. The ER provides membranes for autophagosomes and is itself a target of autophagy. In yeast, selective substrates are recognized by autophagy receptors (for example Atg19 and Atg34) containing the Atg8-interacting motif (AIM) and are delivered to the vacuole. The term ER-phagy was used for the first time by Peter Walter's group in describing how, during UPR, ER becomes selectively degraded by the vacuole [150]. During UPR conditions, the ER significantly enlarges its volume and membrane content. However, soon after, cells start to recover the initial ER homeostasis by eliminating superfluous membrane via vacuolar degradation [151]. Yeast ER-phagy can also function as a detoxification system in which aggregated or unwanted proteins are restricted to specific ER compartments and subsequently eliminated by vacuolar degradation [152]. Yeasts have two ER-phagy receptors, Atg39 and Atg40, which are AIM-containing ER membrane proteins that play key roles in sequestering ER fragments into autophagosomes [153].

b-) ER-Phagy in mammals

In mammalian cells, degradation of ER components by autophagy, initially termed reticulophagy, was discovered as a back-up system for the inefficient proteosomal degradation of ER proteins *via* the ERAD pathway [154-156]. In a process equivalent to what has been described in yeast, ER-phagy includes the re-shaping after ER expansion upon stress, as well as the lysosomal degradation of protein aggregates within the ER lumen. In mammals, the Atg8 homologs are classified into two subfamilies: LC3 and GABARAP. The specialized ER-phagy receptor RETREG1 (also known as FAM134B) was the first one to be described and characterized [148]. Indeed, ablation of RETREG1 or inactivation of its LIR domain have been shown to block ER fragmentation and subsequent lysosomal degradation [157]. Initially, RETREG1 was described as a Golgi protein but was more recently classified as an intra-membrane ER-resident protein, mainly located at the edges of the ER sheets, that is characterized by the presence of a reticulon homology domain. RETREG1 has the intrinsic property to fold double layer ER membranes to form phagophore [148,157].

At least 3 other ER-resident proteins that bind to mammalian Atg8 have revealed that the selective elimination of ER involves different receptors that are specific for different ER subdomains or ER stresses. These include reticulon 3 (RTN) which is a protein that is able to

remodel the ER network and ensure the basal membrane turnover and Sec62 and Ccpg1 that are transmembrane ER receptors were shown to function in response to ER stress signals [158].

Previously, autophagy was thought to be a nonselective bulk degradation pathway; however, it is now clear that some proteins and damaged organelles are selectively recognized and degraded by autophagy [147,149]. Ccpg1 is closely connected to UPR because of its upregulation in response of UPR induction. *In vivo*, Ccpg1-mediated ER-phagy protects pancreatic acinar cells against the aggregation of ER luminal proteins. Therefore, Ccpg1 may act as a bridge between UPR signaling and ER-phagy in a physiological context [159].

However, in contrast to what is seen in yeast, mammalian cells do not appear to use micro-autophagy to re-establish ER shape and homeostasis. This is ensured by the translocon component Sec62, that can mediate ER-phagy through a LIR motif in its C-terminal cytosolic domain [160].

As a summary RETREG1 RTN3, CCPG1 and Sec62 functions may be spatiotemporally different [158,161]. RETREG1 and RTN3L are important for starvation-induced degradation of ER sheets and tubules, respectively [158]. CCPG1 is induced during ER stress and activates autophagic degradation of peripheral ER [159].

ER-phagy is still an emerging pathway, this is why there are few studies about the topic. In 2019 Chino *et al*. [162] identified a new receptor for autophagic degradation, the protein Tex264. TEX264 interacts with LC3 and GABARAP family proteins more efficiently and is expressed more ubiquitously than previously known ER-phagy receptors.

Finally, another recent study also identified ATL3 as an ER-Phagy Receptor for GABARAP-mediated autophagy [163]. This is interesting because ATL3 belongs to atlastins family. Atlastins (ATL1, ATL2, and ATL3), in mammals, are a class of membrane-bound, dynamin-like GTPases that function in ER fusion. Authors show ATL3 specifically binds to GABARAP, but not LC3 via 2 GIMs. The specificity of binding to GABARAP motif may lead to a specific ER-phagy process but much remains to be discovered. All these data of ER-phagy are summarized in **Figure 13-.**

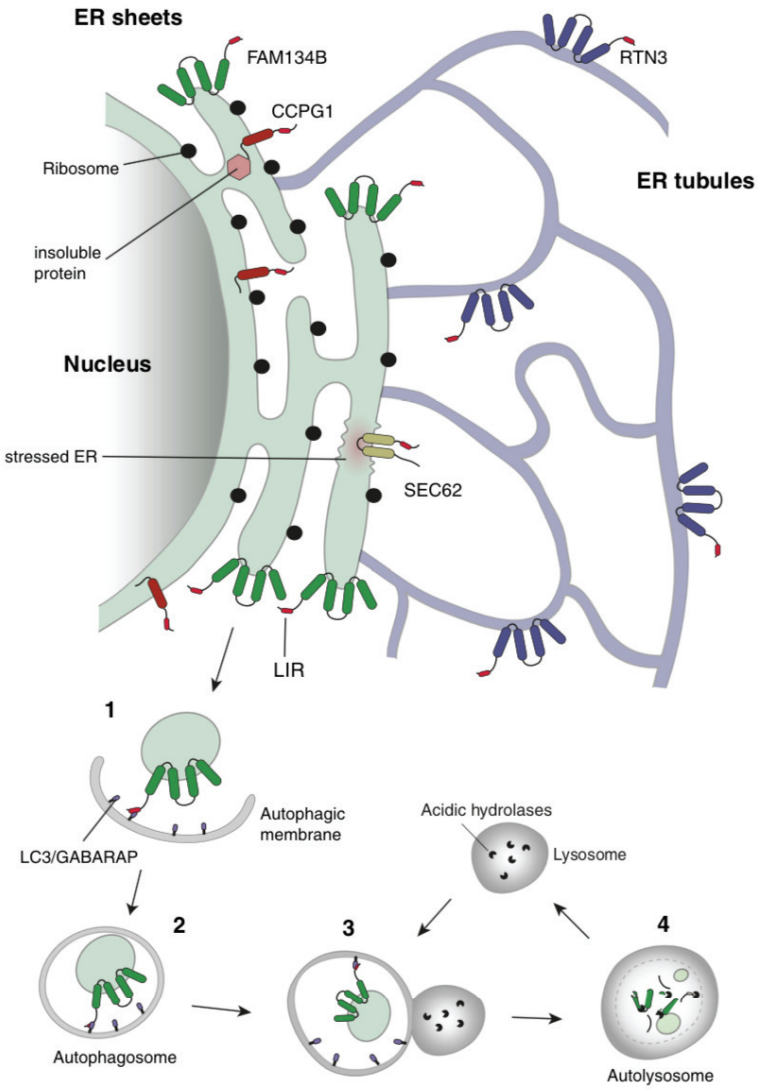

Figure 13- ER-phagy is mediated by ER-phagy receptors localized to distinct subdomains of the ER. FAM134B is restricted to the curved edges of ER sheets. RTN3 is found exclusively on ER tubules. Sec62 is localized to ER sheets following ER-stress. CCPG1 is found in areas of the ER with high content of insoluble proteins. The currently known receptors do not interact or functionally cooperate with each other. All of them contain LIR domains that are able to bind to LC3/GABARAP-decorated autophagic membranes. The process of ER-phagy can be summarized in four steps: 1) cargo sequestration via interaction between LIR and LC3/GABARAP; 2) closure of the autophagic membrane (aka isolation membrane) around the cargo; 3) fusion of the resulting autophagosome with the lysosome; 4) degradation of the enclosed ER fragments by lysosomal hydrolases and acidic pH. Figures and legends extracted from [164]

III-) Herp is a central regulator in the ERQC

Homocysteine-inducible ER stress protein (Herp) is an ER membrane–integrated chaperone-like protein which is a crucial actor of many cellular processes in the ER, very important for ERAD in the retrotranslocation and degradation processes [65]. Due to its

importance for my PhD project, I decided to dedicate one section of this introduction for this protein.

Indeed, Herp (Usa1 in yeast) is demonstrated to be strongly upregulated by ER stress and plays an essential role in ERAD through the interaction with Hrd1, the translocon component Derlin1, the ATPase p97, and the proteasome [165-167]. Herp participates in the retrotranslocation process of ubiquitylated proteins from the ER to proteasomes for degradation thanks to its two important domains: UBA et UBL [165,168,169]. Moreover, highlighting its importance for the cell, Herp depletion accelerates ER stress-induced apoptosis and suppresses ER stress-induced inflammatory reactions [165,170]. Although primarily associated with the ER membrane, Herp can also accumulate in the trans-Golgi network [171].

Even though Herp expression is strongly enhanced by UPR, after ER stress induction, Herp is also rapidly degraded by Ube2g2–gp78-mediated ubiquitylation and proteasomal degradation[165]. At the molecular level, the polyubiquitylation of Herp *in vitro* depends on its physical interaction with the CUE domain of gp78. And the UBL domain of Herp, is essential for Herp degradation *in vivo* during ER stress recovery. Although Herp promotes cell survival under ER stress conditions, sustained high levels of Herp expression can ultimately reduce cell viability under oxidative stress conditions, suggesting that Herp plays a dual role in adaptation to cellular stress [172].

Consequently, a major question that remains unanswered is how Herp expression is regulated according to different levels of ER stress and how Herp switches its pro-survival to pro-death activity. Many studies have investigated the consequences of Herp depletion or overexpression. Knockdown or knockout of Herp were shown to stabilize several ERAD substrates [173,174]. Overexpression of Herp can protect cells from ER stress-induced apoptosis, mainly by interaction with different ERAD components as p97, Derlin1, Os9 and Hrd1 which stimulates degradation of aberrant ER proteins [165,169,175,176]. Gp78 appears to be an Herp regulator because it can ubiquitinate Herp *in vitro* which leads to its degradation in cells [177]. Gp78-mediated Herp turnover represents another way of controlling the Herp protein level in addition to transcriptional upregulation by ER stress inducers [123,165].

At the cellular level, during ER stress, Herp assists Hrd1 in mediating ubiquitination of aberrant ER proteins. After substrates are eliminated, the UBL domain in Herp functions as

a ubiquitin moiety and is recognized by the CUE domain of gp78. As described previously, Gp78 cooperates with Hrd1 in ubiquitin chain assembly. As a result, HERP is ubiquitylated and degraded, thus initiating the ER stress recovery process [178]

Herp was first shown to be highly upregulated by the PERK branch (Ma 2004 Journal of Biological Chemistry) but it now appears that all the UPR pathways directly or indirectly overregulated Herp [13].

Herp is therefore highly unstable and quickly degraded by proteasomes. Any situation that compromises proteasomal activity will increase the levels of Herp and lead to ERAD complex recruitment and compartmentalization. As Herp has the ability to assemble a complex containing the ERAD components Hrd1, Sel1, OS-9, Derlin-1 [169,179], proteasomes and the ubiquitinated substrate [173] it has been proposed that Herp is a master organizer of the ERAD machinery.

IV-) ER stress, UPR and bacterial pathogens

As mentioned before, the UPR is induced in response to a wide variety of cellular perturbations. Microbial infections have long been known to cause stress on the ER and to induce the UPR, especially viral infections probably due to their strict dependency on host protein synthesis. Indeed, several viruses modulate the UPR to ensure viral protein production, replication and cell survival [180]. Furthermore, to gain entrance to the cytosol where they exert their destructive capabilities several viruses were shown to hijack the ER quality control machinery [181]. Not surprisingly, many bacterial pathogens also interfere with UPR and ERQC. Many of these changes are also induced by intracellular bacterial pathogens, which subvert the host immune response and cellular processes to establish a compartment that allows their survival and replication. However, this is still an emerging field with only a few studies available. We will see in the next sessions that according to the pathogens the UPR can be activated or inhibited. This is mainly dependent on the necessity of the bacteria to keep host cell alive or not. Nonetheless, there are still exceptions as we will see with *Brucella* that in specific cells types, induction of ER stress generates inflammation, cell death and dissemination in the environment [138].

1-) Bacteria that induces ER stress

This section does not aim to make an exhaustive list of pathogens that induces UPR. I decided to select 4 pathogens that induces UPR in order to kill cells and 4 others that instead benefit from UPR induction by maintaining cells alive and further controlling the consequences of UPR activation. The specific case of *Brucella* will be discussed in a dedicated **Chapter 3**.

a-) *Mycobacterium tuberculosis*

Mycobacterium tuberculosis is a strict aerobic mycobacterium that is responsible of tuberculosis [182](Fogel 2015 Tuberculosis). It represents a major public health issue nowadays because of the increase of multi-drug resistant strains [183], with 8.7 million of new cases and 1.4 million deaths recently reported [184]. Overall, infection leads to the induction of an apoptotic response. The early secreted mycobacterial antigen ESAT-6 of *Mycobacterium* has been identified as an apoptosis inducer in human macrophages and epithelial cells. In the study of Choi *et al*. [185], they demonstrated that the stimulation of human epithelial A549 cells by ESAT-6 also induces the ER stress response with an increase of intracellular Ca^{2+} concentration. This calcium perturbation results in reactive oxygen species (ROS) accumulation, and therefore induces the molecular hallmarks of ER stress-induced apoptosis [185]. Few years later, another study showed XBP-1 splicing was increased by the same mycobacterial secreted protein ESAT-6. An increase of BiP and CHOP mRNA expressions and protein levels after ESAT-6 treatment in A549 cells was also observed. They also visualized an increase of eIF2α phosphorylation and ATF4 expression which are both associated to the PERK branch of UPR. They also showed that ESAT-6 induced CHOP expression, consistent with pro-apoptotic phenotype during infection, was dependent on the ASK1/JNK signal cascade which is connected to IRE1 pathway. Indeed, ESAT-6 association with IRE1α/ASK-1/JNK causes apoptosis following ER stress induction. More precisely at the molecular level it has been shown that IRE1α binds to TRAF2, and the resultant IRE1α/TRAF2 complex leads to ASK1-JNK activation [112,113]. Once the complex IRE1/ASK-1/JNK is associated, it leads to significant caspase activation which further regulates CHOP expression during the mycobacterial infection of macrophages. This explains why XBP1 splicing is also increased. ESAT-6 acts at two different levels of the UPR, playing an important role in *Mycobacterium* pathogenesis.

These studies on *Mycobacterium* have also shown that the ER stress-mediated apoptosis plays an important role in bacterial pathogenesis [185-187]. Recent evidence suggests that HBHA, another protein secreted from mycobacteria, also induces ER stress responses via intracellular Ca^{2+} release [186], resulting in ER stress-mediated apoptosis in macrophages.

b-) *Listeria monocytogenes*

Listeria monocytogenes is a Gram-positive facultative intracellular bacterium that is mainly transmitted by the ingestion of contaminated food [188]. The bacteria were shown to induce ER expansion as well as UPR prior to entry into host cells. *Listeria* is an inducer of all three ER stress sensors and the main bacterial virulence factor identified is the famous toxin listeriolysin (LLO) because a mutant strain of *Listeria* that does not produce LLO lacked the UPR response. As *Mycobacterium,* sustained *Listeria* infection with host eukaryotic cells resulted in apoptosis. LLO is a "swiss knife" for *Listeria* because it is also involved in membrane permeabilization during infection and can interfere with many cellular processes (eg SUMOylation, Ubiquitination, etc) which gives LLO a very broad spectrum of action but also raises the question of the specificity of its actions. Extracellular delivered LLO induces UPR [189]. Nevertheless, previous studies have revealed that once intracellular, LLO is targeted for host-mediated degradation [190]. LLO is a member of the family of cholesterol-dependent cytolysins (CDCs) known to form large pores in target membranes that leads to the depletion of intracellular Ca^{2+} stores and it is known that rupture in calcium homeostasis provokes ER stress [167]. Splicing of *xbp1* mRNA in effector CD8+ T cells has also recently been demonstrated in mice following infection with *Listeria* and authors suggest that it contributes to the differentiation of effector CD8+ T cells during acute infection [191].

c-) *Helicobacter pylori*

Helicobacter pylori is a Gram-negative bacterium that is naturally present in the stomach of a part of the population. But in case of acute inflammation it can lead to peptitc ulcer disease or the most severe form that is a stomach cancer [192]. In the case of *H. pylori,* it is autophagy that has been shown to be modulated following ER stress induction during infection. The secreted protein HP0175, a peptidyl prolyl cis-trans isomerase of *H. pylori* was identified to promote autophagy in gastric epithelial cells. *H. pylori* was shown to enhance the

expression of PERK and also activate the phosphorylation of PERK in an HP0175-dependent manner [193]. This was also accompanied by phosphorylation of eIF-2α and transcriptional activation of ATF4 and CHOP. Furthermore, silencing of PERK inhibited the conversion of LC3 to LC3II during infection. These findings suggested that the UPR is linked to *H. pylori*-mediated autophagy [194].

Conversely to *Mycobacterium* and *Listeria*, *Helicobacter* invokes UPR that can trigger apoptosis induction but rather for disturbing downstream pathways as autophagy also activated by UPR.

d-) *Orientia tsutsugamushi*

O. tsutsugamushi is an obligate intracellular bacterium that is the etiological agent of nonmalarial febrile illness [195]. This bacterium replicates in the cytosol but the host cellular pathways subverted by this pathogen are poorly defined [196,197]. A recent a study showed that the bacterium induces UPR in the first 48 h of infection *in vitro* and benefits from ER stress. Indeed, in the same period to profit of amino acid nutrients, *O. tsutsugamushi* also impedes ERAD to accumulate misfolded proteins. Interestingly after 72h pi, *Orientia* reverses this process because ER stress is then attenuated and ERAD proceeds unhindered. These data are very interesting because they highlight the adaptation of the bacterial strategy according to the infection kinetics which is not the same at the early and late stages of infection. The authors demonstrated that a prolonged inhibition of ERAD using RNA interference results in an *O. tsutsugamushi* growth defect at 72 h. Thus, *O. tsutsugamushi* temporally blocks ERAD while ERAD-derived amino acids are needed to support its growth but afterwards it can switch mechanisms by controlling both UPR and ERAD. Moreover, they identified the effector Ank4 linked to this phenomenon. Indeed, they show that ectopic expression of Ank4 blocks ERAD, a phenotype that was confirmed during *O. tsutsugamushi* infection. Besides they demonstrated Ank4 interacts with Bat3, a eukaryotic chaperone that is essential for ERAD and especially in retrotranslocation and degradation processes. This is the first study which presents how a bacterial pathogen interferes with ERQC processes and ERAD to satisfy its nutritional virulence requirements [197].

At molecular level they have shown that Bat3 knockdown did not abolish *O. tsutsugamushi* growth what is not surprising given the redundancy of eukaryotic actors in ERAD process. Moreover, *O. tsutsugamushi* as *Helicobacter* can also induce autophagy

without being cleared [193,198]. It is reasonable to think that autophagy may help ERAD to degrade proteins that are accumulated during infection. Amino acids resulting from autophagy have been shown to be beneficial for intracellular growth of *Anaplasma phagocytophilum, Helicobacter pylori* and *Ehrlichia chaffeensis* [199,200], which are also obligate intracellular bacteria that belong of the order *Rickettsiales* with *O. tsutsugamushi*. As a final hypothesis authors suggest *Orientia* alternates autophagy and ERAD to always have nutrients at different steps of infection.

This elegant study highlighted a novel strategy used by an obligate intracellular bacterium to finely modulate cellular ERQC processes to facilitate its replication. This may be a common strategy employed by diverse intracellular pathogens. Finally, this type of study identified the UPR and ERAD pathways that bacterial pathogens modulate as possible pharmacologic targets for treating infectious diseases.

2-) Bacteria that inhibit ER stress

Because UPR is connected to apoptosis and immunity processes, several pathogens subvert the UPR to ensure their survival inside their hosts and to avoid activation of immune mechanisms of the host. Moreover, because some intracellular bacteria need to establish a safe niche, often in very close association with the ER, they use an arsenal of weapons to interfere at different levels of UPR.

a-) *Chlamydia order*

α-) *Simkania negevensis*

Simkania negevensis is a Gram-negative, obligate intracellular bacterium that belongs to the order of *Chlamydiales*. *Simkania*-containing vacuoles in infected eukaryotic cells were shown to be associated with the ER and close to mitochondria [201]. *Simkania* can be maintained in eukaryotic cells for more than 10 days as it strongly inhibits host apoptosis. *Simkania negevensis* was also shown to interfere with UPR by blocking translocation of the transcription factor CHOP into the nucleus. Therefore, authors speculated that *S. negevensis* knockdown of CHOP inhibits ER-stress induced apoptosis [201]. However, the infection cycle is more complex as at early stages of the infection *Simkania* induces an ER-stress response, which is later downregulated. Indeed, authors showed that induction of ER-stress with chemical drugs as thapsigargin or tunicamycin was strongly inhibited in cells infected

with *Simkania*. Similarly, *Simkania* interfered with chemically induced ER-stress cycloheximide (that indirectly induces ER stress by inhibiting host protein synthesis) in infected cells indicating that the pathogen actively inhibits the cellular ER-stress machinery. *Simkania* blocked BiP upregulation at the protein level which is a rather late event in ER stress. In contrast, translocation of transcription factor CHOP is blocked at early time points and CHOP appears to be retained within the *Simkania*-containing vacuoles. The association between bacteria, mitochondria and ER also places Simkania in a perfect position to establish an anti-apoptotic response based on ER-stress inhibition mechanisms.

β-) *Chlamydia pneumoniae*

Chlamydia pneumoniae causes acute infections of the upper and lower respiratory tracts. Species of the genus share a unique biphasic developmental cycle [202] with a persistent latent form and a more infectious productive phase. These 2 states are very important and have distinct impacts on UPR processes. Furthermore, persistent *Chlamydia* infection was associated with the pathogenesis of chronic lung diseases such as chronic obstructive pulmonary disease and asthma [203]. In productive infection, *Chlamydia trachomatis* inclusions directly interact with the ER and the Golgi apparatus to acquire nutrients from host cells [204]. Direct interactions of *Chlamydia pneumoniae* with the ER are essential for intracellular productive infection. Besides, the ER resident chaperone BiP was also identified as an important player *Chlamydia pneumoniae* infections [205]. In this study, authors observed BiP induction at the very early stage of infection and during the persistent phase along with reduced phosphorylation of eIF2α. However, in the late phase of IFN-γ-induced productive infection BiP expression is downregulated accompanied by phosphorylation of eIF2. This is consistent with an active on/off control of BiP expression to ensure that at the end of infection cycle loss of BiP function results in host cell apoptosis important for *Chlamydia* dissemination [206,207].

To conclude BiP plays a key role to restore cells from stress conditions at the early stage of infection in order to establish a persistent form of the bacteria. But it can also be downregulated further to allow bacteria to finish its infection.

b-) *Legionella pneumophila*

Legionella pneumophila is a Gram-negative facultative intracellular bacterium responsible for a pneumonia also-called Legionnaire's disease [208]. It has been shown in several studies that this pathogen also interferes with UPR [209-212]. The used mechanisms of this pathogen provide a good example of how sophisticated can be the bacterial strategy to interfere with UPR. Furthermore, it also illustrates that scientific community has to be very careful on the interpretation of some results when studying UPR modulation by pathogenic bacteria.

Indeed, *L. pneumophila* was demonstrated to induce a global repression of protein translation in the infected host [210,212]. Furthermore, it was also shown that *Legionella* infection impacts mTOR activity which is associated to translational process and confirms this first set of data. Afterwards, it was shown that this inhibition relies of five T4SS *L. pneumophila* effectors *Legionella* glucosyl transferases1,2 and 3 (Lgt1, Lgt2, Lgt3, SidI and SidL). Indeed, These effectors modified a serine residue in eIF2α translation factor which was also shown to result in an inhibition of protein synthesis during *L.pneumophila* infection because the deletion of all these effectors in a mutant strain results in a defect in blocking translation without affecting the growth of the bacteria in both amoeba or human macrophages [213]. The connection between *Legionella* infection and hijacking of UPR process is correlated with 2 other studies where it has been shown that CHOP, XBP1s and BiP are repressed at protein levels even after use of the chemical stress inducer thapsigargin[209,211]. Treacy *et al*. [209] first demonstrated the involvement of the T4SS effectors as mutant strain for the secretion system does not impair host translation. Hempstead *et al*. [211] then later identified the effectors Lgt1 and Lgt2 implicated in the repression of XBP1s at translational level. Nevertheless, the effectors involved in CHOP and BiP repression remained to be found. This study of *Legionella* was also important as it highlights the precautions that we have to take in studying UPR. Indeed, for XBP1s, it was shown in the first time an increase of the mRNA spliced form of XBP1 but not at protein level which *in fine* indicates an UPR inhibition.

In parallel it has been shown that PERK pathway is largely unaffected contrary to IRE1 and ATF6 pathways. It might be to avoid a derived ER-stress induced apoptosis. regarding the 2 other pathways, even if the effectors that may repress these pathways have not yet been found, *Legionella* recruits BiP on its vacuole probably after its dissociation from the sensors to inhibit its function. Thus, Hempstead *et al*. [211] suggest this translational

inhibition may be a common strategy used by pathogens to limit the innate immune response associated with UPR by preventing enhanced proinflammatory response [211].

c-) *Francisella tularensis*

F. tularensis inhibits ER stress by controlling BiP expression and glycosylation by modulating expression of numerous glycosidase and glycosyltransferase genes. As it was previously described, glycosylation is a very important process in protein maturation for the secretory pathway. This is why a subversion of this process can lead to ER disorders and extensive ER stress. *Francisella* especially affects N- and O-glycosylation in infected macrophages. More precisely, *Francisella* was shown to trigger an increased expression and glycosylation of BiP [214]. Indeed, authors have visualized a reduced activation of PERK by decreased phosphorylation following by a decreased expression of CHOP. Although they found a weak activation of ATF6, increased phosphorylation of IRE1 was observed that resulted in a higher activation of IRE1 [214]. As *Francisella* needs to replicate inside infected cells, it is its interest to protect cell from death, probably explaining the differential activation of PERK and ATF6 in contrast to IRE1. In fact, the IRE1 pathway was shown to be important for *Francisella* replication [215]. To my knowledge, this is the only study presenting an example of subversion of the host glycosylation process by a bacterial pathogen, a topic that merits further investigation. Glycosylation is also an important process in the control of ERAD and the folding process. It would be interesting to know how differential glycosylation affects BiP and the consequences on the protein maturation process.

V-) General conclusions

To conclude on this section only few studies are currently published on the subversion of UPR by bacterial pathogens. Moreover, they all focused on the activation or inactivation of the main sensors of UPR pathway, but it is likely that many other molecular actors remain to be found. Consequently, further and deeper studies are required to have a better understanding of how bacteria pathogens inhibit ER stress at the molecular level. Nevertheless, a common strategy emerges for all of the described pathogens to modulate BiP functions because of its association to the three UPR sensors. In addition, PERK and ATF6 are often down-regulated because of its close connection to apoptosis.

Interestingly, invasion alone is sufficient to induce UPR, but bacteria can rapidly regulate different pathways to counteract this activation. Bacteria clearly have many strategies and tools (as secreted effectors) to finely regulate or manipulate UPR as we can see with *Legionella*, which is able to repress XBP1s at translational level using 5 different effectors.

In this chapter I tried to provide a global overview of the importance of the ER for the eukaryotic cell. I mainly focused on protein-associated ER processes because this a subject that is the most documented in the literature and because it is for me a very fascinating topic. It is important to keep in mind that the ER is also associated with many other processes related to other biomolecules or metabolites with a crucial involvement in lipid synthesis and calcium regulation for example. The ERQC is fundamental for maintaining a healthy cellular lifestyle and to avoid its self-destruction. It is also crucial for some innate immune processes.
The 4 processes described in this chapter, folding, ERAD, UPR and ER-phagy are intimately connected and also take part in many cellular processes. Although the UPR is now well described, research must be continued for ERAD and ER-phagy where the molecular mechanisms remain to be found. UPR, ERAD and autophagy processes were historically studied in yeast. These first studies provided strong and solid pedestal of knowledge. Nevertheless, the complexity of these processes in the human system is much higher and requires further development of additional models and techniques to study these pathways in mammals. In addition, the intermingling between ERQC processes significantly complexifies the studies, making it very hard to dissect individual pathways. The study of host-pathogen interactions may provide a wonderful cell biology tool to investigate deeper ER processes. Indeed, the action of effectors that can be directed against one pathway without affecting other pathways may provide a powerful tool.
The study of how bacteria interfere with ERQC is in its early days; overall the molecular mechanisms remain to be determined that will help dissect the consequences for the host and also the benefit for the pathogens, perhaps providing novel therapeutic approaches.

Chapter 2 Mitochondria

I-) Global overview of mitochondria

Mitochondria were for a long time considered simply as the energy central of the cell and their sole purpose was to provide energy by oxidative phosphorylation (after the Krebs cycle). But today mitochondria are known to be associated to a huge variety of processes as apoptosis, innate immunity, autophagy (called mitophagy), redox signaling and calcium metabolism (**Figure 14-**. Moreover, it is well established they communicate with other organelles, although these interactions are still poorly characterized at the molecular level [216].

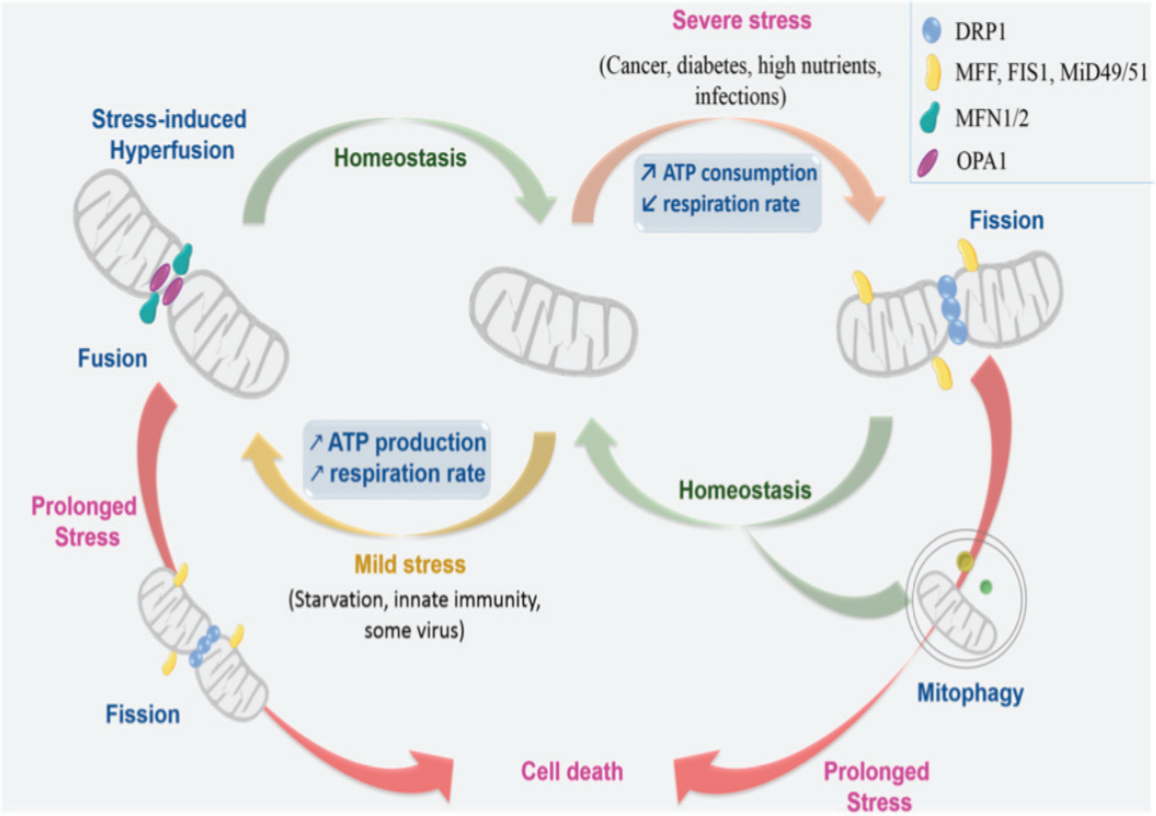

Figure 14- Overview of mitochondrial functions. Figures extracted from [217]

1-) Structure and energy production

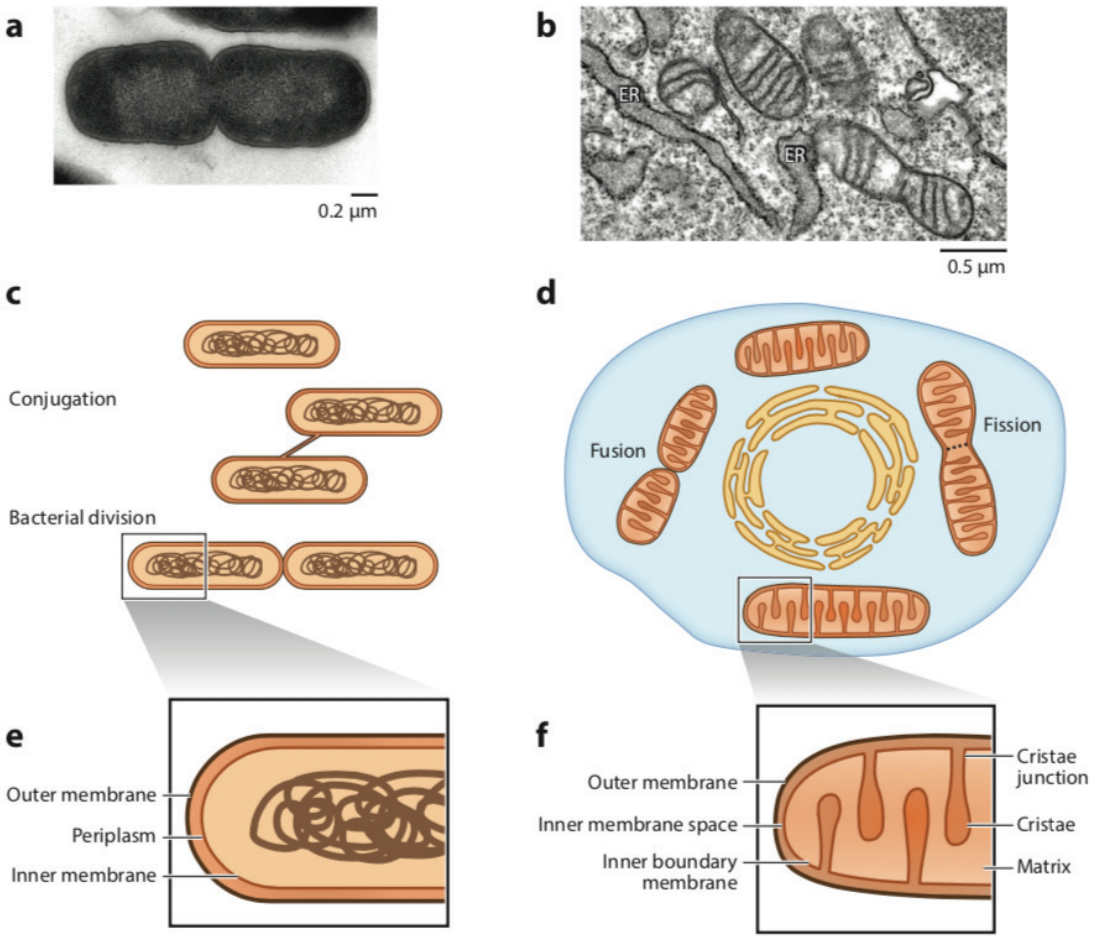

Figure 15- Mitochondria and bacteria are both adapted for intracellular life. (a,b) Transmission electron microscopy (TEM) images depict (a) a dividing bacterial cell and (b) a heterogeneous mitochondrial population, also schematized in panels c and d. (c) Bacterial division and conjugation (transfer of plasmids between bacterial cells) are juxtaposed with (d) mitochondrial fusion and fission processes. (e,f) The architecture of (e) a bacterial cell and (f) a mitochondrion.. Figures and legends extracted from [218].

The mitochondrion is a membraned organelle that originated from the clade α-proteobacteria, considered as a bacteria-like entity that succeeded to establish a symbiotic relationship with the eukaryotic cell (**Figure 15-a-b**) [219]. Thus, not surprising, it has an outer and an inner mitochondrial membrane (OMM and IMM, respectively) separated by a periplasm just as bacteria (Figure 14-d). Mitochondria have their own DNA called mitochondrial DNA (mtDNA) and specific mitochondrial proteins. The OMM is involved in metabolic processes between IMM and the cytosol of the cell and the release of ROS and mtDNA. For the IMM it is composed of 3 distinct regions: the membrane boundary, the cristae junctions, and the cristae [220] (**Figure 15-f**). The cristae are the invaginations of the inner membrane that allows a significant increase of the surface area. This is also the

localization of the different protein complexes that compose the respiratory chain which allow the electron transport chain to provide energy for the cell in a process called oxidative phosphorylation (OXPHOS); explaining why it is important that cristae to occupy the highest surface area as possible [221]. Before the OXPHOS there is the Krebs cycle that takes place in the mitochondria (see **Figure 16-**). OXPHOS will use NADH and FAD into the respiratory complex I and II, respectively to produce electrons. These electrons will move along the respiratory complexes of the mitochondrial respiratory chain while protons are transported from the matrix into the intermembrane space, it will create a proton gradient across the inner membrane, called the electromotive force, very much like a battery that stores energy. This energy will be used by the final complex of the respiratory chain the ATP synthase (also called complex V) which will convert ADP to ATP by adding a phosphate. A small part of the produced ATP is s utilized by mitochondria for its own functions and the rest is released into the cytoplasm as a form of chemical energy that will be used for several cellular processes [216].

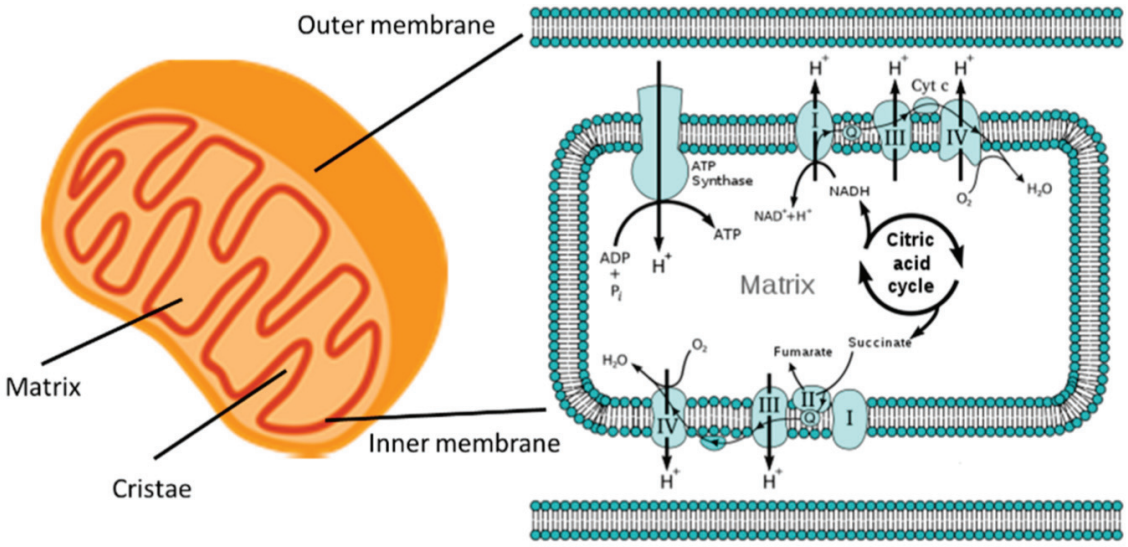

Figure 16- The mitochondria are the powerhouses of the cell. Left: A cartoon of a mitochondrion showing its outer and inner membranes, the cristae, and the matrix. Fat and sugar enter the mitochondria through channels of the outer membrane. Right: The Krebs, or citric acid, cycle feeds the chain of respiratory complexes I through IV which create an electrical and proton (H+) gradient, the electromotive force across the inner membrane. ATP synthase utilizes the electromotive force to generate ATP from ADP and inorganic phosphate (Pi). Figures and legends extracted from [222]

2-) Mitochondrial dynamics

Mitochondria can modulate their structure to create a tubular network coordinated by fission and fusion processes [218] making them a highly dynamic interacting organelles. The regulation between fusion and fission events impacts mitochondrial number size, shape and positioning. Fission is the division of 1 mitochondrion into 2 daughter mitochondria whereas fusion is the association of 2 mitochondria in 1 mitochondrion. A deregulation of these 2 mitochondrial processes severely impacts the mitochondrial network. At the mitochondrial level, an excess of fission results in fragmentation of the mitochondrial network giving rise to round-shape mitochondria; in contrast, an excess of fusion processes results in a hyperfused network with elongated and highly connected mitochondria [223]. Cycles of fusion and fission are required to ensure mitochondrial function but also to adapt to cellular needs for example to respond to nutrient availability and to the metabolic state of the cell [216,224]. Moreover, different morphological states are associated with multiple physiological and pathophysiological conditions [225]. For example, it has been found that some mutations in fusion and fission proteins are linked to Charcot-Maire-Tooth neurodegenerative disease [226,227].

a-) Fusion and fission

As mentioned above, mitochondrial clusters are capable of fusion which will lead to the formation of an interconnected tubular network which can occupy the totality of the volume of the cell. At cellular level this process involves the fusion of both OMM and IMM of 2 separate mitochondria. Interestingly, the mtDNA of each mitochondrion becomes completely mixed upon fusion [228]. At the molecular level, the fusion process involves 3 GTPases: Mitofusin 1 and 2 for OMM fusion (Mfn1 and Mfn2 respectively) and optic atrophy 1 (OPA1) for IMM [218,229]. Astonishingly, it is the OPA1 fusion process that was shown to be dependent of OXPHOS while this not the case for mitofusin mediated fusion [230]. Fusion processes are important for maintaining mitochondrial homeostasis in case of cellular stress [231]. At cellular level Friedman *et al*. [232] demonstrated that mitochondrial fission occurs at positions where ER tubules contact and constrict mitochondria. These constrictions would facilitate the recruitment of Dynamin-related/-like protein 1 (DRP1). Mitochondrial fission also requires the protein Dynamin2 (Dnm2) and is carried out in collaboration with elements of the actin cytoskeleton [218,233,234]. The importance of the cytoskeleton is highlighted by the fact that Drp1 is recruited by microtubules but requires actin microfilaments for targeting of mitochondrial constriction sites. Interestingly, different receptors for Drp1 have been

identified in OMMs. Recently, syntaxin 17 has been found to be involved in mitochondria fission. This protein is found at the ER-mitochondria contact sites where it interacts with Drp1 and modulates the mitochondria fission by regulating Drp1 activity and localization [235]. Fission is necessary for the distribution of mitochondria during cell division and embryonic growth [236]. However, if fission is not controlled and balanced by fusion, the network becomes too fragmented which leads to metabolic and mitochondrial disorders, inducing mitochondrial inner membrane potential decline or the downregulation of ATP production [237].

If mitochondria fusion is reduced or impaired it will lead to mitochondrial fragmentation. Conversely, if this is the fission process that is targeted mitochondrial network become more elongated and excessively interconnected which often over-activates mitochondrial processes [222]. Therefore, tight regulation of these processes needs to be ensured to guarantee cellular homeostasis. Not surprisingly, fusion and fission processes are cross-regulated by sharing several molecular actors and regulators. Indeed, the interaction of 2 heptad-repeat motifs of Mfn2 blocks fusion while their association to Drp1 enhances the fusion process [238]. Another example is the size if OPA1, where the full-length protein mediates fusion contrary to its enzymatic truncated form that promotes mitochondria fission [239]. Moreover, another study reported that the 2 processes may form a continuous fusion/fission cycle to enable mitochondrial renewal and dynamics.

b-) Fragmentation and Hyperfusion

As described above, fragmentation can occur when there is a too much fission or following induction by intrinsic or extrinsic stress, as for example due to an increase of calcium concentration. Very often, mitochondrial fragmentation is linked to mitochondrial dysfunction due to a defect in fusion process or an overregulation of fission process, as this morphological state predominates during elevated stress levels or cell death [217]. Furthermore, a fragmented network is also more sensitive to an induced apoptosis [240]. However, fragmentation is not necessarily connected to induction of cell death; for example, it still occurs under the influence of drug as carbonyl cyanide m-chlorophenyl hydrazone (CCCP) that does not induce apoptosis [241]. Nonetheless, a fragmented network is often associated to metabolism disorders [242].

Mitochondrial fragmentation is also observed in “positive” contexts, for example

during the G2/M phase of the cell cycle where there is a need for enhanced mitochondrial motility, quality control and mtDNA inheritance [241,243]. A second example of "positively" induced fragmentation can be found following accumulation of truncated forms of Opa1, indicative of a role for short Opa1 in cell division. Thus, it is important to keep in mind the notion that a fragmented mitochondrial network is not always associated with increased apoptosis but on the contrary can also protect cells from apoptotic death [223]. Mitochondrial fragmentation also has an important impact on metabolic processes at is was shown that it can enhance glycolysis [244].

The mitochondrial network can also become hyperfused to counteract stress disorders. Indeed, when the mitochondrial network is hyperfused, an improved matrix component distribution is achieved, and it also modifies metabolic processes by stimulating OXPHOS activity [245]. Interestingly Dynamin2-depleted cells or Drp-1depleted cells both were shown to present a hyperfused mitochondrial network, despite the different nature of the depletion. Interestingly, mitochondria hyperfusion was observed during macroautophagy induction by different stress conditions. Mitochondria hyperfuse to escape autophagosome engulfment in order to avoid their degradation and instead to induce cell survival mechanisms [246]. In addition, mitochondria present a hyperfused network during the G1/S transition of the cell cycle [247]. Even if hyperfusion is mainly seen as an adaptive mechanism to counteract some intrinsic and extrinsic disorders, a very recent report showed how this mitochondrial process leads to a neuropathy in *Drosophila* [248]. This discovery opens new ways of research to better understand neuropathologic diseases. To conclude with this first part, depending on the stress type and severity, mitochondria can adapt their form, either by inducing a fragmented or a fused network which can have important functional consequences.

II-) Mitochondrial-Associated Membranes: at the ER mitochondria interface

Mitochondria-associated membranes were the first described inter-organelle contact sites [249], referring to the association between ER and mitochondria. These sites act as hubs that take part in several processes as lipid and calcium metabolism [250,251]. Moreover, as ER was shown to take part in mitochondrial fission it is not surprising to discover that MAMs are also crucial for regulation mitochondrial morphology [232]. Furthermore, MAMs were also shown to be involved in reactive oxygen species (ROS)-induced cell stress (mtROS) [250], autophagy [251] and apoptosis. The study of the function of MAMS is a very exciting

field that is in expansion with the recent characterization of specific markers necessary to better study these structures. To date, the enzyme fatty acid CoA ligase 4 (FACL4), which is involved in triacylglycerol synthesis, is currently considered one of the most reliable MAM marker proteins [252]. To conclude, many studies have focused on the identification of specific proteins and their characterization in relation to mitochondrial and ER related processes. There is indeed a growing list of MAM markers however, the global comprehension of all the coordinated processes dependent on MAMs is still at the very early stages and will require many more years to identify all the molecular actors and to fully understand how they are regulated and inter-connected.

A few of the key functions assigned to MAMs are described in more detailed below.

1-) Calcium metabolism

Calcium is a metabolite that strongly binds ER and mitochondria, with continuous exchanges taking place. MAMs act as the hub that regulates Ca^{2+} transfer from the ER to mitochondria in order to sustain cellular bioenergetic metabolic processes of mitochondria, mitochondrial dynamics but also the induction of cellular processes as apoptosis [253,254]. Ca^{2+} is involved in mitochondria metabolism because ATP production is regulated by Ca^{2+} transfer from the ER to mitochondria and several mitochondrial dehydrogenases of the Krebs cycle require calcium as cofactor during NADH production [255,256]. In the case of Ca^{2+} transfer, it is the inositol-1,4,5-trisphosphate (InsP3) receptor (InsP3R see **Figure 17-**) that interacts with the OMM protein voltage-dependent anion channel isoform 1 (VDAC1) through the molecular chaperone GRP75. MAMs generate microdomains of localized calcium spikes released from the ER through InsP3Rs, thus stimulating calcium uptake by mitochondria [256,257]. Therefore, it has been proposed that GRP75 acts as a bridge between the 2 organelles and indeed, downregulation of GRP75 abrogates the functional interaction between IP3R and the mitochondria. This alteration impairs the normal transfer of Ca^{2+} to the mitochondria while overexpression of VDAC1 has been shown to promote Ca^{2+} uptake into mitochondria [258]. Furthermore, some MAM proteins, such as Mitofusin2 and phosphofurin acidic cluster sorting protein-2 (PACS-2) have been implicated in calcium dependent processes [259-261]. The control of Ca^{2+} exchange between ER and mitochondria is essential also for ER functions. Indeed, Ca^{2+} enables the correct activity of several ER enzymes and chaperones shown previously to be crucial for ERQC like calnexin and calreticulin [262]. This is also the case of another specific MAM marker, the ER protein sigma-1 receptor (Sig-

1R) [263]. Sig-1R is a Ca^{2+} sensitive chaperone complex that binds BiP and prolongs Ca^{2+} signaling from the ER to the mitochondria by stabilizing IP3R subunit 3 at MAMs [263].

In addition to the InsP3R- GRP75-VDAC1 complex, other MAM proteins were proposed to physically connect the ER to the mitochondria at supramolecular level. Indeed, a new kind of structure was found in yeast, called ER-mitochondria encounter structure (ERMES) complex. This complex is composed of ER and mitochondrial proteins, such as the ER protein mitochondrial morphology protein 1 (Mmm1), the mitochondrial distribution and morphology protein 10 (Mdm10) and GTPase EF-hand protein of mitochondria 1 (Gem1) [264]. This complex is also involved in lipid transfer and mitochondrial fission [265]. However, ERMES machinery has not been identified in mammalian cells yet.

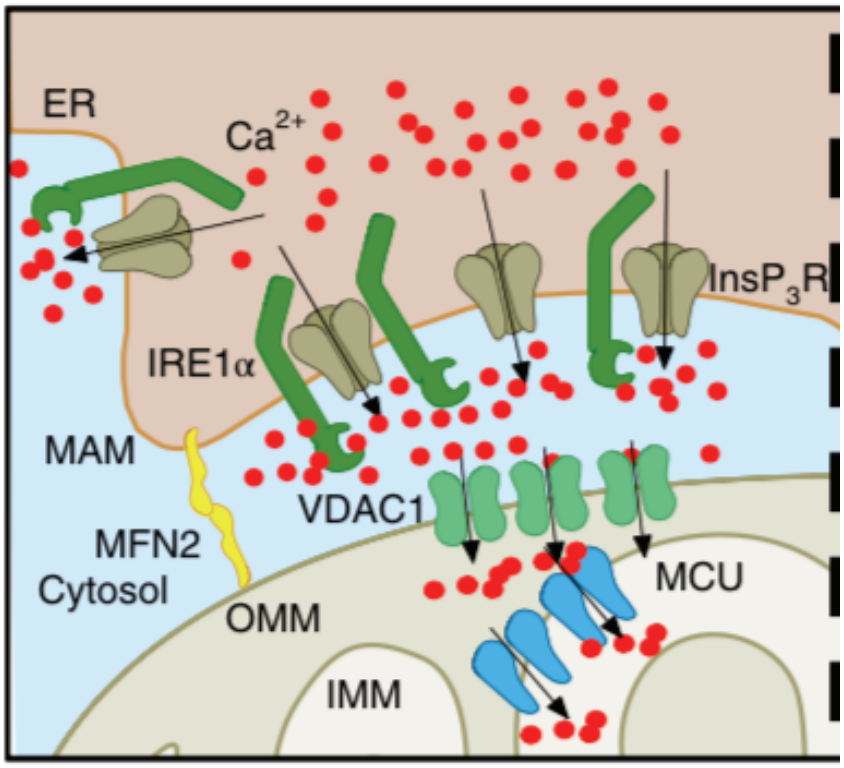

Figure 17- IRE1α expressed at MAMs docks the InsP3Rs at the mitochondrial–ER contact sites possibly through a physical interaction,which may enhance InsP3R channel activity. The presence of IRE1α at MAMs favours calcium transfer into the mitochondria and bursts in ATP production. Figures and legends extracted from [266].

2-) Autophagy

MAMs were also demonstrated to be central for the biogenesis of autophagosomes, as they determine the position of mitochondrial fission and impact the dynamic and the number or mitochondria. Indeed, with fission process it will provide resting membranes for phagophore formation. Given the link of ER and autophagy as described in **Chapter 1 section II-4-b-)**, as well as between mitochondria and autophagy it is not surprising that MAMs are at the center of this process. For mitochondria associated autophagy (considered as a form of macroautophagy) we actually found the term of mitophagy shown to be a recycling process that can occur after recognition of mitochondria damages [267]. Briefly at molecular level, there is still the formation of a phagophore that will enclose mitochondria to be deliver to lysosomes. A study led by the group of Ohsumi [268] reported that MAMs are involved in phagophore assembly. Indeed, upon autophagy induction, ATG14L involved in initiation autophagy complex with LC3 and double FYVE domain-containing protein 1 (DFCP1), known to migrate to omegasomes (Insp3 enriched ER subdomains) during autophagy relocalize to the MAMs to initiate autophagosome formation. Moreover, autophagosome formation marker autophagy-related 5 (ATG5), also shifts to the MAMs after starvation [251](Hamasaki 2013 Nature). Interestingly, syntaxin 17 that participates in mitochondrial fission is also implicated in the autophagosome formation through its interaction with ATG14L promoting the recruitment of phosphatidylinositol 3-phosphate (PI3P) complex [235]. In contrast, the disruption of ER-mitochondria contacts sites reduced the number of autophagosomes. Taken together, all these studies highlight the importance of MAMs in the biogenesis of autophagosome through the recruitment of ATG proteins to the ER-mitochondria contact sites. Further studies are required to better understand the role of molecular components of mitophagy, as it starts to be done for ER-phagy process.

3-) UPR

During early phases of ER stress, in the perinuclear region an enrichment of MAMs was observed. In this cellular context, it highly suggests that connections between ER and mitochondria participate in the regulation of ER stress [269,270]. Indeed, it has been shown that the UPR sensor PERK is enriched at the MAMs, and furthermore, it was demonstrated that PERK is crucial to regulate ROS-induced cell death induced by UPR [250,269]. Moreover, PERK deficiency was associated with a decrease of mitochondrial Ca^{2+} uptake, which results in an ER stress-mediated apoptosis inhibition by the reduction of the release of downstream apoptosis actors as caspases or cytochrome c [250]. A recent study by the group of Zorzano[271] reported that the mitochondrial protein MFN2 physically interacts with

PERK at MAM sites and this binding is required for the regulation of cellular homeostasis upon ER stress. Thus, perturbations of ER-mitochondria contact sites induce ER stress [271].

Indeed, very interesting studies also highlighted the involvement of another major UPR sensor IRE1 in MAM-related functions. The authors demonstrated that IRE1α expression was required to increase metabolism in response to ER stress with the induction of a transient burst in ATP production during the early response to ER stress [270]. Added to that it was visualized that a fraction of IRE1α was also found to be located at MAMs. A separate study showed stabilization of IRE1α by Sig-1R that may enhance its signaling [263,272]. An additional very elegant study deeply associates IRE1α to MAMs integrity and functions. They have established that IRE1α is important for MAMs by regulating mitochondrial calcium uptake [266]. In addition, IRE1α deficiency resulted in marked alterations in mitochondrial physiology and energy metabolism under basal conditions without ER stress. At the molecular level, IRE1α determined the distribution and availability of InsP3Rs at MAMs by operating as a calcium scaffold to modulate OXPHOS and, consequently, ATP production (see **Figure 17-)** [266]. But it is important to note that this IRE 1 activity is independent from its enzymatic domain. Furthermore, it is clear that IRE1α regulates mitochondrial activities because there is an important decrease in ATP in IRE1α-deficient cells and the absence of this sensor induces fragmentation of the mitochondrial network[266].

Interestingly Carreras-Sureda *et* al. observed in a second time an increase of AMP-activated protein kinase (AMPK) phosphorylation IRE1α-deficient cells without any ER stress [266]. However, AMPK is a sensor that detects a decrease of ATP availability. To fulfill this energetic decrease it phosphorylates several targets, in order to increase in ATP generation and/or a reduction in ATP consumption [273]. Moreover, AMPK level is reversely correlated to calcium level. Indeed, it is proven that reduced calcium uptake into mitochondria is also associated with AMPK activation [254], connecting this sensor to IRE1 and supporting the importance of IRE1 on Ca^{2+} regulation.

III-) Mitochondria, MAMs and apoptosis

Apoptosis is a programmed death that is orchestrated by the cell [274](Biala 2014 Trends in cardiovascular medicine). Apoptosis is composed of 2 different pathways: the

extrinsic pathway and the intrinsic pathway (**Figure 18-**) that can be induced by the first one. However, depending on the nature of the stimuli apoptosis can also start directly with the intrinsic pathway as it is shown in the case of terminal UPR. As a reminder many of the pro-death signals from the UPR sensors ultimately converge on the intrinsic mitochondria apoptotic pathway to finally lead to activation of terminal apoptosis actors: the caspases (e.g., caspase-3) [13].

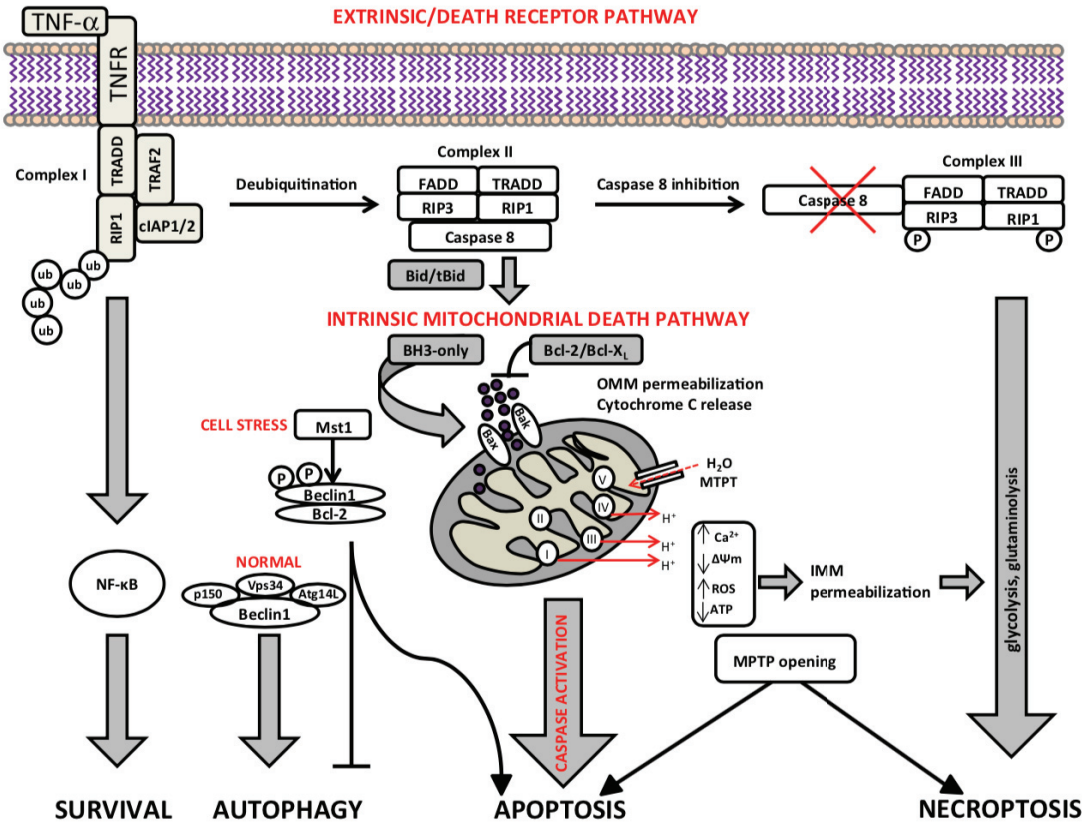

Figure 18- Interplay of cell death signaling pathways. Apoptosis and necrosis are mediated by the death receptor (extrinsic) and mitochondria (intrinsic). In death receptor pathway, TNF-α stimulates formation of complex I comprising TRADD, TRAF2, TRAF5, RIP1, and cIAPs. Complex I activates NF-ϰB signaling and promotes cell survival. Dissociation of complex I from TNF-α receptor, results in the deubiquitination of RIP1, which together with FADD-RIP3 forms complex II. Active caspase-8 can either trigger downstream death effector caspases-3,-6 and -7 or inactivate RIP1/RIP3 complex through RIP1 cleavage. This releases caspase-8 from complex II triggering activation of the intrinsic mitochondrial apoptosis pathway. Apoptotic signaling in response to caspase-8 activation promotes proteolytic cleavage of Bid to t-Bid and recruitment of Bax/Bak proteins to mitochondrial outer membrane (OMM). Oligomerization of Bax/Bak provokes OMM permeabilization, resulting in the release of cytochrome c and other apoptotic proteins from mitochondria, resulting in further caspase activation and apoptosis. Inhibition of caspase-8 results in the formation of complex III, which contains phosphorylated RIP1 and RIP3 and adapter proteins for programmed necrosis. Mitochondrial-associated RIP1/RIP3 promotes glycolysis and glutaminolysis, ROS production, mitochondrial

Ca2+ overload, loss of the inner mitochondrial membrane (IMM) integrity, permeability transition pore opening (mPTP), and necrosis. Mst-1 provides a molecular switch for apoptosis or autophagy through phosphorylation of Beclin-1. During cellular stress, phosphorylation of Beclin-1 by Mst-1 increases Beclin-1-Bcl-2 complexes displacing Bax from Bcl-2 resulting in apoptosis; alternatively, phosphorylation of Beclin-1 diminishes Beclin-1-Vps34-Atg14L complexes and inhibits autophagy. Figures and legends extracted from [274].

Briefly the extrinsic pathway is initiated in response to stimulation of death receptor proteins at the cell surface by the binding of death factors such as Fas ligand (FasL or CD95L) or more generally Tumor Necrosis Factors (=TNF) which induce the formation of the Death-Inducing Signaling Complex (=DISC). This DISC complex (also called complex 1 in the **Figure 18-**) contains the initiator pro-caspase-8, Fas-Associated Death Domain (FADD) and TNF1R-Associated Death Domain (TRADD) [275,276]. Then the caspase 8 is activated by an auto-catalytic process and will proteolytically activate other downstream effector caspases such as caspases-3, -6 and -7. The proteolysis of the BH3-only (BCL2 homology 3) protein BH3 interacting death domain agonist (BID) can also occur at the same time. Its truncated form t-BID is translocated to the mitochondria and activates the intrinsic pathway of apoptosis [276]. Stress stimuli independent of the extrinsic pathway such as cytokine deprivation or DNA damage can also result in cleavage of BID or other BH3-only proteins (BAD, BIK, HRK, BIM, NOXA and PUMA) and directly activate the intrinsic pathway.

Mitochondria are the major players of this arm of apoptosis which is characterized by one key event: mitochondrial outer membrane permeabilization. This is mediated by two proteins of Bcl-2 family BAX and BAK that oligomerize to form the pores in the OMM. After this process cytochrome c and other factors are released in the cell cytosol, such as second mitochondria-derived activators of caspases (SMAC and DIABLO). This process is followed by the recruitment of caspase-9 and apoptotic protease-activating factor 1 (APAF1), resulting in formation of a supramolecular complex known as apoptosome [274-276]. This complex activates caspase-9 which will in turn activate effector caspases and lead to apoptosis. The intrinsic pathway can also lead to caspase-independent cell-death demonstrating the complexity of these signaling cascades. Caspase-2 has also been shown to directly induce mitochondrial outer membrane permeabilization and intrinsic apoptosis but its mechanism remains poorly characterized [274,275].

At molecular level, it is a well-known fact that MAMs are the carrefour in apoptosis induction. Indeed, cytochrome c binds to InsP3R channels during apoptosis induction what

blocks the Ca^{2+}-dependent inhibition of InsP3 function and promotes apoptotic Ca^{2+} release [253,277]. Indeed, the phosphatase and tensin homolog (PTEN) has also been reported to be located at the MAMs and enhances Ca^{2+} signaling to the mitochondria in situations of increased ER stress and pro-apoptotic signaling. Moreover, during apoptosis, mitochondrial network was often shown to be fragmented and increases due to the recruitment of the fission protein DRP1 to the OMM. Then DRP1 was shown to stimulate pro-apoptotic proteins BAX and BAK and after it undergoes their oligomerization. Interestingly, the importance of PACS-2 for MAMs was still demonstrated as its depletion also induced apoptosis [260] and an induction of unfolded protein response (UPR).

IV-) Mitochondria and Immunometabolism focus on the Warburg Effect

1-) Warburg effect and cancer cells

The Warburg effect is a metabolic process that was first discovered in proliferating cancer cells [278]. This particular metabolic state is characterized by a modification of both catabolic and anabolic processes especially in the context of glycolysis and Krebs cycle intermediates that are mainly used for biosynthesis pathways. The classical metabolism starts with glycolysis that is followed by the Krebs cycle. Then the metabolic process ends with mitochondrial respiration with OXPHOS that allows the cell to produce 36 molecules of ATP for 1 consumed molecule of glucose (left panel of Figure 19, oxidative phosphorylation) [279]. Upon a Warburg shift, the fermentation pathway is favoured instead of the Krebs cycle, a process commonly referred to as aerobic glycolysis (right panel, Figure 19) [280]. As a consequence of this shift, the final glycolysis intermediate pyruvate cannot reach the Krebs cycle to be transformed in acetyl-coA but instead accumulates and gets converted into lactate giving rise to only 4 ATP for each consumed Glucose (see **Figure 19-**).

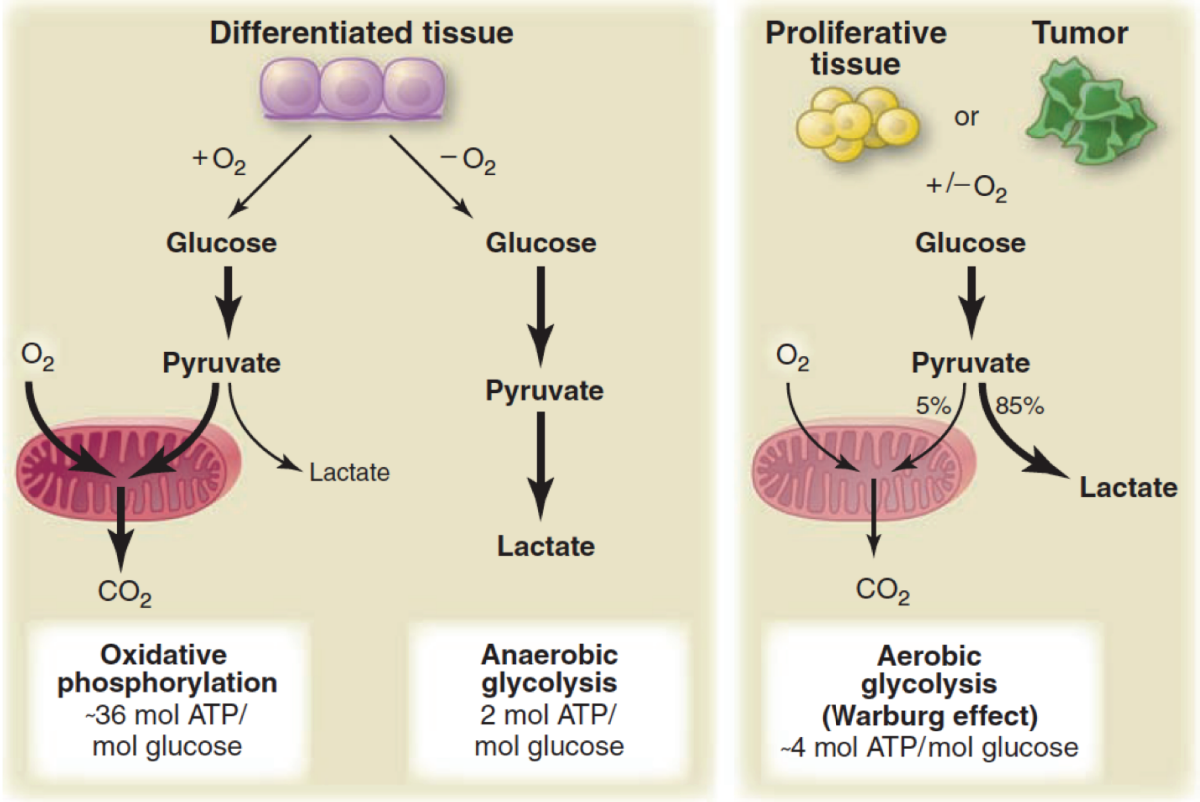

Figure 19- Comparison of glycolytic metabolism between non tumoral cells and tumoral cells. Figures and legends extracted from The Paradox of Cancer's Warburg Effect by Docteur Jason Fung

Consequently, one of the questions that intrigued researchers was to determine the role of mitochondria in cancer cells because their catabolic process dependent of the Krebs cycle associated to OXPHOS was not used anymore. Interestingly, it was found that mitochondria participate in several other metabolic processes including nucleotide, amino acid and lipid biosynthesis. Thus, in the context of a Warburg shift, the mitochondrial anabolism functions are stimulated instead of catabolic degradation of pyruvate glycolysis intermediates.

To conclude, the hallmarks of a metabolic shift that is associate to Warburg metabolism are:

- a huge increase of available glucose that is associated to an exacerbated glycolysis to maintain ATP production. There is also an accumulation of glycolytic intermediates as pyruvate that are used in biosynthetic pathways or for fermentation thus associated to an increase of lactate.

- a differential use of citrate and other Krebs cycle intermediates and acetyl-coenzyme A that are transported from mitochondria to the cytosol and used in lipid and other biosynthesis.

- an accumulation of NADH and NADPH in the cytosol through glycolysis and the pentose

phosphate pathway (PPP), respectively, to be also used for anabolic processes [280,281].

2-) Warburg effect and immune cells

The interplay between immunological and metabolic processes is an exciting emerging field known as immunometabolism. Interestingly, the Warburg process is also observed during immune processes. The current model proposes that innate or non-activated immune cells mainly rely in an OXPHOS metabolism that is shifted to Warburg metabolism upon immune activation [279,282]. For instance, some T-cells were shown to switch to Warburg metabolism upon activation by APCs including TH_1 and TH_{17} helper cells [283,284]. But with several other studies it has been demonstrated that a switch to Warburg metabolism can be observed in a large panel of other immune cells, such as macrophages, DCs, neutrophils, B-cells and natural killer cells [279,285-288]. A few examples where Warburg metabolic shift was observed upon immune activation include macrophages via their PRRs [285,286], T-cells via their cytokines receptors [289] or also B-cells activated by antigen receptors [287]. Interestingly, it has been also shown that Warburg metabolic shift can be associated with precise immune functions as phagocytosis and IL-1β production by macrophages [290], acquisition of costimulatory capacity by DCs [286], T_H17 polarization by activated T-cells [291] and formation of nets by neutrophils [292].

3-) Warburg effect and infected cells

It has also been recently reported that mammalian cells infected with intracellular bacteria have an altered metabolism that resembles the Warburg effect seen in cancer cells [293-295]. In the **Chapter 3** I will further detail the Warburg shift in context of *Brucella* infection. Often for bacterial pathogens, this metabolic shift it associated with an increase of glucose availability that can be used by pathogens as *Legionella, Salmonella* or *Brucella* [294,296,297] for their own replication.

V-) Mitochondria and pathogens

In the context of my work, it is important to highlight a few examples of pathogens that target mitochondria.

1-) *Listeria monocytogenes*

As *Listeria monocytogenes* was shown to induce ER stress (**Chapter 1**), it has been observed by microscopy that this bacterial pathogen fragments the mitochondrial network, in contrast to the nonpathogenic *Listeria innocua*. Again, LLO was identified as responsible of the mitochondrial fragmentation. LLO was sufficient to induce a mitochondrial membrane potential decrease and a drop in ATP level [298]. Interestingly authors conclude in their study that this LLO fragmentation cannot be associated with an apoptosis induction because they do not observe a release of cytochrome c either in infection or following treatment with LLO.

Moreover, mitochondrial dynamics were shown to be important for *Listeria* infection. Indeed, after siRNA treatment that inhibited either fusion or fission processes, a decrease in the rate of infection was observed [298]. However, LLO did not seem to affect mitochondrial dynamics directly.

In another study by Zhang *et al*. [299] it was elegantly demonstrated that *Listeria monocytogenes* interferes with mitochondria associated autophagy (or mitophagy) to avoid being killed. Indeed, it is known that host autophagy can take part in bacterial pathogen clearance. They demonstrated that mitophagy is triggered in macrophages and in weak manner in HeLa cells and that this phenotype was associated to LLO [299]. Authors went on to identify NLRX1 as the target of LLO, the only Nod-like receptor (NLR) family member with a mitochondrial targeting sequence that also contains an LC3-interacting region (LIR). This domain allows a direct association with LC3 after being oligomerized by the LLO that favors the binding of the LIR motif. Thus, *Listeria* promotes mitophagy induction to promote its survival.

2-) *Coxiella burnetii*

Coxiella burnetii is the etiological agent of human Q fever, a zoonotic infection with a worldwide distribution. Because this pathogen represents a threat even at low infectious dose and given its ability to disseminate and to survive *Coxiella* is classified as a category B pathogen by WHO [300,301]. As *Legionella*, *Coxiella* has a T4SS that secretes effectors and during these last year more over 130 Coxiella effector proteins have been identified. Among all these effectors some of them have been shown to be fully required for efficient intracellular replication and CCV biogenesis [302](Larson 2015 Infection and Immunity). A subset of *Coxiella* effectors show mitochondrial localization when they are ectopically

expressed in human cell lines. CBUA0020, CBU1825, CBU1425 and AnkJ all were shown to colocalize with mitochondrial markers [303-305].

For 2 of the mitochondrial located effectors CaeB (CBU1532) and AnkG (CBU0781) it was demonstrated that they have an anti-apoptotic effect by associating with mitochondria [303,306,307]. AnkG acts as a sensor of apoptotic stress at mitochondria, and consequently activate processes to counteract induced apoptosis by interacting with p32 [304,308]. Nevertheless, for CaeB molecular mechanisms it remains to be further investigated in order to find how apoptosis is impaired. Another recent study by Fielden *et al*. further characterized [309](Fielden 2017 Infection and immunity) the effector mitochondrial *Coxiella* effector protein A (MceA), which was previously found to co-localize with lysosomal markers during ectopic expression in HeLa cells [303]. This effector was also shown to localize to the OMM where it interacts with itself to form a multimeric complex. Interestingly it was shown that this effector is farnesylated via a CAAX motif (C for cysteine, A for aliphatic and X for any amino acid) present on the C-terminus, which contributes to the stabilization of the effector at the mitochondrial membrane. Nevertheless, the action of MceA at OMM needs to be further investigated.

3-) *Helicobacter pylori*

We have previously seen that *Helicobacter pylori* modulates UPR with the the secreted protein HP0175. However, contrary to the pathogens *L. pneumophila* or *Coxiella burnetii* which can deliver over 100 effectors, *Helicobacter* seems to have a more restricted repertoire of T4SS effectors. Among these, the best characterized is cytotoxin-associated gene A (CagA) which is responsible for severe damage of host cells by targeting multiple pathways. In contrast the pore-forming toxin VacA induces apoptosis and localizes to mitochondria [192]. Several studies showed that CagA promotes cell survival with an anti-apoptotic effect to counteract VacA-induced apoptosis. VacA mitochondrial localization results in a change of permeabilization of mitochondrial membranes as observed for LLO. This finding is important in the context of long-term infection, which can lead to cancer development after stomach colonization. The pathogen inhibits the cytotoxin VacA using two complementary mechanisms both involving CagA. It is important to highlight that the choice of either mechanism is dependent of the state of phosphorylation of CagA by host kinases. Indeed, when CagA is in a phosphorylated form, it inhibits the entry of the VacA into the cell by preventing its pinocytosis. In contrast, the second mechanism depends on the

unphosphorylated form of CagA to prevent VacA localization at the mitochondrial level, inhibiting the permeabilization of the mitochondrial outer membrane and release of the cytochrome c [310]. In addition, CagA also leads to an increase of Bcl2 anti-apoptotic factors (Bcl-2, Bcl-XL, Mcl-1) that contribute to blocking apoptosis. This coupled action of two effectors VacA/CagA demonstrates a pernicious strategy of the pathogen towards its host. Indeed, firstly VacA is used by *Helicobacter* to colonize and then it is CagA that ensures it can colonize the host durably.

4-) *Ehrlichia chaffeensis*

Ehrlichia chaffeensis is a Gram negative, obligate intracellular bacteria etiologically responsible for human monocytotropic ehrlichiosis considered as an emerging zoonosis [311]. This bacterium also has a T4SS [312] and in 2012 authors identified the effector ECH0825 that is translocated and found to have a mitochondrial localization during infection. Ectopically expressed, ECH0825 was still targeted to mitochondria and resulted in inhibition of apoptosis, associated with a high increase of mitochondrial manganese superoxide dismutase (MnSOD). In infection, this component was indeed increased over 9-fold and the amount of reactive oxygen species (ROS) significantly reduced compared to uninfected cells. This study shows that by up-regulating MnSOD, *Ehrlichia* prevents ROS-induced apoptosis to allow its intracellular infection [313].

5-) *Shigella Flexneri*

Shigella flexneri is a Gram-negative pathogenic bacterium belonging to the Enterobacteriaceae family. It is the responsible agent of dysentery in humans that causes diarrhea and severe inflammation in the gut. Upon entry into the cytoplasm of infected cells, a sub-population of the bacteria hijacks the actin cytoskeleton and stimulates its polymerization on the bacterial surface, forming so-called actin comet tails because of their resemblance of their space homologs [314,315].

I decided to talk about this pathogen because of a very interesting study that demonstrated that the application of mechanical forces lead to mitochondrial fission [316]. The originality of the project is authors used 3 different kind of mechanical forces: infection by *Shigella flexneri,* pressure by an atomic force microscope or via cell migration. For all three processes they observed mitochondrial fission with the recruitment of involved proteins as Drp1. To more develop the aspect by *Shigella* infection, authors observed by time-lapse

microscopy experiments that there are collisions between motile bacteria and the mitochondria. Therefore, these collisions resulted in 60 % of cases in a fission process between 1 to 5 min after collisions. Furthermore, they also observed in rare cases that collisions lead to a loss of fluorescence which indicates a constriction of the mitochondria matrix [316]. Afterwards, they wanted to determine DRP1 involvement in DRP1-depleted cells either with siRNA or shRNA transfection and also after CRISPR-associated protein 9 (CRISPR-Cas9) method. With the 3 different methods of DRP1 down regulation or knock out they observed that *Shigella* could no longer induce mitochondrial fission. This is consistent with another result of the study where they have shown that sites of collisions are associated to DRP1 foci. Nevertheless, it appears that DRP1-depleted cell mitochondria resist less to bacterial collision. Thus, mitochondria undergo fission in the case of *Shigella* infection to counteract mechanic stresses induced by bacterial motility.

6-) *Legionella pneumophila*

As *Brucella* or *Coxiella*, *Legionella* is found in a vacuole called *Legionella*-containing vacuole (LCV). Mitochondria have been shown to be recruited around the LCV independently of the T4SS of *Legionella* [294]. Added to that authors have visualized that LCVs transiently interact with mitochondria. As early as 6 h post-infection mitochondria surround the LCV, interact and then move away. The nature of the contacts requires deeper investigation, nevertheless still in the same study they have found approximately 25% of mitochondrial proteins in the proteome of purified LCVs suggesting membrane exchanges are occurring [294]. Consequently, *Legionella pneumophila* has developed strategies to control mitochondrial functions. Some T4SS effectors have been implicated in modulation of mitochondrial functions. In this part I decided to focus on LpSPL and Mitochondria fragmentation factor (MitF) [294,317].

LpSPL (also known as LegS2) is a T4SS secreted effector that has structural similarity to eukaryotic sphingosine-1-phosphate lyase (SPL). Consequently, it also has the enzymatic activity that catalyzes the irreversible cleavage of sphingosine-1-phosphate. Thus, this effector can finely regulate sphingolipid levels that are involved in autophagosome formation. It is a way to inhibit autophagy known to have a role in bacterial clearance as previously seen with *Helicobacter pylori* in the **Chapter 1-**[278].

Interestingly LpSPL was shown to have different localizations: in the ER [318] and to

mitochondria [319]. Today with the evolution of our knowledge regarding MAMs, it seems reasonable to think that this effector may localize to the MAMs. Moreover, consistent with this hypothesis it has been shown that the substrate of LpSPL sphingosine-1-phosphate is involved in several MAMs processes as calcium transfer [320], lipid metabolism [321], apoptosis [322] and autophagosome formation [251]. Finally, LpSPL was also shown to interfere with mitochondrial functions that can be associated to MAMs as the fission process [323], lipid biosynthesis [318] and autophagosome formations [318].

In 2017 Escoll *et al*. [294] identified a new T4SS effector MitF that induces mitochondrial fragmentation through fission DRP1 protein and Ran binding protein 2 (RanBP2) because silencing of these proteins results in a reduced mitochondrial fragmentation. As *Listeria* it is important to note that DRP1 silencing affects the bacterial replication with a decrease of CFU. Authors showed that this mitochondrial fragmentation consequently affects mitochondrial metabolism by inhibiting OXPHOS even if a glycolysis activation was in parallel observed with a drastic reduction of consumed oxygen. Thus, it is an anaerobic glycolysis that is stimulated, and this is why authors characterized this shift as a Warburg-like effect. This metabolic shift induced by *Legionella* was demonstrated to favor its own replication. Nevertheless, it is important to note that at early stages of the infection (ie up to 1h pi) mitochondrial respiration was upregulated independently of the T4SS.

As mitochondrial fragmentation is often associated to apoptosis, they measured the release of cytochrome c between 6h to 12h pi. Surprisingly cytochrome c was found to stain in the mitochondria which indicates that apoptosis is not induced by the fragmentation. We will see in the **Chapter 4-** that our *Brucella* effector has a similar phenotype.

In summary, with the study of this MitF, authors highlighted again the importance of dynamic mitochondrial processes in host metabolism, as the induction of fragmentation and the impairment of metabolism both are induced by MitF. Finally, in this study DRP1 was found to be a crucial factor for the bacteria to be hijacked in order to manipulate associated-mitochondrial functions.

V-) General conclusions

Emergence of MAMs studies provide new challenges for the scientific community to better understand the relationship between ER and mitochondria. It demonstrated the involvement of both organelles in same processes as illustrated in the section on the calcium

metabolism. Otherwise for bacterial pathogens, mitochondria constitute an attractive target to manipulate given its link to energetic and biosynthetic metabolism but also for the control of the programmed cell death. Indeed, this latter process is crucial to be controlled if the pathogen wants to establish a safe niche in the cell and have the time to replicate.

Future studies should carefully follow the advancement of MAMs characterization to help study the function of bacterial effectors that are probably associated to MAMs especially if both ER and mitochondria localizations were found during infection. On the other hand, bacterial effectors can also provide original tools to help decipher the functions and molecular components of MAMs as they often have very specific functions with “smoother” effects in contrast to chemical drugs or RNA interference treatments that can lead to some undesirable side-effects.

Chapter 3 Brucella

I-) Global overview of a fascinating pathogen

1-) *Brucella* epidemiology

The *Brucella* genus belongs to the α2-subdivision of the proteobacteria (represented

Figure 20- which includes several animal pathogens such as *Bartonella henselae*, *Rickettsia ricketsii* and the phytopathogen *Agrobacterium tumefasciens* [324]. Bacteria from the *Brucella* genus are the aetiological agents of brucellosis, also called Malta or Mediterranean fever. It is still considered by the World Health Organization (WHO) as an important neglected zoonosis re-emerging in poverty associated regions with 500 000 referenced human cases by year and because of its impact on agriculture given the ability of *Brucella* to infect a large spectrum of hosts [325-327].

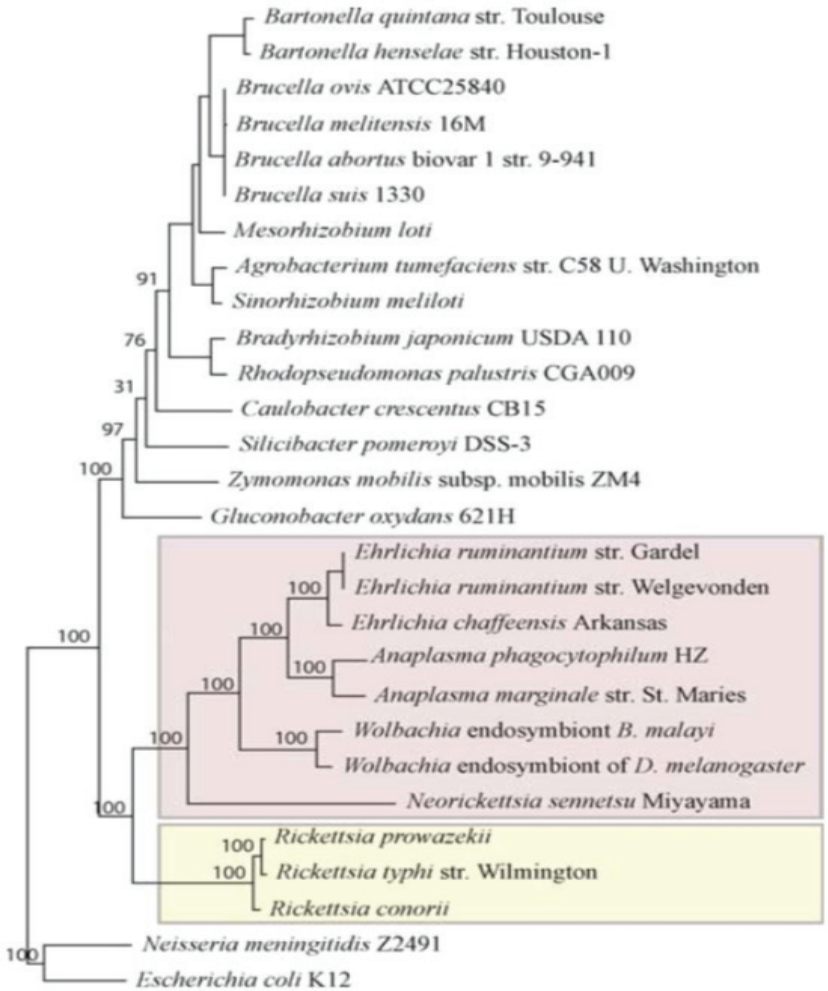

Figure 20- Phylogenetic Tree of the α-Proteobacteria. The protein sequences of select conserved genes were concatenated and aligned, and a phylogenetic tree was inferred of all sequenced α-Proteobacteria. The Anaplasmataceae (purple) and the Rickettsiaceae (yellow) are highlighted. Figures and legends extracted from [324]

Brucellosis is still endemic and a threat in the Mediterranean region, Asia (except Japan and Corea), sub-Saharan Africa and some countries in Latin America [326,328]. In the developing world, it is often associated with absence of competent veterinary services and political structure. Moreover, these regions practice an intensive pastoral agriculture that increases the risk of animal brucellosis and complicates the diagnostics of the cattle because of the high number of animals. Overall, we are still facing major challenges to contain or eradicate brucellosis outbreaks worldwide [328]. To add to this problem, *Brucella* spp. are also prevalent in marine and terrestrial wild-life (e.g. dolphins, seals, bison, elk, wild-boar) which hampers eradication. The recent identification of a growing number of atypical strains, such as those isolated from amphibians and voles point towards a common ancestor in the soil and suggest that new *Brucella* environmental niches are yet to be discovered.

2-) History, vaccines

a-) History and discovery

Brucellosis was first reported in 1859 (and the strain was first isolated in 1887 by the English officer David Bruce. Almost a century later the first animal vaccine against caprine brucellosis was developed: Rev1[329]. Since then, several vaccines are used in the field to control animal brucellosis. It is important to note that no vaccine is yet available for humans. Among animal vaccines 2 are mainly used today: S19 and RB51.

b-) *Brucella* vaccines: a balance between risk and benefit

Firstly, S19 is a live attenuated vaccine good to immunize calves. But the major problem of this vaccine is the antibody production, which cannot be distinguished from an antibody response induced by an infection. Consequently, the main restriction of this vaccine is the age of the vaccination, which has to be injected at the youngest age of the cheptel to be sure that antibody detection is not the result of an infection. S19 for agriculture is an interesting vaccine because it does not induce abortion nor sterility and still gives a good vaccine cover contrary to other vaccines[330].

The second vaccine, RB51, is also considered a good vaccine and does not have this age restriction problem. It is also a live strain derived from *Brucella abortus* but with a rough morphology, due to absence of the O-polysaccharide, the most external component of the lipopolysaccharide (LPS). However, vaccination with RB51 of pregnant animals can cause abortion. For male animals it can lead to infertility, which not surprisingly represents a major inconvenient in agriculture. Another issue with RB51 is that this vaccine needs to be applied several times. Nevertheless, the main advantage of this vaccination is that the antibody response, which is different, compared with classical *Brucella* infection. Indeed, we can make the difference between infected animals compared with vaccinated animal. Thus, with RB51 we can be monitor immunization with standard serology tests [331].

Regarding humans, it is important to notice that these vaccines are dangerous because they both can cause infections in humans. Consequently, their use requires safety training which adds a high cost difficult to support for developing countries.

Despite of all the negative points discussed above, S19 and RB51 are the officially approved vaccine strains. Vaccinology research has to continue in order to find a better vaccine with less inconveniences that can be used for livestock, without associated abortion or infertility and inducing an immune response different from *Brucella* infection. Finally, it would be desirable that the future vaccine is also efficient for humans to protect farmers and veterinary personal[331].

Consequently, nowadays the control of animal brucellosis and indirectly of human brucellosis is dependent on strict food hygiene, animal management measures and milk pasteurization. In North America, Australia, and some northern European countries, control of *Brucella* in the zoonotic reservoir species by massive vaccination programs and killing of infected animals has strongly reduced the incidence of human brucellosis. However, in several countries brucellosis is still prevalent and far from being controlled. This is the case for example of Africa bovine brucellosis with more than 250 outbreaks/year reported since 2003 and also in China/Mongolia regions [332]. It is clear that a global coordinated effort has to be set in place to encourage official veterinary services and public health officers to collect and share epidemiological data for designing improved control and eradication plans in these regions against this bacterial agent.

c-) Symptoms and dissemination

The clinical symptoms of brucellosis are very different between humans, and animals and depend of the stage of infection. Indeed "farm animals" can be colonized for life without any major symptoms and bacteria mainly affects reproductive organs and establishes its replicative niche inside the placenta and foetus, which results in abortion at middle or late stages of the pregnancy. It can also lead to sterility of male animals or arthritis[11] as it was reported in pigs after *B. suis* infection [333]. However, in some cases, animals can present a fever, inflammation of the mammary gland in the breast (mastitis) and hygromas which are pockets of inflammation containing synovial liquid associated to joints [333,334]. And if the pregnant female can succeed to deliver its offspring it often results in very weak progeny.

For the marine mammals and especially cetaceans, 2 species are the main etiological agents: *B. ceti* and *B. pinnipedialis*. Abortion cases have also been reported in infected dolphins [335]. They are often associated with skin and cutaneous lesions. The pathology can evolve in more severe forms with spinal discopondylitis, meningoencephalitis and some other neurologic disorders [336].

In humans, we can distinguish two different phases for brucellosis. At the beginning, the acute phase is characterized by a febrile illness, which resembles flu with undulant fever. In absence of therapeutics, brucellosis can evolve into a more severe and debilitating illness with cardiac and neurological complications and the formation of infectious foci in bone joints [325,326]. There are no major differences according to the gender [337]. The disease is accompanied with significant increase of the size of the spleen and liver, not surprisingly because of their involvement in immunity. In clinics, list of symptoms used for diagnostic of *Brucella* infection in addition to fever are hepatomegaly, splenomegaly, hepatosplenomegaly and arthritis. Prompt diagnosis is vital to rapidly treat the disease and to avoid the further complications. These can include endocarditis, which requires surgery and a heavy treatment to clear the bacteria but can also be mortal [338]. Neurological complications have also been reported, with the entry of the bacteria in the central nervous system. This invasion leads to meningitis or meningoencephalitis and demyelination disorders [333]. Degradation of the optic nerve has also been reported during neurobrucellosis [339]. Thus, brucellosis remains an infectious disease that requires careful diagnosis and surveillance even if few human cases are reported in the year the disease can become extremely debilitating, associated with significant morbidity worldwide.

We have seen that symptoms are different between marine and aquatic animals and humans. Unfortunately, there does not seem to be a species barrier that could block a

transmission between “natural” animal hosts. This transmission can be horizontal with these above described actions as:

- Inhalation of bacterial aerosol from an abortion for example
- Contact with body fluids from infected animals
- Genital contact during the mating [340]

Thankfully for humans the most effective route for infection is the inhalation of contaminated aerosols that might occur in laboratory or animal slaughterhouses. Indeed, the majority of human brucellosis cases are caused by ingestion of unpasteurized milk and dairy products. In addition, the last important part of human brucellosis comes from exposure in a professional context for people in contact with infected animals: farmers, veterinarians and butchers [325]. There is currently no evidence of transmission between humans except in pregnancy, where *Brucella* can pass to the unborn fetus and cause abortion in the first trimester of pregnancy.

d-) *Brucella* tropism and infected tissues

In animals *Brucella* has a preferential tropism for the genital tract. Indeed, the infections of mammary gland and placenta allow the bacteria perfect setting for effective dissemination because *Brucella* can use these organs as a way to spread in the environment through the milk, the genital secretions and aborted foetus. The genital tract is a free highway for *Brucella* dissemination because this conduct in mammals has developed immunology particularities to tolerate foreign antigens such as those generated by spermatozoid and the foetus [341].

In humans, only few studies characterized *in vivo* the nature of infected cells as most of the experiments are carried out in mice. However, given the nature of the symptoms that are previously mentioned, *Brucella* can infect immune cells as it is a safe niche to replicate without being detected. Following inoculation, infection can progress undetected for many months. And given the cardiac and the neurological complications it may suggest that *Brucella* can infect a large variety of cells. This is confirmed in *in vitro* experiments where *Brucella* was shown to infect a huge spectrum of human cell types with a high capacity to infect and to replicate within immune cells as macrophages, dendritic cells (DCs), but also osteoblasts and fibroblasts as well as epithelial cells and trophoblasts [342-347]. Indeed, cultured epithelial cell lines are considered as a routine model for laboratories because they

are easy to manipulate and adequate for microscopy experiments.

A little focus on the trophoblast which appears to be an important cellular target for *Brucella* pathogenesis in both animals and humans. Indeed, it is important to note that *Brucella* was demonstrated for the first time to establish its replicative niche in the ER in infected goat and bovine placenta indicating a tropism for trophoblast cells [348]. Furthermore, in infected placenta, it has been shown by microscopy *Brucella* localizes to trophoblasts and replicates in placental trophoblasts [348]. More recently it has been shown that late in gestation *Brucella* localizes both in trophoblasts and extracellular which explains its spread after infection [341]. Nonetheless, recent investigations of *Brucell*a spp. infection of human trophoblasts revealed interesting differences in intracellular trafficking that will be discussed latter in this chapter.

II-) *Brucella* and host immunity, a game of hide-and-seek

We have seen that *Brucella* has different species that can infect many animals and humans. An important topic occupying researcher is how do these bacteria succeed to persist in infected hosts without being killed by the immune system. The immune response to *Brucella* infection has been characterized most extensively in the mouse model. Many studies show that *Brucella spp*. evolved different strategies using both passive and active mechanisms to avoid immune detection by its host by maintaining low the immune surveillance. Yet, it manages at critical times and in specific tissues to induce important inflammatory responses that contribute to pathology of the disease. In this section a global overview of different mechanisms will be discussed.

1-) *Brucella* and its structural modification

As a passive mechanism to avoid innate immunity it has been shown that *Brucella* evades detection by complement, TLRs and most NLRs through a stealthy design of its cell envelope. First of all, it has been shown that *Brucella* does not express any pili, fimbriae or capsule which are considered as PAMPs and can be recognized by the immune system [349]. As several other bacteria, *Brucella* has a flagellum on its surface, but the pathogen has modified the flagellin protein constituting the flagellum in order to activate less TLR5 contrary to a normal flagellum [350,351].

Another component of the bacterial cell envelope is the lipopolysaccharide (LPS) complex which is composed of 3 components: the O antigen, an oligosaccharide core and a

lipid A. These 3 components are highly variable in their composition and in the case of *Brucella* the modification of its own LPS allows avoidance of immune activation. Indeed, it has been shown that *Brucella spp*. passively evade detection by TLR4 via modification of the lipid A moiety of LPS. Indeed, the difference of the lipid A results in a reduction of phosphate groups and the presence of the long acyl chains found also in plant bacteria as Rhizobium which belong to the same clade (See **Figure 20-**) [352]. Besides, a second anti-inflammatory feature of *Brucella* LPS is its resistance to deposition of complement component C3 which avoids bacterial lysis or opsonization [353]. Finally, as a last modification of the LPS it has also been shown that the O chain antigen of the LPS associates with major histocompatibility complexes (MHC) class II. This association inhibits the ability of macrophages to present *Brucella* antigen in order to further activate $CD4^+$ T lymphocytes [354].

2-) *Brucella* and its type IV secretion system

Bacterial secretion systems are huge macromolecular machines that allow bacteria to secrete proteins from their cytoplasm to their environment or in a target cell. They are involved in many processes in the lifestyle of bacteria that have some secretion systems as bacterial killing with the type VI secretion system or conjugation for the type IV secretion system (T4SS). This research area is too broad to summarize here, and this is why I will focus on the VirB T4SS of *Brucella* which is a major virulence factor. However, it is important to mention that, there are other identified secretion systems as type I and V that are present in *Brucella* genome. The T1SS is involved in the export of proteins from the cytoplasm to the extracellular environment in a single step without involving periplasmic intermediate. As secreted proteins of this kind of system we can usually find toxins, proteases, cell surface proteins and lipases. Moreover, this system can also transport non-proteic substrates as the cyclic β-glucans and polysaccharides [355]. In the case of *Brucella* there are no toxins and over two third of the T1SS are ABC transporters.

The T5SS is associated with the Sec/Tat pathways which are used to cross the cytoplasmic membrane into the periplasm. The protein is then secreted in the extracellular medium thanks to the T5SS [356]. To date three different of T5SS were referenced: Va, Vb and Vc. In the case of *Brucella,* it is the T5SSVc that is identified with the identification of YadA protein. For the bacteria it allows the adhesion as it was demonstrated to secrete adhesins and might also contribute to the virulence process [356].

The T4SS secretion system was firstly identified in the phytopathogen *Agrobacterium tumefasciens* where it is genetically encoded by the Vir operon. This system has been referenced in both Gram negative and positive bacteria. T4SS can be divided in 2 groups given the nature of the involved operon and protein subunits: type A with VirB operon which was mentioned above and the type B more closely resembling the Dot/Icm operon [357,358]. *Brucella* encodes for a T4SSA, composed of VirB1-11 and an additional VirB12. Interestingly, *Brucella* lacks the gene encoding for VirD4. In addition, VirB1, VirB7 and VirB12 do not seem to be essential for persistence in the mouse model [356]. Electronic microscopy revealed that T4SS form a protuberance called pilus, whose function is still not entirely elucidated. It may be involved possibly in the transport of secreted molecules and/or a device for attachment to the target bacterial cell. The T4SS pili (which should not be confused with the type IV pilus associated with type 2 secretion) is composed of the VirB2 and VirB5 subunits. All other VirB proteins are the structural core of the system forming a large complex inserted in inner and outer bacterial membranes. This secretion system is ancestrally associated to conjugation systems and are involved in horizontal gene transfer and virulence. This bacterial process mediates transfer of plasmids and other mobile, extra-chromosomic genetic elements. These DNA transfer processes are very well studied because transferred plasmids containing arrays of antibiotics-resistance genes can be propagated through bacterial populations thanks to this contributing to the spread of antibiotic resistance which is a major public health issue.

A number of bacterial pathogens use T4SS for pathogenicity such as *Legionella spp*., *Bartonella* spp., *Brucella* spp., *Coxiella* spp. and *Helicobaceter pylori*. In the context of bacterial pathogenicity, the T4SS allows them to inject proteins often called effectors in plant or animal cell targets. These effectors will first cross the bacterial membranes, a secretion process requiring ATP. Then effectors are translocated into eukaryotic cells, where they can modulate cellular functions. Bacterial effectors can be considered as potent “weapons” or « tools » that ensure bacterial multiplication. Most of the effectors have a eukaryotic-like domain suggesting an interaction with proteins in the infected host cell [359].

The *Brucella* T4SS has an essential role in intracellular survival and replication[360-364]. Indeed, it has been highlighted the inability of *virB* mutant bacteria to replicate inside host cells. The absence of the T4SS prevents the translocation of effectors essential for controlling several host functions and mediate fusion with the ER which is the replicative compartment of *Brucella* [360,363,365-367]. But as we will see in a later part *Brucella* also has to avoid phago-lysomal degradation in early stage of infection.

It has been reported that *Brucella* requires a functional T4SS to elicit innate immune responses in mice [368]. Indeed, early during infection of mice, it has been shown that the host response is a T helper 1 (T_H1) response, with gamma interferon (IFN-γ) production by T cells and natural killer (NK) cells. T4SS is critical for inducing production of IFN-γ and other proinflammatory chemokines. *virB* mutants failed to elicit any inflammatory response. In addition to an early TH1 response, *B. abortus* also induces the anti-inflammatory cytokine interleukin-10 (IL-10 produced by CD4 cells B cells and macrophages) [369,370]. IL-10 can inhibit the microbicidal activity of macrophages against *Brucella* as well as antagonizing the activity of IFN-γ [371]. Therefore, the T4SS plays a complex role contributing to induction of inflammation but also as an active mechanism to counteract the host innate immune system. As it was mentioned in this study of Christelle Roux *et al*. [368] in 2007 "it is possible that the VirB T4SS of *Brucella* elicits inflammation by translocating either conserved bacterial ligands or T4SS effectors that trigger proinflammatory signaling via cytosolic innate immune receptors". Indeed, *Brucella* secretes at least 1 effector VceC that elicits immune response and 2 TIR domain-containing effectors BtpA (also known as TcpB) and BtpB that allow it to actively manipulate the immune system and reduce inflammation in the infected host. It is not clear yet how these opposing effects are regulated but it may be related to specific cellular targets and steps of the infection. It is possible that VceC shown to induce inflammation and associated abortion is acting mainly on macrophages and trophoblasts in the context of placental colonization whereas BtpA and BtpB would be involved in down-modulation in specific types of migratory macrophages and DCs, important in dissemination, lymph node colonization and granuloma formation. It is also likely that these sets of effectors intervene at different chronological stages of the infection cycle, for example to contribute towards reducing an immune response induced by the T4SS in order to ensure long term persistence in the host. These effectors and their molecular modes of action are discussed in greater detail in the **section IV-4**-).

3-) Granuloma formation

The generation of a mild inflammatory response has important consequences for persistence of *Brucella* spp. in tissue. Indeed, *Brucella* does not exert a total inhibition of immune processes. Another point that is important to mention is *Brucella* infection induces granulomatous "bodies" that can be observed in histology biopsy samples from both mice and

humans. These analyses reveal small granulomas in liver, spleen, bone marrow, and more generally all targeted tissues by bacteria [372]. Those granulomas are developed by the host in attempt to wall off the bacteria that cannot be eliminated by macrophages. These granulomas contain epithelioid macrophages (macrophages with an increased amount of cytoplasm) and are a site of bacterial persistence during *Brucella* infection [372]. This type of granulomas is better studied in context of *Mycobacterium* tuberculosis infection. Indeed, it has been shown with *Mycobacterium tuberculosis* that granulomas serve as a niche of persistent mycobacterial infection, in which bacteria may multiply and eventually spread to other sites in the host[373]. This latent strategy perfectly highlights how the bacteria optimize all the processes of its host to establish chronic infection.

As a conclusion for this part, we have seen how *Brucella* benefits from important modifications of its own surface components to adapt to its host in order to avoid extensive immune recognition that would lead to its destruction. Moreover, with its T4SS, the bacteria actively manipulate host immune processes to counteract the establishment of an adaptive immunity by avoiding the activation of the key factor NF-κB at molecular level or the antigen presentation at cellular level. Additional mechanisms have been implicated in modulation of host immunity during *Brucella* infection but are beyond the scope of this thesis. These include for example, the protein L-Omp19 that inhibits MHC-II expression and studies showing *Brucella* also acts on MHC-I expression by retaining the immune complex in the Golgi apparatus [374], interfering with adaptative immune response and activation of $CD8^+$T lymphocytes.

III-) *Brucella* intracellular lifestyle: from trafficking to replication and bacterial release

1-) Entry of the bacteria

The success of *Brucella* infection is associated to its ability to invade or be taken up by host cells. Therefore, the pathway of entry is determinant for bacterial fate. The integrity of the smooth LPS has been shown to be key for this process. Indeed, interaction between the O antigen of *Brucella* smooth LPS and the class A scavenger receptors located in the lipid rafts of host cell membrane is essential for the intracellular survival [375,376]. Therefore, rough mutants for LPS do not enter through lipid rafts and are quickly degraded by lysosomes [377].

Moreover, as mentioned above, *Brucella* can infect phagocytic and non-phagocytic

cells [378]. The nature of the infected cell line obviously impacts the mechanisms of internalization. Little is known on the mechanisms of entry into non-phagocytic cells. The entry of bacteria has mostly been characterized in immune cells where 2 different pathways were described for the *Brucella* uptake and the difference resides in the opsonized state of the bacteria. In the case of non-opsonized *Brucella*, internalization requires a lipid raft-mediated entry [375]whereas opsonized bacterial entry is independent of lipid rafts and involves Fc receptors for IgG [379]. After the recognition by the receptors *Brucella* is taken up by phagocytosis or macropinocytosis. Another example has been described for dendritic cells where it has been shown that opsonized *Brucella* fail to persist in murine bone marrow-derived DCs [343] and its entry partially requires lipid rafts [380]. These examples show that *Brucella* can present multiple "sophisticated" mechanisms to enter host eukaryotic cells.

2-) From endosomal compartments to ER: the endosomal *Brucella*-containing vacuole

Once inside cells, the early stages of infection start to be well characterized. In this section, we will summarize the current knowledge on the trafficking of the bacteria through the endosomal compartments until the establishment of the replicative niche in the host eukaryotic ER.

After the uptake within professional or non-professional phagocytes, *Brucella* is found inside a membrane compartment called *Brucella*-Containing Vacuole (BCV). This vacuole is a phagosome that is modified by the bacterium with acquisition of early endosome marker at the beginning of infection: early endosomal antigen1 (EEA1), the transferrin receptor TfR and the small GTPase Rab5. The acquisition of these proteins on the surface of the BCVs will allow bacteria to benefit from interactions with the host endosomal pathway. Given the nature of acquired EEA1 and Rab5, this first stage of vacuole trafficking has the name of endosomal BCV (eBCV) [360].

Afterwards, *Brucella* will acquire late endosomal and lysosomal components in order to partially acquire phagolysosomal properties [381]. The transient acquisition of the late endosomal membrane proteins 1 and 2 (LAMP1 and LAMP2), the multi-vesicular body marker CD63 and the small GTPase Rab7 is followed by an acidification (pH around 4.5), necessary for the induction of the T4SS [382,383]. Added to that it is important to note that *Brucella* was initially thought to avoid lysosome fusion without acquiring specific proteins of the lysosome. Nevertheless, Starr *et al*. (2008 Traffic) alerts that it can be due to the preparation of the microscopy samples as it has been shown previously on *Salmonella* study [384]). The authors have shown that there was a loss of antigen markers because of fixation

and permeabilization steps. In Starr *et al* they consequently used the fluorescent markers in live cells to assess if eBCVs acquire lysosomal markers. They found an acquisition of lysosomal markers and even a proteolytic activity which a hallmark of lysosome.

It is important to note that even *Brucella* strategy seems perfectly established to avoid degradation by the endocytic pathway, almost 90% of bacteria do not succeed to reach the ER and are killed by macrophages as it was reported in different studies [360,381]. Consequently, it asks the question of why *Brucella* uses this dangerous pathway to reach the ER. The answer is simple as eBCV stage represents only a transitional but also necessary step towards rBCV biogenesis and allows the acidification of the BCV to induce T4SS which is crucial for downstream processes. Furthermore, it has been established that *Brucella* modulates its cell cycle during the eBCV stage. Indeed, it has been shown that *Brucella* cell cycle is blocked in the G1 phase until 6 h pi. And surprisingly the bacterium resumes its cell cycle and chromosomal replication whilst still in the eBCV stage [385].

3-) Replicative *Brucella* containing vacuole strongly requires secretory pathway

Between 8 and 12h pi eBCVs will reach a sub-compartment of the ER the Endoplasmic Reticulum Exit Sites (ERES). BCV interactions with ERES allow subsequent fusion with the ER cisternae, transforming the eBCVs into an ER-derived organelle. Thus, the bacteria will progressively loose endosomal and lysosomal markers, which are replaced by specific markers of the ER (calnexin, calreticulin, sec61β) [345,360,381]. These new markers are characteristic of the replicative vacuole of *Brucella*.

Thus, the bacteria will start to replicate in this new vacuole [345,360,381] known as replicative BCVs (rBCVs). Added to that, in a recent study where they performed 3D electron microscopy, we can visualize in detail the fusion process of BCV and ER. With this resolution authors clearly show that BCVs are ER-derived compartments that are continuous to ER cisternae which gives all the sense to the name of ER-derived vacuole [386]. Interaction with ERES is an essential first step for onset of rBCVs. These ER compartments are specialized in the formation of COPII cargo vesicles, essential components of the secretory pathway. The importance of the secretory pathway for *Brucella* is highlighted by the use of Brefeldin A, that blocks a major regulator of the secretory pathway the small GTPase ARF1 [387]. The consequence of inhibited ARF1 was *Brucella* failed to acquire ER membranes required for rBCV biogenesis. Afterwards, several GTPases were identified to be important for *Brucella* pathogenesis, as Rab1 and Rab2 that control anterograde and retrograde vesicular

traffic between the ER and Golgi apparatus [388,389] and the small GTPase Sar1, which controls COPII coat assembly, ERES formation and function. They were all shown to be important for *Brucella abortus* [387,390,391]. For example, in the case of a deficient Sar1, an impairment in rBCV biogenesis and bacterial replication was observed consistent with the specific interactions of BCVs with COPII components [387,392]. A few years later the importance of Sar1 and COPII components was once again highlighted with Taguchi *et al*. who showed that *Brucella* infection upregulates production of Sar1 but also Sec23 and Sec24D which are COPII components [392]. Conjointly these studies have highlighted the importance of controlling vesicle trafficking to promote rBCV biogenesis.

Thus, rBCVs are the replicative vacuole of *Brucella*, and it is in this vacuole that the longest stage of the *Brucella* infection cycle takes place to allow extensive intracellular multiplication (until 48h pi). We have seen in this section the complex and crucial role of vesicular trafficking and secretory pathway for eBCV conversion and then the establishment of *Brucella* replicative niche. Moreover, we have seen the intermingling between different processes of the secretory pathway. We are going to discuss now a second level of complexity associated with *Brucella* multiplication, its link to the UPR. The best study that highlights this increasing complexity was made by Taguchi *et al*. [392] They identified a new eukaryotic protein Yip1A that is associated to ER secretion processes and also ER stress.

4-) *Brucella*, ER stress and UPR

As mentioned in the **Chapter 1**, pathogenic bacteria are more and more known to interfere with UPR. Given the localization of the rBCV for bacterial proliferation, it is not surprising to learn that *Brucella* also induces ER stress and interferes with the UPR. There are several studies that demonstrated UPR induction by *Brucella* is found in different cell lines as HeLa cells, macrophages and trophoblasts. To date UPR induction by *Brucella* was reported to be mainly dependent of IRE1 pathway [138,161,361,392] even if the study of Smith *et al* is the only one that observed an induction of the three branches of UPR with *Brucella melitensis* [161]. Interestingly with *Brucella* it has been demonstrated in 2 studies that UPR is also necessary for *Brucella* replication. Indeed, in a first example authors infected IRE1 knock-out mice and a drastic reduction of bacterial replication was observed [215]. In the second case in Smith *et al*. used a chemical inhibitor of ER stress TUDCA and they also observed an impairment of *Brucella* replication. Another point which is important to be highlighted is *Brucella* seems to be inducing ER stress early in infection as phosphorylated activation of

IRE1 was detected at 4h pi [161,392]. It seems counter intuitive that a pathogen would induce UPR given its link to innate immunity processes [137]. More recently, important studies have begun to shed light on the consequences of ER stress. In the context of placental colonization, *Brucella* relies on ER stress for strong induction of inflammation and subsequently causing abortion. This phenotype is dependent on a specific effector called VceC discussed in the next section of this chapter.

Indeed, it is clear that UPR induction is not a side effect due to bacterial replication as we will see later that several effectors specifically trigger ER stress. Taguchi *et al*. [392] were the first to find a good reason for the bacteria to induce UPR, by showing a connexion with ERES and rBCV biogenesis with Yip1A.

First of all, they identified that IRE1α activation is dependent of the ERES-localized protein Yip1A. Indeed, they have demonstrated that Yip1A is involved in the phosphorylation step required for IRE1 dimerization because knock-down of Yip1A by RNA interference does not show any increased level of phosphorylated IRE1. Furthermore, this eukaryotic factor was reported to be essential for *Brucella* replication. They infected knock-down Yip1A cells and they visualised that *Brucella* does not succeed to generate rBCVs, resting in endosomal compartments. This is consistent with the fact that *Brucella* was shown to fail to replicate without an IRE functional pathway [215], Yip1A is essential for IRE1 functionality and Yip1A is the linker between ERES dependent processes and UPR. Moreover, authors have shown that Yip1A is required for the upregulation of Sar1, Sec23 and Sec24D during infection with *B. abortus* essential for formation of rBCVs and explaining why *Brucella* remains in endosomal compartments.

In addition, authors finally showed that the formation of large vacuoles requires autophagic proteins as Atg9 and WIPI1. Based on the roles of UPR and more specifically IRE1α in autophagy or specialized ER-phagy, authors hypothesized Yip1A might coordinate the intersection between the secretory pathway, UPR and ER-phagy pathways at ERES by activating IRE1. The identification of autophagic proteins is consistent with early studies of BCV intracellular trafficking which already proposed the involvement of the autophagy pathway in rBCV biogenesis [345] and the study of Wang *et al*. [219] that found that COPII vesicles can be hijacked by the autophagic pathway to supply membranes for autophagosome formation.

We will now see in the that autophagy is also important for the end of the *Brucella* intracellular lifestyle, highlighting that fine-tuning of cellular pathways in a kinetically defined manner enables bacteria to highjack host mechanisms for their own benefit.

5-) Autophagy for terminal BCV formation: time to say goodbye

At the end of the bacterial replication (around 48h pi), *B. abortus* was demonstrated to exit cells by using an autophagy process in order to disseminate and to infect neighbouring cells or to spread in the environment [393]. rBCVs were shown to use organelle membranes as those from ER to form phagophores where there will be one or several bacteria. Unlike at other stages of BCV formation, these vesicles contain late endosomal and lysosomal markers and their formation depends on very specific autophagy-related proteins as ULK1, ATG14L and Beclin1 while rBCV required ATG9 and WIPI1 [392,393]. These final BCVs are thus called autophagic BCVs (aBCVs). However, aBCV formation was independent of the autophagy elongation proteins ATG5, ATG16L1, ATG4B, ATG7, and LC3B. Thus, *Brucella* ends its intracellular cycle with aBCVs by subverting only autophagy-initiation/nucleation complexes.

This highlights how *Brucella* only uses what it needs for its intracellular cycle by selectively subverting autophagic components as it also selectively subverted a subset of endosomal markers earlier in its trafficking.

This aBCV stage is important for *Brucella* pathogenesis because it allows exit from the infected cell by "bubbling" without killing the infected cell. Moreover, it has been shown in Starr *et al* that an alteration of aBCV formation process results in inhibition of bacterial egress. Indeed, authors visualized secondary bacterial infections while aBCV formation stage is still occurring in primary infected cells. All the cycle is summarized in the **Figure 21-**) extracted from Celli *et al*. [394].

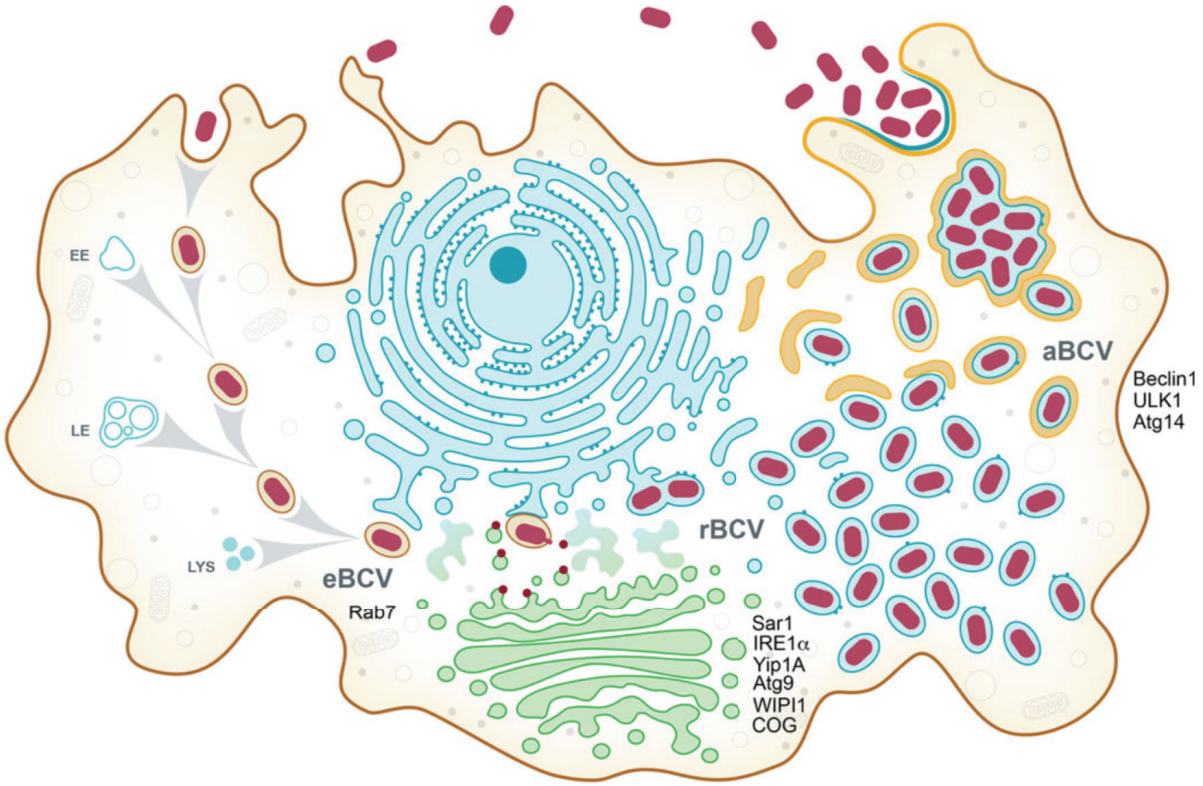

Figure 21 Model of the *Brucella* intracellular cycle in macrophages. Following phagocytic uptake by macrophages, Brucella spp. reside in the first 8 to 12 h post infection within a membrane bound vacuole that undergoes endosomal maturation via sequential interactions with early (EE) and late (LE) endosomes and lysosomes (LYS) to become an acidified, endosomal Brucella-containing vacuole (eBCV). The host small GTPase Rab7 contributes to eBCV maturation, which provides physicochemical cues promoting expression of the VirB Type IV secretion system (T4SS), which translocates effector proteins (red) that mediate eBCV interactions with ER exit site and acquisition of ER and Golgi-derived membranes. These events lead to the biogenesis of replication permissive, ER-derived BCVs, called replicative BCVs (rBCVs). The host proteins Sar1, IRE1α, Yip1A, Atg9, WIPI1 and the COG complex contribute to rBCV biogenesis. Bacteria then undergo extensive replication in rBCVs between 12 and 48 h pi, after which rBCVs are captured within autophagosome-like structures in a VirB T4SS-dependent manner, to become autophagic BCVs (aBCVs). aBCV formation requires the host autophagy proteins Beclin1, ULK1 and Atg14. aBCVs harbors features of autolysosomes and are required for bacterial egress and new cycles of intracellular infections. Figures and legends extracted from [394].

6-) *Brucella* atypical niches

The intracellular life cycle described above occurs in the vast majority of cell types studied to date. However, a few exceptions are worth mentioning. *B. abortus* and *B. suis* can replicate in large endosomal inclusions in extra-villous trophoblasts (EVTs) JEG-3 [395] whereas *B. melitensis* mostly replicated in the typical ER-derived compartment. These

inclusions were shown to exclude LC3 and did not present with double membrane characteristic of autophagosomes, but it would be interesting to investigate if other autophagy proteins are involved in their formation. This phenotype was specific for EVT as *B. abortus* and *B. suis* still replicate within the ER in other trophoblast lineages as BeWo, JAR and HTR8 corresponding to villous trophoblasts [341,386]. Surprisingly, in JEG cells bacterial replication was partly independent from the T4SS [395]. So, EVTs represent another model cell line that is interesting to further explore to improve or knowledges on *Brucella* replication mechanisms. Interestingly, *Brucella papionis* (associated with stillbirth in primates) also infects human trophoblasts. However, it replicates actively in CTB, whereas its replication is very restricted within EVT; [396].

It is also important for me to note that *Brucella* does not have the same trafficking when it is Immunoglobulin G opsonized. Indeed, it has been shown that *B. abortus* is found in a LAMP-1 positive vacuole that will not be acidified in the human monocytic cell line THP1 [379]. Thus, opsonization seems to alter the intracellular trafficking of the bacteria by changing the nature of the eBCV but further work needs to be carried out to confirm these results.

Together these studies suggest *Brucella* presents some versatility and ability to adapt and replicate in alternative niches. How these niches are formed, what are the bacterial factors involved and the relevance of these atypical niches *in vivo* remains to be characterized.

IV-) *Brucella* effectors a cold war arsenal

This part does not aim to exhaustively list all the discovered *Brucella* effectors. This information can be found in **Table (2)** which regroups all the published effectors. But for this part of my thesis I class them given their mode of action or given the targeted process.

Table 2

Effectors	Chromosomal positions	Translocated	T4SS dependent	Ectopic localization	Eukaryotic domain	Eukaryotic target (s)	References
BtpA	BAB1_0279	Yes	No		TIR	TIRAP Myd88 MAL	Salcedo PLoS Pathogens 2008
BtpB	BAB1_0756	Yes	Yes		TIR	MyD88	Salcedo Frontiers 2013
VceA	BAB1_1652	Yes	Yes				deJong 2008 Molecular Microbiology
VceC	BAB1_1058	Yes	Yes	ER		BiP	deJong 2008 Molecular Microbiology
BPE123	BAB2_0123	Yes	Yes			ENO-1	Marchesini *et al*. 2011
BPE275	BAB1_1275	Yes	Yes				
BPE005	BAB1_2005	Yes	Yes				
BPE865			No				
RicA	BAB1_1279	Yes	No	On BCV (infection)		Rab2	Marchesini et al. 2011
SepA	BAB1_1492	Yes	Yes	On BCV (infection)			Döhmer *et al*. (2014)
PrpA	BAB1_1800	yes	unknown			NMIIA	Spera 2006 PNAS
BspA	BAB1_0678	Yes	Yes	ER			Myeni *et al*. 2013
BspB	BAB1_0712	Yes	Yes	ER		COG complex	
BspC	BAB1_0847	Yes	Yes	Perinuclear area consistent with Golgi apparatus			
BspD	BAB1_1611	Yes	did not work	ER			
BspE	BAB1_1671	Yes	Yes	peri-nuclear area			
BspF	BAB1_1948	Yes	Yes	cytoplasm and plasma membrane protusion	GNAT-family acetyltransferase domain		
BspG	BAB1_0227	Yes	no	cytosol/nucleus			
BspH	BAB1_1864	Yes	non conclusive	cytosolic	Armadillo repeat motifs		
BspI	BAB1_1865	Yes	non conclusive	cytosolic	GTPase Activating Protein (GAP) domain		
BspJ	BAB2_0119	Yes	Yes	cytosol nucleus			
BspK	BAB2_0541	Yes	no	ER			

1-) Secreted effector protein A (SepA) interferes with the endosomal pathway

SepA is an effector which was shown to be translocated in host cell in a *virB* dependent-manner and the only one that was shown to be important for *Brucella* trafficking in the endosomal pathway. Indeed, SepA seems to accumulate on the vacuolar membrane at the early stages of infection. Moreover, a *ΔsepA* mutant strain shows a significant defect in early stages of intracellular trafficking as it remains in a vacuole devoid of the typical eBCV marker LAMP1. Surprisingly, *ΔsepA* mutants are also more efficiently inactivated during the first stages of the replication process but have an increase capacity to invade host cells. Thus, the authors suggest that SepA could allow the bacteria to select the phagocytosis route, but this remains to be formally demonstrated [397].

2-) The secretory pathway targeted by multiple effectors

In many ways, it has been shown eBCVs undergo T4SS-dependent, sustained interactions with ERES structures during the eBCV/rBCV conversion stage. The importance of the secretory pathway for *Brucella* is today well established and accepted in the field. This is why to date, several effectors (further described below) are already identified to interfere with host secretory pathway [391,398,399].

The first identified effector is Rab2 interacting conserved protein A (RicA) which was established to preferentially bind the GDP form of the GTPase Rab2. This is consistent with the essential role of Rab2 in *Brucella* pathogenesis, shown to be recruited on the BCVs during infection [390]. For the bacteria it has been demonstrated that Rab2 has to be functional to allow the bacteria to establish its ER-derived niche [398]. Indeed GDP-locked form of Rab2 blocks the trafficking of the bacteria, which stay in late endosomal compartments. Although it is clear that Rab2 contributes to the maturation of the BCV its precise role and why it is the GDP-form of Rab2 that is preferentially bound by RicA remains to be determined.

Afterwards several effectors were identified in the same study to be associated to the subversion of some secretory pathway processes [399]. After an *in-silico* screen and an experiment of TEM1-β-lactamase to confirm that identified proteins are effectors, Myeni *et al*. [399] co-transfected these new identified effectors with a secretion reporter: Secreted Enzyme Alkaline Phosphatase (SEAP) which is an excellent reporter of a functional ER

secretion pathway. They showed that ectopically expressed *Brucella* secreted proteins A, B and F (BspA, B and F) inhibit the secretory pathway. The importance of BspB and F in the control of ER secretion was sustained in infection as cells infected with mutants of *bspB* and *bspF* did not show any secretion inhibition contrary to the bspA mutant. The importance of these Bsp proteins was further confirmed in infection as a *bspA*, *bspB* and *bspF* triple mutants failed to replicate as efficiently as the wild-type strain in murine macrophages [399].

In a more recent study, the same team more deeply investigated the mechanism of action of BspB. Indeed, they demonstrated that BspB interacts with the Conserved Oligomeric Golgi (COG) [391], a complex reported to be crucial for Golgi vesicular trafficking [400]. Moreover, this COG complex was shown to be a regulatory “carrefour" for secretory Rab GTPases known to be important for *Brucella* virulence.

Therefore, BspB modulates Golgi membrane traffic by interacting with COG. This interaction leads to a competition for Golgi-derived vesicles normally used for the protein secretion. Thus, the Golgi apparatus appears to be another source of membrane for rBCV biogenesis in addition to ER-derived membranes.

Finally, the same study showed that an inhibition of Rab2 GTPase via depletion of Rab2 counteracts the deleterious effect of a Δ*bpsB* mutant suggesting that BspB may affect retrograde secretory traffic to redirect COG-dependent Golgi vesicular traffic to the BCV [391].

3-) Effectors that targets UPR: Playing with Fire

Previously we have shown that UPR is necessary for *Brucella* replication. Consequently, several teams have tried to identify whether some effectors can be responsible of this phenotype.

One major effector involved in the induction of ER stress is the effector VceC. This effector was identified in a study which wanted to identify *virB*-coregulated genes [401]. Indeed, in this study they hypothesized that associated T4SS effectors will be genetically encoded close to the *virB* operon for genetic ergonomy and this is in this way after β-lactamase experiment that they identified 2 effectors VceA and VceC.

Few years later, they published another study regarding VceC. Transfection of VceC in HeLa cells showed extensive co-localization of this effector with ER markers. Moreover, they also observed a disruption of the ER morphology with the formation of particular

structures resulting in a vacuolation of the ER. Given the localization of the effector, they looked for putative partners of VceC and identified the ER chaperone BiP which is a major actor of ER stress process (see **Chapter 1**). Monitoring splicing of Xbp1 by RT-PCR and Western Blot they observed the apparition of 2 bands indicating an activation of the IRE1 pathway [361]. They also observed in infection and dependent of the translocation of this effector an up-regulation of pro-inflammatory responses with an increase of IL-6 and TNF-α secretion [361]. Thus, this study was the first to associate an effector with the induction of inflammation in macrophages.

To complete these first results the same team further investigated the importance of VceC for *Brucella* infection associated to ER stress, inflammation and immunity processes [138]. This study is very powerful as we have seen from work by Martinon *et al*. [137] PRRs are associated to ER stress but their exact involvement remained unclear. Interestingly, by studying the function of VceC, authors highlighted the association of NOD1 and NOD2, two NLRs that successfully associate to IRE1α via TRAF2 because NOD1/NOD2 both have TRAF2 motifs. When TRAF2 associates to IRE1 it leads to the induction of inflammation process with the translocation of NF-κB (see **Chapter 1**). Authors then elucidated if *Brucella* could induce the same pathways. As a control, they showed that the ER stress inducer thapsigargin induces IL-6 in a NOD1/NOD2 dependent manner, and they observed the same kind of induction with *Brucella* dependent of the T4SS identified effector VceC [138,361].
Furthermore, they demonstrated the importance of TRAF2 in this new pathway with the transfection of VceC in HEK293 cells which induced NF-κB activation. Nevertheless, if VceC is ectopically expressed in cells with dominant negative forms of TRAF2 the induction of NF-κB is abrogated [138].
All these processes led by VceC trigger ER stress that induces the IRE1-NOD1/2-dependent pro-inflammatory branch of the UPR could be linked with the abortion phenomenon observed during *B. abortus* infection. Authors went further and extended their study to another pathogen *Chlamydia muridarum* a bacterial pathogen also known to induce ER stress [204]. They infected HeLa cells and they also observed an activation of the NOD1/NOD2 dependent pathway [138]. It took 13 years to have the complete story for this fascinating effector, but it highlights how the research on bacterial effectors can also allow a better understanding of cellular fundamental processes.

Surprisingly Smith *et al*. [161] is the only study that shows that *B. melitensis* infection up regulated expression of the 3 UPR pathways after measuring by qPCR the mRNA of target genes BiP, CHOP, ERdj4, and spliced XBP1 in murine macrophages [161].
They also showed that *Brucella virB* mutant harbors an intact UPR induction while a *btpA* mutant presented reduced BiP, CHOP and ERdj4 expression. These results are surprising when we have seen the importance of VceC or with the new effector that we will present in the next chapter of Results: *Brucella* secreted protein L (BspL).
As what has been described for VceC they also showed that transfection of BtpA induced the overexpression of UPR genes and affects the morphology of the ER with again vacuolation of the ER network. Logically with their first results they observed that a *btpA* mutant less fragmented the ER [161].

The identification of these 2 effectors involved in ER stress represents a hot topic for *Brucella* characterization. In addition, in Myeni *et* al. the authors identified 3 other effectors: BspC, G and K demonstrated to induce ER stress [399] with the upregulation of BiP chaperone which let us to think an involvement in UPR. Otherwise we will see in the next chapter that our team characterized a new effector that induces ER stress and surprisingly for a new function.

4-) Effectors and host immunity processes: BtpA, BtpB and PrpA

Brucella was shown to down-modulate the maturation of dendritic cells and to inhibit the production of pro-inflammatory cytokines (such as TNF-α). This was in part due to a translocated effector called BtpA because of its ability to interfere with TLR2 and TLR4 signalling.

After these first observations, other studies from several groups further investigated how BtpA acts on the TLR pathways identifying Myd88 and TIRAP as targets. It was shown that BtpA efficiently blocks TIRAP-induced NF-ϰB. Interestingly it was also shown that BtpA can induce degradation of phosphorylated TIRAP by enhancing its poly-ubiquitination [402]. Consequently, these first papers demonstrated that BtpA can interact with a same target in order to interfere in downstream processes. Moreover authors deduced that BtpA controls inflammatory responses because ectopic BtpA has been shown to interact with phosphoinositides at the plasma membrane and modulate microtubule dynamics to misplace some specific adaptor molecules within the cell [373].

For the second target mentioned above, BtpA was shown to directly interact with MyD88 via the Death Domain and not the TIR domain of the adaptor. However, other groups have failed to detect an interaction with MyD88 [403]. Nevertheless, further work is now required to fully understand the molecular mechanism by which BtpA controls TLR signalling, which may involve interaction and/or competition with both MyD88 and TIRAP and maybe other immune players.

As BtpA, BtpB also contributes to the control of DC activation during infection [404]. Indeed, *btpB* mutant strain presents higher translocation of NF-κB and higher level of MHC-II at the surface and co-stimulatory molecules when compared with WT strain infection[27]. Even if BtpB shares some similarity sequence with BtpA they do not act as the same manner as BtpB can block all TLR *receptors in vitro* and seems to more strongly impact IL12 production by infected inflammatory DCs.

Interestingly susceptible IFNγ-/- mice infected with *btpB* mutant survived longer than those infected with the WT strain and this phenotype was even more striking for the double *btp1btp2* mutants which were highly attenuated in this model which confirms the major importance of BtpA and BtpB *in vivo*.

Otherwise another secreted protein was identified in *Brucella abortus* to induce the proliferation of B-cells. This protein is called Proline racemase protein A (PrpA) and was firstly demonstrated to induce the production of IL10 [405,406]. It induces a transient nonresponsive state of splenocytes, acts as a potent IL-10 inducer, and participates in the efficient establishment of a chronic infection in mice [406]. This protein is translocated during the replicative phase of *Brucella* and is able to bind macrophages through nonmuscular myosin IIA (NMM-IIA) in order to induce B-cell proliferation. Interestingly they also demonstrated that neutralization of NMM-IIA with the use of polyclonal antibody inhibits the interaction. Thus NMM-IIA can be considered either as a receptor or an adaptor for PrpA, in every case involved in a signaling process for B-cell proliferation [405].

V-) *Brucella* targets host metabolism

1-) *Brucella* modulates host metabolic pathways

As we have previously seen in the **Chapter 1** with *Orientia tsutsugamushi*, intracellular pathogens are in competition with host cell metabolism process for nutrient

acquisition. In the study of Rodino *et al*. it was for the acquisition of amino acid, but it can be generalized to other metabolites as glucose or calcium [407]. *Brucella* is no exception as nutrient uptake is certainly vital during infection. Moreover, it is today known that some pathogens induce metabolic shift in the infected host cells reminiscent of the Warburg effect initially described in cancer cells and in immune cells (see **Chapter 2**). As a reminder the glycolysis without a fully functioning Krebs cycle leads to an over production of lactic acid which is a hallmark of Warburg effect (see **Chapter 2**). Understanding the capacity of *Brucella* to play with all the different metabolic pathways will be essential for obtaining a full picture of the intracellular life cycle and has recently started to be investigated with two main studies. The first one of Xavier *et* al. [297] perfectly illustrates the link between metabolism shift induced by *Brucella abortus* and the activation of some immune cells as macrophages that were separated in two groups: classically activated macrophages (CAMs or M1) and alternatively activated macrophages (AAM or M2). The nature of the macrophages depends of the host inflammatory response according to the produced cytokines. Indeed, CAMs are induced by IFN-γ and are known to exert an anti-microbicidal activity by secreting pro-inflammatory cytokines. Whereas for AAMs it has been established the involvement of IL-4 and 13 in their differentiation. AAMs are known to be less efficient in host immunity defense as they present a reduced microbicidal activity and secrete anti-inflammatory cytokines which is consistent with *Brucella* strategy infection mentioned with Btp proteins. As mentioned above the transition of CAMs to AAMs is accompanied by a metabolism shift [408]. It has been demonstrated that CAMs mainly use glucose for an anaerobic metabolism associated with Krebs cycle and oxidative phosphorylation. On the contrary it has been shown that AAMs use the β-oxidation pathways as nutrients to produce energy. Indeed, glucose levels are higher in AAMs than in CAMs so it is more interesting for the bacteria to differentiate macrophages in AAMs where there will be more available glucose. Moreover, in AAMs bacteria can use alternative pathway as β-oxidation or fermentation process for its own replication as it can use some metabolic substrates to produce energy. Nevertheless, and interestingly authors have shown that a *gluP* mutant strain defective for glucose transporter presented both a reduced intracellular survival in AAMs and persistence in mice. These results sustain the importance of glucose for *Brucella* proliferation even if the pathogen can adapt itself to different metabolisms.

To go further Xavier *et al*. [297] identified the cellular actor that is responsible of the metabolic shift in AAMs: the peroxisome proliferator activated receptor γ (PPARγ). This

protein was demonstrated to be able to increase intracellular glucose availability. Indeed, Signal transduction through the nuclear peroxisome proliferator-activated receptors PPARγ and PPARδ orchestrates the patterns of gene expression required for the development of AAMs [409]. Thus, it is the increased availability of glucose as a carbon and energy source that makes AAMs a permissive site for intracellular replication of the brucellae during chronic infection rather than the fact that AAMs have reduced bactericidal activities compared to CAMs. Given the importance of PPARγ to promote chronic persistence and enhance bacterial survival of *B. abortus* within AAM it can represent an interesting target to counteract *Brucella* infection.

The second study confirms in macrophage-like cells (Thp1) that *Brucella* induces a metabolic shift [410]. In this study, the Krebs cycle was shown to be altered which is correlated with a decrease of amino acid degradation and an increase of lactate level which looks like to a Warburg effect. Indeed, *Brucella* inhibits the Krebs cycle to force the cell to make more glucose available to increase glycolysis for their own benefit [410]. This inhibition of Krebs cycle forced the cell towards fermentation and production of alternative metabolites as lactate that can be used as a carbon source for *Brucella*.

Authors demonstrated that *B. abortus* infection of Thp1 cells impairs mitochondrial function and localization, with a "polarization" of all the mitochondria. As explained in the previous chapter mitochondria are very important for metabolic processes because this is where the Krebs cycle undergo. This is why the authors of Czych *et al.* [410] tested the respiratory chain activity associated to mitochondria function. Their results demonstrated that *B. abortus* infection acts as mitochondrial inhibitors and inhibits human THP-1 cells to utilize amino acids as an energy source. Furthermore, they shown that an increased MOI of *Brucella* leads to an increase consumption of glucose [410]. And finally, *B. abortus* required lactate dehydrogenase for normal intracellular survival in THP-1 cells which is consistent with the increased concentration of lactate

2-) *Brucella* and mitochondria: a new target for this pathogen

Given the multiple functions ensured by mitochondria and the two previous studies on the metabolism it now appears crucial to investigate the connexion between *Brucella* and this organelle. In infected cells, *Brucella* was shown to be tightly associated to mitochondria by electron microscopy even if this close association does not result in any cytoskeleton

reorganization [411]. Interestingly the experiment was reproducible with *in vitro* cell lines (HeLa cells) and primary cells (trophoblasts from BALB/c mice). They next used confocal microscopy to visualize the mitochondrial network. Surprisingly they observed fragmentation of the mitochondrial network in different cell lines after *B. abortus* and *B. melitensis* infection. In spite of this strong phenotype *Brucella* replication was not affected. Authors then tried to identify the cellular partner hijacked by *Brucella* to induce this fragmentation. They focused on Drp1 as it is connected with mitochondrial fission processes, but it appears that the fragmentation was Drp1 independent. As a final hypothesis, authors suggested the observed fragmentation may be related to defects in the fusion process during *Brucella* infection, which remains to be investigated.

Because this paper came after those from Czych *et al.* [410] and Xavier *et al.* [297] they decided to study another process of the mitochondria the regulation mitochondrial reactive oxygen species (mtROS) production. But again, they did not observe any consequences for bacterial replication with the modulation of mtROS. In the continuity of the previous studies they blocked the mitochondrial respiration and without surprise they did not observe any effect which is consistent that *Brucella* not requiring oxidative phosphorylation and surviving with aerobic mitochondrial metabolism. Because mitochondria and ER are connected via MAMs and given the importance of the calcium in MAM-dependent processes, they also measured the impact on mitochondrial calcium uptake. But again, the calcium levels were not found to be responsible for the observed mitochondrial morphology.

Finally, they tested if the fragmentation could be related to interference with apoptosis. Indeed, given the link of mitochondria to the intrinsic pathway of apoptosis they induced apoptosis with TNF-α to see if the mitochondrial fragmentation could confer to bacteria protection from apoptosis but they did not observe any protective effect of the induced mitochondrial fragmentation.

Brucella-induced fragmentation does not impact replication nor TNF-α induced apoptosis, which would have been an interesting explanation of how *Brucella* controls host cell death as reported in several studies. It is important to note that a few studies, reported that in some cell lines *Brucella* can induce apoptosis but given their controversy, this topic remains to be further investigated and will be further discussed in the **Chapter 6**.

Chapter 4 Results Part 1: Manuscript in submission

Brucella effector targets Herp, seizing the endoplasmic reticulum quality control machinery to prevent premature egress

Jean-Baptiste Luizet[1], Julie Raymond[1], Thais Lourdes Santos Lacerda[1], Magali Bonici[1], Frédérique Lembo[2], Kévin Willemart[3], Jean-Paul Borg[2], Jean-Pierre Gorvel[4], Suzana P. Salcedo[#1]

[1]Laboratory of Molecular Microbiology and Structural Biochemistry, Centre National de la Recherche Scientifique UMR5086, Université de Lyon, Lyon, France.

[2]CRCM, Inserm, Institut Paoli-Calmettes, Aix-Marseille Université, CNRS, Marseille, France

[3]Research Unit in Microorganisms Biology, University of Namur, B-5000 Namur, Belgium

[4]Aix-Marseille Univ, CNRS, INSERM, CIML, Marseille, France

[#]Corresponding author and lead contact: suzana.salcedo@ibcp.fr

Abstract

Perturbation of the endoplasmic reticulum (ER), a central organelle of the cell, can have critical consequences for cellular homeostasis. An elaborate surveillance system known as ER quality control ensures that cells can respond and adapt to stress *via* the unfolded protein response (UPR) and that only correctly assembled proteins reach their destination. Interestingly, several bacterial pathogens have been shown to hijack the ER to establish an infection. However, it remains poorly understood how bacterial pathogens exploit ER quality control functions to complete their intracellular cycle. *Brucella* spp. replicate extensively within an ER-derived niche, which evolves into specialized vacuoles suited for exit from infected cells. Here we present BspL, a new *Brucella abortus* type IV secretion system effector that targets Herp, a key component of ER-associated degradation (ERAD) machinery. We found that BspL strongly enhances ERAD, independently of the UPR. Targeting of Herp allows tight control of the kinetics of autophagic *Brucella*-containing vacuole formation, delaying the last step of its intracellular cycle and preventing premature bacterial egress from infected cells. This study highlights a new mechanism by which an intracellular bacterial pathogen hijacks ERAD components for fine regulation of its intracellular trafficking.

Keywords: *Brucella*, ERAD, trafficking, Herp, ERQC

Introduction

The endoplasmic reticulum (ER) is the largest organelle in the cell and plays numerous functions vital for maintaining cellular homeostasis. It is the major site for protein synthesis of both secreted and integral membrane proteins as well as exporting of newly synthesised proteins to other cellular organelles. Disturbance or saturation of the folding-capacity of the ER leads to a complex stress response that has evolved to help cells recover homeostasis or, if necessary, commit them to death. The ER relies on a complex surveillance system known as ER quality control that ensures handling of misfolded, misassembled or metabolically regulated proteins [1]. Once retained in the ER, these proteins are retrotranslocated into the cytosol to be ubiquitinated and degraded by the proteasome, a process known as ER-associated degradation (ERAD) [2]. Alternatively, ERAD-resistant proteins can be degraded *via* ER-phagy [3]. In response to perturbations of ER quality control, ER stress ensues and cells activate a set of inter-connected pathways that are collectively referred to as the unfolded protein response (UPR), critical for restoring homeostasis [4].

The homocysteine-inducible ER stress protein (Herp) is an ER membrane protein that is highly upregulated during ER stress by all UPR branches [5,6]. Herp is a key component of ERQC that plays a protective role in ER stress conditions [7,8]. It is an integral part of the ERAD pathway, enhancing the protein loading and folding capacities of the ER. In addition, it acts as a hub for membrane association of ERAD machinery components, stabilizing their interactions with substrates at ER quality control sites [9] and facilitating their retrotranslocation [10]. Furthermore, as Herp is also in a complex with the proteasome it may aid delivery of specific retrotranslocated substrates to the proteasome for degradation [11,12].

Given its importance for cellular homeostasis, the ER quality control represents a prime target for microbial pathogens. Indeed, a growing number of bacterial pathogens have been shown to modulate UPR [13]. This is the case of *Brucella* spp., a facultative intracellular pathogen that causes brucellosis, a zoonosis still prevalent worldwide. *Brucella abortus* has been shown to induce UPR [14,15], and more specifically the IRE1 pathway, contributing to enhanced inflammation, a process particularly relevant in the context of colonization of the placenta and abortion [16]. However, activation of IRE1 is also important for *Brucella* trafficking and subsequent *Brucella* multiplication [15,17]. After cellular uptake, *Brucella* is found in a membrane bound compartment designated endosomal *Brucella*-containing vacuole (eBCV) which transiently interacts with early and late endosomes, undergoing limited fusion with lysosomes [18]. Bacterial are then able to sustain interactions with ER exit sites (ERES) a process that requires the activity of the small GTPases Sar1 [19] and Rab2 [20] and results in the establishment of an ER-derived compartment suited for multiplication (replicative or rBCV)[21]. UPR induction by *Brucella* is necessary for this trafficking step, as the formation of rBVCs is dependent on IRE1 activation by the ERES-localized protein Yip1A, which mediates IRE1 phosphorylation and dimerization [22]. Once rBCVs are established, *Brucella* is capable of extensive intracellular replication, without induction of cell death. Instead, at late stages of the intracellular cycle, rBCVs reorganize and fuse to form large autophagic vacuoles (aBCVs) that will mediate bacterial exit from infected cells [23]. The bacterial factors behind the switch between rBCVs and aBCVs remain uncharacterized.

Brucella relies on a type 4 secretion system (T4SS), encoded by the *virB* operon and induced during eBCV trafficking to translocate bacterial effectors into host cells and directly modulate cellular functions, including the biogenesis of rBCVs [24-26] and formation of aBCVs [27]. However, only a few effectors have been characterized and for which we have a full grasp of how they contribute towards pathogenesis. This system has been implicated in the induction of UPR

during infection and a subset of these effectors has been shown to modulate ER-associated functions. VceC interacts with the ER chaperone BiP to activate the IRE1 pathway, which results in NOD1/NOD2 activation and up-regulation of inflammatory responses [14,16]. BspA, BspB and BspF have all been implicated in blocking of ER secretion [28]. In particular, BspB was shown to interact with the conserved oligomeric Golgi (COG) complex to redirect vesicular trafficking towards the rBCVs [29]. Several other effectors that localize in the ER when ectopically expressed have been shown to induce UPR or control ER secretion, but the mechanisms involved remain uncharacterized.

In this study, we identify a new T4SS effector of *Brucella abortus,* that we designate as *Brucella*-secreted protein L (BspL) that targets a component of the ERAD machinery, Herp. BspL enhances ERAD and delays the formation of aBCVs, preventing early bacterial release from infected cells which helps maintain cell to cell spread efficiency.

Results

BspL is a *Brucella* T4SS effector protein

Bacterial effectors often contain domains and motifs that are characteristic of eukaryotic proteins. This is the case for example of SifA from *Salmonella enterica* [30,31] and AnkB from *Legionella pneumophila* [32,33] that contain a carboxyl-terminal CAAX tetrapeptide motif (C corresponds to cysteine, A to aliphatic amino acids and X to any amino acid) that serves as a lipidation site to facilitate membrane attachment. Previous work highlighted several *Brucella* encoded proteins that contain putative CAAX motifs [32] which could therefore be T4SS

121 effectors. In this study, we focused on one of these proteins encoded by the gene BAB1_1533
122 (YP_414899.1), that we have designated BspL for *Brucella*-secreted protein L.
123
124 We first determined if BspL was translocated into host cells during infection. We constructed
125 a strain expressing BspL fused to the C-terminus of the TEM1 ß-lactamase (encoded by *bla*)
126 and infected RAW macrophage-like cells for different time-points. A Flag tag was also included
127 for control of protein expression. The fluorescent substrate was added and the emission of
128 coumarin, resulting from cleavage by the cytosolic TEM1 lactamase, was detected by confocal
129 microscopy. This assay is widely used in the *Brucella* field and we included the T4SS effector
130 VceC as a positive control [34], which showed the highest level of secretion at 24h post-infection
131 in our experimental conditions (Figure 1A). We found that TEM1-BspL was secreted into host
132 cells as early as 4h post-infection, with a slight peak at 12h post-infection, CCF2 cleavage was
133 still detected at 24h post-infection (Figure 1A). This phenotype was fully dependent on the
134 T4SS as a Δ*virB9* mutant strain did not show any coumarin fluorescence (Figure 1A and B).
135 This was not due to lack of expression of TEM1-BspL as both the wild-type and the Δ*virB9*
136 strains carrying the *bla*::*bspL* plasmid showed equivalent levels of TEM1-BspL (Figure 1C).
137 Together, these results show BspL is a T4SS effector.
138
139 **Ectopically expressed BspL accumulates in the ER, does not interfere with host protein**
140 **secretion but induces the UPR**
141 BspL is very well conserved in the *Brucella* genus, it is 170 amino acids long (Figure S1A) and
142 is approximately 19 kDa. BspL does not share any homology to eukaryotic proteins nor to other
143 bacterial effectors. Its nucleotide sequence encodes for a sec secretion signal, a feature
144 commonly found in other *Brucella* effectors [35]. In addition, it contains a hydrophobic region as
145 well as a proline rich domain, with seven consecutive prolines. To gain insight into the function

146 of BspL we ectopically expressed HA, myc or GFP-tagged BspL in HeLa cells. We found BspL
147 accumulated in the ER, as can be seen by the co-localization with calnexin (Figure 2A and S1B,
148 S1C), an ER membrane protein and chaperone. Unlike what has been reported for VceC [14], the
149 structure of the ER remained relatively intact upon BspL expression. Deletion of the C-terminal
150 tetrapeptide sequence had no effect on the ER localization of BspL in transfection (Figure S1B,
151 bottom panel), as it significantly overlapped with the full-length protein when co-expressed in
152 the same cell (Figure S1C).
153
154 Our observations suggest BspL is part of a growing number of *Brucella* effectors that
155 accumulate in the ER when ectopically expressed, including VceC, BspB and BspD [14,28]. We
156 therefore investigated if BspL shared any of the ER modulatory functions described for other
157 effectors, notably interference with ER secretion as BspB [28,29] or induction of ER stress as VceC
158 [14,16].
159 To determine the impact of BspL on host protein secretion we used the secreted embryonic
160 alkaline phosphatase (SEAP) as a reporter system. HEK cells were co-transfected with the
161 vector encoding SEAP and vectors encoding different *Brucella* effectors. We chose to work
162 with HA-BspL, to allow direct comparison with previously published HA-BspB that blocks ER
163 secretion and HA-BspD as a negative control [28]. Expression of the GDP-locked allele of the
164 small GTPase Arf1[T31N], known to block the early secretory pathway, was used as a control
165 for efficient inhibition of secretion (Figure S1D). As previously reported, we found that
166 expression of HA-BspB drastically reduced SEAP secretion (Figure S1D). In contrast, HA-
167 BspL did not impact SEAP secretion to the same extent as BspB, having an effect equivalent
168 to HA-BspD previously reported not to affect host protein secretion [28].
169

We next investigated whether ER targeting of BspL was accompanied with activation of the UPR, an important feature of *Brucella* pathogenesis [16,17,22]. In the case of *B. abortus*, IRE1 is the main pathway activated [14] which leads to splicing of the mRNA encoding the transcription factor X-box-binding protein 1 (XBP1) which in turn induces the expression of many ER chaperones and protein-folding enzymes. The second branch of the UPR dependent on PERK may also be of relevance in *Brucella* infection [15]. Under prolonged stress conditions, this UPR branch leads to the up-regulation of the transcription factor C/EBP-homologous protein (CHOP) which induces expression of genes involved apoptosis. We therefore monitored *XBP1s* and *CHOP* transcript levels following ectopic expression of HA-BspL, in comparison to HA-VceC, established as an ER stress inducer and HA-BspB, known not to induce ER stress. Treatment with tunicamycin, a chemical ER stress inducer was also included. We found that over-expression of HA-BspL induced an increase of both *XBP1s* and *CHOP* transcription, to levels even higher than HA-VceC (Figure 2B and C). These results suggest BspL may induce ER stress.

BspL is not involved in establishment of an ER-derived replication niche but is implicated in induction of ER stress during infection

As UPR has been implicated in the establishment of rBCVs [22] and intracellular replication [15,17,22] of *Brucella* we next investigated the intracellular fate of a *B. abortus* 2308 strain deleted for *bspL* in comparison with the wild-type. Two cellular models were used, HeLa cells and an immortalized cell line of bone marrow-derived macrophages (iBMDM). We found that the Δ*bspL* strain replicated as efficiently as the wild-type in both iBMDM (Figure S2A) and HeLa cells (Figure S2B). In terms of intracellular trafficking no obvious differences were observed in the establishment of rBCVs at 24 and 48h post-infection, as Δ*bspL* BCVs were nicely decorated with the ER marker calnexin in both cell types (Figure 2D and E) as observed for the

wild-type strain (Figure S2C and D). As this is the first report to our knowledge to use iBMDM in *Brucella* infections, we confirmed this observation by quantifying the percentage of BCVs positive for calnexin and the lysosomal associated membrane protein 1 (LAMP1) in comparison with the wild-type at 24 and 48 post-infection (Figure S2E and F, respectively). The wild-type strain in this cellular model behaved as expected forming the typical rBCVs.

As in transfected cells we found that BspL induced UPR, we next monitored the levels of *XBP1s* and *CHOP* transcripts during infection. Since the rate of infected cells is too low to detect ER stress in HeLa cells, these experiments were only performed in iBMDMs. As expected, the wild-type *B. abortus* strain induced an increase in the levels of transcription of *XBP1s* in relation to the mock-infected control iBMDM at 48h post-infection (Figure 2F). In contrast, Δ*bspL* infected macrophages showed decreased *XBP1s* transcript levels compared to the wild-type (Figure 2F). Furthermore, the wild-type phenotype could be fully restored by expressing a chromosomal copy of *bspL* in the Δ*bspL* strain, confirming that BspL specifically contributes towards induction of the IRE1 branch of the UPR during infection (Figure 2F). We did not observe an increase in *CHOP* transcript levels in iBMDM infected with the wild-type nor Δ*bspL* strains in comparison to the mock-infected cells (Figure 2G), suggesting that *B. abortus* does not significantly induce the PERK-dependent branch of the UPR at this stage of the infection.

BspL interacts with Herp, a key component of ERQC

To gain insight into the function of BspL we set out to identify its interacting partners. A yeast two-hybrid screen identified 7 candidates: eukaryotic translation initiation factor 4A2 (EIF4A2), pyruvate dehydrogenase beta (PDHB), MTR 5-methyltetrahydrofolate-homocysteine methyltransferase, Bcl2-associated athanogene 6 (BAG6), ARMCX3 armadillo

repeat containing protein (Alex3), homocysteine-inducible ER protein with ubiquitin like domain (Herpud1 or Herp) and Ubiquilin2 (Ubqln2).

In view of our previous results for BspL showing ER localization and induction of UPR we decided to focus on Alex3, Herp and Ubiquilin2 which are rarely present or even absent in the database of false positives for this type of screen (http://crapome.org/). Alex3 is a mitochondrial outer membrane protein that has been implicated in regulation of mitochondrial trafficking [36]. As ER and mitochondria extensively interact, Alex3 could constitute an interesting target. Herp is an ER membrane protein playing a role in both the UPR and the ERAD system whereas Ubiquilin2 is implicated in both the proteasome and ERAD and, interestingly, shown to interact with Herp [37]. In view of these different targets we decided to carry out an endogenous co-immunoprecipitation in cells expressing HA-BspL. As controls for detecting non-specific binding, we also performed co-immunoprecipitations from cells expressing two other ER-targeting effectors, HA-BspB and HA-VceC. We then probed the eluted samples with antibodies against Alex3, Ubiquilin2 or Herp to detect if any interactions could be observed. We found that Alex3 was co-eluted with all 3 effectors suggesting a potentially non-specific interaction with the effectors or the resin itself (Figure 3A). In contrast, no interactions were observed with Ubiquilin2, which was detected only in the flow through fractions. However, we found that endogenous Herp specifically co-eluted with HA-BspL and not the other effectors (Figure 3A), suggesting Herp and BspL form a complex within host cells. To confirm these results, we co-expressed GFP-BspL with Flag-Herp in HeLa cells and carried out a co-immunoprecipitation. Despite much higher levels of GFP expression, only GFP-BspL was able to co-immunoprecipitate Flag-Herp (Figure 3B) confirming they are part of the same complex. Taken together with the yeast two-hybrid data, we can conclude that BspL directly interacts

243 with Herp. Consistently, over-expressed BspL co-localized with Herp by microscopy (Figure
244 3C).
245
246 **BspL facilitates degradation of TCRα *via* ERAD independently of ER stress**
247 Herp is a key component of ERAD, strongly up-regulated upon ER stress [6]. Indeed, during *B.*
248 *abortus* infection we observed an up-regulation of *HERP* transcripts (Figure S3A), consistent
249 with *XBP1s* induction, although these differences were not statistically significant with the
250 number of replicates carried out. However, inhibition of Herp using siRNA (Figure S3B)
251 showed that ER stress induced following ectopic expression of BspL was not dependent on
252 Herp (Figure S3C and D), suggesting BspL interaction with Herp is mediating other functions
253 in the cell.
254
255 Therefore, we next investigated if BspL could directly impact ERAD. We used expression of
256 T cell receptor alpha (TCRα) as reporter system, as this type I transmembrane glycoprotein has
257 been shown to be a canonical ERAD substrate, quickly degraded [38,39]. TCRα is transferred
258 across the ER membrane, where is becomes glycosylated and fails to assemble. This in turn
259 induces its retrotranslocation to the cytosol to be degraded by the proteasome. Cycloheximide
260 treatment for 4 h was used to block protein synthesis, preventing replenishment of TCR pools
261 and allowing for visualization of ERAD-mediated degradation of TCRα. When HEK-293T
262 cells, which do not naturally express TCR were transfected with HA-TCRα and treated with
263 cycloheximide, a decrease in HA-TCRα was observed, indicative of degradation (Figure 4A,
264 red arrow). Strikingly, expression of BspL induced very strong degradation of TCRα (Figure
265 4A). This is accompanied by the appearance of a faster migrating band at around 25 KDa (blue
266 arrow), that nearly disappears upon cycloheximide treatment suggesting this TCRα peptide is
267 efficiently degraded by the proteasome. It is important to note that the 25 KDa band is also

present when HA-TCRα is expressed alone (lane 2 of Figure 4A, blue arrow) suggesting it is a natural intermediate of HA-TCRα degradation.

To determine if the enhanced effect of BspL on TCRα degradation is a side-effect of ER stress, cells were treated with TUDCA which strongly inhibited both *XBP1s* and *CHOP* transcript levels induced by either tunicamycin, BspL or VceC (Figure S3E and F). In the presence of TUDCA, BspL was still found to enhance HA-TCRα degradation showing this is occurring in an ER stress-independent manner (Figure S4).

As the TCRα subunit undergoes N-glycosylation in the ER, we wondered if the faster migrating band of TCRα induced by BspL corresponded to non-glycosylated form of TCRα. We therefore treated samples with EndoH, which deglycosylates peptides. Upon EndoH treatment we observed deglycosylated HA-TCRα (second lane, Figure 4B, black arrow), confirming the reporter system is being processed normally. In the BspL expressing samples (lanes 3 and 4, Figure 4B), a slight band corresponding to the non-glycosylated TCRα could also be detected particularly after EndoH treatment, confirming that BspL does not prevent TCRα from entering the ER and being glycosylated. The dominant TCRα band induced upon BspL expression (around 25 KDa, blue arrow) migrates faster than the non-glycosylated form resulting from EndoH treatment (black arrow) and does not appear to be sensitive to EndoH. This may therefore correspond to a natural truncated non-glycosylated form of HA-TCRα. Consistently, this band is also present in the absence of BspL (lane 1, Figure 4B, blue arrow).

Together these data indicate that BspL is a strong inducer of ERAD, implicating for the first time this process in *Brucella* pathogenesis. We therefore decided to block ERAD during infection using eeyarestatin, an established inhibitor of this system that targets the p97-

293 associated deubiquinating process and sec61-dependent protein translocation at the ER.
294 Unfortunately, prolonged treatment at the concentration necessary for full inhibition of ERAD
295 induced detachment of infected iBMDM. Nonetheless, we were able to carry out this
296 experiment in HeLa cells, which showed significant resistance to the eeyarestatin treatment.
297 Total CFU counts after addition of eeyarestatin at 2h post-infection showed a significant
298 decrease in bacterial counts at 48h, suggesting a potential inhibition of replication (Figure S5A).
299 However, microscopy observation of infected cells at this time-point clearly showed extensive
300 replication of bacteria even in the presence of eeyarestatin (Figure S5B). To confirm this
301 possibility, we counted by microscopy the number of bacteria per cell at 24h post-infection and
302 indeed found a higher replication rate upon eeyarestatin treatment (Figure S5C). These results
303 suggest that blocking of ERAD during early stages of infection favour intracellular replication,
304 a phenotype clearly not dependent on BspL, as we have shown it is not implicated in the
305 establishment of rBCVs and when ectopically expressed it induces ERAD. Therefore, we
306 hypothesized that the drop of CFU observed upon inhibition of ERAD at 48h post-infection
307 was a result of enhanced exit of bacteria from infected cells rather than inhibition of intracellular
308 replication.
309
310 **BspL delays premature bacterial egress from infected cells**
311 The late stage of the intracellular cycle of *Brucella* relies on induction of specific autophagy
312 proteins to enable the formation of aBCVs characterized as large vacuoles decorated with
313 LAMP1 containing multiple bacteria [23]. In our experimental conditions aBCVs could be clearly
314 observed in iBMDM infected for 65h with wild-type *B. abortus* (Figure 5A). We therefore
315 investigated if BspL was involved in formation of aBCVs. Strikingly, Δ*bspL* aBCVs could be
316 detected as early as 24h, with nearly 30% of infected cells showing aBCVs at 48h post-infection
317 compared to less than 10% for wild-type infected cells (Figure 5B and C). Importantly,

318 complementation of the Δ*bspL* strain fully restored the wild-type phenotype. These results show
319 that BspL is involved in delaying the formation of aBCVs during *B. abortus* macrophage
320 infection. As aBCV formation was previously linked to *Brucella* exit from infected cells and
321 spread to neighbouring cells [23,27] we next searched for re-infection events. Wild-type infected
322 iBMDM at 48h post-infection showed none or few signs of re-infection with most cells showing
323 extensive perinuclear ER-like distribution of bacteria (Figure 5D). In contrast, imaging of
324 Δ*bspL* infected iBMDM at the same time-point revealed the presence of high numbers of
325 extracellular bacteria as well as cells with single bacteria or a single aBCV (Figure 5D),
326 suggestive of re-infection and reminiscent of what was previously described for wild-type *B.*
327 *abortus* at 72 h post-infection [23].
328
329 In view of our results and the fact that BspL interacts with Herp, we hypothesized that secretion
330 of BspL during *Brucella* infection modulates ERAD machinery to control aBCV formation and
331 prevent premature bacterial egress from infected cells. To test this hypothesis, we next analysed
332 aBCV formation in cells either depleted for Herp or upon blocking ERAD with eeyarestatin.
333 We took advantage of our HeLa cell model, in which aBCVs can still be monitored although
334 the vacuoles formed are much smaller in size [23]. We first confirmed that BspL was also
335 implicated in formation of aBCV in this cell type by quantifying the number of cells containing
336 aBCVs, in our case defined as a vacuole with a least 4 bacteria surrounded by a single LAMP-
337 positive membrane. We found that at 48h post-infection a strain lacking *bspL* formed
338 significantly more aBCVs than the wild-type and complemented strains (Figure 6A), as we
339 observed for iBMDM.
340 As initial blocking of ERAD enhances intracellular replication and may therefore impact early
341 trafficking events we decided to inhibit ERAD and Herp at 24h post-infection to allow normal
342 establishment of rBCVs. Interestingly, we found eeyarestatin enhanced aBCV formation at 65h

(Figure 6B). These results suggest ERAD contributes towards aBCV formation at late stages of the cell cycle. However, these results contrasted with the observations made for Δ*bspL,* in which aBCV formation is precocious. In contrast, inhibition of Herp at 24h post-infection resulted in higher percentage of cells with aBCVs being formed at 48h compared to siControl treated cells (Figure 6C), perfectly mimicking the results obtained with Δ*bspL.* Together these results show that blocking of ERAD impacts aBCV formation but is not sufficient to account for the aBCV phenotypes observed at 48h, which require full inhibition of Herp. Therefore, we propose that BspL delays aBCV formation by directly modulating Herp functions.

Discussion

In this study, we characterize a previously unknown T4SS effector of *B. abortus* and its role in virulence. We found this effector hijacks the Herp, a component of the ERAD machinery to regulate the late stages of the *Brucella* intracellular cycle. Although many bacterial pathogens have been shown to control UPR, very little is known about the impact of ERAD, a downstream process following UPR, in the context of intracellular bacterial infections. To our knowledge there are only two examples. The obligatory intracellular pathogen *Orientia tsutsugamushi,* the cause of scrub thypus, is an auxotroph for histidine and aromatic amino acids and was shown to transiently induce UPR and block ERAD during the first 48h of infection [40]. This in turn enables release of amino acids in the cytosol, necessary for its growth [40]. The second example is *Legionella pneumophila*, that recruits the AAA ATPase Cdc48/p97 to its vacuole, that normally recognizes ubiquitinated substrates and can act as a chaperone in the context of ERAD to deliver misfolded proteins to the proteasome. Recruitment of Cdc48/p97 to the *Legionella* vacuole is necessary for intracellular replication and helps dislocate ubiquitinated proteins from the vacuolar membrane, including bacterial effectors [41].

368 In the case of BspL we found it directly interacts with Herp, a component of ERAD which is
369 induced upon UPR. Our data suggest that BspL enhances ERAD and this prompted us to further
370 investigate the role of ERAD during *Brucella* infection. Interestingly, we found that inhibition
371 of ERAD is beneficial during early stages of intracellular trafficking and enhances bacterial
372 multiplication. It is possible that *Brucella* is transiently blocking ERAD during rBCV formation
373 and initial replication, potentially *via* a specific set of effectors or a particular cellular signal yet
374 to be identified. This could, as demonstrated for *Orientia*, release amino acids into the cytosol
375 that would be critical for bacterial growth. Alternatively, or in parallel, a block of ERAD could
376 potentially enhance autophagy [42] to deal with the ER stress that would in turn favour rBCV
377 formation.
378
379 As a permanent block of ERAD could become damaging to the cell under prolonged stress and,
380 as we observed, speed up the bacterial release from infected cells potentially prematurely,
381 *Brucella* translocation of BspL could counteract these effects by enhancing ERAD and slowing
382 down aBCV formation. We could not directly show BspL ERAD induction is dependent on
383 Herp as its depletion would itself block ERAD [12,43]. However, in the presence of BspL no
384 glycosylated ER loaded HA-TCRα was observed indicative of enhanced processing through
385 the ERAD pathway. Instead, only a truncated unglycosylated TCRα intermediate was detected,
386 which disappeared in the presence of cycloheximide suggesting it is efficiently degraded. These
387 likely correspond to a backlog of peptides awaiting proteasomal degradation, generated by an
388 abnormal ERAD flux induced by BspL.
389
390 Further work is now required to establish the precise mechanisms that enables BspL to facilitate
391 ERAD. It is possible that BspL interaction with Herp stabilizes it, preventing its degradation
392 and would therefore help sustain ERAD. Indeed, ER stress significantly induces Herp levels

393 but Herp was shown to be quickly degraded, enabling efficient modulation of ERQC [44].
394 Alternatively, BspL may favour Herp accumulation at ERQC sites that would also enhance its
395 ability to assist protein retrotranslocation and delivery to proteasomes.
396
397 This study focuses on BspL-Herp interactions, nevertheless we cannot exclude the participation
398 of other potential targets identified in the yeast-two hybrid screen, notably Ubiquilin2 and Bag6.
399 Ubiquilin2 functions as an adaptor protein between the proteasome and ubiquination machinery
400 and therefore participates in ERAD. Ubiquilin2 also interacts with Herp [37] and very
401 interestingly has been shown to play a role in control of autophagy [45]. Our co-
402 immunoprecipitation experiment did not reveal any binding but perhaps a weak or transient
403 interaction is taking place not detectable with our current *in vitro* conditions. Another
404 interesting target is Bag6, (also known as Bat3) a chaperone of the Hsp70 family that is also
405 involved in delivery of proteins to the ER or when they are not properly folded to the
406 proteasome. Bag6 was shown to be the target of the *Orientia* Ank4 effector that blocks ERAD
407 [40] and to be targeted by multiple *Legionella* effectors to control host cell ubiquitination
408 processes [46]. Therefore, it is possible that Bag6 may contribute towards BspL control of ERAD
409 functions during *Brucella* infection.
410
411 In addition to ERAD, we found that BspL itself was implicated in induction of UPR. However,
412 this phenotype was independent of Herp and may be an indirect effect due to its ER
413 accumulation or *via* another cellular target yet to be characterized. Furthermore, the increased
414 ERAD activity upon BspL expression was not a result of increased ER stress; suggesting that
415 BspL is independently controlling these two pathways. There is growing evidence that the
416 induction of IRE1-dependent UPR by multiple effectors is linked to modulation of *Brucella*
417 intracellular trafficking and intracellular multiplication [15,22]. Our data allow us to add another

418 piece to this complex puzzle, and place for the first time the ERAD pathway at the centre of
419 *Brucella* regulation of its intracellular trafficking. Further work is now required to decipher all
420 the molecular players involved.
421
422 In conclusion, our results show that Herp modulation by BspL enables *Brucella* to temporarily
423 delay the formation of aBCVs and avoid premature egress from infected cells, highlighting a
424 new mechanism for fine-tuning of bacterial pathogen intracellular trafficking.
425
426
427 **Acknowledgements**
428 This work was funded by the ERA-Net Pathogenomics *CELLPATH* grant (ANR 2010-PATH-
429 006), the FINOVI foundation under a Young Researcher Starting Grant, ANR *NUCPATH*
430 (grant n° ANR-15-CE15-0011) and the ANR *charm-Ed* (grant n° ANR-18-CE15-0003), all
431 obtained by SPS. JBL was supported by a doctoral contract from the Région Rhônes-Alpes
432 ARC1 Santé. SPS is supported by an INSERM staff scientist contract. We are very grateful to
433 Linda Hendershot (St Judes Medical School, USA) for sending us the pcDNA-TCRα and for
434 all the help with setting up the ERAD assay and discussion of the results. We thank Renée
435 Tsolis (University of California at Davis, USA) and Jean Celli (Washington State University,
436 USA) for advice for the construction of the following plasmids TEM1-VceC, HA-VceC, HA-
437 BspB and HA-BspD, as the French Agency ANSM has prevented us from importing these
438 vectors directly from them. We also thank Thomas Henry (CIRI, Lyon, France) for the
439 iBMDM. A final special thanks to Jean Celli (Washington State University, USA) for sending
440 us several protocols and vectors (pSEAP and pmini-Tn7 vectors) as well as providing us
441 constant guidance for the SEAP assay, complementation and observation of aBCVs. The two-
442 hybrid screening was hosted by the Marseille Proteomics platform (JPB, FL) supported by

443 Institut Paoli-Calmettes, IBISA (Infrastructures Biologie Santé et Agronomie), Aix-Marseille
444 University, Canceropôle PACA and the Région Sud Provence-Alpes-Côte d'Azur. JPB is a
445 scholar of Institut Universitaire de France. We thank Steve Garvis, Amandine Blanco and
446 Arthur Louche for critical reading of the manuscript.
447
448 **Author contributions**
449 Conceptualization: JBL, JPB, JPG and SPS. Investigation: JBL, JR, TLSL, MB, FL, KW and
450 SPS; Writing of Original Draft: JBL and SPS; Writing, Review & Editing: all authors; Funding
451 Acquisition: SPS.
452
453 **Declaration of Interests**
454 The authors declare no competing interests.
455
456 **Figure Legends**
457 **Figure 1. BspL is a T4SS effector translocated into host cells during *B. abortus* infection.**
458 (A) Macrophage-like cell line (RAW) was infected with *B. abortus* carrying a plasmid encoding
459 for *bla* fused with BspL (p*bla::bspL*) to enable expression of TEM-BspL. Cells were infected
460 with either wild-type *B. abortus* or Δ*virB9* carrying this plasmid. A positive control of wild-
461 type expressing *bla::vceC* was included. At 4, 12 or 24h post-infection, cells were incubated
462 with fluorescent substrate CCF2-AM, fixed and the percentage of cells with coumarin emission
463 quantified using an automated plugin. More than a 1000 cells were quantified for each condition
464 from 3 independent experiments and data represent means ± standard deviations. Kruskal-
465 Wallis with Dunn's multiple comparisons test was used and P = 0.0019 between wild-type
466 p*bla::bspL* and Δ*virB9* p*bla::bspL* at 12h (**) and 0.171 at 24h (*). Not all statistical
467 comparisons are shown.

(B) Representative images of cells infected for 24h with *B. abortus* wild-type or Δ*virB9* carrying p*bla::bspL*. Cells were incubated with CCF2 and the presence of translocated TEM1-BspL detected by fluorescence emission of coumarin (red). Scale bars correspond to 5 µm.
(C) The expression of TEM1-BspL in the inocula of wild-type and Δ*virB9* strains was controlled by western blotting thanks to the presence of a FLAG tag in the construct. The membrane was probed with an anti-Flag antibody (top) or anti-Omp25 (bottom) as a loading control. A sample from wild-type without the plasmid was included as a negative control. Molecular weights are indicated (KDa).

Figure 2. BspL does not impact early BCV trafficking but contributes to UPR induction at late stages of the infection.
(A) Confocal microscopy image showing the intracellular localization of HA-BspL expressed in HeLa cells labelled with an anti-HA antibody (green) and ER marker calnexin (red). Phalloidin (cyan) was used to label the actin cytoskeleton and Dapi (white) for the nucleus.
(B) Quantification of mRNA levels of *XBP1s* and (C) *CHOP* by quantitative RT-PCR obtained from HeLa cells expressing HA-BspL, HA-VceC or HA-BspB for 24h. Cells transfected with empty vector pcDNA3.1 were included as a negative control and cells treated tunicamycin at 1µg/µl for 6h as a positive control. Data correspond to the fold increase in relation to an internal control with non-transfected cells. Data are presented as means ± standard deviations from at least 4 independent experiments. One-way ANOVA with Dunnett's multiple comparisons test was used to compare each value to the negative control. In the case of *XBP1s*, P = 0.0045 for HA-BspL (**). In the case of *CHOP,* P = 0.0001 for tunicamycin (****); 0.0001 for HA-BspL (****); 0.0018 for HA-VceC (**). All other comparisons ranked non-significant.
(D) Representative images of rBCVs from Δ*bspL*-expressing DSred infected iBMDM or (E) HeLa cells at 24 and 48h post-infection, labelled for calnexin (green).

493 (F) Quantification of mRNA levels of *XBP1s* and (G) *CHOP* by quantitative RT-PCR obtained
494 from iBMDMs infected with wild-type, Δ*bspL* or the complemented Δ*bspL::bspL* strains for
495 48h. Mock-infected cells were included as a negative control. Data correspond to the fold
496 increase in relation to an internal control with non-infected cells. Data are presented as means
497 ± standard deviations from at least 3 independent experiments. One-way ANOVA with
498 Dunnett's multiple comparisons test was used to compare each value to the negative control. In
499 the case of *XBP1s*, P = 0.0201 for wild-type infected cells (*) and 0.0048 for the complemented
500 Δ*bspL::bspL* infected cells (**). All other comparisons ranked non-significant with this test.
501
502 **Figure 3. BspL specifically interacts with the ERAD component Herp.**
503 (A) Co-immunoprecipitation (co-IP) from cell extracts expressing either HA-BspL, HA-BspB
504 and HA-VceC using HA-trapping beads. Flow through and elutions were probed with
505 antibodies against Alex3, Ubiquilin (Ubqln) and Herp in succession. The level of each effector
506 bound to the beads was revealed with an anti-HA antibody and 15% of the input used for the
507 co-IP shown (at the bottom). Molecular weights are indicated (KDa).
508 (B) Co-IP assay from cells expressing GFP-BspL and Flag-Herp. GFP was used as a control
509 for non-specific binding. The co-IP was revealed using an anti-Herp antibody, the fraction
510 bound to GFP-trapping beads using an anti-GFP antibody and the inputs (shown on the bottom
511 two images) using both anti-Herp and anti-GFP antibodies. Molecular weights are indicated
512 (KDa).
513 (C) Representative confocal micrograph of HeLa cells expressing HA-BspL (green) and
514 labelled for Herp (red). Scale bar corresponds to 5 μm.
515
516 **Figure 4. BspL enhances ERAD degradation of TCRα.**

(A) HEK 293T cells were transfected with HA- TCRα in the absence or presence of myc-BspL for 24h. Where indicated, cells were treated with 50 μg/ml cycloheximide for the last 4h. The blot was probed first with an anti-TCR antibody followed by anti-actin. The same samples were loaded onto a separate gel (separated by dashed line) for probing with an anti-myc and anti-actin to confirm the expression of myc-BspL. Molecular weights are indicated (KDa) and relevant bands described in the text highlighted with different coloured arrows.

(B) HEK 293T cells were transfected with HA- TCRα in the absence or presence of myc-BspL for 24h and samples treated with EndoH where indicated. The blot was probed first with an anti-TCR antibody followed by anti-actin. The same samples were loaded onto a separate gel (separated by dashed line) for probing with an anti-myc and anti-actin to confirm the expression of myc-BspL. Molecular weights are indicated (KDa) and relevant bands described in the text highlighted with different coloured arrows.

Figure 5. BspL is implicated in delay of aBCV formation.

(A) Representative confocal images of iBMDM infected with wild-type DSred for 65h labelled for LAMP1 (green). Scale bar corresponds to 5 μm.

(B) Representative confocal images of iBMDM infected with Δ*bspL* DSred for 24h (top), 48h (middle) and 65h (lower), labelled for LAMP1 (green). Scale bars correspond to 5 μm.

(C) Quantification of the percentage of cells with aBCVs, in iBMDMs infected with either wild-type, Δ*bspL* or the complemented Δ*bspL::bspL* strains for 24, 48 or 65h. Data correspond to means ± standard deviations from 5 independent experiments. A two-way ANOVA was used yielding a $P < 0.0001$ (****) between wild-type and Δ*bspL* as well as Δ*bspL* and Δ*bspL::bspL* at 48h. Other comparisons are not indicated.

(D) Representative confocal image of iBMDM infected with either wild-type DSRed or Δ*bspL* for 48h, labelled for calnexin (red). Bacteria shown in white. Scale bars correspond to 5 μm.

Figure 6. Delay of aBCV formation is dependent on Herp.

(A) Quantification of the percentage of cells with aBCVs, in HeLa cells infected with either wild-type, Δ*bspL* or the complemented Δ*bspL::bspL* strains for 24, 48 or 65h. Data correspond to means ± standard deviations from at least 3 independent experiments. A two-way ANOVA was used yielding a P = 0.0422 (*) between wild-type and Δ*bspL* and P = 0.0445 (*) for Δ*bspL* and Δ*bspL::bspL* at 48h.

(B) Quantification of the percentage of cells with aBCVs, in HeLa cells infected with wild-type *B. abortus* for 24, 48 or 65h either untreated or in the presence of eeyarestatin added at 24h post infection. Data correspond to means ± standard deviations from 3 independent experiments. A two-way ANOVA was used yielding at 65h post-infection, P = 0.0074 (**) for wt and wt+ eeyarestatin added at 24h.

(C) siControl or siHerp were added at 24h post-infection. A two-way ANOVA was used yielding a P = 0.0001 (***) between wild-type (wt) and wt+siHerp and P = 0.0031 (**) for wt+siControl and wt+siHerp at 48h. In the case of 65h, P < 0.0001 (****) between wild-type (wt) and wt+siHerp and P = 0.0032 (**) for wt+siControl and wt+siHerp. A non-specific effect of the siControl was observed at this time point in relation to untreated cells P = 0.0063.

Supplementary Figure Legends

Figure S1. BspL targets the ER independently of its CAAX motif without impacting ER secretion.

(A) Schematic diagram of BspL and its domains, namely the Sec secretion signal, hydrophobic region, Prolin-rich region (PRR) and potential CAAX motif with amino acid C, T, A and N.

(B) Representative confocal images of HeLa cells expressing myc-BspL (top panel) or myc-BspLΔCAAX (bottom panel) labelled for the ER marker calnexin (red). Scale bars correspond to 2 µm.

(C) HeLa cells were co-transfected with GFP-BspL (green) and myc-BspLΔCAAX (cyan) for 24h and labelled for the ER marker calnexin (red).

(D) Quantification of SEAP secretion in HEK 293T cells expressing either control empty vector (pcDNA3.1), dominant negative form of Arf1 (HA-ARF[T31N]), HA-BspL, HA, BspB or HA-BspD. Measurements were done at 24h after transfection and the secretion index corresponds to means ± standard deviations. Kruskal-Wallis with Dunn's multiple comparisons test was used and P = 0.0164 between pcDNA control and HA-ARF[T31N] (*) and 0.0005 between pcDNA and HA-BspB (***). All other comparisons ranked non-significant.

Figure S2. Equivalent intracellular trafficking of wild-type and *bspL* mutant strains.

(A) Bacterial counts using colony forming units (CFU) at 2, 24 and 48h post-infection with either the wild-type (red) or Δ*bspL* strains (black) of iBMDM or (B) HeLa cells. Data correspond to means ± standard deviations from 3 independent experiments.

(C) iBMDM or (D) HeLa cells were infected with wild-type *B. abortus* DSRed (red) for 24 or 48h and labelled for the ER marker calnexin (green). Zoomed insets are indicated. Scale bars correspond to 5 µm.

(E) Quantification of the percentage of BCVs positive for calnexin or (F) LAMP1 at 24 or 48h post-infection of iBMDM with either wild-type or Δ*bspL* DSRed-expressing strains. Data are presented as means ± standard deviations from at 6 independent experiments. Kruskal-Wallis with Dunn's multiple comparisons test was used and all comparisons between the wild-type and the mutant strain yielded P > 0.05, considered as non-significant.

Figure S3. BspL induction of ER stress is independent of Herp.

(A) Quantification of mRNA levels of *HERP* by quantitative RT-PCR obtained from iBMDMs infected with wild-type, Δ*bspL* or the complemented Δ*bspL::bspL* strains for 48h. Mock-infected cells were included as a negative control. Data correspond to the fold increase in relation to an internal control with non-infected cells. Data are presented as means ± standard deviations from 3 independent experiments. Kruskal-Wallis with Dunn's multiple comparisons test was used and yielded non-significant differences.

(B) Western blot of cell lysates from HeLa cells treated with siRNA control (siCtrl) or siRNA Herp (siHerp) for 48h. A sample from non-treated cells was included as a negative control. Membrane was probed with an anti-Herp antibody followed by anti-actin for loading control.

(C) Quantification of mRNA levels of *XBP1s* or (D) *CHOP* by quantitative RT-PCR obtained from HeLa cells expressing HA-BspL or HA-VceC for 24h. Where indicated, HeLa cells were treated with siRNA control (siCtrl) or siRNA Herp (siHerp). Cells transfected with empty vector pcDNA3.1 were included as a negative control and cells treated tunicamycin at 1µg/µl for 6h as a positive control. Data correspond to the fold increase in relation to an internal control with non-transfected cells. Data are presented as means ± standard deviations from at least 3 independent experiments. Kruskal-Wallis with Dunn's multiple comparisons test was used and yielded P=0.0184 (*) between negative siCtrl and BspL siCtrl, 0.0277 (*) between negative siHerp and BspL siHerp and 0.0485 (*) between negative siCtrl and tunicamycin siCtrl. No significant differences for observed for *CHOP*.

(E) Quantification of mRNA levels of *XBP1s* or (F) *CHOP* by quantitative RT-PCR obtained from HeLa cells expressing HA-BspL, HA-VceC or HA-BspB for 24h. Were indicated, cells were treated with 0.5 nM of TUDCA for 22h. Cells transfected with empty vector pcDNA3.1 were included as a negative control and cells treated tunicamycin at 1µg/µl for 6h as a positive control. Data correspond to the fold increase in relation to an internal control with non-

transfected cells. Data are presented as means ± standard deviations from 3 independent experiments. One-way ANOVA with Tukey's correction was used for multiple comparisons and yielded P=0.0287 (*) between BspL and BspL+TUDCA. For *CHOP,* P=0.0018 (**) between tunicamycin and tunicamycin+TUDCA, 0.0032 (**) between BspL and BspL+TUDCA and 0.0185 (*) between VceC and VceC+TUDCA. Not all comparisons are indicated.

Figure S4. BspL induction of ERAD is ER stress-independent.

HEK 293T cells were transfected with HA- TCRα in the absence or presence of myc-BspL for 24h. Where indicated, cells were treated with 50 μg/ml cycloheximide for the last 6h or 0.5 nM of TUDCA for 22h. The blot was probed first with an anti-TCR antibody followed by anti-actin. The same samples were loaded onto a separate (separated by dashed line) for probing with an anti-myc and anti-actin to confirm the expression of myc-BspL. Molecular weights are indicated (KDa) and relevant bands described in the text highlighted with different coloured arrows.

Figure S5. Blocking of ERAD at early stages of the infection enhances intracellular replication and accelerates bacterial release.

(A) Bacterial counts (CFU) at 2, 24 and 48h post-infection with either the wild-type without any treatment (wt, black) or in the presence of 8 μM eeyarestatin (wt+Eeya, red) or the equivalent amount of DMSO (wt+DMSO, green). Data correspond to means ± standard deviations from 6 independent experiments. A two-way ANOVA was used yielding a P < 0.0001 (****) between wild-type+DMSO with wild-type+Eeya at 48h. Other comparisons are not indicated.

(B) Representative confocal images of HeLa cells infected with the wild-type DSRed or following treatment eeyarestatin at 48h post-infection.

(C) Microscopy bacterial counts at 24h post-infection with either the wild-type with DMSO or in the presence of 8 μM eeyarestatin. Data is presented as the percentage of cells containing 1 to 5 bacteria per cell (red), 6 to 30 (black), 30 to 40 (blue) or more than 50 (green). Data correspond to means ± standard deviations from 3 independent experiments. A two-way ANOVA test was used yielding a P= 0.0003 (***) between wild-type+DMSO with wild-type+Eeya at 48h. Other comparisons are not indicated.

Material and methods

Cell culture

HeLa, RAW and HEK293T cells obtained from ATCC were grown in DMEM supplemented with 10% of fetal calf serum. Immortalized bone marrow-derived macrophages from C57BL/6J mice were obtained from Thomas Henry (CIRI, Lyon, France) and were maintained in DMEM supplemented with 10% FCS and 10% spent medium from L929 cells that supplies MC-CSF.

Transfections and siRNA

All cells were transiently transfected using Torpedo® (Ibidi-Invitrogen) for 24 h, according to manufacturer's instructions. siRNA experiments were done with Lipofectamine® RNAiMAX Reagent (Invitrogen) according the protocol of the manufacturers. Importantly, siRNA depletion of Herp was done by treatment with 3μM siRNA the day after seeding of cells and again at 24h. Depletion was achieved after 48h total. Depletion was confirmed by western blotting with an antibody against Herp. ON-TARGETplus siRNA SMARTpool (L-020918)

were used for Herp and for the control ON-TARGETplus Non-targeting pool (D-001810) both from from Dharmacon. For both transfections and siRNA cells were weeded 18h before at $2x10^4$ cells/well and $1x10^5$ cells/well for 24 and 6 well plates, respectively.

Bacterial strains and growth conditions

Brucella abortus 2308 was used in this study. Wild-type and derived strains were routinely cultured in liquid tryptic soy broth and agar. 50 µg/ml kanamycin was added for cultures of DSRed or complemented strains.

Construction of BspL eukaryotic expression vectors

The BspL constructs were obtained by cloning in the gateway pDONR™ (Life Technologies) and then cloned in the pENTRY Myc, HA or GFP vectors. The following primers were used 5'-GGGGACAAGTTTGTACAAAAAAGCAGGCTTCAATCGATTTTTGAAGATCACTAT-3' and 5'-GGGGACCACTTTGTACAAGAAAGCTGGGTCCTAGTTGGCCGTGCAGAAATG-3'. For the construct without CAAX the following reverse primer was used: 5'-GGGGACCACTTTGTACAAGAAAGCTGGGTCCTAGAAATGGTCGCGACCGTCA-3'. The final constructs were verified by sequencing and expression of tagged-BspL verified by western blotting.

Construction of *bspL* mutant and complementing strain

B. abortus 2308 knockout mutant Δ*bspL* was generated by allelic replacement. Briefly, upstream and downstream regions of about 750 bp flanking the *bspL* gene were amplified by PCR (Q5 NEB) from *B. abortus* 2308 genomic DNA using the following primers: (i) SpeI_Upstream_Forward: actagtATGTCGAGAACTGCCTGC, (ii) BamHI_XbaI_Upstream_Reverse: CGGGATCCCGGCTC

691 TAGAGCGCGGCTCCGATTAAAACAG, (iii) BamHI_XbaI_Downstream_Forward:
692 CGGGATCC CGGCTCTAGAGCACCGAACCGATCAACCAG and (iv)
693 SpeI_Downstream_Reverse: actagtCC CTATACCGAGTTGGAGC. A joining PCR was used
694 to associate the two PCR products using the following primers pairs: (i) and (iv). Finally, the
695 Δ*BspL* fragment was cloned in a SpeI digested suicide vector (pNPTS138). The acquisition of
696 this vector by *B. abortus* after mating with conjugative S17 *Escherichia coli* was selected using
697 the kanamycin resistance cassette of the pNPTS138 vector and the resistance of *B. abortus* to
698 nalidixic acid. The loss of the plasmid concomitant with either deletion of a return to the wild
699 type phenotype was then selected on sucrose, using the *sacB* counter selection marker also
700 present on the vector. Deletant (Δ) strain was identified by diagnostic PCR using the following
701 primers: Forward: CACTGGCAATGATCAGTTCC and Reverse:
702 CTGACCATTATGTGTGAACAGG (Amplicon length: WT-2000 bp, Δ - 1500 bp).
703 The complementing strain was constructed by amplifying BspL and its promoter region (500
704 bp upstream) with the PrimeStar DNA polymerase (Takara) using the following primers: Fw:
705 AAAGGATCCGACAATCAGAAGGTTTCCTATGAAACG and Rev:
706 AAAACTAGTTCAGTTGGCCGTGCAGAAATG. Insert and pmini-Tn7 [28] were digested
707 with BamHI and SpeI and ligated overnight. Transformants were selected on kanamycin 50
708 μg/mL and verified by PCR and sequencing. To obtain the complementing strain the Δ*bspL*
709 mutant was electroporated with pmini-Tn7-*bspL* with the helper plasmid pTNS2.
710 Electroporants were selected on tryptic soy agar plates with kanamycin 50 μg/mL and verified
711 by PCR.
712
713 **HA-TCRα**
714 The pcDNA-TCRα was obtained from Linda Hendershort (St Judes Medical School, USA) and
715 it corresponds to the A6-TCRα [38]. The HA tag was introduced by sequence and ligation

716 independent cloning (SLIC) method with the following primers: TCR-Fw:
717 CGAGCTCGGATCCACTAGTCCAGTGTGGTGGAATTCTACCCATACGATGTTCCAG
718 ATTACGCTATGGGCATGATCAGCCTG and TCR-
719 Rv:GAGCGGCCGCCACTGTGCTGGATATCTGCAGAATTCTTACTAGCTAGACCACA
720 G. Briefly, pcDNA-TCRα was digested with EcoRI and incubated with purified PCR product
721 amplified with the PrimeStar DNA polymerase (Takara – Ozyme) for 3 min at RT followed by
722 10 min on ice. The following ratio was used for the reaction: 100 ng vector + 3x PCR insert.
723
724 **Infections**
725 Bacterial cultures were incubated for 16h from isolated colonies in TSB shaking overnight at
726 37 °C. Culture optical density was controlled at 600 nm. Bacterial cultures diluted to obtain the
727 appropriate multiplicity of infection (MOI) for HeLa 1:500 and iBMDMs 1:300 in the
728 appropriate medium. Infected cells were centrifuged at 400 x g for 10 minutes to initiate
729 bacterial-cell contact followed by incubation for 1h at 37°C and 5% CO_2 for HeLa cells and
730 only 15 min for iBMDMs. After the cells were washed 3 times with DMEM and treated with
731 gentamycin (50 μg/mL) to kill extracellular bacteria for 1h. At 2 hours pi the medium was
732 replaced with a weaker gentamycin concentration 10 μg/mL. Cells are plated 18h before
733 infection and seeded at $2x10^4$ cell / well and $1x10^5$cells/well for 24 and 6 well plates
734 respectively. For qRT-PCR experiments, 10 mm cell culture plates were used at a density of
735 $1x10^6$cell/plate. At the different time points cells were either harvested of coverslips fixed for
736 immunostaining. In the case of bacterial cell counts, cells were lysed in 0.1% Triton for 5 min
737 and a serial dilution plated for enumeration of bacterial colony forming units (CFU).
738
739 **Immunofluorescence microscopy**

740 At the appropriate time point, coverslips were washed twice with PBS, fixed with AntigenFix
741 (MicromMicrotech France) for 15 minutes and then washed again 4 times with PBS. For ER
742 and Herp immunostaining, permeabilization was carried out with a solution of PBS containing
743 0.5% saponin for 30 minutes followed by blocking also for 30 minutes in a solution of PBS
744 containing 1% bovine serum albumin (BSA), 10% horse serum, 0.5% saponin, 0.1% Tween
745 and 0.3 M glycine. Coverslips were then incubated for 3h at room temperature or at 4 °C
746 overnight with primary antibody diluted in the blocking solution. Subsequently, the coverslips
747 were washed twice in PBS containing 0.05% saponin and incubated for 2h with secondary
748 antibodies. Finally, coverslips were washed twice in PBS with 0.05 % saponin, once in PBS
749 and once in ultrapure water. Lastly, they were mounted on a slide with ProLongGold (Life
750 Technologies). The coverslips were visualized with a Confocal Zeiss inverted laser-scanning
751 microscope LSM800 and analyzed using ImageJ software. For Lamp1 immunostaining no pre-
752 permeabilization and blocking were done and coverslips were directly incubated with antibody
753 mix diluted in PBS containing 10% horse serum and 0.5% saponin for 3h at room temperature.
754 The remaining of the protocol was the same as described above.
755
756 **Western blotting**
757 Cells were washed 1x with PBS and the 1x with ice-cold PBS. Cells were scrapped ince-cold
758 PBS, centrifuged for 5 min at 4 °C at 80 g. Pellets where then ressuspended in cell lysis buffer
759 (Chromotek) supplemented with phenylmethylsulfonyl fluoride (PMSF) and proteinase
760 inhibitors tablet cocktail (complete Mini, Roche). Samples resolved on SDS-PAGE and
761 transferred onto PVDF membrane Immobilon-P (Millipore) using a standard liquid transfer
762 protocol. Membranes were blocked using PBS with 0.1% Tween 20 and 5% skim milk for 30
763 min and the probed using relevant primary antibodies overnight at 4 °C, washed 3 times with
764 PBS with 0.1% Tween 20 and then incubated with HRP-conjugated secondary anti-goat, mouse

765 or rabbit antibodies, diluted in PBS with Tween 20 0.1% and 5% skim milk for 1 h. Western
766 blots were revealed using ECL Clarity reagent (BioRad). Signals were acquired using a Fusion
767 Camera and assembled for presentation using Image J.
768
769 **TEM1 translocation assay**
770 RAW cells were seeded in a 96 well plates at $1x10^4$ cells/well overnight. Cells were then
771 infected with an MOI of 300 by centrifugation at 4 °C, 400 g for 5 min and 1 at 37 °C 5% CO_2.
772 Cells were washed with HBSS containing 2.5 mM probenicid. Then 6 µl of CCF2 mix (as
773 described in the Life Technologies protocol) and 2.5 mM probenicid were added to each well,
774 and incubated for 1.5 h at room temperature in the dark. Cells were finally washed with PBS,
775 fixed using Antigenfix and analysed immediately by confocal microscopy (Zeiss LSM800).
776
777 **RNA isolation and real-time quantitative polymerase chain reaction (qRT-PCR)**
778 HeLa cells were seeded in 100x100 culture dishes at $1x10^6$ cells/plate for each condition and
779 were either transfected with HA-tagged BspL, VceC or BspB for 24h or infected with wild-
780 type, mutant or complemented strains for 48h. Cells were then washed 1x in PBS, scrapped in
781 buffer RLT (Qiagen) supplemented with ß-mercaptoethanol and transfered on a Qiashredder
782 column (Qiagen). Then several wash steps were performed and total RNAs were extracted
783 using a RNeasy Mini Kit (Qiagen). 500 ng of RNA were reverse transcribed in a final volume
784 of 20 µl using QuantiTect Reverse Transcription Kit (Qiagen). Real-time PCR was performed
785 using SYBR Green PowerUp (ThermoScientific) with an QuantiTect Studio 3
786 (ThermoScientific). Specific primers for human cells: *HERP* fw:
787 CGTTGTTATGTACCTGCATC and *HERP* rev: TCAGGAGGAGGACCATCATTT ; *XBP1s*
788 fw: TGCTGAGTCCGCAGCAGGTG and *XBP1s* rev: GCTGGCAGGCTCTGGGGAAG;
789 *CHOP* fw: GCACCTCCCAGAGCCCTCACTCTCC and *CHOP* rev:

GTCTACTCCAAGCCTTCCCCCTGCG. The *HPRT*, and *GAPDH* expressions were used as internal controls for normalization and fold change calculated in relation to the negative control. Primers were *HPRT* fw: TATGGCGACCCGCAGCCCT and *HPRT* rev: CATCTCGAGCAAGACGTTCAG; *GAPDH* fw: GCCCTCAACGACCACTTTGT and *GAPDH* rev: TGGTGGTCCAGGGGTCTTAC.

For murine cells: *HERP* fw: CAACAGCAGCTTCCCAGAAT and *HERP* rev: CCGCAGTTG GAGTGTGAGT; *XBP1s* fw: GAGTCCGCAGCAGGTG and *XBP1s* rev: GTGTCAGAGTCCATGGGA; *CHOP* fw: CTGCCTTTCACCTTGGAGAC and *CHOP* rev: CGTTTCCTGGGGATGAGATA and for the internal controls for normalization primers were *18S* fw: GTAACCCGTTGAACCCCATT and *18S* rev: CCATCCAATCGGTAGTAGCG; *GAPDH* fw: TCACCACCATGGAGAAGGC and *GAPDH* rev: GCTAAGCAGTTGGTGGTGCA. Data were analyzed using Prism Graph Pad 6.

ERAD evaluation

HEK293T cells seeded in 100 mm culture plates at $8x10^5$ cells/plate overnight and then co-transfected for 24h with Torpedo (Ibidi) with vectors encoding HA-TCR (5 µg) and myc-BspL (5 µg). Cycloheximide 50 µg/ml was added 6h before lysis. Where indicated, TUDCA was added 2h after transfection at 0.5 mM. Cells were harvested as described above (western blotting) and lysed in 200 µl of lysis buffer (Chromotek). EndoH (New England Biolabs) treatment was carried out following the manufacturers protocol for 1h at 37 °C. Sample buffer was then added (30 mM Tris-HCl pH 6.8, 1% SDS, 5% glycerol, 0.025% bromophenol blue and 1.25 ß-mercaptoethanol final concentration). Western blotting was done as described above using anti-TCR antibody. Actin levels were also analyzed as a loading control.

Secretion assay

HEK293T cells were harvested and seeded in 6-well plates at $1x10^5$ cells/well and co-transfected with plasmids encoding *Brucella* secreted proteins (300 ng DNA) and the secreted embryonic alkaline phosphatase (SEAP) (300 ng DNA) provided by Jean Celli. Total amount of transfected DNA was maintained constant using an empty vector pcDNA 3.1 for the positive control. At 18 h post transfection, the transfection media was removed and then cells were still incubated at 37°C 5% CO_2. Fourty-eight hours later, media containing culture supernatant (extracellular SEAP) was removed and collected. To obtain intracellular SEAP, each well was washed with PBS and then incubated with a solution of PBS-Triton X-100 0.5% for 10 minutes. An incubation of each fraction was performed at 65 °C following a centrifugation at maximum speed for 30 seconds. Then cells were incubated with a provided substrate 3-(4-methoxyspiro [1,2-dioxetane-3,2'(5'-chloro)-tricyclo(3.3.1.13,7) decane]-4-yl)phenyl phosphate (CSPD) by SEAP reporter gene assay, chemiluminescent kit (Roche Applied Science). Chemiluminescence values were obtained with the use of a TECAN at 492 nm. Data are presented as the SEAP secretion index, which is a ratio of extracellular SEAP activity to intracellular SEAP activity.

Yeast two-hybrid

BspL was cloned into pDBa vector, using the Gateway technology, transformed into MaV203 and used as a bait to screen a human embryonic brain cDNA library (Invitrogen). Media, transactivation test, screening assay and gap repair test were performed as described [47-49].

Antibodies

For immunostaining for microscopy the following antibodies were used:

Rat anti-HA antibody clone 3F10 (Roche, #1867423) was used at a dilution 1/50 and mouse anti-HA (Covance, clone 16B12, #MMS-101R), at 1/500. Rabbit anti-calnexin (Abcam,

#ab22595) was used at 1/250. Rabbit anti-Herp EPR9649 (Abcam, #ab150424) at 1/250. The mouse anti-myc antibody clone 9E10 (developed by Bishop, J.M.) was used at 1/1000. Rat anti-LAMP1 clone ID4B (developed by August, J.T.) was used 1/100 for mouse cells and mouse anti-LAMP1 clone H4A3 (developed by August, J.T. / Hildreth, J.E.K.) was used 1/100 for human cells. All LAMP1 and Myc antibodies were obtained from the Developmental Studies Hybridoma Bank, created by the NICHD of the NIH and maintained at the University of Iowa. Secondary anti-mouse, rabbit and rat antibodies were conjugated with Alexas-555, -488 or -647 fluorochromes all from Jackson Immunoresearch at a dilution 1/1000. Phallodin Atto-647 (Sigma, #65906) was used at a dilution of 1/1000. Dapi nuclear dye (Invitrogen) was used at a dilution of 1/1000.

For western blotting the following antibodies were used:

rabbit anti-FLAG (Sigma, #F7425) at 1/1000 ; rabbit anti-Alex3 (Sigma, # HPA000967) at 1/100; rabbit anti-Ubiquilin 2 (Abcam, #ab217056) at 1/1000; rabbit anti-Herp EPR9649 (Abcam, # ab150424) at 1/1000; mouse anti-HA (Covance, clone 16B12, ref. MMS-101R) at 1/1000; rabbit anti-TCR clone 3A8 (Invitrogen, #TCR1145) at 1/1000; mouse anti-myc antibody clone 9E10 at 1/1000 ; mouse anti-actin AC-40 (Sigma, #A4700) at 1/1000. Anti-mouse (GE Healthcare) or rabbit-HRP (Sigma) antibodies were used at 1/5000.

Drug treatments

All drug treatments are indicated in the specific protocols. To summarize the concentrations used were: TUDCA (Focus Biomolecules) at 0.5 nM; Cycloheximide (Sigma) at 50 µg/ml; Eeyarstatin (Sigma) at 8 µM; Tunicamycin (Sigma) at 1 µg/µl; Probenicid (Sigma) at 2.5 mM.

Co-immunoprecipitation

HeLa cells were cultured in 100 mm x 20 mm cell culture dishes at $1x10^6$ cells/dish overnight. Cells were transiently transfected with 30 uL of Torpedo ^{DNA} (Ibidi) for 24h for a total of 10 µg of DNA/plate. On ice, after 2 washes with cold PBS cells were collected with a cell scraper and centrifuged at 80g at 4 °C during 10 min. Cell lysis and processing for co-immunoprecipitation were done as described with the PierceTM HA Epitope Antibody Agarose conjugate (Thermo scientific) or GFP-Trap (Chromotek).

Statistical analysis

All data sets were tested for normality using Shapiro-Wilkinson test. When a normal distribution was confirmed we used a One-Way ANOVA test with a Dunnett correction for statistical comparison of multiple data sets with the negative control or Tukey's correction for multiple comparisons. For two independent variables, a Two-Way ANOVA test was used. For data sets that did not show normality, a Kruskall-Wallis test was applied, with Dunn's correction, or Mann-Whitney U-test for two sample comparison. All analyses were done using Prism Graph Pad 6.

References

1. Braakman, I. & Bulleid, N. J. Protein Folding and Modification in the Mammalian Endoplasmic Reticulum. *Annu. Rev. Biochem.* **80,** 71–99 (2011).
2. Wu, X. & Rapoport, T. A. Mechanistic insights into ER-associated protein degradation. *Curr Opin Cell Biol* **53,** 22–28 (2018).
3. Houck, S. A. *et al.* Quality Control Autophagy Degrades Soluble ERAD-Resistant Conformers of the Misfolded Membrane Protein GnRHR. *Molecular Cell* **54,** 166–179 (2014).
4. Walter, P. & Ron, D. The unfolded protein response: from stress pathway to homeostatic regulation. *Science* **334,** 1081–1086 (2011).
5. Kokame, K., Agarwala, K. L., Kato, H. & Miyata, T. Herp, a New Ubiquitin-like Membrane Protein Induced by Endoplasmic Reticulum Stress. *J Biol Chem* **275,** 32846–32853 (2000).
6. Ma, Y. & Hendershot, L. M. Herp is dually regulated by both the endoplasmic reticulum stress-specific branch of the unfolded protein response and a branch that is shared with other cellular stress pathways. *J Biol Chem* **279,** 13792–13799 (2004).
7. Chan, S. L. *et al.* Herp stabilizes neuronal Ca2+ homeostasis and mitochondrial

function during endoplasmic reticulum stress. *J Biol Chem* **279,** 28733–28743 (2004).
8. Tuvia, S. *et al.* The ubiquitin E3 ligase POSH regulates calcium homeostasis through spatial control of Herp. *J Cell Biol* **177,** 51–61 (2007).
9. Leitman, J. *et al.* Herp coordinates compartmentalization and recruitment of HRD1 and misfolded proteins for ERAD. *Mol Biol Cell* **25,** 1050–1060 (2014).
10. Huang, C.-H., Chu, Y.-R., Ye, Y. & Chen, X. Role of HERP and a HERP-related protein in HRD1-dependent protein degradation at the endoplasmic reticulum. *Journal of Biological Chemistry* **289,** 4444–4454 (2014).
11. Kny, M., Standera, S., Hartmann-Petersen, R., Kloetzel, P.-M. & Seeger, M. Herp regulates Hrd1-mediated ubiquitylation in a ubiquitin-like domain-dependent manner. *Journal of Biological Chemistry* **286,** 5151–5156 (2011).
12. Okuda-Shimizu, Y. & Hendershot, L. M. Characterization of an ERAD pathway for nonglycosylated BiP substrates, which require Herp. *Molecular Cell* **28,** 544–554 (2007).
13. Celli, J. & Tsolis, R. M. Bacteria, the endoplasmic reticulum and the unfolded protein response: friends or foes? *Nature Publishing Group* 1–12 (2014). doi:10.1038/nrmicro3393
14. de Jong, M. F. *et al.* Sensing of Bacterial Type IV Secretion via the Unfolded Protein Response. *mBio* **4,** e00418–12–e00418–12 (2012).
15. Smith, J. A. *et al.* Brucella Induces an Unfolded Protein Response via TcpB That Supports Intracellular Replication in Macrophages. *PLoS Pathog* **9,** e1003785 (2013).
16. Keestra-Gounder, A. M. *et al.* NOD1 and NOD2 signalling links ER stress with inflammation. *Nature* 1–15 (2016). doi:10.1038/nature17631
17. Qin, Q.-M. *et al.* RNAi screen of endoplasmic reticulum-associated host factors reveals a role for IRE1alpha in supporting Brucella replication. *PLoS Pathog* **4,** e1000110 (2008).
18. Starr, T., Ng, T. W., Wehrly, T. D., Knodler, L. A. & Celli, J. Brucella intracellular replication requires trafficking through the late endosomal/lysosomal compartment. *Traffic* **9,** 678–694 (2008).
19. Celli, J., Salcedo, S. P. & Gorvel, J.-P. Brucella coopts the small GTPase Sar1 for intracellular replication. *Proc Natl Acad Sci USA* **102,** 1673–1678 (2005).
20. Fugier, E. *et al.* The glyceraldehyde-3-phosphate dehydrogenase and the small GTPase Rab 2 are crucial for Brucella replication. *PLoS Pathog* **5,** e1000487 (2009).
21. Sedzicki, J. *et al.* 3D correlative electron microscopy reveals continuity of *Brucella*-containing vacuoles with the endoplasmic reticulum. *J Cell Sci* 1–36 (2018).
22. Taguchi, Y. *et al.* Yip1A, a Novel Host Factor for the Activation of the IRE1 Pathway of the Unfolded Protein Response during Brucella Infection. *PLoS Pathog* **11,** e1004747 (2015).
23. Starr, T. *et al.* Selective Subversion of Autophagy Complexes Facilitates Completion of the Brucella Intracellular Cycle. *Cell Host Microbe* 1–14 (2011). doi:10.1016/j.chom.2011.12.002
24. Delrue, R. M. *et al.* Identification of Brucella spp. genes involved in intracellular trafficking. *Cell Microbiol* **3,** 487–497 (2001).
25. Comerci, D. J., Martínez-Lorenzo, M. J., Sieira, R., Gorvel, J. P. & Ugalde, R. A. Essential role of the VirB machinery in the maturation of the Brucella abortus-containing vacuole. *Cell Microbiol* **3,** 159–168 (2001).
26. Celli, J. *et al.* Brucella evades macrophage killing via VirB-dependent sustained interactions with the endoplasmic reticulum. *J Exp Med* **198,** 545–556 (2003).
27. Smith, E. P., Miller, C. N., Child, R., Cundiff, J. A. & Celli, J. Postreplication Roles of the Brucella VirB Type IV Secretion System Uncovered via Conditional Expression of

947 the VirB11 ATPase. *mBio* **7,** 215 (2016).
948 28. Myeni, S. *et al.* Brucella Modulates Secretory Trafficking via Multiple Type IV
949 Secretion Effector Proteins. *PLoS Pathog* **9,** e1003556 (2013).
950 29. Miller, C. N. *et al.* A Brucella Type IV Effector Targets the COG Tethering Complex
951 to Remodel Host Secretory Traffic and Promote Intracellular Replication. *Cell Host*
952 *Microbe* **22,** 317–329.e7 (2017).
953 30. Boucrot, E., Beuzón, C. R., Holden, D. W., Gorvel, J.-P. & Méresse, S. Salmonella
954 typhimurium SifA effector protein requires its membrane-anchoring C-terminal
955 hexapeptide for its biological function. *J Biol Chem* **278,** 14196–14202 (2003).
956 31. Reinicke, A. T. A Salmonella typhimurium Effector Protein SifA Is Modified by Host
957 Cell Prenylation and S-Acylation Machinery. *Journal of Biological Chemistry* **280,**
958 14620–14627 (2005).
959 32. Price, C. T. D., Al-Quadan, T., Santic, M., Jones, S. C. & Abu Kwaik, Y. Exploitation
960 of conserved eukaryotic host cell farnesylation machinery by an F-box effector of
961 Legionella pneumophila. *J Exp Med* **207,** 1713–1726 (2010).
962 33. Ivanov, S. S., Charron, G., Hang, H. C. & Roy, C. R. Lipidation by the host
963 prenyltransferase machinery facilitates membrane localization of Legionella
964 pneumophila effector proteins. *Journal of Biological Chemistry* **285,** 34686–34698
965 (2010).
966 34. de Jong, M. F., Sun, Y.-H., Hartigh, den, A. B., van Dijl, J. M. & Tsolis, R. M.
967 Identification of VceA and VceC, two members of the VjbR regulon that are
968 translocated into macrophages by the Brucella type IV secretion system. *Mol Microbiol*
969 **70,** 1378–1396 (2008).
970 35. Marchesini, M. I., Herrmann, C. K., Salcedo, S. P., Gorvel, J.-P. & Comerci, D. J. In
971 search of Brucella abortus type IV secretion substrates: screening and identification of
972 four proteins translocated into host cells through VirB system. *Cell Microbiol* **13,**
973 1261–1274 (2011).
974 36. Serrat, R. *et al.* The non-canonical Wnt/PKC pathway regulates mitochondrial
975 dynamics through degradation of the arm-like domain-containing protein Alex3. *PLoS*
976 *ONE* **8,** e67773 (2013).
977 37. Kim, T.-Y., Kim, E., Yoon, S. K. & Yoon, J.-B. Herp enhances ER-associated protein
978 degradation by recruiting ubiquilins. *Biochem Biophys Res Commun* **369,** 741–746
979 (2008).
980 38. Feige, M. J. & Hendershot, L. M. Quality control of integral membrane proteins by
981 assembly-dependent membrane integration. *Mol Cell* **51,** 297–309 (2013).
982 39. Lippincott-Schwartz, J., Bonifacino, J. S., Yuan, L. C. & Klausner, R. D. Degradation
983 from the endoplasmic reticulum: disposing of newly synthesized proteins. *Cell* **54,**
984 209–220 (1988).
985 40. Rodino, K. G. *et al.* Orientia tsutsugamushiModulates Endoplasmic Reticulum-
986 Associated Degradation To Benefit Its Growth. *Infect Immun* **86,** e00596–17–16
987 (2017).
988 41. Dorer, M. S., Kirton, D., Bader, J. S. & Isberg, R. R. RNA Interference Analysis of
989 Legionella in Drosophila Cells: Exploitation of Early Secretory Apparatus Dynamics.
990 *PLoS Pathog* **2,** e34–13 (2006).
991 42. Quiroga, C. *et al.* Herp depletion protects from protein aggregation by up-regulating
992 autophagy. *BBA - Molecular Cell Research* **1833,** 3295–3305 (2013).
993 43. Hori, O. *et al.* Role of Herp in the endoplasmic reticulum stress response. *Genes to*
994 *Cells* **9,** 457–469 (2004).
995 44. Yan, L. *et al.* Ube2g2-gp78-mediated HERP polyubiquitylation is involved in ER
996 stress recovery. *J Cell Sci* **127,** 1417–1427 (2014).

997 45. Şentürk, M. *et al.* Ubiquilins regulate autophagic flux through mTOR signalling and
998 lysosomal acidification. *Nat Cell Biol* 1–19 (2019). doi:10.1038/s41556-019-0281-x
999 46. Ensminger, A. W. & Isberg, R. R. E3 Ubiquitin Ligase Activity and Targeting of
1000 BAT3 by Multiple Legionella pneumophila Translocated Substrates. *Infect Immun* **78,**
1001 3905–3919 (2010).
1002 47. Thalappilly, S. *et al.* Identification of multi-SH3 domain-containing protein
1003 interactome in pancreatic cancer: A yeast two-hybrid approach. *Proteomics* **8,** 3071–
1004 3081 (2008).
1005 48. Walhout, A. J. & Vidal, M. High-throughput yeast two-hybrid assays for large-scale
1006 protein interaction mapping. *Methods* **24,** 297–306 (2001).
1007 49. Orr-Weaver, T. L. & Szostak, J. W. Yeast recombination: The association between
1008 double-strand gap
1009 repair and crossing-over. *Proc Natl Acad Sci USA* **80,** 4417–4421 (1983).
1010

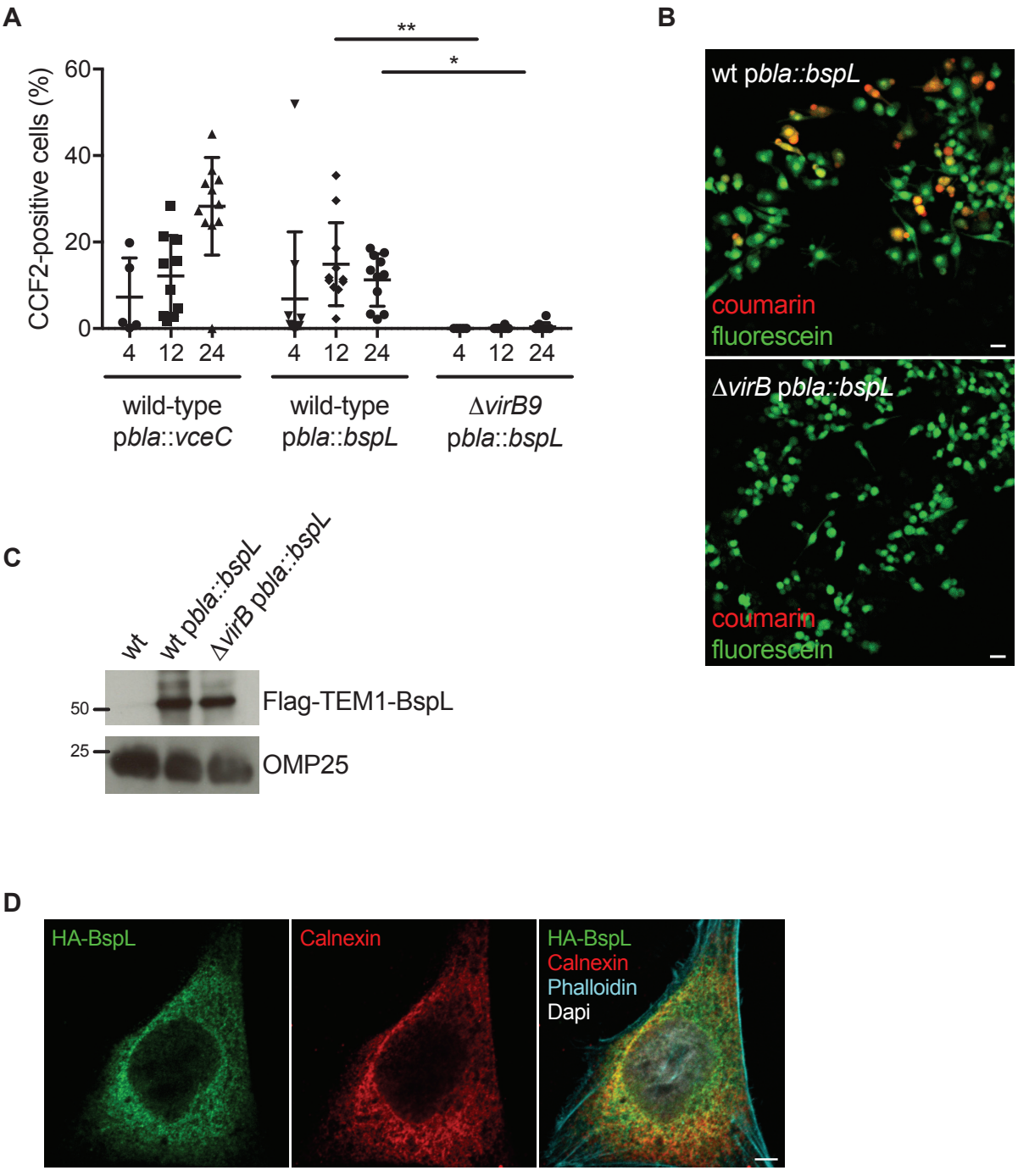
A
**
*
CCF2-positive cells (%)
60
40
20
0
4 12 24 4 12 24 4 12 24
wild-type pbla::vceC
wild-type pbla::bspL
ΔvirB9 pbla::bspL
B
wt pbla::bspL
coumarin
fluorescein
ΔvirB pbla::bspL
coumarin
fluorescein
C
wt
wt pbla::bspL
ΔvirB pbla::bspL
50
Flag-TEM1-BspL
25
OMP25
D
HA-BspL
Calnexin
HA-BspL
Calnexin
Phalloidin
Dapi

Figure 1

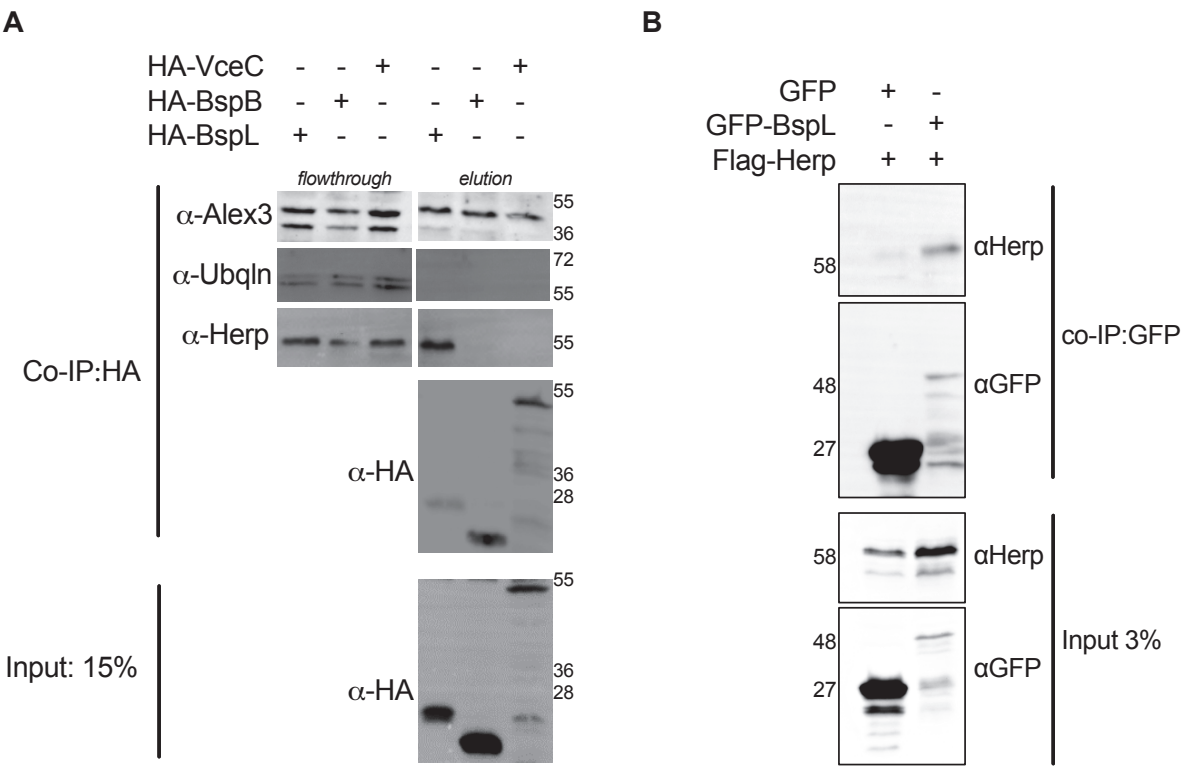
A
HA-VceC - - + - - +
HA-BspB - + - - + -
HA-BspL + - - + - -
flowthrough
elution
α-Alex3
α-Ubqln
α-Herp
α-HA
α-HA
Co-IP:HA
Input: 15%
55
36
72
55
55
55
36
28
55
36
28
B
GFP + -
GFP-BspL - +
Flag-Herp + +
58
48
27
58
48
27
αHerp
αGFP
αHerp
αGFP
co-IP:GFP
Input 3%

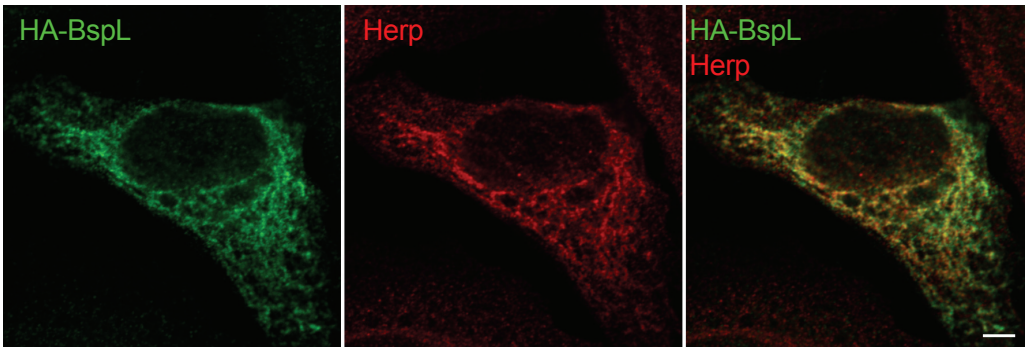
C
HA-BspL
Herp
HA-BspL
Herp

Figure 2

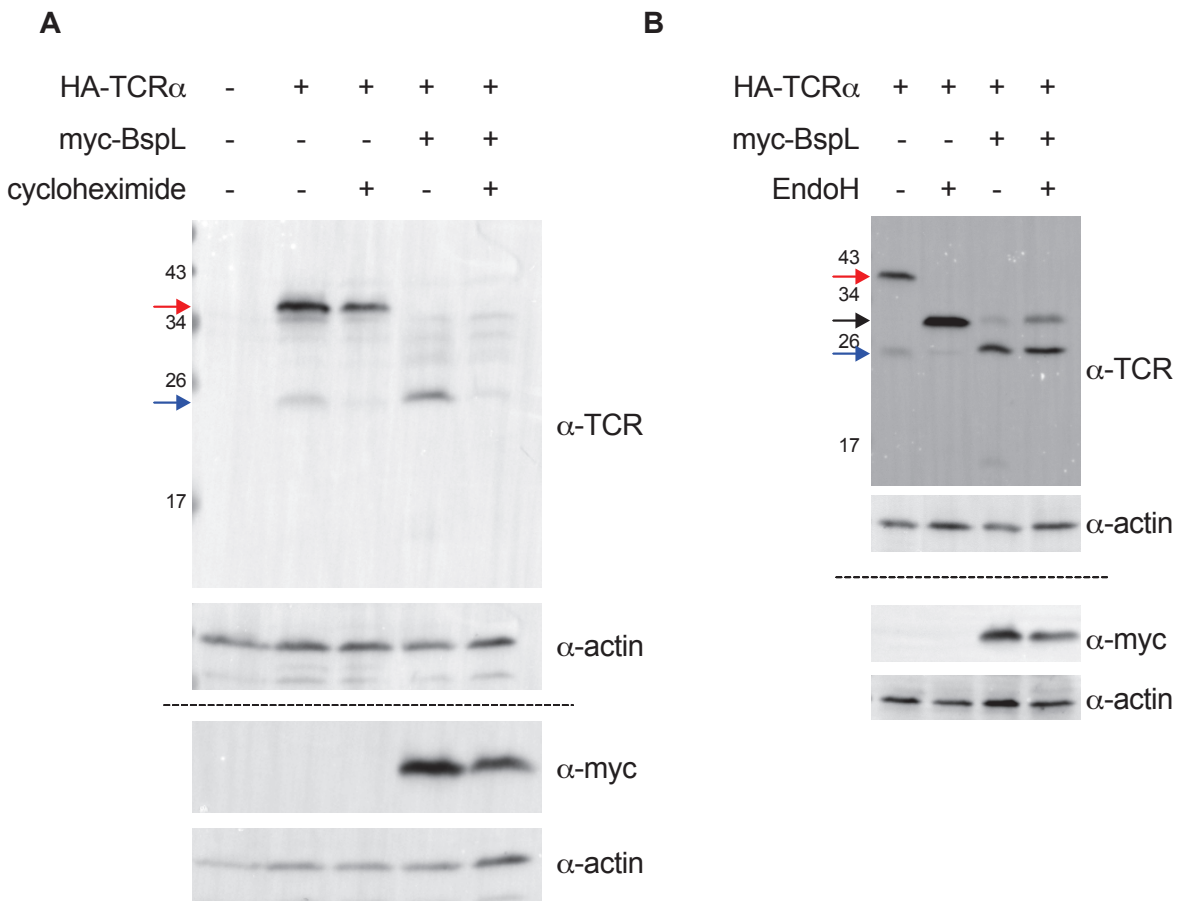
A
HA-TCRα - + + + +
myc-BspL - - - + +
cycloheximide - - + - +
43
34
26
17
α-TCR
α-actin
α-myc
α-actin
B
HA-TCRα + + + +
myc-BspL - - + +
EndoH - + - +
43
34
26
17
α-TCR
α-actin
α-myc
α-actin

Figure 3

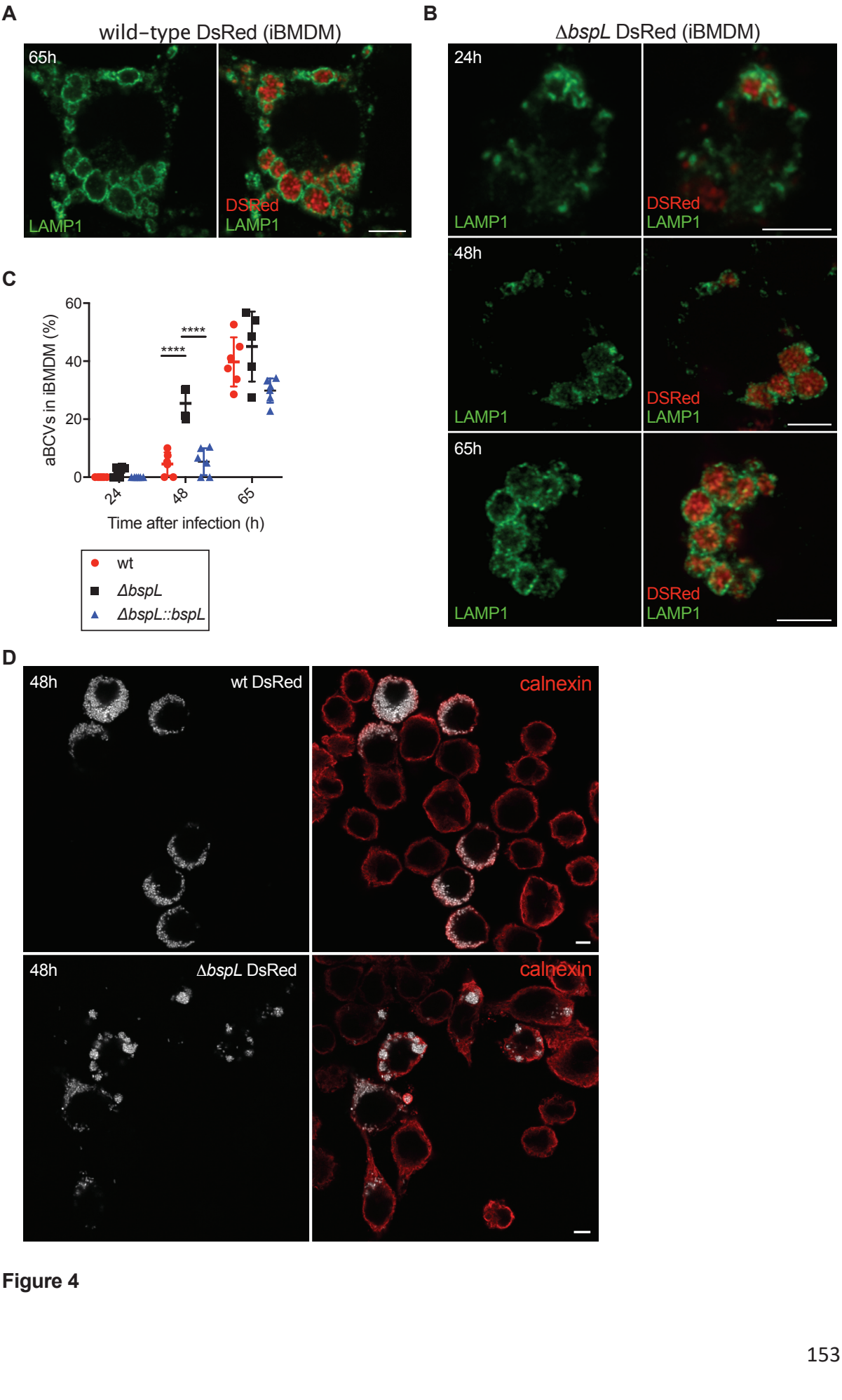
A
wild-type DsRed (iBMDM)
65h
LAMP1
DSRed
LAMP1
B
ΔbspL DsRed (iBMDM)
24h
LAMP1
DSRed
LAMP1
48h
LAMP1
DSRed
LAMP1
65h
LAMP1
DSRed
LAMP1
C
aBCVs in iBMDM (%)
60
40
20
0
****
****
24
48
65
Time after infection (h)
wt
ΔbspL
ΔbspL::bspL
D
48h
wt DsRed
calnexin
48h
ΔbspL DsRed
calnexin

Figure 4

A

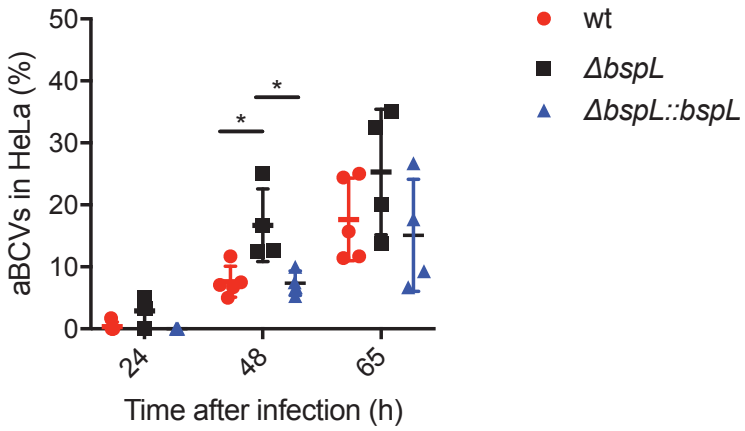
aBCVs in HeLa (%)
50
40
30
20
10
0
24
48
65
Time after infection (h)
*
*
wt
ΔbspL
ΔbspL::bspL

B

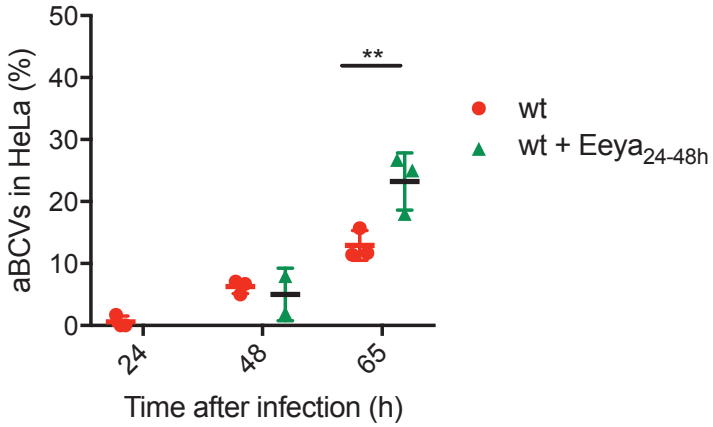
aBCVs in HeLa (%)
50
40
30
20
10
0
24
48
65
Time after infection (h)
**
wt
wt + Eeya24-48h

C

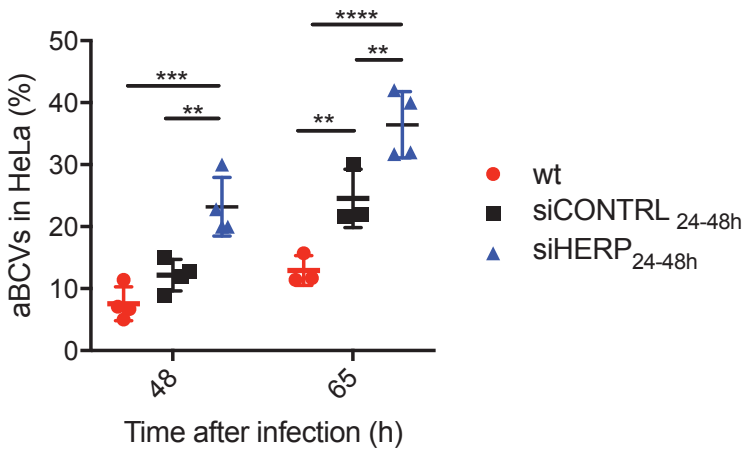
aBCVs in HeLa (%)
50
40
30
20
10
0
48
65
Time after infection (h)
***
**
**
****
**
wt
siCONTRL 24-48h
siHERP24-48h

Figure 5

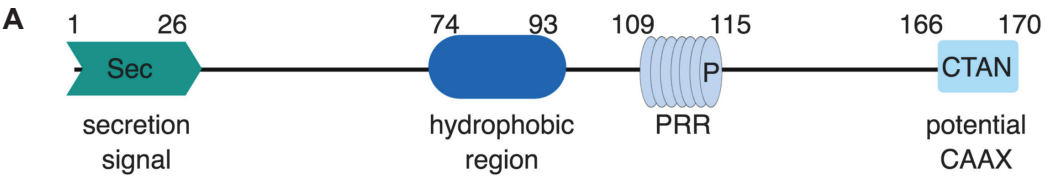
A
1
26
74
93
109
115
166
170
Sec
P
CTAN
secretion signal
hydrophobic region
PRR
potential CAAX

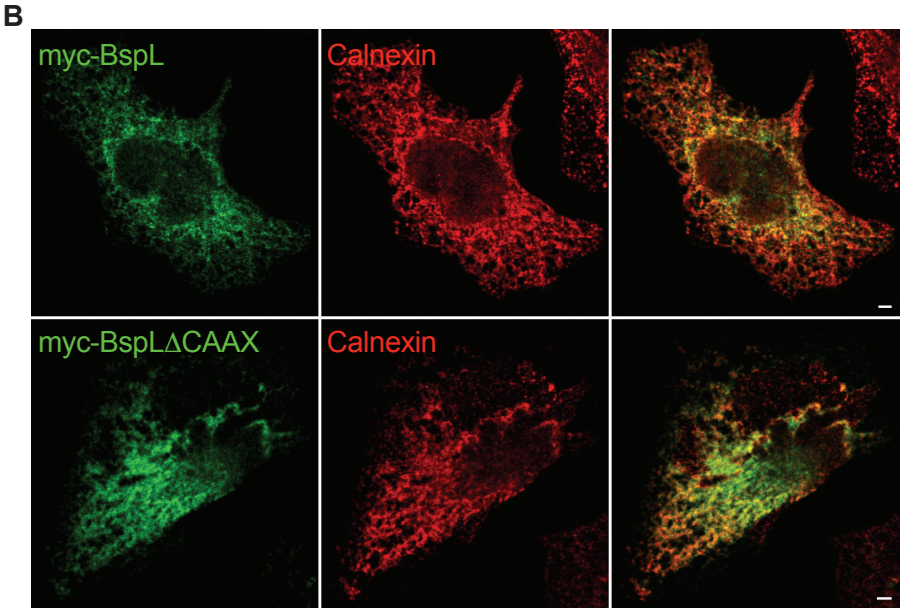
B
myc-BspL
Calnexin
myc-BspLΔCAAX
Calnexin

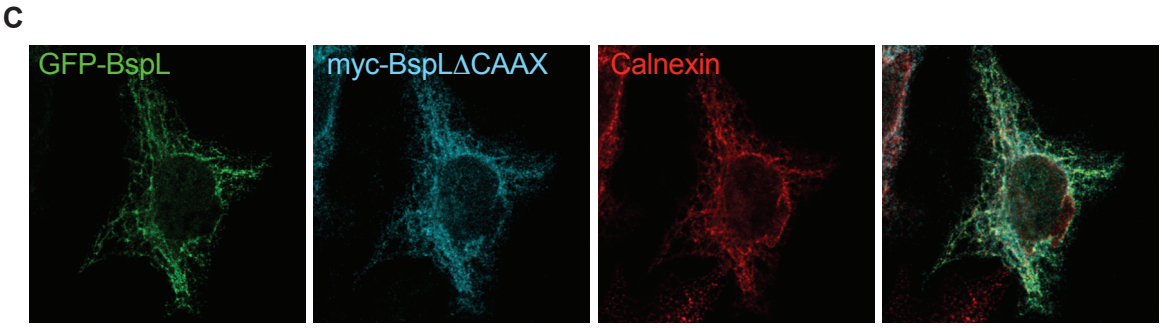
C
GFP-BspL
myc-BspLΔCAAX
Calnexin

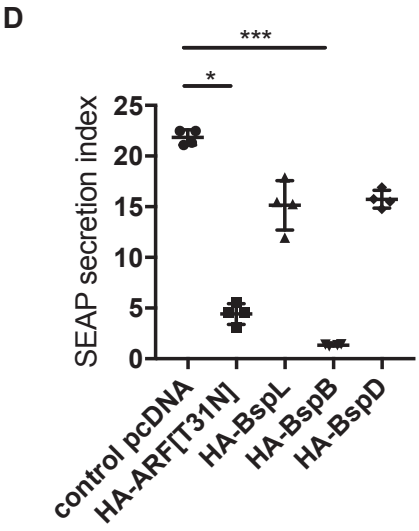
D
***
*
SEAP secretion index
25
20
15
10
5
0
control pcDNA
HA-ARF[T31N]
HA-BspL
HA-BspB
HA-BspD

Figure S1

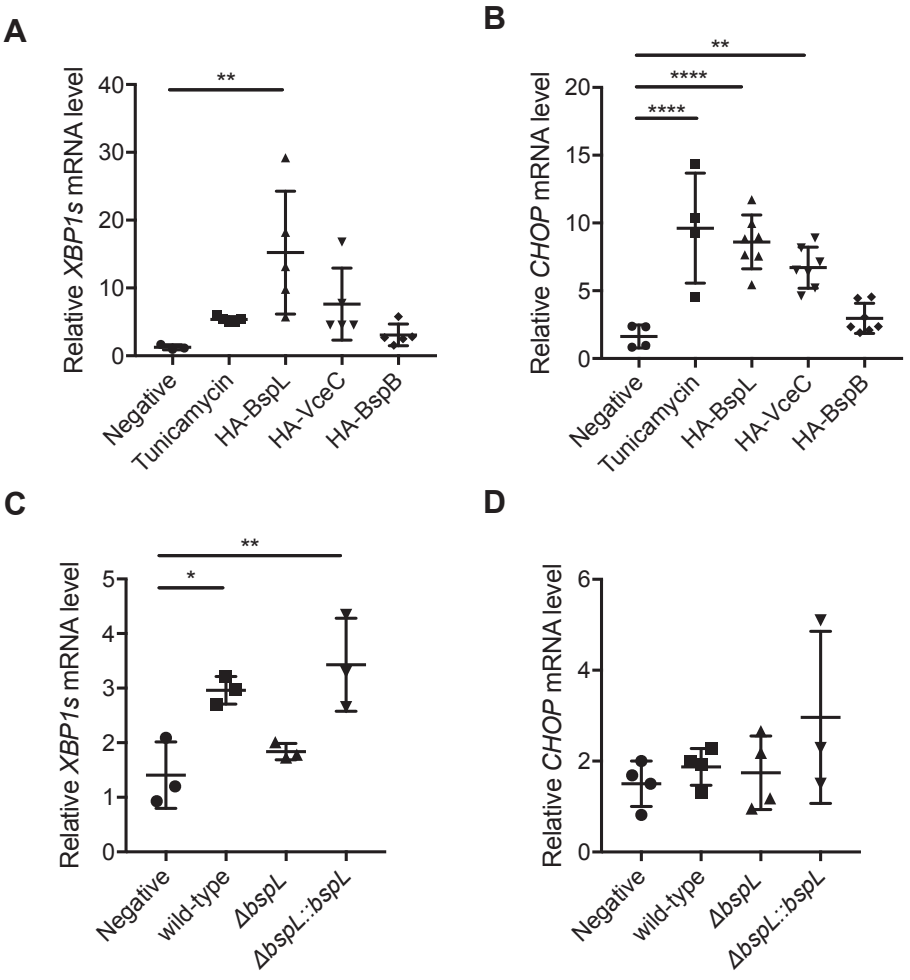
A
Relative XBP1s mRNA level
40
30
20
10
0
**
Negative
Tunicamycin
HA-BspL
HA-VceC
HA-BspB
B
Relative CHOP mRNA level
20
15
10
5
0
**
****
****
Negative
Tunicamycin
HA-BspL
HA-VceC
HA-BspB
C
Relative XBP1s mRNA level
5
4
3
2
1
0
**
*
Negative
wild-type
ΔbspL
ΔbspL::bspL
D
Relative CHOP mRNA level
6
4
2
0
Negative
wild-type
ΔbspL
ΔbspL::bspL

Figure S2

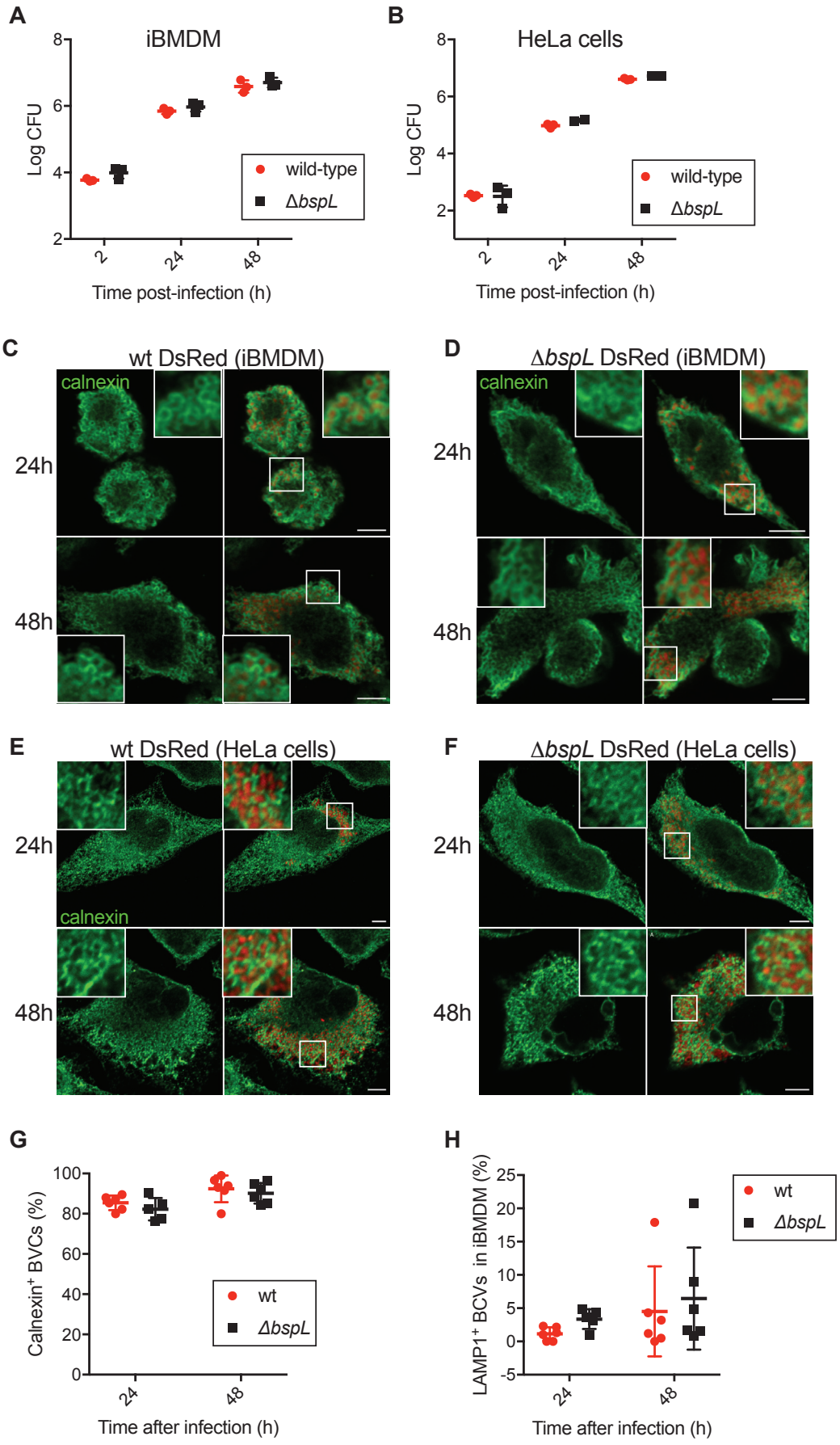
A
iBMDM
Log CFU
8
6
4
2
wild-type
ΔbspL
2
24
48
Time post-infection (h)
B
HeLa cells
Log CFU
8
6
4
2
wild-type
ΔbspL
2
24
48
Time post-infection (h)
C
wt DsRed (iBMDM)
calnexin
24h
48h
D
ΔbspL DsRed (iBMDM)
calnexin
24h
48h
E
wt DsRed (HeLa cells)
24h
calnexin
48h
F
ΔbspL DsRed (HeLa cells)
24h
48h
G
Calnexin+ BVCs (%)
100
80
60
40
20
0
wt
ΔbspL
24
48
Time after infection (h)
H
LAMP1+ BCVs in iBMDM (%)
25
20
15
10
5
0
-5
wt
ΔbspL
24
48
Time after infection (h)

Figure S3

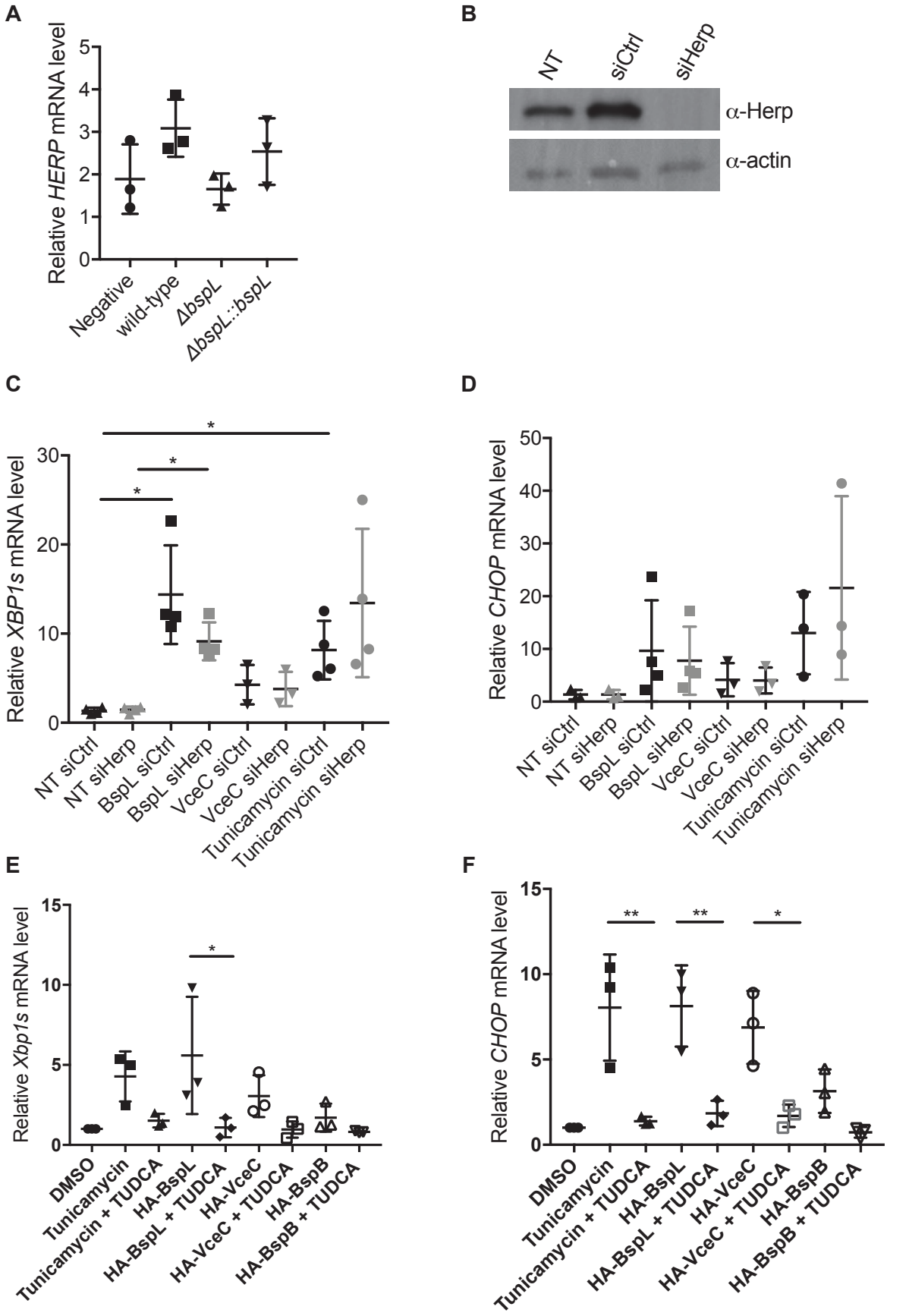
A
Relative HERP mRNA level
Negative
wild-type
ΔbspL
ΔbspL::bspL
B
NT
siCtrl
siHerp
α-Herp
α-actin
C
Relative XBP1s mRNA level
NT siCtrl
NT siHerp
BspL siCtrl
BspL siHerp
VceC siCtrl
VceC siHerp
Tunicamycin siCtrl
Tunicamycin siHerp
D
Relative CHOP mRNA level
E
Relative Xbp1s mRNA level
DMSO
Tunicamycin
Tunicamycin + TUDCA
HA-BspL
HA-BspL + TUDCA
HA-VceC
HA-VceC + TUDCA
HA-BspB
HA-BspB + TUDCA
F
Relative CHOP mRNA level

Figure S4

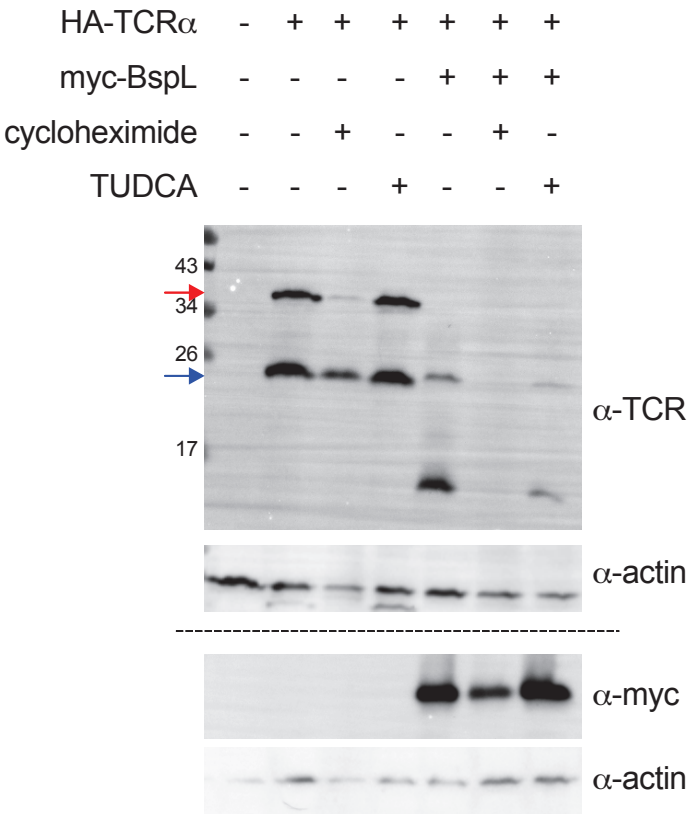
HA-TCRα - + + + + + +
myc-BspL - - - - + + +
cycloheximide - - + - - + -
TUDCA - - - + - - +
43
34
26
17
α-TCR
α-actin
α-myc
α-actin

Figure S5

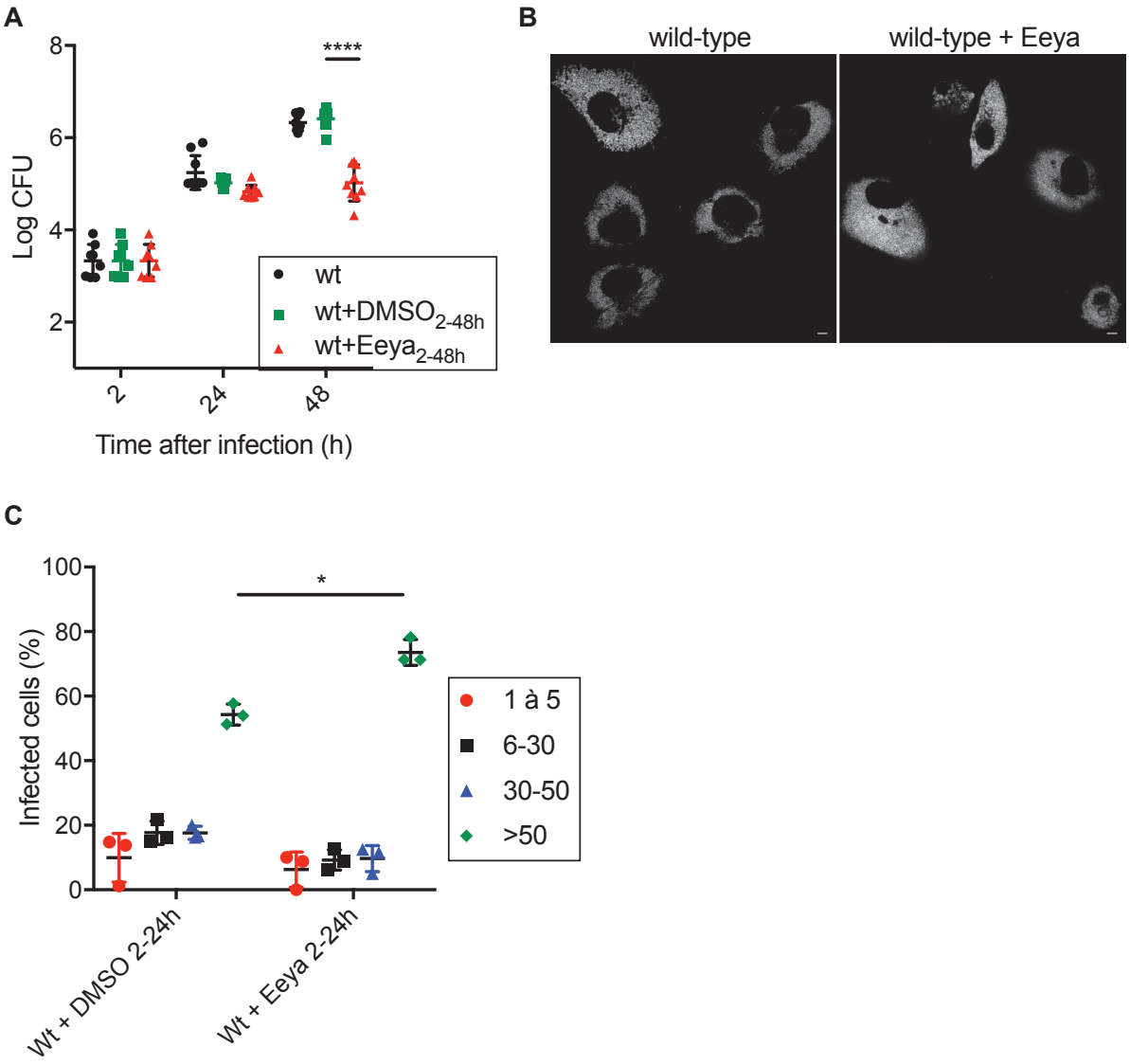
A
B
C
wild-type
wild-type + Eeya
Log CFU
Time after infection (h)
wt
wt+DMSO2-48h
wt+Eeya2-48h
****
*
Infected cells (%)
1 à 5
6-30
30-50
>50
Wt + DMSO 2-24h
Wt + Eeya 2-24h

Figure S6

Chapter 5 Results Part2: BspL fragments mitochondrial network

This work was initiated in parallel of the characterization of BspL impact on the endoplasmic reticulum presented in the **Chapter 4**. Before presenting these results, I would like to explain why we investigated a potential impact of BspL on the mitochondrial network. The first reason was the significant amount of data that support mitochondria and ER are very closely connected organelles. Indeed, ER and mitochondria can be physically associated as the ER participates in the mitochondrial fission process, by constricting the organelle [232]. In addition, the identification of the point of contacts called MAMs of theses 2 organelles strengthens this connection.

The second reason was that ER stress induction is known to affect mitochondria and we observed early on during our studies that BspL was a strong inducer of stress [423].

The third reason was that at the time we started this project, the laboratory of Thierry Arnould contacted us with evidence that *Brucella* was inducing mitochondrial fragmentation during infection and we wanted to test if BspL could be the effector mediating this phenotype.

The fourth and last reason was that one of the putative targets of BspL identified by yeast two-hybrid was the mitochondrial protein Alex3. Indeed, when we started this second project, we did not know yet the result of the co-immunoprecipitation experiment where we found non-specific interactions of Alex3 with BspB and VceC effectors.

This work was done with the help of an excellent M2 student, Magali Bonici, that I supervised. She performed the majority of counting microscopy experiments of mitochondrial fragmentation after *Brucella* infection in HeLa and trophoblasts cells.

I-) Results

1-) BspL induces mitochondrial fragmentation

First of all, we overexpressed BspL to see if there was some colocalization between mitochondria and our effector that could suggest an action of BspL on this organelle. Although we did not observe any significant co-localization, we observed BspL induces mitochondrial fragmentation (**Figure 1A**). To quantify this phenotype, 65 images of transfected cells labeled with an antibody against the mitochondrial chaperone Grp75were

taken by confocal fluorescence microscopy and submitted to the Fiji software to calculate the Aspect Ratio, which nicely reflects the state of the mitochondrial network as it measure the connectivity of the network and particularly the elongation of the network (**Figure 1B)** [424]. We decided to attribute a rank for each value of aspect ratio that better reflects the tendency of the aspect of the mitochondrial network. In non-transfected HeLa cells (negative control), mitochondria form a network throughout the cell covering the whole cytoplasm and the aspect ratio is therefore high (with a mean value around 2.5, data not shown). However, in HeLa cells transfected with BspL, the connectivity of the mitochondrial network is perturbed, forming disparate dots in the cytoplasm (**Figure 1A**,). In some cases, we observed that mitochondria were absent from the periphery of the cell, with all fragmented mitochondria seemed to be close to the nucleus. We found that, cells expressing BspL had a low aspect ratio value (with a mean value around 1,5, data not shown) compared to the negative control indicating a strong fragmentation of the mitochondria (**Figure 1B**). We next sought to determine if expression of other *Brucella* effectors that accumulate in the ER when over-expressed in HeLa cells resulted in mitochondrial fragmentation. We chose VceC, known to localize to the ER and induce ER vacuolation as well as ER stress [361].. We also compared with BspB, another ER-targeting *Brucella* effector in transfection but that does not induce ER stress and instead modulates ER to Golgi transport [391,399]. Interestingly, fragmentation of mitochondria in HeLa cells transfected with VceC was also observed when compared to the negative control but at much lower levels than those induced by BspL (**Figure 1B**), and only in cells expressing high levels of VceC (data not shown). In contrast, in cells expressing BspB the mitochondrial network was intact (**Figure 1A**) and the aspect ratio was similar to that of negative cells (**Figure 1B**). Therefore, BspB does not induce mitochondrial fragmentation. These results indicate that BspL induces a strong mitochondrial fragmentation. Moreover, we found the same results using a different tag for BspL (**Figure 1C**), indicating that the observed phenotype is not due to the tag but to the effector.

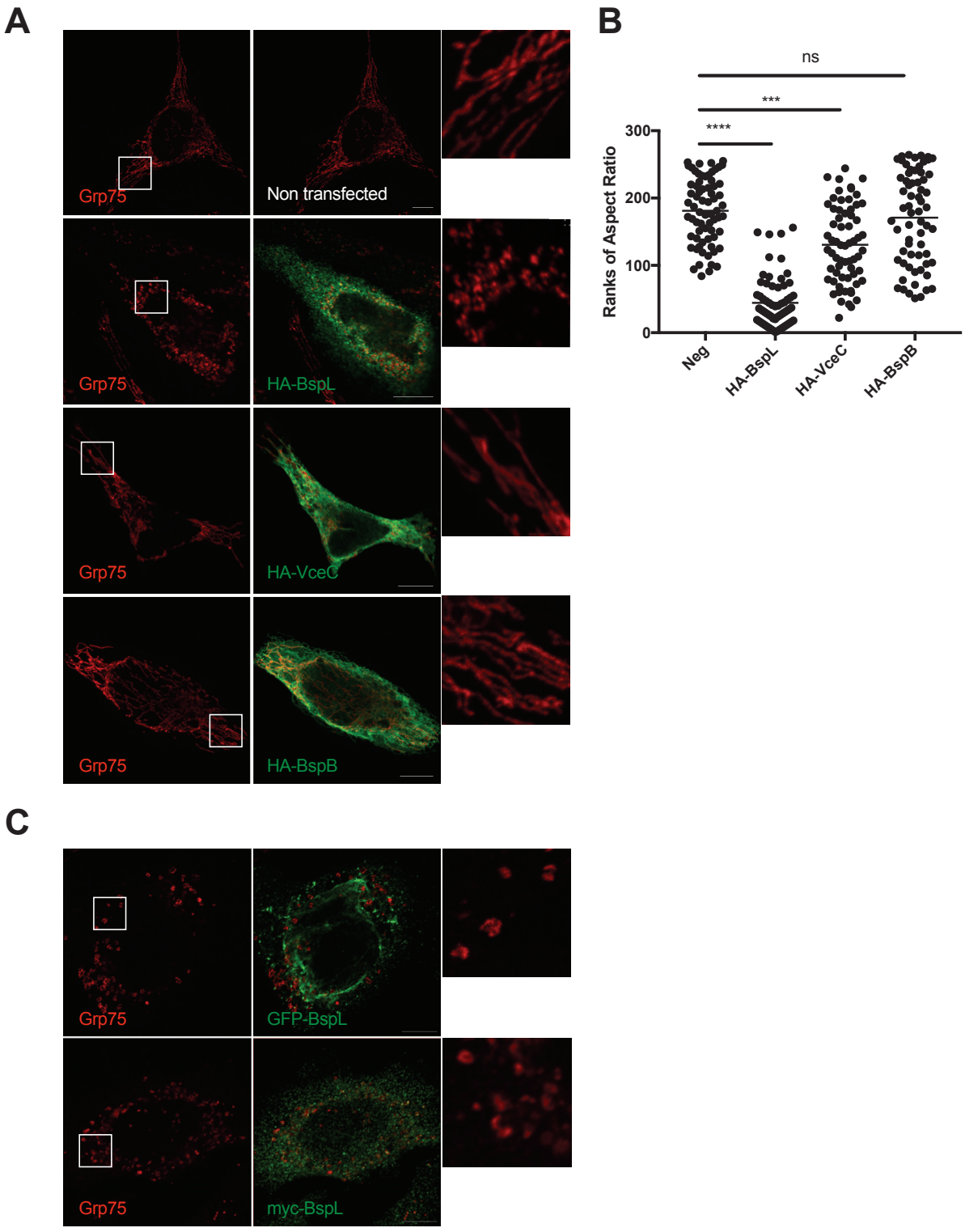

Figure 1- BspL induces mitochondrial fragmentation. (A) HeLa were transiently transfected for 24 h with plasmids encoding HA-BspL, BspB or VceC and fixed. Cells were labeled for mitochondrial chaperone protein Grp75 (red) and an antibody against the HA tag was used to label the effectors (green). Representative of confocal microscopy images are shown. Scale bars correspond to 10 µm. Zoom insets of mitochondria are indicated with white boxes. **(B)** Aspect ratio of the mitochondrial network was calculated with the software ImageJ in transfected cells. Non-transfected cells were also quantified as a control (Neg). A total of 65 cells were counted for the control and each effector. Results represent the rank of each aspect ratio from 3 independent

experiments. The bar corresponds to the mean of the ranks. Statistical analysis was done with a Kruskal-Wallis: "****" for $p < 0.0001$, "***" for $p < 0.001$. (**C**) HeLa were transiently transfected for 24 h with plasmids encoding GFP-BspL or myc-BspL and fixed. Cells were labeled for mitochondrial chaperone protein Grp75 (red) and an antibody against the myc tag was used to label the effector (green). Representative of confocal microscopy images are shown. Scale bars correspond to 10 μm. Zoom insets of mitochondria are indicated with white boxes.

2-) BspL still induces mitochondrial fragmentation independently of ER stress

Although our results suggest that BspL may induce fragmentation of the mitochondrial network, it is possible that the observed fragmentation was a secondary effect of the ER stress induced by BspL or VceC and not a direct action of the effector. Therefore, we next investigated if inhibition of ER stress, using a well-established treatment with TUDCA, would impact the phenotypes observed in cells expressing BspL and VceC. As seen in the previous chapter, in our conditions TUDCA can counteract ER stress induced by tunicamycin and also inhibited ER stress induced by BspL and VceC as seen by a decrease in transcript of CHOP and spliced XBP1 (**Chapter 4**, **Figure S3E and F**). These results show that TUDCA inhibits stress not only induced by tunicamycin but also by VceC and BspL effectors. We next quantified the aspect ratio of mitochondria of HeLa cells transfected with different effectors and treated with TUDCA. As observed previously, the aspect ratio for the negative control cells and BspB transfected cells was high and the mitochondrial network remained intact (**Figure 2A and B**). These results also allow us to conclude that treatment with TUDCA does not impact mitochondrial aspect ratio. Interestingly, incubation with TUDCA following transfection with VceC resulted in normal aspect ratio values equivalent to those obtained for negative control and BspB transfected cells (**Figure 2B**), suggesting this treatment prevents mitochondrial fragmentation induced by VceC. In contrast, even in the presence of TUDCA, the aspect ratio of mitochondria in HeLa cells transfected with BspL was significantly lower than the negative control and mitochondria were still clearly heavily fragmented (**Figure 2A and B**). Furthermore, the aspect ratio was similar between cells transfected with BspL and cells transfected with BspL and treated TUDCA which clearly shows that this phenotype is independent of ER stress. In conclusion, VceC-induced mitochondrial fragmentation is mostly likely due to the induction of ER stress as it was abrogated by TUDCA treatment. However, the fact that, even in the absence of ER stress, BspL is still able to induce mitochondrial fragmentation suggests that this effector may act directly on mitochondrial integrity.

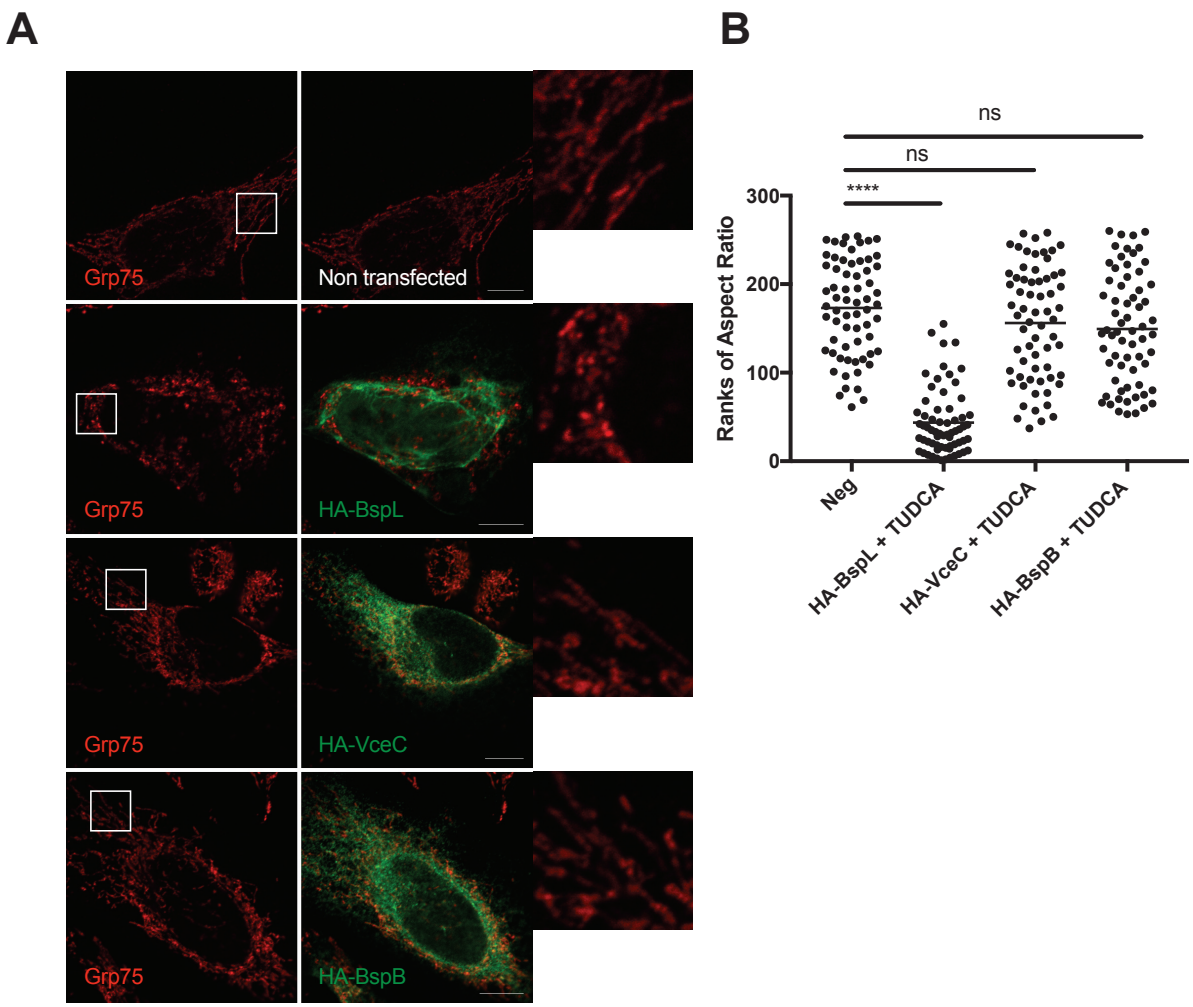

Figure 2- BspL still induces mitochondrial fragmentation independently of ER stress. (A) HeLa cells were transiently transfected for 24 h with plasmids encoding HA-BspL, BspB or VceC effectors. 2 h after transfection cells were treated with 0.5 mM TUDCA and fixed. Cells were labeled for mitochondria with an anti-Grp75 antibody (red) and an antibody against the HA tag (green). Representative images obtained by confocal microscopy are shown. Scale bars correspond to 10 µm. Zoom insets of mitochondria are indicated with white boxes. **(B)** A total of 65 cells were counted for the control and each effector. Results represent the rank of each aspect ratio from 3 independent experiments. The control is non-transfected and non-treated with TUDCA. The bar corresponds to the mean of the ranks. Statistical analysis was done with a Kruskal-Wallis test: "****" for $p <$ 0.0001.

3-) BspL contributes to mitochondrial fragmentation in infection

As the previous experiments all relied on ectopic expression of BspL, we next investigated the mitochondrial fragmentation during *Brucella* infection. HeLa cells were infected 24h or 48h with *Brucella abortus* WT strain expressing DSRed (**Figure 3A**) and, as previously, the aspect ratio was quantified (**Figure 3C**). We found that the aspect ratio of mitochondria in infected HeLa cells after 24h and 48h were lower than that of uninfected cells

(**Figure 3C**). Therefore, we can conclude that *Brucella* infection results in fragmentation of the mitochondria at 24h post-infection. Similar results were also observed in BeWo cells, a trophoblast cell line established as a model for this pathogen [341], in which slight fragmentation was observed at 24h, which significantly increased at 48h (**Figure 4A-B**). Together, these results show that *Brucella* induces mitochondrial fragmentation during infection.

We next investigated if this mitochondrial fragmentation was dependent on BspL by infecting HeLa cells with the *ΔbspL* strain. At 24 h after infection, the *ΔbspL* mutant infected cells displayed lower fragmentation than those infected with the WT strain. However, this was no longer the case at 48h after infection (**Figure 3B**). These results suggest that the *ΔbspL* mutant is still able to induce strong mitochondrial fragmentation during infection, but this phenotype is delayed compared to WT (**Figure 3C**), suggesting BspL is contributing to induction of mitochondrial fragmentation early on during infection.

As it is well established that *Brucella* induces ER stress, especially at late stages of the infection, which could explain the induction of mitochondrial fragmentation, we next tested the impact of adding TUDCA to block ER stress during infection. Indeed, we found a low aspect ratio, equivalent to that of untreated wt-infected cells and therefore a high fragmentation of the mitochondria induced by *Brucella* infection (**Figure 3C**). This result indicates that during infection with the WT strain, the observed fragmentation is not a side effect of *Brucella*-induced ER stress. Interestingly, we also found a reduction of the aspect ratio and therefore a high fragmentation of the mitochondria induced by *Brucella ΔbspL* infection following TUDCA treatment in comparison to the untreated *ΔbspL* infected cells (**Figure 3C**). However, this fragmentation is significantly less than that induced by the WT *Brucella* strain in the presence of TUDCA (**Figure 3C**). Together, these results suggest that BspL may play a role in the fragmentation of mitochondria during infection, but we must now complement the mutant phenotype to confirm these results.

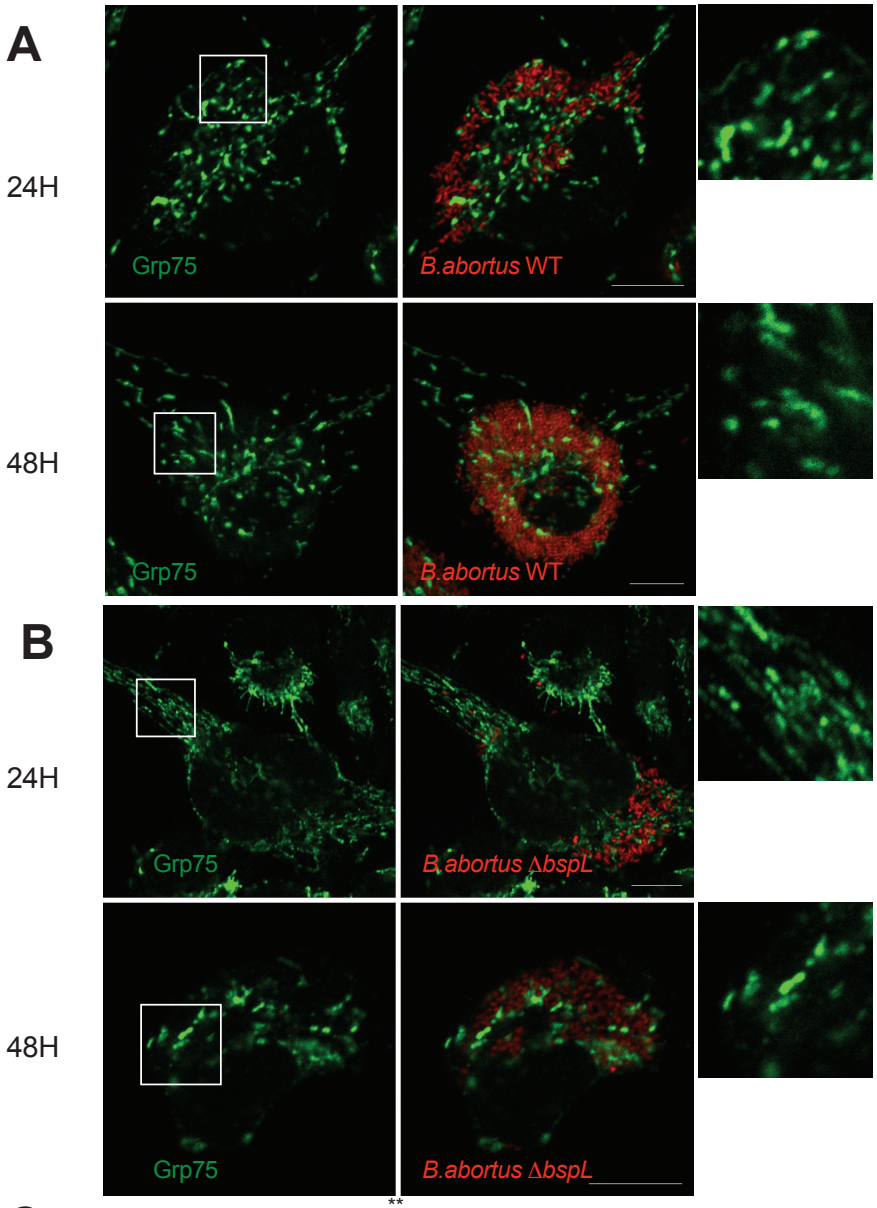
A
24H
Grp75
B.abortus WT
48H
Grp75
B.abortus WT
B
24H
Grp75
B.abortus ΔbspL
48H
Grp75
B.abortus ΔbspL
C
Ranks of Aspect Ratio
500
400
300
200
100
0
**
****
****
****
**
****
****
**
Neg 24H
WT 24H
ΔbspL 24H
Neg 48H
WT 48H
ΔbspL 48H
WT 48H + TUDCA
ΔbspL 48H + TUDCA

Figure 3- BspL contributes to mitochondrial fragmentation in infected HeLa cells. HeLa cells were infected with WT *B. abortus* (**A**) and *ΔbspL* DsRed (**B**) strains for 24h (top panel) and 48h (bottom panel). Cells were fixed and labelled for mitochondria with antibody against Grp75 (green). **(C)** Aspect ratio of the mitochondrial network was determined in HeLa infected for 24h or 48h with either *Brucella abortus* WT or with *ΔbspL*, treated or not with TUDCA 0.5 mM. A total of 60 cells were counted for the control and each infection condition. Results represent the rank of each aspect ratio from 3 independent experiments. The control is non-infected and non-treated with TUDCA. The bar corresponds to the mean of the ranks. Statistical analysis was done with a Kruskal-Wallis test, "****" for $p < 0.0001$, "***" for $p < 0.001$, "**" for $p < 0.01$.

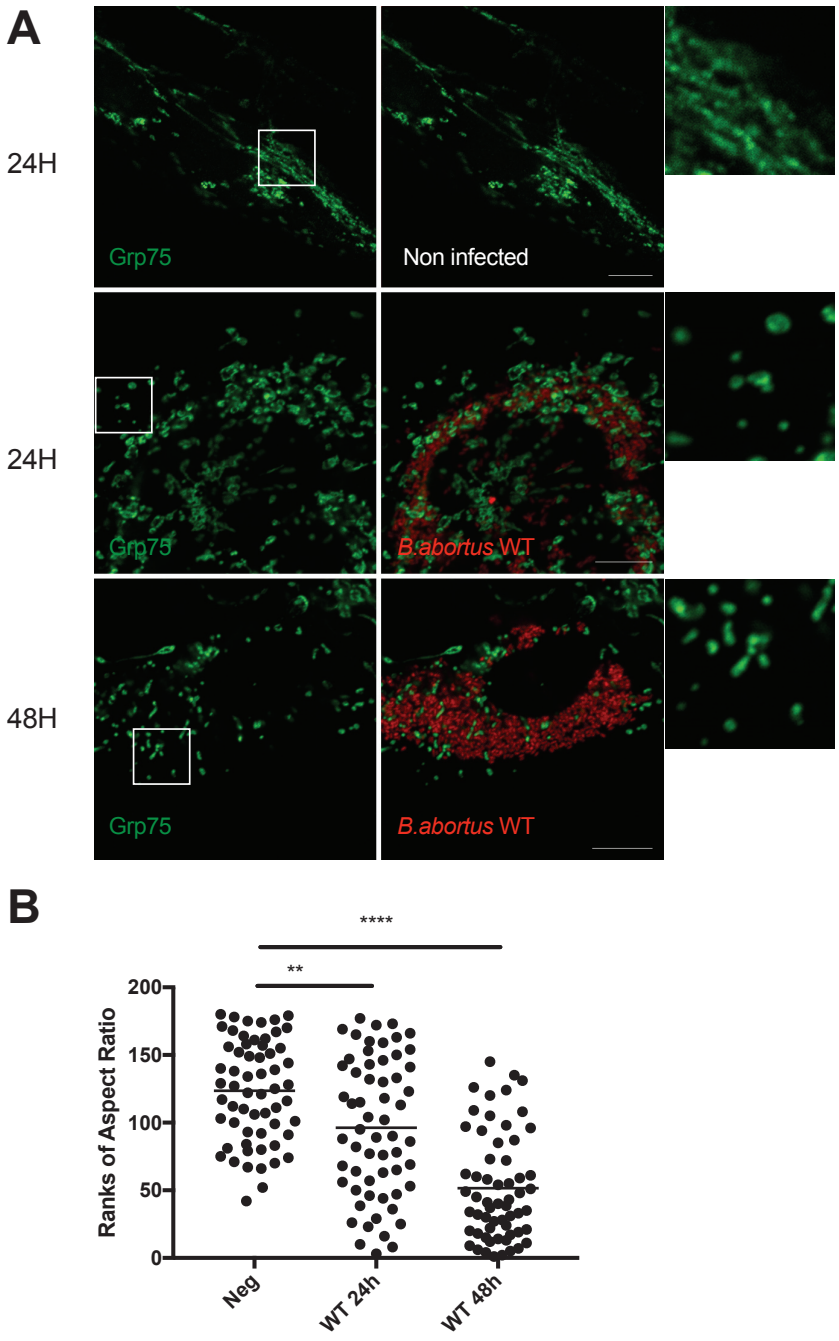

Figure 4- BspL also contributes to mitochondrial fragmentation in infected BeWo cells. (**A**) BeWo cells were infected with WT DsRed strain for 24h or 48h. Cells were fixed and labelled for mitochondria with

antibody against Grp75 (green). Scale bars correspond to 10 μm. **(B)** Aspect ratio of the mitochondrial network was determined in BeWo infected or non-infected cells. Non-infected cells were used as the negative control. A total of 65 cells were counted for the control and each infection condition. Results represent the rank of each aspect ratio from 3 independent experiments. The bar corresponds to the mean of the ranks. Statistical analysis was done with a Kruskal-Wallis test: "****" for $p < 0.0001$, "***" for $p < 0.001$, "**" for $p < 0.01$

4-) BspL induces mitochondrial network fragmentation independently of Herp

Previously we identified Herp as a partner of BspL (see **Chapter 4**). Herp is connected to many cellular processes as described in the chapter 2 and 4, namely regulating ERAD and also protecting mitochondrial dysfunctions and ER stress induced apoptosis [170]. Therefore, we hypothesized that BspL could induce mitochondrial fragmentation by targeting Herp. To test this hypothesis, we used siRNA to down regulate the expression of Herp in cells expressing BspL. In addition, we used tunicamycin to induce ER stress as it is well established ER stress can result in mitochondrial fragmentation. First of all, we observed in BspL transfected cells that the mitochondrial network is still fragmented after siRNA control (ctrl) treatment (**Figure 5A and B**). Similarly, as expected, after tunicamycin treatment in siRNA ctrl treated cells, the mitochondrial network is fragmented. However, down-regulation of Herp did not significantly prevent BspL-induced mitochondrial fragmentation (**Figure 5A and B)** suggesting BspL interaction with Herp does not impact mitochondria. In contrast, Tunicamycin was no longer able to induce mitochondrial fragmentation following Herp silencing, highlighting an important link between Herp and mitochondria stability. This is particularly interesting, as we know from our previous study that silencing of Herp in tunicamycin treated cells in fact enhances ER stress. We are now in the process of quantifying additional experiments and including other *Brucella* effectors. We will also analyze this phenotype in infected cells.

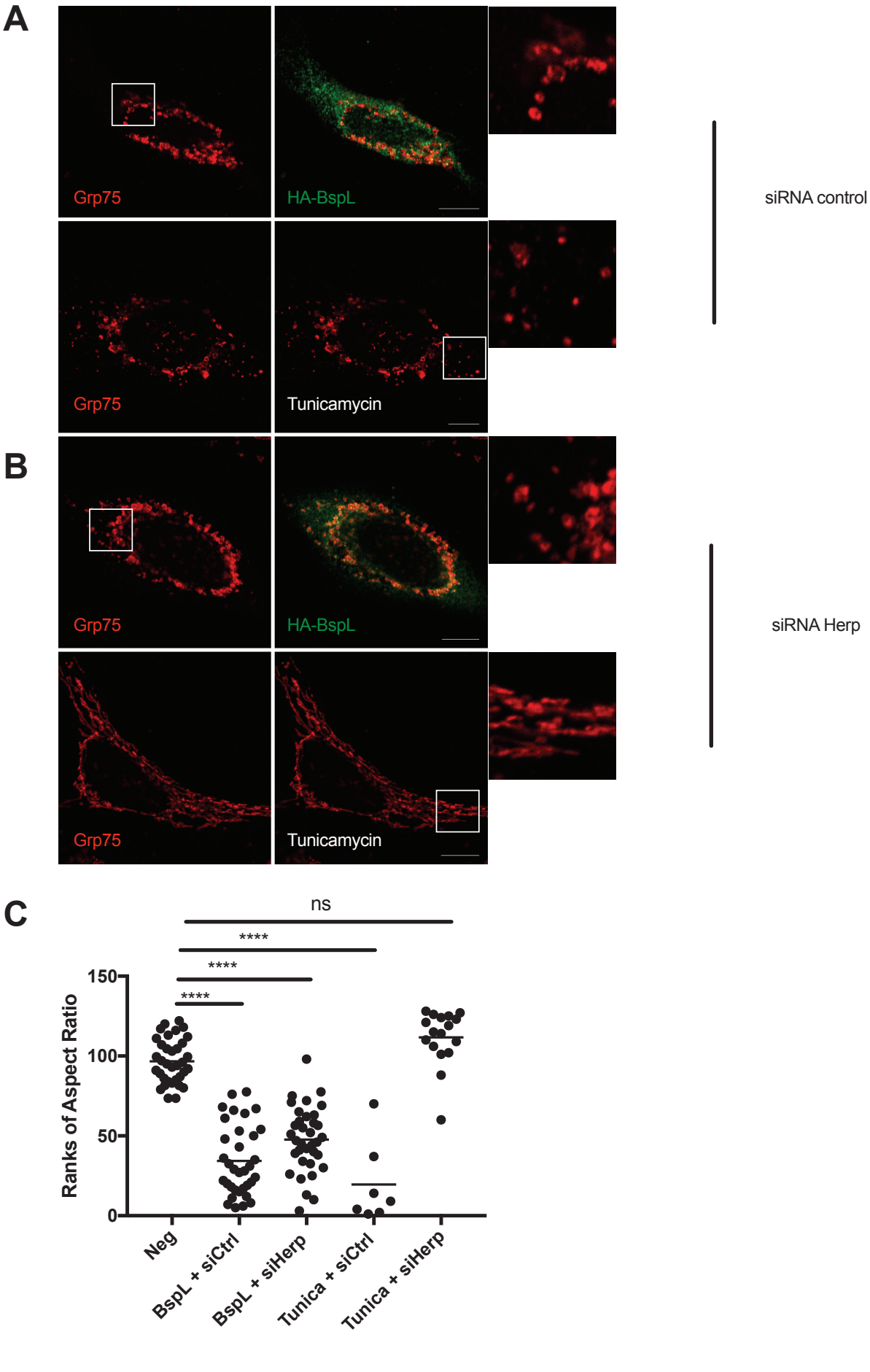
A
Grp75
HA-BspL
Grp75
Tunicamycin
siRNA control
B
Grp75
HA-BspL
Grp75
Tunicamycin
siRNA Herp
C
ns
****
****
****
150
100
50
0
Ranks of Aspect Ratio
Neg
BspL + siCtrl
BspL + siHerp
Tunica + siCtrl
Tunica + siHerp

Figure 5- BspL induces mitochondrial network fragmentation independently of Herp. HeLa were transiently transfected for 24 h with siRNA control **(A) or** against HERP (**B**) and 22h later for plasmid encoding HA-BspL or treated with tunicamycin at 1 µg/µL 6h before harvested. Cells were labeled for mitochondrial chaperone protein Grp75 (red) and an antibody against the HA tag was used to label the effectors (green). Scale bars correspond to 10 µm. Zoom insets of mitochondria are indicated in the white box. (**C**) Aspect ratio of the mitochondrial network was calculated with the software ImageJ in HeLa transfected cells 24h with either siRNA against Herp or control and either BspL or tunicamycin treated cells. Non-transfected cells were also quantified as a control (Neg). A total of 30 cells were counted for the control and BspL-transfected cells. Only 7 cells for tunicamycin and siRNA control treated cells and 15 cells for tunicamycin and siRNA against Herp treated cells. Results represent the rank of each aspect ratio from 1 experiment. The bar corresponds to the mean of the ranks. Statistical analysis was done with a Kruskal-Wallis test: "****" for $p < 0.0001$

5-) BspL does not induce apoptosis

Mitochondrial fragmentation is often associated to apoptosis induction [217] and *Brucella* is known to inhibit apoptosis process [411]. This is why we decided next to test if BspL could be involved in the control of apoptosis or more generally cell death processes. We first measured the level of activation of caspases 3 and 7, key mediators of mitochondrial induced apoptosis, after infection with WT and *ΔbspL* mutant strains (**Figure 6A**). For this assay we infected 2 kinds of cells HeLa and iBMDM to ensure *Brucella* would not be differentially modulating these host cell processes depending on the nature of the infected cell line. We did not observe any differences in apoptosis induction between the WT strain and the mutant strain in both cell types (**Figure 6A**). To ensure we were not simply missing a phenotype for specifically focusing on caspase 3 and 7 we next carried a broader cytotoxicity test by measuring LDH release. We obtained the same results, with no differences observed between the 2 strains and the 2 kinds of infected cells (**Figure 6B**). Thus, BspL is not involved in the

control of apoptosis.

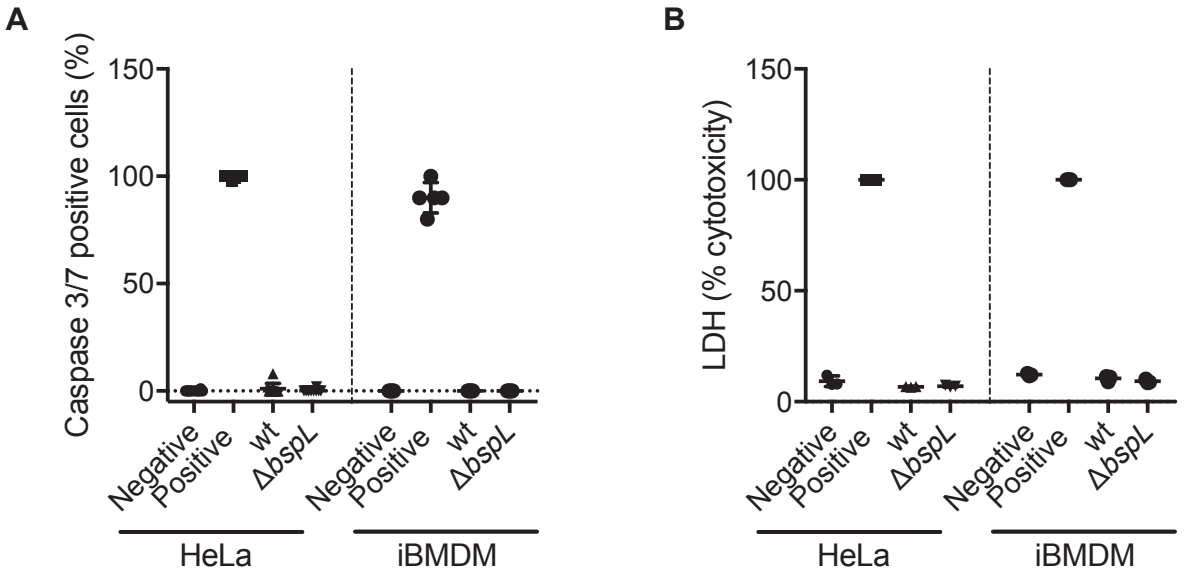

Figure 6- BspL does not induce apoptosis. (A) HeLa (left panel) and iBMDM (right panel) cells were infected with WT *B.abortus* and *ΔbspL* DsRed strains for 48h. Non-infected were also quantified as a negative control and treated cells with a high concentration of 50 µM of Eeyarestatin were quantified as a positive control. Then the coverslips were visualized by confocal microscopy to see if caspase 3 or 7 are activated. More than 100 cells were quantified for each condition from 2 independent experiments and data represent mean +/- standard deviations. (**B**) HeLa (left panel) and iBMDM (right panel) cells were infected with WT *B. abortus* and *ΔbspL* DsRed strains for 48h. Non-infected were also quantified as a negative control and treated cells with a high concentration of 50 µM of Eeyarestatin were quantified as a positive control. Absorbance were quantified after an enzymatic reaction with release LDH and the synthetic substrate, with a TECAN spectrophotometer at 490 nm. Data was obtained from 3 independent experiments and correspond to means +/- standard deviations.

6-) General conclusion

In this chapter we have demonstrated that BspL participates in the induction of mitochondrial fragmentation following transfection and in infected cells. Indeed, with the comparison with the other effectors VceC and BspB and the quantification of the aspect ratio it is clear that BspL specifically impacts the mitochondrial network and independently from an induced ER-stress. Besides, this phenotype is observed in different cell lines, so it will be interesting to determine what kind of mitochondrial functions are targeted by BspL as a result of this induced fragmentation. Furthermore, we found that Herp is not the molecular partner of BspL implicated in these phenotypes as its knockdown does not prevent the mitochondrial fragmentation in BspL transfected cells. We are still in the process of repeating some of the experiments to allow us to perform statistical analysis as well as complementing the mutant

phenotype during infection to validate BspL involvement. Further experiments investigating the impact of different mitochondria functions are also ongoing.

II-) MATERIALS AND METHODS

Cell culture

HeLa epithelial cell line was maintained in Dulbecco's Modified Eagle Medium (DMEM) and Bewo trophoblast cell line in Ham's Nutrient Mixture F12 (Kaighn's) Medium (F12K) with 5 mM of L-glutamine and 10% fetal calf serum (FCS) at 37°C and 5% CO_2.

Bacterial strains

Brucella abortus 2308 is a CO_2-independent, virulent, smooth strain. The *B. abortus* 2308 DsRed strain constitutively expresses fluorescent DsRed due to the integration of the DsRed coding sequence and a kanamycin resistance cassette. DsRed *Brucella abortus* wild-type and mutant strains were grown into tryptic soy agar (TSA) with kanamycin plates for 5 days and then inoculated for 16 hours in tryptic soy broth (TSB) with kanamycin (50 µg/mL).
B. abortus 2308 knockout mutant Δ*bspL* was generated by allelic replacement. Briefly, upstream and downstream regions of about 750 bp flanking the *bspL* gene were amplified by PCR (Q5 NEB) from *B. abortus* 2308 genomic DNA using the following primers:
(i) SpeI_Upstream_Forward: actagtATGTCGAGAACTGCCTGC,
(ii) BamHI_XbaI_Upstream_Reverse: CGGGATCCCGGCTC TAGAGCGCGGCTCCGATTAAAACAG, (iii) BamHI_XbaI_Downstream_Forward: CGGGATCCCGGCTCTAGAGCACCGAACCGATCAACCAG
(iv) SpeI_Downstream_Reverse: actagtCC CTATACCGAGTTGGAGC.
A joining PCR was used to associate the two PCR products using the following primers pairs: (i) and (iv). Finally, the Δ*BspL* fragment was cloned in a SpeI digested suicide vector (pNPTS138). The acquisition of this vector by *B. abortus* after mating with conjugative S17 *Escherichia coli* was selected using the kanamycin resistance cassette of the pNPTS138 vector and the resistance of *B. abortus* to nalidixic acid. The loss of the plasmid concomitant with either deletion of a return to the wild type phenotype was then selected on sucrose, using the *sacB* counter selection marker also present on the vector. Deletant (Δ) strain was identified by diagnostic PCR using the following primers: Forward:

CACTGGCAATGATCAGTTCC and Reverse: CTGACCATTATGTGTGAACAGG (Amplicon length: WT-2000 bp, Δ - 1500 bp). Deletion was also confirmed by sequencing.

Cell infection

Bacterial growth was measured by monitoring the culture optical density at 600 nm. Bacterial cultures were seeded for appropriate multiplicity of infection (MOI) (for HeLa 1:500, BeWo 1:500, iBMDMs 1:50) in the appropriate medium. Infected cells were centrifuged at 400 x g for 10 minutes to initiate bacterial-cell contact followed by incubation for 1h at 37°C and 5% CO_2 for HeLa and BeWo cells and only 10 min for iBMDMs . After the cells were washed 3 times with DMEM or F12K free media. At 1h post-infection (pi), cells were treated with gentamycin (50 µg/mL) to kill extracellular bacteria and at 2 hours pi the medium was replaced with a weaker gentamycin concentration 10 µg/mL. Cells are plated 18h before infection and seeded at 2.10^4 cell / well and 1.10^6cell for 24 and 6 well plates respectively.

Transfection, TUDCA treatment and siRNA treatment

The cells were plated and seeded respectively at $1x10^5$ (for HeLa cells) in culture plates of 6 wells and at $1x10^6$ in 100mm dish. Plasmids coding for different tagged and secreted *Brucella* proteins were introduced into the cells with the transfection reagent Torpedo (Ibidi). The cells were then incubated for 24h at 37°C and 5% $C0_2$, to be then harvested. For TUDCA treatment cells were incubated 18h before transfection or infection experiments with TUDCA (0,5 mM). For siRNA treatment, HeLa were incubated for 48 h with 3 µM ON-TARGETplus SMARTpool siRNAs (GE Dharmacon) directed against human Herp or a non-targeting (si ctrl). For the siRNA transfection Lipofectamine (Thermo Fisher Scientific) reagent was used. siRNA have been bought in the manufacturer Dharmacon, consequently the sequences are not available for confidentiality reasons. Nevertheless, here are the references of the manufacturer
siRNA against Herp: ON-TARGETplus Human Herpud1 Reference L-020918-00
siRNA control: ON-TARGETplus Non-targeting Pool Reference D-001810-10-20

Microscopy and immunofluorescence

After transfection, the coverslips were washed twice with 1X PBS, fixed with Antigen Fix for 15 minutes and then washed again 4 times with PBS. Permeabilization was carried out with a solution of PBS containing 0.5% saponin for 30 minutes and blocking also for 30 minutes was carried out in a solution of PBS containing 1% bovine serum albumin (BSA), 10% horse serum, 0.5% saponin, 0.1% Tween and 0.3 M glycine. Coverslips were then incubated for 3h at room temperature with primary antibody solution, which is the same that blocking solution, or overnight at 4°C. Subsequently, the coverslips were washed twice in PBS containing 0.05% saponin and incubated for 2h with secondary antibodies. Finally, coverslips were washed twice in PBS with 0.05 % saponin, once in PBS and once in ultrapure water. Lastly, they were dried and mounted on a slide with ProLongGold (Life Technologies). The coverslips were visualized with a Confocal Zeiss inverted laser-scanning microscope LSM800 and analyzed using ImageJ software. The bacterial effectors were tagged with either the green fluorescent protein (GFP) or HA tags. We therefore used anti-HA antibodies from rat (dilution 1/50; Sigma). Mitochondria was stained with an antibody against the mitochondrial chaperone Grp75 from mouse (dilution 1/250; Abcam). Secondary anti-mouse and rat antibodies were conjugated with Alexa555 or Alexa 488 fluorochromes (dilution 1/1000).

RNA isolation and real-time polymerase chain reaction (qRT-PCR)

HeLa cells were seeded in Petri Dish at 1.10^6 for each condition were transfected with BspL, VceC or BspB and treated or not with TUDCA (0,5 mM). Next, cells were scrapped to be harvested and to be places on a Qiashredder column in order to isolate nucleic acids and proteins. Then several wash steps were performed and total RNAs were extracted using a RNeasy Mini Kit (Qiagen). 500ng of RNA was reverse transcribed in a final volume of 20 ul to cDNA using QuantiTect Reverse Transcription Kit (Qiagen). Real-time PCR was performed using Brilliant III SYBR Green QPCR (Agilent Technologies, Santa Clara, CA, USA) with an AriaMx Real-Time PCR System (Agilent Technologies). Specific primers are listed in Table 1. The *HPRT*, and *GAPDH* expressions were used as internal controls for normalization and fold change calculated in relation to the DMSO control. Data were analyzed using Prism Graph Pad 5 with a Kruskal-Wallis test (n = 3).

LDH and Apoptosis assays

Apoptosis was monitored in both HeLa and iBMDM cells. To perform this experiment, we used the commercial kit from Thermofisher CellEventTM Caspase-3/7 Green Detection Reagent. This kit contains a fluorescent reagent which is the association of 4 amino acids DEVD conjugated to a nucleic acid that indicates if the caspases 3 and 7 are activated. Cells were infected with WT or mutant strains for 48h. As a positive control of apoptosis induction, the chemical drug Eeyarestatin was used at a lethal concentration of 50 μM. After incubation of the drug or infection with the different strains, the medium was removed to add the reagent for 30 minutes at 37 °C at 10 μM. Then the cells were fixed with the 3% paraformaldehyde solution and the coverslips were visualized with a Confocal Zeiss inverted laser-scanning microscope LSM800. LDH assay was monitored in both HeLa and iBMDM cells with the help of a commercial kit from Roche company. It is composed of 2 reagents: one that will be catalyzed by the release LDH and one dye solution. The absorbance was monitored with a Tecan spectrophotometer. Several controls were performed with the addition of Triton-X100 at 1% in 1 well as a positive control of cytotoxicity, another well only has untreated cells as a negative control and a last well only contains the used medium to estimate the background. Absorbance background was then subtracted to all the samples. Then the % of cytotoxicity was calculated by normalizing with the positive control and the negative control for both HeLa and iBMDM cells. Positive control is considered at 100% of cytotoxicity.

Chapter 6 Discussion

I-) Infectiology a neglected research topic

The 20th century was considered as the cancer century because of its discovery and its incidence on public health. I think the 21st century will be that of microbiological infections and could represent a step back into the past. In part this is due to extensive anti-vaccination campaigns around the world that are responsible for the reemergence of some bacterial pathogens [425]. Although antibiotherapy has allowed countries to fight against major bacterial infections, nowadays this is becoming more and more difficult due to the increase in antibiotic resistance. Indeed, extreme antibiotic resistance has been observed for several bacterial pathogens as *Acinetobacter baumannii* and *Mycobacterium tuberculosis*, with strains that resist to 90% of antibiotics [426,427].

Furthermore, there is an alarming tendency of re-emerging infectious diseases in the world as the plague caused by *Yersinia pestis* a serious human infection [428] as well as animal diseases as brucellosis, considered by the WHO as an re-emerging zoonosis. Brucellosis was considered eradicated in most of Europe, notably in France, but the 2 outbreaks in 2012 and 2014 in "le massif du Bargy" highlight its presence even in previously considered "brucellosis-free" countries [429].

Re-emergence of human and animal diseases act as a reminder for us continue studying these kinds of pathogens, improve disease control and enforce better human and animal vaccination programs. In the case of animal diseases as brucellosis, the study of local wildlife is often neglected which in my opinion is a mistake because they represent an important reservoir of bacteria that can become a threat. The perfect illustration of the importance of this biodiversity is the identification of new *Brucella* species in wildlife hosts, including amphibians, marine mammals, baboons and wild rodents [430]. It is therefore, in my opinion, important that the scientific community continue to convince governments of the importance of studying these kinds of pathogens because zoonotic bacteria represent a public health issue with important economic consequences.

In recent years, our knowledge on bacterial pathogenesis has consistently increased with for instance the identification and characterization of secretion systems. However, secreted effectors still require further studies so we can understand the eukaryotic pathways targeted during disease. Indeed, one could compare secretion systems as molecular guns where effectors are their bullets with a very high specificity in the targeting. It is fascinating

from an evolution and functional point of view how secretion systems are relatively well conserved between bacteria but not the associated secreted effectors making the challenge harder. Moreover, it is also surprising to see a bacterium as *Legionella* which has more than 300 identified effectors compared with *Helicobacter pylori* which seems to control its infection process with a very restricted catalog of effectors.

II-) Impact of BspL on *Brucella* pathogenesis and ERQC processes

BspL could have been yet another *Brucella* effector that is located in the ER to induce stress and disorder for the cell. This was in fact what we were thinking at the beginning of our project after the obtention of our first data about its localization and the induction of ER stress in transfection. But, the identification of Herp as a target of BspL lead us to investigate the cellular pathways targeted further. Indeed, it is known that Herp is over-regulated during ER stress, but why would be BspL induce ER stress if interacting with Herp?

Analyzing previously described functions of Herp allowed us to find the role of BspL for *Brucella*. Indeed, as presented in the **Chapters 1** and **4** Herp is involved in several ERQC processes as ERAD and autophagy. Concerning ERAD process, and with the help of a TCR reporter we clearly demonstrated that ERAD is affected by BspL with a higher degradation of glycosylated TCR. It will be important now to investigate which step of the ERAD BspL is targeting. Herp is involved in multiple stages, including stabilization of ER complexes at specific sites, retrotranslocation and delivery to the proteasome. Further molecular studies are required and use of pulse-chase experiments essential to follow in greater detail the ERAD pathway. In my opinion, it would also be interesting to analyze other reporters, for example, unglycosylated proteins or Herp-independent targets for ERAD.

We also highlighted the importance of ERAD at different stages of infection for *Brucella*. We were surprised to observe that ERAD blocking enhanced replication whilst BspL has a clear opposite effect on the ERAD process. It would be interesting to test all ER-targeting effectors, VceC, BspA-K and BtpA to determine if one of more effectors could be blocking ERAD at earlier stages of the infection. Our results with BspL make it clear that ERAD is finely controlled by *Brucella* to have the time to ensure its replication in the infected cell.

Thanks to the study by Starr *et al*. for aBCV formation and the associated role of Herp of autophagy regulation we were prompted to investigate if BspL could be involved in the

formation of aBCVs. The difference in the kinetics of aBCV formation between the mutant strain and the wild-type strain clearly sustains an implication of BspL in the process of aBCV formation. However, as it stands, the connection with ERAD remains circumstantial. It will be essential to monitor ERAD throughout the infection cycle and pinpoint when HERP-dependency mediated via BspL is occurring. Experiments using siRNA in macrophages could be useful but are technically challenging. Herp has a very quick turnover and we cannot successfully do siRNA treatments throughout 48 and 65h, the time points in which aBCVs begin to be formed. Unfortunately, we did not succeed to make CRISPR KO of Herp. This would have been the ideal tool.

As discussed in the discussion of Chapter 4, our study highlighted for the first time a role for hijacking of ERAD in control of intracellular trafficking. This may be a more widespread topic in bacterial pathogenesis. Most papers that study interference of pathogens on ERQC mainly focus on UPR and particularly the 3 UPR sensors and the associated chaperone BiP. The identification and the characterization of HERP in infection context as the importance of ERAD for *Brucella* bring an important novel concept to the *Brucella* field.

III-) Impact of BspL on mitochondria

In parallel, the implication of BspL in the fragmentation of mitochondrial network is also an exciting set of data as this is the first *Brucella* effector shown to fragment in different cell lines as HeLa and trophoblast BeWo. As MitF *Legionella* effector [431], there is no induced cell death after ectopic expression or *Brucella* infection. Consequently, it will be interesting to test also the concentration of some metabolites as glucose or lactate. Indeed, some studies referred that some pathogens including *Brucella* are able to induce a metabolic shift [297,410]. So, it will be very interesting to determine if BspL is the responsible effector of the shift that allows the differentiation of macrophages [297]. It will be also interesting to find how BspL induces mitochondrial fragmentation by identifying the mitochondrial partner. We have seen that this is not subverted via Herp interaction as its downregulation by RNA interference did not prevent mitochondrial fragmentation after BspL ectopic expression. In addition, with the study of Lobet *et al*. [411] we also know that it is not dependent on DRP1 contrary to *Legionella* [294]. To try to address this question I would focus on Alex3 which is one of the putative BspL targets identified after the yeast two-hybrid presented in the **Chapter 4.** Indeed, Alex3 is an interesting candidate because of its localization in the OMM

and it has been shown to be involved in mitochondrial dynamics and trafficking [421]. At the beginning of my Ph.D., we have tried to perform co-immunoprecipitation and microscopy experiments. However, it was not possible to co-transfect BspL with Alex3 because of cytotoxicity. We found endogenous Alex3 to interact with BspL, VceC and BspB. Consequently, we did not pursue our experiments because we conclude there the interaction between BspL and Alex3 may not be specific. However, it is also a possibility that we did not succeed to set the right experimental conditions to analyze Alex3 interactions. Thus, it would be worth to take more time to try to better characterize this mitochondrial protein with BspL overexpression and in *Brucella* infection context. If Alex3 is a false positive that often occurs in yeast two-hybrid experiments, we should use a global approach to find other putative partners of BspL as co-immunoprecipitation coupled to mass spectrometry, such as using a BioID approach.

Finally, to conclude with this axis, it is important to note that in infected cells, mitochondrial fragmentation is significantly enhanced at late stages of the infection and when the cell is full of bacteria. It is possible that the space occupied by these bacteria results in perturbation of the network just by mechanical force as shown by Helle *et al* [316] . Further work has to be done to confirm this hypothesis and determine if lack of significant difference in mitochondrial fragmentation at 48h is due to replication-induced space restrictions or the action of other unknown effectors.

As mentioned in the end of the **Chapter 3**, we have to be careful interpreting data on effectors that target both the ER and mitochondria. To further characterize BspL it will be interesting to try to localize the effector in infection by building a 4HA-tag effector which could be followed by microscopy, a strategy now successfully implemented in the lab for other *Brucella* effectors. Indeed, we could precisely determine when and where this effector is translocated and then where it is located during infection. We could see if the effector uniquely resides in the ER or moves or transiently interacts with mitochondria. Moreover, and in the same aim, we could make a subcellular fractionation as an alternative technic to localize BspL. It will be good to succeed to isolate ER, mitochondria and MAM fractions because it could give us important details to further investigate. However, it remains nowadays very complicated to perfectly separate these 3 fractions as ER is often found in all subcellular fractions. Besides it is also hard to have an enough quantity of purified MAMs especially when we are working on single cells. Thus, the investigation of BspL localization will require to overcome technical challenges to answer these questions on BspL

Otherwise, as illustrated in the **Chapter 2** the variation of calcium flux is crucial as it was demonstrated to impact several processes as apoptosis and metabolism. Several tools are available as some fluorescent probes as Fluo4-AM or Fura2. With the help of these probes, it is possible to visualize calcium concentration at contact sites of ER mitochondria but also the calcium that is coming from ER [432]. I think we can apply this kind of study in the context of *Brucella* infection. Indeed, given the link with cellular metabolism and the impact of *Brucella* on major metabolic pathways, I think it is of utmost importance to study how *Brucella* impacts calcium concentration and even the associated flux.

IV-) Bacterial effectors and eukaryotic motifs

Since a few years many researchers have highlighted the presence of motifs or eukaryotic domains in bacterial effector proteins [359,433]. This is also the case for BspL which presents a putative eukaryotic CAAX motif whose the function remains to be determined in context of *Brucella* infection. This tetrapeptide most often corresponds to the enchainment of 1 cystein, 2 aliphatic amino acids and any amino acid. This motif in eukaryotic cell is known to be a posttranslational lipid modified termed prenylation. Prenylation is the addition of either farnesyl or geranylgeranyl lipid groups to the cysteine [434]. For eukaryotic proteins this modification is important for the anchoring of the protein into cellular membranes as illustrated by the G proteins or Rho GTPases. Consequently, it is intriguing to find this motif in bacterial protein even if the anchoring function could explain why bacteria keep this motif in their protein. Several effectors have been shown to contain CAAX motifs, or derivatives such as SifA identified in *Salmonella enterica* [418] or AnkB from *Legionella penumophila* [407,419,435]. In some cases, such as for SifA from *Salmonella*, there is no need for two aliphatic acids for it to be a functional CAAX. The key residue is the cysteine that in the case of SifA is modified by isoprenoid addition by a host geranylgeranyl transferase I and is required for virulence. We tested the impact of this protein signature on the ER localization of BspL and we did not find any change. Nevertheless, a study has shown that the palmitoylation (another lipid modification) of the ER calnexin chaperone was shown to interact with MAMs with an ER located pump participating in Ca^{2+} regulating signaling. In contrast, its non-palmitoylated form remains in the ER to mediate protein folding and quality control [436]. Consequently, it would be great to perform other experiments with BspL depleted for its CAAX motif and to test the consequences on mitochondria or more generally in MAMs. It is

possible that the CAAX motif contributes to sub-ER localization or accumulation in MAMs. Alternatively, this CAAX might not be involved in the localization of the effector but rather in some specific protein interactions.

In our case, this eukaryotic-like domain led us to identify BspL as a new effector following from an *in-silico* screen, a widely used approach to identify new secreted bacterial proteins in genome database. From an evolution point of view, it is reasonable to think that these bacterial proteins with eukaryotic domains may result from a horizontal gene transfer from eukaryotes to bacteria [399]. Furthermore, the possession of eukaryotic domains is certainly likely to be involved in interaction and / or modulation of host factors. We must now further investigate if BspL undergoes any lipid modifications to determine if this C-terminal tetrapeptide is indeed a CAAX motif with relevance during infection.

V-) *Brucella* effectors: a potential new direction following UPR and intracellular trafficking studies

This last decade the studies on *Brucella* effectors mainly focused on those that induce ER stress or are involved in the intracellular trafficking especially between the maturation of eBCV to rBCV. Nevertheless, there are still some gaps in knowledge regarding *Brucella* pathogenesis that could be explained by the identification and the characterization of new effectors. I would like to discuss two recent studies, that characterized 2 effectors that may provide another path of research in terms of the control of innate immunity and more excitingly immunometabolism processes.

The first one is BPE005 that directly impacts innate immunity in special cells from the liver. Authors demonstrated that the effector induces a fibrotic phenotype [437]. This particular phenotype is important in the establishment of chronic infection as it contributes to a reduction of antibiotic penetration because it seems to induce granuloma formation of liver cells. They have also shown that the effector inhibits in transfection and infection the metalloproteinase 9 (MMP9). This result is particularly interesting because this kind of proteins are linked to innate immunity as they allowed the recruitment of inflammatory cells and consequently regulate their functions [438]. Thus, the identification of this effector initially described in 2011 has added a new complexity to the pathogenicity of *Brucella* after the characterizations of VceC, BtpA, BtpB and PrpA. Indeed, it seems that according to the infected cell type or tissue there are some different strategies that are used by *Brucella* to decrease or induce specific immune responses [437]. Although the functions of the effector

are not related to my work, it is important to keep in mind that only the full characterization of all *Brucella* effectors will be able to provide a comprehensive understanding of the cellular pathways targeted during infection.

In another study more relevant in the context of the work presented in this thesis, the BPE123 effector was found to participate in the recruitment of Enolase 1 (ENO-1 or ENO-α) on BCVs [439]. Briefly enolases or 2-phospho-D-glycerate hydrolases are enzymes that are involved in glycolysis and gluconeogenesis metabolic pathways. There are three different enolase isoforms alpha or 1, beta or 2 and gamma or 3-enolase. Interestingly ENO-1 is associated mitogenic stimulation in lymphocytes [440] and after inflammatory stimuli and cytokines production [441]. Thus, ENO1 is as bound to metabolism processes as to immune responses. Moreover, given the link of ENO1 with glycolysis it perfectly sustains the involvement or a possible hijacking of glycolysis during *Brucella* infection as previously demonstrated by Xavier *et al*. [297] and Czych *et al*. [410] Furthermore, BPE123 is the first effector that is associated to metabolic processes. It will be interesting to investigate more its precise role on metabolic intermediates and at which stage of infection it is contributing the most. Interestingly authors have shown that ENO-1 depletion by siRNA impaired *B. abortus* replication in HeLa cells which confirms again the importance of glycolysis for *Brucella* and particularly ENO1 as ENO-1 activity levels were enhanced upon *B. abortus* infection of THP-1 macrophagic cells, and this activation is highly dependent on BPE123. Furthermore, the depletion of this effector impacts the bacterial replication. This suggests that this effector is involved in early stages of infection. Control of host metabolism during infection is a topic that deserves additional research in the context of *Brucella* infection [439]. To support this, recent work from our lab has highlighted that BtpA and BtpB, the TIR domain-containing effectors retain NAD consuming activity during infection inducing a decrease in intracellular NAD^+ levels. This coenzyme plays not only a key role in bioenergetics namely glycolysis but has also been found to have a prominent function in cell signalling and immunomodulation. In addition, as BspL induces fragmentation of mitochondria it is likely to play a role in immunometabolism regulation during infection. Therefore, this is, in my opinion, a very interesting topic to pursue in the future.

VI-) 2011-2019 What is new on *Brucella*?

In 2011, at the end of the review of Atluri *et al*. six questions were raised by the authors [341]

in the discussion about future perspectives to investigate for a better understanding of *Brucella* pathogenesis. I decided to select a subset of these questions to illustrate the recent advances in the field. Among the questions, there was: "What is the role of the previously and newly described T4SS substrates in promoting intracellular persistence?" and "Are there additional T4SS substrates that mediate ER localization of *Brucella*?" In 2011, only 10 T4SS effectors had been identified and remained weakly characterized. Today, there are 25 referenced effectors (see **Table 2**). So, I think that during this last decade the *Brucella* community has succeeded to increase our knowledge on the "previously described T4SS substrates", identify new ones that are still being characterized (BPE123 for example) and in a few cases undertake the deep molecular functional study such as the case of BspB and VceC. I am excited that my work on BspL, once published, will also contribute towards advancement of our comprehension of *Brucella* pathogenesis. BspL was identified in 2014 and it took my full thesis work to propose a function for this effector and its first characterization. One interesting area to explore in *Brucella* pathogenesis is the association of effector functions and their kinetics. As I mentioned above, there are several effectors that manipulates ER stress processes as VceC, BspL and some Bsp proteins. Although several of them induce ER stress, they have distinct functions during infection with VceC inducing inflammation and BspL modulating ERAD. It is necessary now to determine the chronological action of *Brucella* effectors particularly regarding trafficking and ER stress. It is very likely that the function of several effectors is to compensate the activity of others. This has become particularly obvious having studied BspL that slows down aBCV formation and induces ERAD, most likely to compensate for the action of another effector blocking ERAD at an earlier stage of the intracellular cycle. Indeed, we have demonstrated at early stage that inhibition of ERAD could be beneficial for replication. However, a permanent inhibition of ERAD seems to result in a truncated cell cycle with premature aBCVs formation. We have unfortunately not been able to block ERAD long enough to monitor aBCV formation in macrophages due to the toxicity of the drug used but we could observe in epithelial cells premature exit from infected cells at 48h post-infection. In summary, it would not be surprising to find in the future different effectors that modulate ERAD in a different manner and at different time point post infection.

The second question of the review was "How does residence in the ER-associated compartment provide an intracellular growth advantage to *Brucella*?". I think the identification of ER targeted effectors including BspL, helps to begin answering this question.

As explained in the first chapter of my introduction, the ER is crucial for eukaryotic cells. *Brucella* establishes its niches in ER that are prolongment of ER cisternae as shown in the paper of Sedzicki *et al*. [386] Thus, the interest in *Brucella* to be close with this organelle is to rapidly target specific components to subvert many associated functions. This location allows *Brucella* control of UPR to modulate the inflammation process, control of ERAD to regulate its proliferation and the control of ER secretion to impact protein maturation and intercept vesicular trafficking as a source of membrane or nutrients. To conclude, this ER localization niche is a great advantage for *Brucella* because at this place the pathogen can totally control the cell given its connection to almost all the cell processes. In this context, I think we should address how other organelles than ER are triggered by the bacteria. This has already begun for the ERGIC [391] and us, with characterizations of fragmented mitochondria.

Finally, I will end with a last question which remains unsolved: "How do *Brucella* inhibit apoptosis of infected host cells?".

Indeed, I selected this last question even though with BspL characterization, I do not contribute to answer this question. Despite the fact that BspL contributes to fragmentation of the mitochondrial network, we did not observe any apoptosis induction or inhibition. Indeed, as described in the **chapter 3 section III-5-)** *Brucella* does not induce cell death to quit the cells at the end of its cycle. Moreover, what I did not mention previously is it has also been shown that *Brucella* actively prevents apoptosis in few studies [442,443]. Indeed, in 2000, it was already shown that *Brucella* infection upregulated BCL2A1, a member of the BCL2 family known to have an antiapoptotic activity [443]. Few years later another study has shown that globally *Brucella melitensis* represses mitochondrial genes involved in apoptosis induction [444]. To date some studies are published to try to identify the *Brucella* mechanisms to inhibit apoptosis. Cui *et al*. [442] also worked on this topic where they also found an inhibition of apoptosis in macrophages via the degradation of the calcium dependent protein Nedd4. Thus, even if there are some attempts to determine that apoptosis is inhibited by different mechanisms in different cell lines or different *Brucella* strains we still do not know if this is dependent of T4SS effectors or other bacterial molecules. This topic remains open and unexplored and will require perhaps large-scale approach to identify several putative proteins involved in the control of cell death.

For the future, it will be very important in my opinion to use system biology approaches which regroup several disciplines to better answer these biological questions

particularly in the context of host-pathogen relationships. Indeed, today this topic of research requires a deep characterization of the molecular mechanisms when studying bacterial effectors. In addition, it is important when we try to characterize the impact on bacterial proteins on cell eukaryotic process, to ensure that the observed consequences are directly due to the effector and not a side effect of the infection itself or due to experimental procedures as for example in the case of transfections. Furthermore, interactions between components of a system such as individual effectors with individual targets, is beginning to reveal numerous phenotypes and properties that cannot be understood from the study of each component individually. To understand the infection process as a whole, a more comprehensive understanding of the relationships between different effectors and *Brucella* components within the host cell or even the whole organism will allow for more accurate knowledge of the system's behavior. Thus, system biology approaches may help to connect all the data generated, molecular and cellular, all the pathways targeted and each effector function in the timeline of the infection cycle. Combined with artificial intelligence for processing all the data and decipher its complexity maybe one day we will have a full understanding of the molecular mechanisms governing *Brucella* infection!

Chapter 7 Secondary Projects and Contributions

In this chapter I include the papers where I had the opportunity to take part in. Before the pdf of the article, I briefly summarize bellow the context of the studies and the main results. I also include a description of what experiments I carried out to show my precise contribution for each of these publications.

I-) Unsaturated Fatty Acids Affect Quorum Sensing Communication System and Inhibit Motility and Biofilm Formation of *Acinetobacter baumannii*

Nicol *et al*. 2018

International Journal of Molecular Sciences

Acinetobacter baumannii (*Ab*) is a nosocomial emerging pathogen representing an increasing threat for public health because of its incidence in hospitals [445,446]. Indeed, *Acinetobacter* can persist on abiotic and biotic surfaces for several weeks and can resist to dessication or chemical treatments used for disinfection [445](Peleg 2008 Clinical Microbiology Reviews). *Ab* strains have shown a significant increase antimicrobial resistance, with prevalence of Multiple Drug Resistant (MDR) and even Extensively Drug Resistant (XDR) strains in certain countries. For all these reasons, WHO has placed *Ab* as top research priority from the "ESKAPE" pathogen list which regroups 6 bacterial pathogens (*Enterococcus faecium*, *Staphylococcus aureus*, *Klebsiella pneumoniae*, *Pseudomonas aeruginosa* and *Enterobacter* spp.). These pathogens are becoming extremely difficult to treat and therefore will represent an increasing problem if we cannot find alternative therapies [447].

In this study authors highlighted a potentially promising treatment against *Ab* with the use of palmitoleic (PoA) and myristoleic (MoA) fatty acids. Indeed, the authors demonstrated an efficient antibiofilm activity and a biofilm dispersing effect after the use of these drugs.

Moreover, they also showed an impairment on the bacterial motility. We found that these small molecules down regulate the expression of *abaR*, a gene from the LuxIR-type quorum sensing (QS) communication system AbaIR [448] [449]). The consequence of this is a reduction of the *N*-acyl-homoserine lactone production which is a crucial compound in the development of the biofilm [450].

My contribution for this paper was to perform quantitative PCR to measure the level of the regulator *abaR* after different treatments with Virstatin, PoA and MoA on *Acinetobacter baumannii* cultures. I had to establish the protocol for RNA extraction from *Acinetobacter* as well as test multiple housekeeping genes to find those best suited for internal controls under the experimental conditions tested. These results are presented in the Figure 2A in the published paper below. This study was mainly led by the Principal Investigator Dr. Emmanuelle Dé, so I thank her to have given me the chance to take part in this project.

International Journal of
Molecular Sciences

MDPI

Article

Unsaturated Fatty Acids Affect Quorum Sensing Communication System and Inhibit Motility and Biofilm Formation of *Acinetobacter baumannii*

Marion Nicol [1,2], Stéphane Alexandre [1,2], Jean-Baptiste Luizet [3], Malena Skogman [4], Thierry Jouenne [1,2], Suzana P. Salcedo [3] and Emmanuelle Dé [1,2,*]

1 Normandie University, Unirouen, 76000 Rouen, France; marion.nicol@etu.univ-rouen.fr (M.N.); stephane.alexandre@univ-rouen.fr (S.A.); thierry.jouenne@univ-rouen.fr (T.J.)
2 CNRS, UMR 6270, Polymers, Biopolymers, Surfaces Laboratory, F-76821 Mont-Saint-Aignan, France
3 Laboratory of Molecular Microbiology and Structural Biochemistry, University of Lyon, Centre National de la Recherche Scientifique, F-69367 Lyon, France; jean-baptiste.luizet@ibcp.fr (J.-B.L.); suzana.salcedo@ibcp.fr (S.P.S.)
4 Department of Pharmaceutical Biosciences, Faculty of Pharmacy, University of Helsinki, Viikinkaari 5E, FI-00014 Helsinki, Finland; malena.skogman@helsinki.fi
* Correspondence: emmanuelle.de@univ-rouen.fr; Tel.: +33-2-35-14-66-99

Received: 21 November 2017; Accepted: 8 January 2018; Published: 10 January 2018

Abstract: The increasing threat of *Acinetobacter baumannii* as a nosocomial pathogen is mainly due to the occurrence of multidrug-resistant strains that are associated with the real problem of its eradication from hospital wards. The particular ability of this pathogen to form biofilms contributes to its persistence, increases antibiotic resistance, and promotes persistent/device-related infections. We previously demonstrated that virstatin, which is a small organic compound known to decrease virulence of *Vibrio cholera* via an inhibition of T4-pili expression, displayed very promising activity to prevent *A. baumannii* biofilm development. Here, we examined the antibiofilm activity of mono-unsaturated chain fatty acids, palmitoleic (PoA), and myristoleic (MoA) acids, presenting similar action on *V. cholerae* virulence. We demonstrated that PoA and MoA (at 0.02 mg/mL) were able to decrease *A. baumannii* ATCC 17978 biofilm formation up to 38% and 24%, respectively, presented a biofilm dispersing effect and drastically reduced motility. We highlighted that these fatty acids decreased the expression of the regulator *abaR* from the LuxIR-type quorum sensing (QS) communication system AbaIR and consequently reduced the *N*-acyl-homoserine lactone production (AHL). This effect can be countered by addition of exogenous AHLs. Besides, fatty acids may have additional non-targeted effects, independent from QS. Atomic force microscopy experiments probed indeed that PoA and MoA could also act on the initial adhesion process in modifying the material interface properties. Evaluation of fatty acids effect on 22 clinical isolates showed a strain-dependent antibiofilm activity, which was not correlated to hydrophobicity or pellicle formation ability of the tested strains, and suggested a real diversity in cell-to-cell communication systems involved in *A. baumannii* biofilm formation.

Keywords: palmitoleic acid; myristoleic acid; biofilm; pellicle; quorum sensing

1. Introduction

Acinetobacter baumannii is a bacterial pathogen causing nosocomial outbreaks worldwide and is responsible for many infections, such as pneumonia and bloodstream infections, especially in intensive cares units [1,2]. Due to its exceptional adaptability to detrimental environmental conditions, this bacterial species has rapidly emerged as a Multi-Drug Resistant (MDR), but also XDR (extensively-DR) and now, more and more often, as a PDR (Pan-DR) organism. This led the

World Health Organization to classify *A. baumannii* among the "Critical" bacterial agents (priority 1), for which research and development of new and effective antibiotic treatments are urgently required. Besides, this pathogen is also problematic for its long-time survival in hospital settings owing to its great ability to survive desiccation [3] or treatment with disinfectants [4]. This persistence is mostly linked to its capacity to form biofilms [5,6]. Virstatin is known to inhibit expression of cholera toxin (encoding by *ctx* genes) and toxin co-regulated pilus (a type IV pilus, T4P, encoding by *tcp* genes), two major virulence factors of *Vibrio cholerae*. We previously demonstrated that this small organic molecule prevents *A. baumannii* biofilm production possibly via inhibition of pili biosynthesis [7–9]. Virstatin antibiofilm activity was recently confirmed on *Acinetobacter nosocomialis* [10], and could be due to an inhibition of the Quorum-sensing (QS) system. QS is a communication system that orchestrates bacterial behaviors within a microenvironment to promote community establishment by the regulation of specific genes. In most gram-negative bacteria, signal molecules, called acyl-homoserine lactones (AHLs), are diffusible autoinducers that are characterized by a length variable acyl-chain coupled with a homoserine lactone ring [11]. In *A. baumannii*, different type of AHLs have been described [12], the most commonly described ones are long chain AHLs with C_{10} or C_{12} acyl chains [13–15]. When considering its crucial involvement in biofilm development, QS is an interesting target for the development of antibiofilm strategies that can act either by inhibiting the signal molecule synthesis, or by degrading or quenching this signal in the external environment [12]. Some mono-unsaturated fatty acids (UFAs) as palmitoleic (*cis*-9-hexadecenoïc, C16:1Δ9, PoA) and myristoleic (*cis*-9-tetradecenoïc, C14:1Δ9, MoA) acids were shown to inhibit *tcp* genes expression in *V. cholerae* [16,17]. These molecules prevent the interaction between their transcriptional regulator ToxT and the DNA [18]. Bactericidal activity of UFAs, in particular against cutaneous pathogens, has already been described [19–21]. Besides, UFAs can also affect virulence factor expression, initial adhesion, or motility [20]. In this study, we evaluated the efficacy of unsaturated fatty acids, PoA and MoA, as antibiofilm compounds and investigated their effect on *A. baumannii* QS system.

2. Results and Discussion

2.1. Effect of UFAs on A. baumannii ATCC 17978 Biofilm Growth and Motility

Activity of PoA and MoA was preliminary tested on *A. baumannii* ATCC 17978 reference strain forming both a biofilm at the solid-liquid interface and a pellicle. In the planktonic growth mode, MICs of 4 mg/mL were obtained for each UFA. To investigate the antibiofilm activity of these compounds, we used sub-inhibitory concentrations at least 100-fold lower than the MICs, i.e., 0.01, 0.02 and 0.05 mg/mL, concentrations in agreement with those used to decrease production of T4P in *V. cholerae* [17]. At these concentrations, fatty acids did not modify bacterial growth (Figure S1). The biofilm formation inhibition by fatty acids is clearly depicted by the Figure 1a. Addition of PoA reduced significantly the biofilm formation at the three tested concentrations (up to 37% and 39% reduction at 0.02 and 0.05 mg/mL, respectively), whereas MoA exhibited a significant activity only at 0.02 and 0.05 mg/mL (decrease of 28% and 42% respectively). These results showed that UFAs display a biofilm inhibition activity that is similar to that of virstatin, for which the decrease reached 32%, MoA being however less active than PoA at lower concentrations. Biofilm dispersion activity of UFAs was investigated on 24 h-static biofilms. Incubation of biofilms with MoA or PoA for anadditional 24 h demonstrated that these UFA displayed significant dispersive activity as compared to virstatin (decrease of 24% for MoA and PoA at 0.05 mg/mL, Figure 1a). Finally, *A. baumannii* surface motility was tested on semi-solid medium plate (0.3% agar) with or without UFAs (Figure 1b at 0.02 mg/mL and Table S1). PoA impeded motility when added at 0.02 and 0.05 mg/mL and MoA also significantly decreased the motility up to 73% at 0.05 mg/mL.

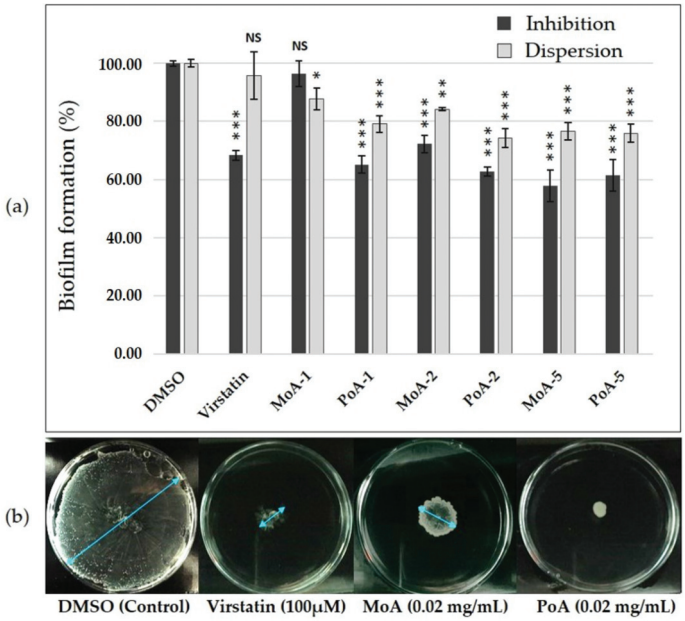

Figure 1. UFAs activity on *A. baumannii* ATCC 17978 motility and biofilm formation. (**a**) Inhibition and dispersion of biofilms quantified by crystal violet staining method. 24 h-biofilms were treated with or without virstatin (100 µM), palmitoleic acid (PoA) or myristoleic acid (MoA) at different concentrations (0.01 (UFA-1), 0.02 (UFA-2) or 0.05 (UFA-5) mg/mL) and DMSO as control; (**b**) Activity on motility. Blue arrows measure the diameter of surface motility. Results are presented as (mean ± standard error of mean). "***" for $p < 0.0001$, "**" for $p < 0.01$, "*" for $p < 0.05$ and "NS" for non-significant difference.

These results showed that UFAs prevent significantly motility and biofilm formation on *A. baumannii* ATCC 17978 at sub-inhibitory concentrations (0.01, 0.02 and 0.05 mg/mL) with a better activity of PoA (C16:1Δ9) than MoA (C14:1Δ9). This is in agreement with the observation that, in *V. cholera*, UFAs activity, reducing the *tcp* gene expression, was improved by an increase of the length chain and was also related to the presence of unsaturated bond and to the conformation (*cis*/*trans*) of the molecule [16,17]. Moreover, unlike virstatin, PoA and MoA were shown to significantly disperse 24 h-biofilms. Some Gram-bacteria produced *cis*-UFAs, also called Diffusible Signaling Factors (DSF). These QS signals have been shown to be involved in cell-to-cell communication and could regulate biofilm lifestyle [22]. For example, the UFA *cis*-2-decenoic acid (CDA) from the DSF family was shown to be an autoinducer of the biofilm dispersion in *P. aeruginosa* and in many others species [23–26]. PoA and MoA might possess similar activity in *A. baumannii* biofilms. It was already shown that the addition of an exogenous DSF, i.e., *cis*-2-dodecenoic (BDSF), inhibits *P. aeruginosa* biofilm formation by interfering with the production of AHL [27]. This prompted us to further examine the impact of UFAs on *A. baumannii* QS.

2.2. Impact of UFAs on Quorum Sensing

It was previously shown that virstatin could interfere with QS system of *A. nosocomialis*, by decreasing the expression of the *anoR* regulator of the LuxI/R-type AnoIR system [10]. This decrease of *anoR* expression, in reducing the activation of *anoI*, gene that codes for the autoinducer synthase, could decrease AHLs production. In order to determine if virstatin or UFAs could also impact the QS

system in *A. baumannii* ATCC 17978, we examined the expression of the regulator *abaR* gene of the AbaIR system (homologue of the *anoR* gene in *A. nosocomialis*). We found that virstatin, MoA or PoA significantly decreased *abaR* expression suggesting these UFAs can interfere with the AbaIR QS system of *A. baumannii* (Figure 2a and Table S1).

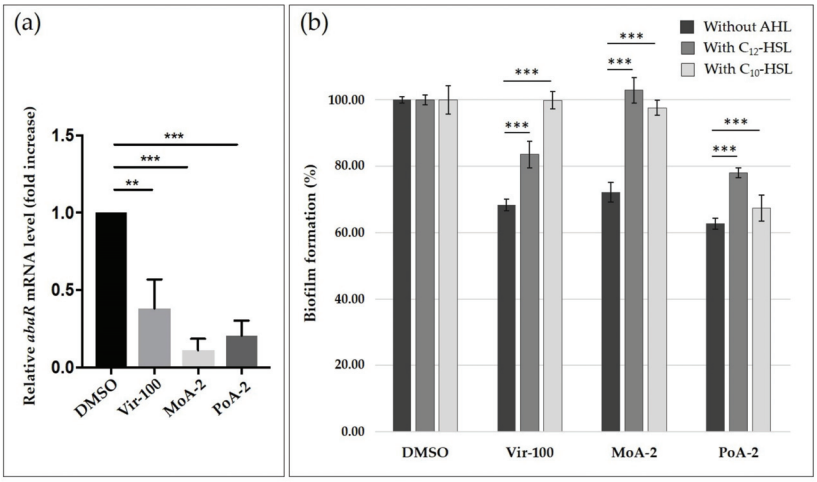

Figure 2. UFAs activity on *A. baumannii* ATCC 17978 quorum sensing system. (**a**) *abaR* gene expression quantified by real time PCR of the total RNA isolated from bacteria grown in the presence of virstatin (100 µM, Vir-100), PoA or MoA at 0.02 mg/mL (PoA-2 and MoA-2) relative to that of the bacteria grown in DMSO alone; (**b**) UFAs activity on biofilm formation in presence of AHLs (500 nM) quantified by crystal violet staining method. 24 h-biofilm formation with or without virstatin (100 µM), PoA or MoA at 0.02 mg/mL and DMSO as control. Results are presented as (mean ± standard error of mean). "***" for $p < 0.0001$, "**" for $p < 0.01$ and "NS" for non-significant difference.

To confirm the impact of these compounds on the production of AHLs, we first performed cross-streaking of *A. tumefaciens* and *C. violaceum* biosensors against *A. baumannii* ATCC 17978 to determine the type of AHLs, i.e., short or/and long-type, which are produced by this strain [28]. In agreement with previous studies [13,14], we only detected the production of long-AHLs by *A. baumannii* ATCC 17978 (Figure S2). To further examine the activity of UFAs and virstatin on AHLs production, we evaluated the activity of these compounds on the *A. baumannii* biofilm formation in presence of 500 nM of the main AHLs already described, i.e., OH-C_{12}-HSL or N-C_{10}-HSL [13–15] (Figure 2b). If OH-C_{12}-HSL addition completely restored the biofilm formation when *A. baumannii* was treated by MoA, it only partially counteracted the activity of virstatin and PoA (recovery of 54 and 38% of the phenotype, respectively). The addition of N-C_{10}-HSL also totally inhibited the effect of MoA as well as the effect of virstatin (98% and 100% of recovery, respectively), whereas no significant activity of N-C_{10}-HSL was shown on biofilms treated with PoA (only 4% of recovery, Figure 2b). Addition of AHLs on motility plates did not restore the motility of *A. baumannii* ATCC 17978 abolished by virstatin or UFAs. Finally, we tested virstatin and UFAs via the QS screening platform developed by Skogman et al. [29]. Neither virstatin nor UFAs (up to 400 µM) could be characterized as quorum quencher or quorum inhibitor of short AHLs production.

In line with the previous data obtained on *A. nosocomialis* [10], these overall results indicate that virstatin, but also UFAs, could prevent biofilm formation via an inhibition of *abaR* gene expression. The consequent *abaI* autoinducer synthase gene repression could thus lead to an inhibition of the

long-AHLs production. It has been shown that a deletion of the *abaI* in *A. baumannii* M2 displayed a 40% reduction of biofilm formation [13], a decrease that is similar to the one induced by virstatin or UFAs. For PoA, the partial recovery of biofilm formation after addition of C_{10}- or C_{12}-HSL suggests that this UFA alters the AHLs production, but could also act on another QS communication system not yet characterized.

2.3. UFAs Affect Biofilm Architecture

We next investigated pellicles formed by ATCC 17978 after treatment with either virstatin or UFAs. The pellicle formed by the ATCC 17978 strain showed aggregates on the air-facing side (the "ball-shaped" morphogroup according to [30]) in control growth or in the presence of virstatin. After 24 h of UFA treatment, these aggregates disappeared (Figure 3a). Pellicles were further characterized by AFM. After 6 h of growth, control and virstatin-treated pellicles exhibited a similar macroscopic aspect with merging microcolonies characterized by a diameter of about 50–100 µm and an average thickness of (360–460 ± 40) nm (Figure 3b). However, with UFAs, tridimensional architecture was abolished, leading to a monolayer structure with an average thickness of (230 ± 40) nm and (150 ± 40) nm with PoA and MoA, respectively. This monolayer cellular organization appeared to be less cohesive after PoA treatment than after the MoA one. We also observed elongated cells inside the pellicle formed with and without UFAs (up to 20 µm of length versus 1 µm average for normal cells, Figure 3b). When these elongated cells were inside the biofilm, they exhibited the same thickness than normal cells (black circles in Figure 3b). However, in the presence of PoA or MoA, a large part of these atypical cells seem to be lysed and their membranes expelled from the community (white arrows in Figure 3b). UFC counts in the biofilms after 24 h with or without the presence of UFAs or virstatin were similar (Figure S1).

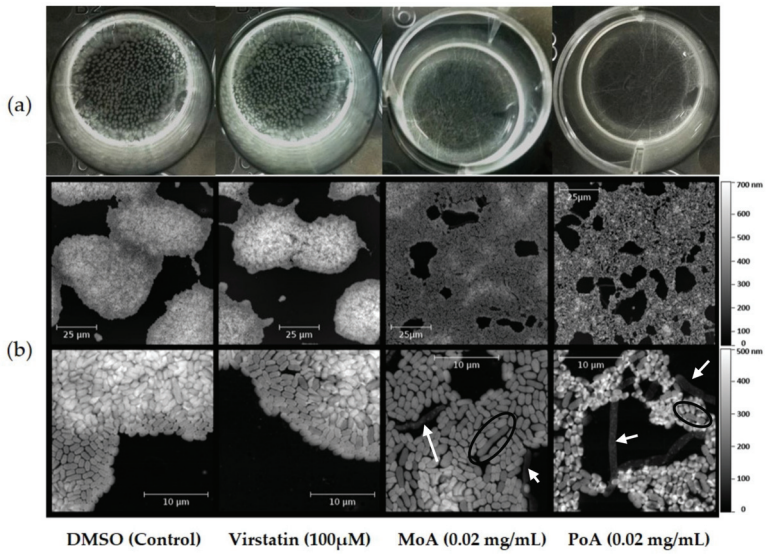

Figure 3. UFAs activity on air-liquid biofilm organization. Pellicles were observed after growth with or without virstatin, PoA or MoA. (**a**) Visual aspect of pellicle surface after 24 h treatment (**b**) Atomic Force Microscopy (AFM) images of pellicle water-facing sides after 6 h treatment. From left side to right side: DMSO control, pellicle formation with 100 µM virstatin, with 0.02 mg/mL MoA and with 0.02 mg/mL PoA. Elongated cells with a normal thickness are black encircled and lysed elongated cells are pointed out with white arrows.

These observations suggest a specific action of UFAs during the initial steps of biofilm formation, i.e., on the cell adhesion. Indeed, due to their amphiphilic nature, UFAs go spontaneously at the air-liquid interface where they could locally accumulate and lead to a first antibiofilm action. In agreement with this hypothesis, it was previously shown that oleic acid (C18:1Δ^9, OA) inhibited the primary adhesion step of *S. aureus* on polystyrene surfaces [31]. We also observed that the addition of UFAs in MH medium significantly reduced the air/liquid surface tension. It has been already demonstrated that this type of interface alteration, due to addition of biosurfactants, for an example, significantly reduced pellicle formation or induced biofilm dispersion [32,33]. Finally, the observation of the air-liquid interface by Brewster Angle Microscopy [30] demonstrates that if DMSO did not influence the organization of the monolayer formed by the growth medium molecules, in the presence of UFAs, the fluidity of this monolayer drastically increased. The influence of this parameter on the pellicle formation is difficult to evaluate, but one might suggest that the irreversible adhesion step, preluding microcolony formation during biofilm development, might be more difficult to achieve for bacteria on fluid surface. Taken together, these overall results suggest that, besides its action on QS system, the antibiofilm activity of UFAs could also be due, at least in initial steps of biofilm formation, to several modifications of the interfaces on which the biofilm settles.

2.4. UFAs Effect on Biofilm Formation and Mobility of Clinical Isolates

To evaluate more broadly the UFAs activity on *A. baumannii* biofilms, we tested MoA and PoA on 22 clinic isolates from different origins [34]. We quantified the biofilm formation of these strains grown with or without UFAs at 0.02 mg/mL. PoA decreased significantly the biofilm formation in 13 of strains with a maximum reduction of 44% (Figure S3). With MoA, eight strains exhibited a significant reduction of their biofilm formation ability. As observed with the ATCC 17978 strain, PoA displayed a better antibiofilm activity than MoA, but no relationship between the antibiofilm activity of virstatin and the one of UFAs could be emphasized [7]. UFAs antibiofilm activity seems not to be correlated to the pellicle formation ability or hydrophobicity of the strain (Figure S3). For some strains, UFAs addition slightly promoted the biofilm formation. Cross-streaking of *A. tumefaciens* biosensor against these isolates confirmed the efficiency of the AHL QS system by long AHL production. Several hypotheses can be proposed to explain this increase. In *S. aureus*, it was shown that OA could promote biofilm formation, probably by interaction between positive charges of adhesion factors and negative charges of UFAs [31,35]. Expression of adhesion factors in *A. baumannii* was shown to be strain-dependent [36] and might explain this increasing effect. One can notice also that the quorum quencher enzyme MomL displayed on *A. baumannii* biofilms a similar activity as UFAs, with a maximum 42% decrease of the biomass formation and a strain-dependence of its activity [37], suggesting that other cell-to-cell communication systems or factors could be recruited during *A. baumannii* biofilm formation. In *V. cholerae*, UFAs (PoA and OA) were shown to interact and prevent the DNA interaction of the AraC-type regulator, ToxT [17]. Additional interaction of UFAs with such regulators in clinical isolates may also explain an increased biofilm formation. This demonstrates that the UFAs activity is not limited to an activity an *abaR* gene.

3. Materials and Methods

3.1. Bacterial Strains and MICs Determination

To evaluate fatty acid activity, we used two reference strains of *A. baumannii* (i.e., ATCC 17978 and ATCC 19606) and a panel of 22 *A. baumannii* clinical isolates previously described [7,34]. Fatty acids, *cis*-9-hexadecenoic acid (C16:1Δ9, palmitoleic acid, PoA, Sigma Aldrich, Lyon, France) and *cis*-9-tetradecenoic acid (C14:1Δ9, myristoleic acid, MoA, Sigma Aldrich, France) and virstatin (4-[*N*-(1,8-naphthalimide)]-n-butyric acid, Bachem, Bubendorf, Germany) were solubilized in dimethyl sulfoxide (DMSO, Sigma, St. Louis, MO, USA). Determination of UFAs minimal inhibitory concentrations (MIC) were performed by the microdilution method, as previously described by [7].

3.2. UFAs Activities on Biofilm Formation and Motility of A. baumannii Strains

A. baumannii biofilms were grown on 24-well plates in Mueller Hinton broth (MHB, Difco, Sparks, NV, USA) at 37 °C as previously described [7]. To test their inhibition activity on *A. baumannii* biofilms, fatty acids were introduced at final concentration of 0.02 mg/mL (as well as 0.01 and 0.05 mg/mL for ATCC 17978 strain), using DMSO as negative control and 100 µM virstatin as positive control [7,17]. In case of strains forming pellicle in addition to biofilms on plate walls, the sub-phase was gently removed allowing the pellicle to stick onto the plate walls, then the overall remaining biomass (i.e., biofilm on solid surface and pellicle) was quantified, as described by [38]. Biofilm dispersion activity of UFAs was investigated only on 24 h-biofilms formed by ATCC 17978 strain in MHB. Twenty four-hour biofilms were incubated in fresh medium for an additional 24 h in the presence of fatty acids (at 0.01, 0.02, or 0.05 mg/mL) using DMSO or virstatin 100 µM as controls. Surface motility of *A. baumannii* strains was investigated in 0.3% Luria Bertani agar (LB; Difco) Petri dishes supplemented or not with UFAs and DMSO as control and incubated overnight at 37 °C [39]. All of the experiments were performed at least in triplicate. Data were statically analyzed using Prism Graph Pad 5 with a *t*-test to determine a significant effect of UFAs.

3.3. Effect of Virstatin and UFAs on Quorum Sensing

The *N*-acyl-homoserine lactone (AHL) production in *A. baumannii* ATCC 17978 or *A. baumannii* clinical isolates was determined, as described by [28] with *P. aeruginosa* PAO1 and *E. coli* ATCC 10536 as positive and negative controls, respectively. To investigate the potential quorum-quenching activity of UFAs and virstatin on short-HSLs, we used the screening platform described by [29]. The effect of the addition of long-HSLs, i.e., *N*-(3-hydroxydodecanoyl)-DL-homoserine lactone (OH-C_{12}-HSL, Sigma Aldrich) and *N*-decanoyl-DL-homoserine lactone (N-C_{10}-HSL, Sigma Aldrich) solubilized in DMSO, on biofilms pretreated by virstatin and UFAs was investigated. Five hundred nM of each HSL were added concomitantly to 0.02 mg/mL of UFAs and 100 µM virstatin. DMSO enriched with HSL (500 nM) was used as control. Biofilm formation was quantified and the results significance was analyzed, as described in the previous section. The effect of virstatin and UFAs on *abaR* gene expression using q-RT-PCR was also investigated. *A. baumannii* was grown overnight in MH medium and diluted to OD600 of 0.01 and incubated for 24 h under agitation at 37 °C with DMSO (negative control), virstatin (100 µM), MoA (0.02 mg/mL), or PoA (0.02 mg/mL). Total RNAs were extracted using RNeasy-Mini kit (Qiagen, Valencia, CA, USA), followed by a supplementary DNase treatment (Ambion, Carlsbad, CA, USA), and a verification of absence of contaminating DNA by PCR. RNAs were reverse-transcribed using QuantiTect Reverse Transcription Kit (Qiagen). Real-time PCR was performed using Brilliant III SYBR Green QPCR (Agilent Technologies, Santa Clara, CA, USA) with an AriaMx Real-Time PCR System (Agilent Technologies). Specific primers are listed in Table S1. The *rpoB* expression was used as an internal control for normalization and fold change calculated in relation to the DMSO control. Data were analyzed using Prism Graph Pad 5 with a one-way ANOVA ($n = 4$).

3.4. Impact of UFAs on A. baumannii Biofilm Morphology

Morphological changes of liquid-facing sides of *A. baumannii* ATCC 17978 pellicles were visualized by Atomic Force Microscopy (AFM) after 6h of growth with or without 0.02 mg/mL of UFAs or 100 µM virstatin, DMSO being used as control [7]. Modifications of air-water interfaces in presence of UFAs and virstatin, were determined either by Brewster's angle microscopy [30] or by surface tension measurements using a Wilhelmy pressure sensor with a filter paper plate (R & K, Wiesbaden, Germany).

4. Conclusions

Involved in device-related infections and in persistence in hospital settings, the biofilm formation is a major cause of concern in the battle against *A. baumannii* and deserves the research of new therapeutic compounds. In this context, we previously demonstrated that virstatin, a factor decreasing

T4P-pili expression in *V. cholera* [17], inhibits *A. baumannii* biofilm formation [7]. In this study, we demonstrated that MoA and PoA also decreasing T4P-pili expression in *V. cholera* [16,17], inhibit the biofilm formation and motility in *A. baumannii*. By decreasing the expression of the QS system regulator, *abaR*, these three compounds inhibit AHLs production that could be restored by AHL exogenous addition. However, UFAs, as hydrophobic compounds, also modify material interfaces, as shown here by the modification of the air-liquid interface, precluding initial steps of biofilm formation. Additional bacterial responses that are uncorrelated to QS communication system or sensing of surfaces might also be induced by the use of these compounds, like overexpression of genes involved in stress response, or the regulation of peptidoglycan biosynthesis highlighted in *S. aureus* under OA treatment [40], and merit further investigation.

Supplementary Materials: Supplementary materials can be found at www.mdpi.com/1422-0067/19/1/214/s1.

Acknowledgments: We thank the "Laboratoire de biotechnologie et chimie marines" for providing us the *Agrobacterium tumefasciens* NTI and *Chromobacterium violaceum* CV026 strains. Our thanks to Sylvie Chevalier and Emeline Bouffartigues for helpful discussions. MN is a recipient of doctoral fellowship from the IRIB and SeSa research networks of the Region Haute Normandie (France). JBL was funded by a Région Rhônes-Alpes ARC1 Santé fellowship and his work funded by the FINOVI foundation under a Young Researcher Starting Grant awarded to SPS. We thank the Spanish Group for the Study of Nosocomial Infections (GEIH) to provide us *A. baumannii* clinical isolates.

Author Contributions: Marion Nicol, Thierry Jouenne, Emmanuelle Dé conceived and designed the experiments. Marion Nicol, Stéphane Alexandre, Jean-Baptiste Luizet, Malena Skogman, Suzana P. Salcedo performed the experiments. Marion Nicol, Stéphane Alexandre, Jean-Baptiste Luizet, Malena Skogman, Suzana P. Salcedo, Thierry Jouenne, Emmanuelle Dé analyzed the data. Stéphane Alexandre, Malena Skogman, Suzana P. Salcedo contributed to materials/technical support. Marion Nicol, Emmanuelle Dé wrote the paper. All authors read and approved the final manuscript.

Conflicts of Interest: The authors declare no conflict of interest.

Abbreviations

AFM	Atomic force microscopy
AHL	*N*-acyl-homoserine lactone
ATCC	American type culture collection
DMSO	Dimethyl sulfoxide
HSL	Homoserine lactone
MIC	Minimal inhibitory concentration
MoA	Myristoleic acid
PoA	Palmitoleic acid
OA	Oleic acid
PCR	Polymerase chain reaction
QS	Quorum sensing
UFA	Unsaturated fatty acid

References

1. Peleg, A.Y.; Seifert, H.; Paterson, D.L. *Acinetobacter baumannii*: Emergence of a successful pathogen. *Clin. Microbiol. Rev.* **2008**, *21*, 538–582. [CrossRef] [PubMed]
2. Lee, C.-R.; Lee, J.H.; Park, M.; Park, K.S.; Bae, I.K.; Kim, Y.B.; Cha, C.-J.; Jeong, B.C.; Lee, S.H. Biology of *Acinetobacter baumannii*: Pathogenesis, Antibiotic Resistance Mechanisms, and Prospective Treatment Options. *Front. Cell. Infect. Microbiol.* **2017**, *7*, 55. [CrossRef] [PubMed]
3. Espinal, P.; Martí, S.; Vila, J. Effect of biofilm formation on the survival of *Acinetobacter baumannii* on dry surfaces. *J. Hosp. Infect.* **2012**, *80*, 56–60. [CrossRef] [PubMed]
4. Wisplinghoff, H.; Schmitt, R.; Wöhrmann, A.; Stefanik, D.; Seifert, H. Resistance to disinfectants in epidemiologically defined clinical isolates of *Acinetobacter baumannii*. *J. Hosp. Infect.* **2007**, *66*, 174–181. [CrossRef] [PubMed]

5. Wisplinghoff, H.; Bischoff, T.; Tallent, S.M.; Seifert, H.; Wenzel, R.P.; Edmond, M.B. Nosocomial bloodstream infections in US hospitals: Analysis of 24,179 cases from a prospective nationwide surveillance study. *Clin. Infect. Dis.* **2004**, *39*, 309–317. [CrossRef] [PubMed]
6. Ellis, D.; Cohen, B.; Liu, J.; Larson, E. Risk factors for hospital-acquired antimicrobial-resistant infection caused by *Acinetobacter baumannii*. *Antimicrob. Resist. Infect. Control* **2015**, *4*. [CrossRef] [PubMed]
7. Nait Chabane, Y.; Mlouka, M.B.; Alexandre, S.; Nicol, M.; Marti, S.; Pestel-Caron, M.; Vila, J.; Jouenne, T.; Dé, E. Virstatin inhibits biofilm formation and motility of *Acinetobacter baumannii*. *BMC Microbiol.* **2014**, *14*, 62. [CrossRef] [PubMed]
8. Hung, D.T.; Shakhnovich, E.A.; Pierson, E.; Mekalanos, J.J. Small-molecule inhibitor of *Vibrio cholerae* virulence and intestinal colonization. *Science* **2005**, *310*, 670–674. [CrossRef] [PubMed]
9. Shakhnovich, E.A.; Hung, D.T.; Pierson, E.; Lee, K.; Mekalanos, J.J. Virstatin inhibits dimerization of the transcriptional activator ToxT. *Proc. Natl. Acad. Sci. USA* **2007**, *104*, 2372–2377. [CrossRef] [PubMed]
10. Oh, M.H.; Choi, C.H. Role of LuxIR homologue AnoIR in *Acinetobacter nosocomialis* and the effect of virstatin on the expression of *anoR* gene. *J. Microbiol. Biotechnol.* **2015**, *25*, 1390–1400. [CrossRef] [PubMed]
11. Churchill, M.E.A.; Chen, L. Structural basis of acyl-homoserine lactone-dependent signaling. *Chem. Rev.* **2011**, *111*, 68–85. [CrossRef] [PubMed]
12. Bhargava, N.; Sharma, P.; Capalash, N. Quorum sensing in *Acinetobacter*: An emerging pathogen. *Crit. Rev. Microbiol.* **2010**, *36*, 349–360. [CrossRef] [PubMed]
13. Niu, C.; Clemmer, K.M.; Bonomo, R.A.; Rather, P.N. Isolation and characterization of an autoinducer synthase from *Acinetobacter baumannii*. *J. Bacteriol.* **2008**, *190*, 3386–3392. [CrossRef] [PubMed]
14. Anbazhagan, D.; Mansor, M.; Yan, G.O.S.; Md Yusof, M.Y.; Hassan, H.; Sekaran, S.D. Detection of quorum sensing signal molecules and identification of an autoinducer synthase gene among biofilm forming clinical isolates of Acinetobacter spp. *PLoS ONE* **2012**, *7*, e36696. [CrossRef] [PubMed]
15. Erdönmez, D.; Rad, A.Y.; Aksöz, N. Quorum sensing molecules production by nosocomial and soil isolates *Acinetobacter baumannii*. *Arch. Microbiol.* **2017**. [CrossRef] [PubMed]
16. Childers, B.M.; Cao, X.; Weber, G.G.; Demeler, B.; Hart, P.J.; Klose, K.E. N-terminal residues of the *Vibrio cholerae* virulence regulatory protein ToxT involved in dimerization and modulation by fatty acids. *J. Biol. Chem.* **2011**, *286*, 28644–28655. [CrossRef] [PubMed]
17. Lowden, M.J.; Skorupski, K.; Pellegrini, M.; Chiorazzo, M.G.; Taylor, R.K.; Kull, F.J. Structure of *Vibrio cholerae* ToxT reveals a mechanism for fatty acid regulation of virulence genes. *Proc. Natl. Acad. Sci. USA* **2010**, *107*, 2860–2865. [CrossRef] [PubMed]
18. Plecha, S.C.; Withey, J.H. Mechanism for inhibition of *Vibrio cholerae* ToxT activity by the unsaturated fatty acid components of bile. *J. Bacteriol.* **2015**, *197*, 1716–1725. [CrossRef] [PubMed]
19. Kabara, J.J.; Swieczkowski, D.M.; Conley, A.J.; Truant, J.P. Fatty acids and derivatives as antimicrobial agents. antimicrob. *Agents Chemother.* **1972**, *2*, 23–28. [CrossRef]
20. Desbois, A.P.; Smith, V.J. Antibacterial free fatty acids: Activities, mechanisms of action and biotechnological potential. *Appl. Microbiol. Biotechnol.* **2010**, *85*, 1629–1642. [CrossRef] [PubMed]
21. Desbois, A.P.; Lawlor, K.C. Antibacterial activity of long-chain polyunsaturated fatty acids against *Propionibacterium acnes* and *Staphylococcus aureus*. *Mar. Drugs* **2013**, *11*, 4544–4557. [CrossRef] [PubMed]
22. Zhou, L.; Zhang, L.-H.; Cámara, M.; He, Y.-W. The DSF Family of Quorum Sensing Signals: Diversity, Biosynthesis, and Turnover. *Trends Microbiol.* **2017**, *25*, 293–303. [CrossRef] [PubMed]
23. Jennings, J.A.; Courtney, H.S.; Haggard, W.O. *Cis*-2-decenoic acid inhibits *S. aureus* growth and biofilm in vitro: A pilot study. *Clin. Orthop.* **2012**, *470*, 2663–2670. [CrossRef] [PubMed]
24. Sepehr, S.; Rahmani-Badi, A.; Babaie-Naiej, H.; Soudi, M.R. Unsaturated fatty acid, *cis*-2-decenoic acid, in combination with disinfectants or antibiotics removes pre-established biofilms formed by food-related bacteria. *PLoS ONE* **2014**, *9*, e101677. [CrossRef] [PubMed]
25. Amari, D.T.; Marques, C.N.H.; Davies, D.G. The putative enoyl-coenzyme a hydratase DspI is required for production of the *Pseudomonas aeruginosa* biofilm dispersion autoinducer *cis*-2-decenoic acid. *J. Bacteriol.* **2013**, *195*, 4600–4610. [CrossRef] [PubMed]
26. Rahmani-Badi, A.; Sepehr, S.; Mohammadi, P.; Soudi, M.R.; Babaie-Naiej, H.; Fallahi, H. A combination of *cis*-2-decenoic acid and antibiotics eradicates pre-established catheter-associated biofilms. *J. Med. Microbiol.* **2014**, *63*, 1509–1516. [CrossRef] [PubMed]

27. Deng, Y.; Boon, C.; Chen, S.; Lim, A.; Zhang, L.-H. *Cis*-2-dodecenoic acid signal modulates virulence of *Pseudomonas aeruginosa* through interference with quorum sensing systems and T3SS. *BMC Microbiol.* **2013**, *13*, 231. [CrossRef] [PubMed]
28. Gallique, M.; Decoin, V.; Barbey, C.; Rosay, T.; Feuilloley, M.G.J.; Orange, N.; Merieau, A. Contribution of the *Pseudomonas fluorescens* MFE01 Type VI secretion system to biofilm formation. *PLoS ONE* **2017**, *12*, e0170770. [CrossRef] [PubMed]
29. Skogman, M.E.; Kanerva, S.; Manner, S.; Vuorela, P.M.; Fallarero, A. Flavones as quorum sensing inhibitors identified by a newly optimized screening platform using *Chromobacterium violaceum* as reporter bacteria. *Molecules* **2016**, *21*, 21. [CrossRef] [PubMed]
30. Nait Chabane, Y.; Marti, S.; Rihouey, C.; Alexandre, S.; Hardouin, J.; Lesouhaitier, O.; Vila, J.; Kaplan, J.B.; Jouenne, T.; Dé, E. Characterisation of pellicles formed by *Acinetobacter baumannii* at the air-liquid interface. *PLoS ONE* **2014**, *9*, e111660. [CrossRef] [PubMed]
31. Stenz, L.; François, P.; Fischer, A.; Huyghe, A.; Tangomo, M.; Hernandez, D.; Cassat, J.; Linder, P.; Schrenzel, J. Impact of oleic acid (*cis*-9-octadecenoic acid) on bacterial viability and biofilm production in *Staphylococcus aureus*. *FEMS Microbiol. Lett.* **2008**, *287*, 149–155. [CrossRef] [PubMed]
32. Irie, Y.; O'toole, G.A.; Yuk, M.H. *Pseudomonas aeruginosa* rhamnolipids disperse *Bordetella bronchiseptica* biofilms. *FEMS Microbiol. Lett.* **2005**, *250*, 237–243. [CrossRef] [PubMed]
33. Bartlett, J.A.; Bartlett, J.; Gakhar, L.; Penterman, J.; Singh, P.K.; Singh, P.; Mallampalli, R.K.; Porter, E.; McCray, P.B. PLUNC: A multifunctional surfactant of the airways. *Biochem. Soc. Trans.* **2011**, *39*, 1012–1016. [CrossRef] [PubMed]
34. Marti, S.; Nait Chabane, Y.; Alexandre, S.; Coquet, L.; Vila, J.; Jouenne, T.; Dé, E. Growth of *Acinetobacter baumannii* in pellicle enhanced the expression of potential virulence factors. *PLoS ONE* **2011**, *6*, e26030. [CrossRef] [PubMed]
35. Götz, F. Staphylococcus and biofilms. *Mol. Microbiol.* **2002**, *43*, 1367–1378. [CrossRef] [PubMed]
36. McQueary, C.N.; Actis, L.A. *Acinetobacter baumannii* biofilms: Variations among strains and correlations with other cell properties. *J. Microbiol.* **2011**, *49*, 243–250. [CrossRef] [PubMed]
37. Zhang, Y.; Brackman, G.; Coenye, T. Pitfalls associated with evaluating enzymatic quorum quenching activity: The case of MomL and its effect on *Pseudomonas aeruginosa* and *Acinetobacter baumannii* biofilms. *PeerJ* **2017**, *5*, e3251. [CrossRef] [PubMed]
38. O'Toole, G.A.; Kolter, R. Initiation of biofilm formation in *Pseudomonas fluorescens* WCS365 proceeds via multiple, convergent signalling pathways: A genetic analysis. *Mol. Microbiol.* **1998**, *28*, 449–461. [CrossRef] [PubMed]
39. Eijkelkamp, B.A.; Stroeher, U.H.; Hassan, K.A.; Papadimitrious, M.S.; Paulsen, I.T.; Brown, M.H. Adherence and motility characteristics of clinical *Acinetobacter baumannii* isolates. *FEMS Microbiol. Lett.* **2011**, *323*, 44–51. [CrossRef] [PubMed]
40. Kenny, J.G.; Ward, D.; Josefsson, E.; Jonsson, I.-M.; Hinds, J.; Rees, H.H.; Lindsay, J.A.; Tarkowski, A.; Horsburgh, M.J. The *Staphylococcus aureus* response to unsaturated long chain free fatty acids: Survival mechanisms and virulence implications. *PLoS ONE* **2009**, *4*, e4344. [CrossRef] [PubMed]

II-) A Pseudomonas aeruginosa TIR effector mediates immune evasion by targeting UBAP1 and TLR adaptors

Imbert *et al*. 2016

EMBO Journal

Bacterial pathogens developed several strategies to escape innate immunity of their hosts to enable them to succeed to colonize the host [451]. *Pseudomonas aeruginosa* is also in the ESKAPE list mentioned above, known to cause hospital acquired infections but also to be a major cause of morbidity and mortality in cystic fibrosis patients [447]. One of the research axis in the team of my supervisor Dr Suzana Salcedo is the characterization of bacterial proteins that contain a TIR domain which are well known to interfere with components of innate immunity as it was described in **Chapter3** with BtpA and BtpB. In our laboratory another PhD student Paul Imbert identified a new TIR protein in the nosocomial pathogen *Pseudomonas aeruginosa* called *Pseudomonas* UBAP1 Modulator A (PumA). To sum up PumA inhibits the translocation of an important activator of the innate immunity, NF-κB. As Btp *Brucella* proteins, PumA was shown to interact with TIR adaptors TIRAP and Myd88. In addition, Ubiquitin Associated Protein 1 (UBAP1) was also shown to be a partner of PumA, a very interesting result. Indeed, UBAP1 was mainly characterized and associated to endosomal components especially in endosomal-sorting complex required for transport I (ESCRT-I) [452]. This complex is associated to diverse functions as the transport of ubiquitinated endosomal cargo for degradation [452]. We showed that PumA was able to interfere with TNF receptor signaling in addition to TLRs. Moreover, a few months before this paper another team characterized the role of UBAP1 in TNF receptor activation [453](Maminska 2016 Cell Biology). The identification and characterization of the new bacterial protein PumA was very interesting the interaction between PumA and UBAP1 constituted a new strategy for bacterial inhibition of innate immune signaling during infection.

My contribution for this work was to perform qPCR to show no differences in the induction of NF-κB between the wild-type, mutant and complemented strains. And in second time for the review process I performed co-immunoprecipitation between the C-Terminal (C-Ter) part of PumA and full-length TIRAP, MyD88 and UBAP1 to confirm that the interactions do not involved the C-ter extremity of PumA. All these results are presented in supplementary data.

Published online: May 8, 2017

Article

SOURCE DATA | TRANSPARENT PROCESS | OPEN ACCESS

THE EMBO JOURNAL

A *Pseudomonas aeruginosa* TIR effector mediates immune evasion by targeting UBAP1 and TLR adaptors

Paul RC Imbert[1], Arthur Louche[1], Jean-Baptiste Luizet[1], Teddy Grandjean[2], Sarah Bigot[1], Thomas E Wood[3], Stéphanie Gagné[1], Amandine Blanco[1], Lydia Wunderley[4], Laurent Terradot[1], Philip Woodman[4], Steve Garvis[5], Alain Filloux[3], Benoit Guery[2] & Suzana P Salcedo[1,*]

Abstract

Bacterial pathogens often subvert the innate immune system to establish a successful infection. The direct inhibition of downstream components of innate immune pathways is particularly well documented but how bacteria interfere with receptor proximal events is far less well understood. Here, we describe a Toll/interleukin 1 receptor (TIR) domain-containing protein (PumA) of the multi-drug resistant *Pseudomonas aeruginosa* PA7 strain. We found that PumA is essential for virulence and inhibits NF-κB, a property transferable to non-PumA strain PA14, suggesting no additional factors are needed for PumA function. The TIR domain is able to interact with the Toll-like receptor (TLR) adaptors TIRAP and MyD88, as well as the ubiquitin-associated protein 1 (UBAP1), a component of the endosomal-sorting complex required for transport I (ESCRT-I). These interactions are not spatially exclusive as we show UBAP1 can associate with MyD88, enhancing its plasma membrane localization. Combined targeting of UBAP1 and TLR adaptors by PumA impedes both cytokine and TLR receptor signalling, highlighting a novel strategy for innate immune evasion.

Keywords *Pseudomonas*; TIR domain; TLR adaptors; UBAP1; virulence
Subject Categories Microbiology, Virology & Host Pathogen Interaction
DOI 10.15252/embj.201695343 | Received 27 July 2016 | Revised 29 March 2017 | Accepted 5 April 2017 | Published online 8 May 2017
The EMBO Journal (2017) 36: 1869–1887

Introduction

Microbial pathogen recognition by innate immune receptors initiates a progression of molecular interactions and signalling events assuring host defence. In bacterial infections, detection of surface components, such as peptidoglycan, lipopolysaccharides and flagellin by Toll-like receptors (TLR) 2, 4 and 5, respectively, is essential for induction of pro-inflammatory cytokines and type I interferon (IFN) responses. Specific sorting and signalling adaptor proteins bridge activated receptors with downstream kinases to initiate signalling cascades via Toll/interleukin 1 receptor (TIR) domains present on both the adaptors and the cytosolic face of TLRs (Brubaker *et al*, 2015). Upon TLR2 or TLR4 activation, the TIR-containing adaptor protein (TIRAP) recruits myeloid differentiation primary response 88 (MyD88) that interacts with the TLR via its TIR domain (Fitzgerald *et al*, 2001; Horng *et al*, 2001; Kagan & Medzhitov, 2006). MyD88 oligomerization and recruitment of specific kinases leads to the formation of myddosomes, signalling platforms that induce NF-κB translocation into the nucleus and subsequent transcription of pro-inflammatory associated genes (Nagpal *et al*, 2011; Bonham *et al*, 2014). TLR4 activation also results in induction of a type I IFN via another set of adaptors, TRAM and TRIF (Fitzgerald *et al*, 2001; Yamamoto *et al*, 2002; Kagan *et al*, 2008). In the case of the MyD88-dependent TLR5, the identity of a sorting adaptor remains undefined and the role of TIRAP unclear although it has been implicated in proper TLR5 signalling in epithelial cells (Choi *et al*, 2013).

Microbial pathogens have been shown to counter these host defence pathways. Most bacterial immune-modulatory proteins described to date rely on inhibition of downstream signalling components, such as MAP kinases and transcription factors (reviewed in Rosadini & Kagan, 2015). In contrast, few examples of direct blocking at the level of initial receptor–adaptor complexes are known. Some bacterial pathogens rely on TIR domain-containing proteins to perturb TIR-dependent interactions (Newman *et al*, 2006; Cirl *et al*, 2008; Salcedo *et al*, 2008, 2013), essential in innate immune signalling. The growing number of bacterial TIR proteins recently identified in both Gram-negative and Gram-positive human

1 Laboratory of Molecular Microbiology and Structural Biochemistry, Centre National de la Recherche Scientifique, University of Lyon, Lyon, France
2 EA 7366 Recherche Translationelle Relations Hôte-Pathogènes, Faculté de Médecine Pôle Recherche, Université Lille 2, Lille, France
3 MRC Centre for Molecular Bacteriology and Infection, Imperial College London, London, UK
4 School of Biological Sciences, Faculty of Biology Medicine and Health, University of Manchester, Manchester Academic Health Science Centre, Manchester, UK†
5 Laboratoire de Biologie et Modelisation, Ecole Normal Supérieur, UMR5239, Lyon, France
*Corresponding author. Tel: +33 437652915; E-mail: suzana.salcedo@ibcp.fr
†Correction added on 3 July 2017, after first online publication: affiliation 4 has been corrected

pathogens (Spear *et al*, 2012; Askarian *et al*, 2014; Zou *et al*, 2014) highlights the importance of this immune evasion strategy in disease. However, the molecular mechanisms underlying most TIR-dependent virulence strategies remain to be defined.

We focused on a previously uncharacterized TIR domain-containing protein of the multi-drug resistant pathogen *Pseudomonas aeruginosa* PA7, that we called PumA. *P. aeruginosa* PA7 lacks genes encoding the type III secretion system (T3SS) and its cognate effector proteins that are normally associated with strong induction of cell death, a hallmark of acute *P. aeruginosa* infections (reviewed by Filloux, 2011). In addition, PA7 does not show high lytic capacity towards epithelial cells due to exolysin A (ExlA) as described for the haemorrhagic pneumonia-causing strain of the same family (Elsen *et al*, 2014; Reboud *et al*, 2016). We thus took advantage of the absence of traditional virulence factors in this *P. aeruginosa* strain to study the molecular interactions involved in TIR-mediated bacterial targeting of events proximal to receptor–adaptor signalling complexes and to dissect PumA function. We found that the PumA *Pseudomonas* TIR domain-containing protein is essential for PA7 virulence conferring a previously unrecognized ability to *Pseudomonas* to down-modulate innate immune responses during infection. We show that PumA directly interacts with both TIRAP and MyD88 to control TLR signalling. Uniquely, it also targets the ubiquitin-associated protein 1 (UBAP1), a recently discovered component of the endosomal-sorting complex required for transport I (ESCRT-I; Stefani *et al*, 2011). UBAP1 is known to play a key role in selective sorting of ubiquitinated endosomal cargo on multi-vesicular bodies (MVB), via its interaction with VPS37A and other components of ESCRT-I namely TSG101 (Wunderley *et al*, 2014), as well as with the ESCRT regulator, His domain protein tyrosine phosphatase (HDPTP; Stefani *et al*, 2011). UBAP1 has been shown to control endosomal sorting of ubiquitinated EGFR (Stefani *et al*, 2011) as well as ubiquitin-dependent degradation of antiviral surface proteins (Agromayor *et al*, 2012) and integrins (Kharitidi *et al*, 2015). More recently, UBAP1 was shown to modulate steady-state trafficking of cytokine receptors in non-stimulated cells (Mamińska *et al*, 2016). UBAP1 is expressed in a wide range of tissues, but when deleted in mice, it is lethal for embryos (Agromayor *et al*, 2012).

We propose that this novel *Pseudomonas* effector modulates UBAP1 function, hence the name PumA (for *Pseudomonas* UBAP1 modulator A), which confers to this TIR domain-containing protein the distinctive ability to also interfere with cytokine receptor signalling. Targeting of both TLR adaptors and UBAP1 by PumA is not spatially restricted as we found UBAP1 can associate with MyD88 in host cells. Our results thus highlight a novel role of bacterial TIR domains and place UBAP1 sorting in the context of TLR signalling.

Results

PumA is required for *Pseudomonas aeruginosa* PA7 virulence *in vivo*

In *Pseudomonas*, TIR domain-containing proteins were first identified in an *in silico* study in *P. aeruginosa* and the plant pathogen *P. syringae* (Zhang *et al*, 2011). Analysis of currently available genomes shows that several plant strains encode such proteins as well as additional human pathogenic strains of *P. stutzeri* and *P. aeruginosa*. The closest orthologue is found in the plant pathogen *P. viridiflava*. The TIR domain of PumA spans the first 136 amino acids of PumA (Appendix Fig S1A and B), with no significant sequence/structure homologies detected for the C-terminal domain (amino acid 137–303) and no signal peptide. Analysis of the PA7 genome shows *pumA* (*PSPA7_2375*) is within the genomic island RGP56, which displays a G+C content of 58.5% in contrast to the average 66.5% in the remaining genome. Interestingly, using Geneious (Kearse *et al*, 2012), we found the *pumA* gene itself has an even larger reduction in G+C content (46.6%) (Appendix Fig S1C), suggesting that it is not a conserved gene within its immediate genetic context.

We assessed the potential role of PumA in virulence by infecting the nematode *Caenorhabditis elegans*, a well-established model for *P. aeruginosa* allowing for rapid assessment of virulence (Garvis *et al*, 2009). Infection with the highly virulent strain *P. aeruginosa* PA14 which contains virulence factors such as the T3SS but no TIR protein resulted in 50% lethality at day 5. The PA7 wild-type strain caused 50% lethality 7 days after inoculation. In contrast, we found that the PA7 Δ*pumA* mutant showed a slight but significant attenuation in virulence in *C. elegans* (Fig 1A). These differences were not due to an *in vitro* growth defect of the mutant (Appendix Fig S2A) nor to a problem in expression of PumA in the wild-type *P. aeruginosa* PA7 strain (Appendix Fig S2B).

We then used an acute *in vivo* infection model to evaluate the involvement of *pumA* in *P. aeruginosa* induced lung injury. Mice infected with Δ*pumA* showed a clear increased survival compared to wild-type strain (Fig 1B). A dose of 4.10^7 CFU of PA7 induced 100% lethality after 52 h against 62.5% survival after 96 h for the Δ*pumA* mutant. Bacterial clearance and cellular recruitment were then analysed with a lower inoculum of 3.10^7 CFU. PA7Δ*pumA* infected mice showed decreased cell recruitment (Fig 1C) and an enhanced lung bacterial clearance in bronchoalveolar lavages (BAL) compared to the wild-type strain (Fig 1D). The bacterial dissemination measured with the spleen bacterial load was equivalent between the two groups (Fig 1E). Together these results show that PumA is required for *P. aeruginosa* PA7 infection.

PumA inhibits NF-κB translocation into the nucleus during infection *in vitro*

As bacterial TIR proteins down-modulate NF-κB activation (Newman *et al*, 2006; Cirl *et al*, 2008; Salcedo *et al*, 2008, 2013; Spear *et al*, 2012; Askarian *et al*, 2014; Zou *et al*, 2014), we infected the lung carcinoma epithelial cell line A549, a well-established cellular model for *Pseudomonas* infection and analysed NF-κB translocation into the nucleus after one hour of infection by confocal microscopy. We developed an automated analysis of p65/RelA fluorescence in relation to DAPI labelling using a specific ImageJ plugin from images obtained by confocal microscopy (Fig EV1A) which allowed us to clearly differentiate between TNFα-treated and mock-infected cells (Figs 2A and EV1B). Infection with the three heat-killed *P. aeruginosa* strains, wild-type PA7, isogenic mutant Δ*pumA* or wild-type PA14 resulted in significant induction of NF-κB translocation into the nucleus, although to a lower level than TNFα-treated cells (Fig 2A). When cells were infected with PA7, there was no significant induction of

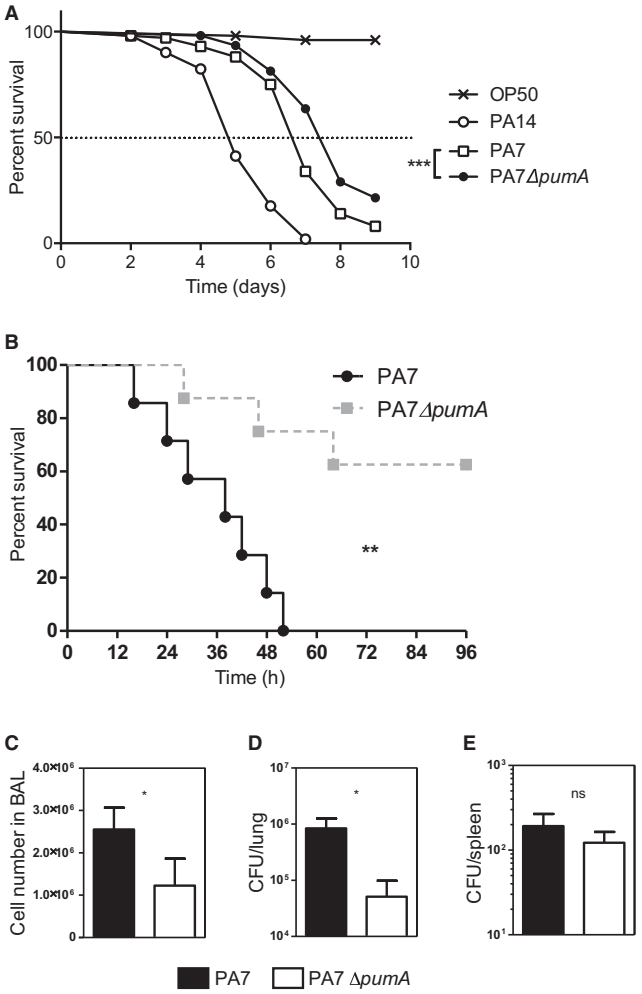

Figure 1. PumA is required for *Pseudomonas aeruginosa* PA7 virulence *in vivo*.

A *Caenorhabditis elegans* survival curve. Fifty *C. elegans* were infected with *E. coli* OP50 and with highly virulent strain *P. aeruginosa* PA14. One hundred *C. elegans* were infected with *P. aeruginosa* PA7 and PA7 Δ*pumA*. Test of Mantel–Cox was used with ***P = 0.0002.

B To establish an *in vivo* model of acute infection, mice were intranasally infected with 4 × 10^7 CFU *P. aeruginosa* PA7 or PA7Δ*pumA* strains (n = 7/group). Lethality was monitored for 96 h, and a test of Mantel–Cox was used, with **P = 0.0035.

C–E Mice were intranasally infected with 3 × 10^7 CFU *P. aeruginosa* PA7 or PA7Δ*pumA* strains (n = 7/group). Cells from bronchoalveolar lavage (BAL) were counted (C). Bacterial load in the lungs (D) and dissemination (E) were assessed through cultured lung or spleen homogenate. Non-parametric two-tailed Mann–Whitney test was carried out with (C) *P = 0.0173, (D) *P = 00364 and (E) P = 0.3629. All data correspond to mean ± standard error.

NF-κB when compared with the mock-infected negative control (Fig 2B), suggesting PA7 blocks NF-κB translocation into the nucleus. In contrast, Δ*pumA* infection promoted NF-κB nuclear translocation, attaining activation levels similar to those observed with heat-killed bacteria. The inability of *pumA* mutants to block NF-κB nuclear transport was complemented by chromosomal expression of this gene under an arabinose-inducible promoter (Fig 2C). Importantly, when *pumA* expression was repressed with glucose, no complementation of NF-κB inhibition was observed (Fig 2B). Addition of arabinose had no effect on NF-κB

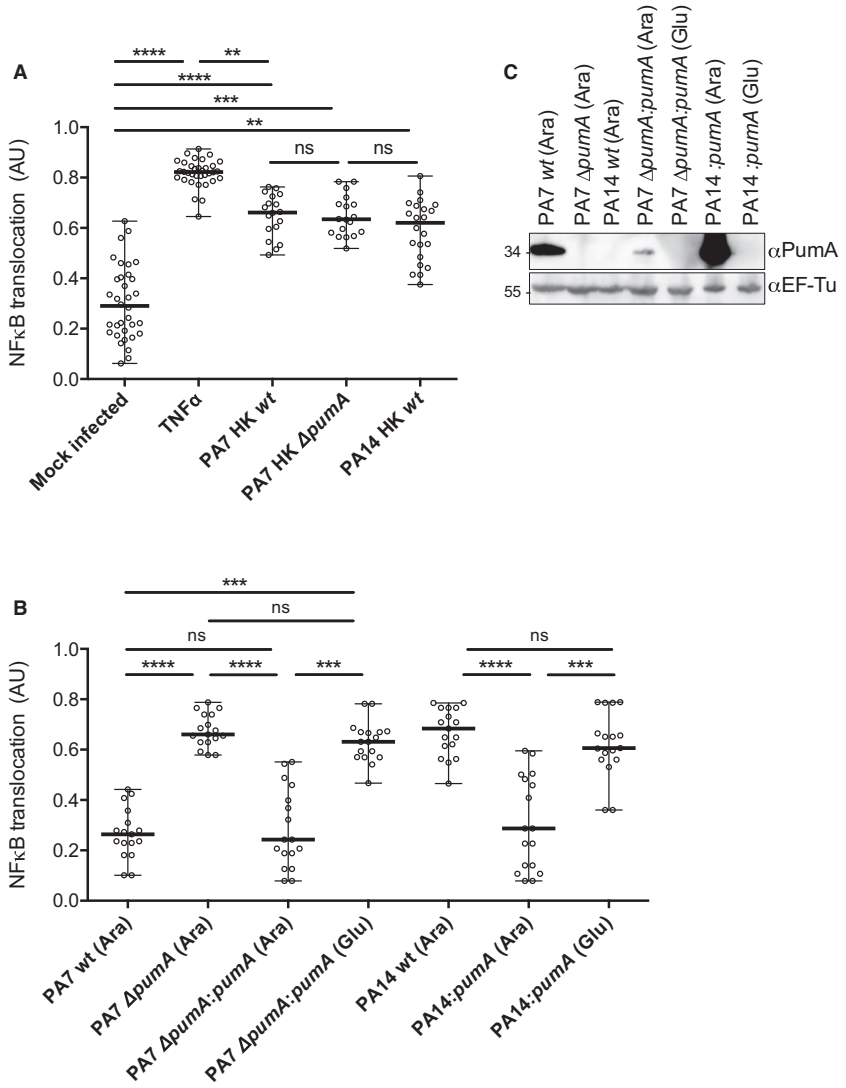

Figure 2. PumA is essential for control of NF-κB translocation into the nucleus during *Pseudomonas aeruginosa* infection of human A549 lung epithelial cells.

A Quantification of fluorescence ratio between nuclear NF-κB (p65) and nuclear DAPI staining. Negative control corresponds to uninfected cells that underwent all steps of the experiment. Positive control corresponds to full NF-κB activation with TNFα (1 μg/ml). A549 cells were incubated for 1 h with heat-killed (HK) bacteria to establish maximum activation induced by *Pseudomonas* infection.

B Cells were infected for 1 h with either *P. aeruginosa* PA7 wt, Δ*pumA*, Δ*pumA*:*pumA* (Ara) induced with 1% arabinose, Δ*pumA*:*pumA* (Glu) repressed with 0.5% glucose, PA14 wt, PA14:*pumA* (Ara) induced with 1% arabinose and PA14:*pumA* (Glu) repressed with 0.5% glucose. For consistency, arabinose was also included for the infections with wild-type and deletion mutant strains.

C Western blots from representative inocula used for the infection experiments, showing expression of PumA (34 kDa) in the different *P. aeruginosa* strains visualized using a polyclonal rabbit anti-PumA with control blot against the standard cytoplasmic protein EF-Tu (45 kDa) below.

Data information: For (A) and (B), between 200 and 400 cells per condition were counted and data correspond to median ± standard error from three independent experiments. Non-parametric one-way ANOVA Kruskal–Wallis test, with Dunn's multiple comparisons test was performed; ****$P < 0.0001$, ***$P < 0.001$, **$P < 0.01$.

translocation (Fig 2B versus EV1B). Furthermore, absence of NF-κB nuclear translocation was not due to reduced immune detection of the mutant strain as incubation of host cells with heat-killed Δ*pumA* resulted in equivalent levels of NF-κB activation to the wild-type PA7 (Fig 2A). To further support that the differences observed relate to PumA and are not indirect, we verified that all strains showed equivalent levels of membrane permeability (Fig EV2A), the global protein composition of the cell envelope was not altered in a *pumA* mutant (Fig EV2B), and no differences were observed in cytotoxicity (Fig EV2C and D) nor host cell adhesion (Fig EV2E) between wild-type PA7 and isogenic Δ*pumA* mutant. Together these results show that PumA is responsible for *P. aeruginosa* PA7 inhibition of NF-κB nuclear translocation during infection.

We then investigated whether expression of PumA alone could confer the ability to block NF-κB translocation to a different *Pseudomonas* strain. We chose PA14, which does not contain *pumA* and is known to be more virulent due to the presence of several virulence factors, namely those secreted by the T3SS. As expected, cells infected with wild-type PA14 showed high levels of NF-κB translocation into the nucleus (Fig 2B). Induction of *pumA* from the PA14 chromosome, which did not impact membrane permeability (Fig EV2A), was sufficient to enable this highly virulent strain to block NF-κB accumulation in the nucleus of infected cells (Fig 2B). These data indicate that PumA expression in *P. aeruginosa* is necessary and sufficient for NF-κB inhibition, highlighting its central role in immune evasion.

PumA translocation into host cells during infection *in vitro*

We next sought to determine whether PumA could be secreted by *Pseudomonas*. Fractionation of bacterial cells grown in liquid culture indicates that PumA is mostly cytoplasmic and to a lesser extent associated with the inner membrane (Appendix Fig S3A). The protein was not detected in the outer membrane fractions nor could it be found in the supernatant indicating absence of secretion into the extracellular milieu *in vitro*. To determine whether PumA could be found inside host cells during infection, we fused chromosomal PumA with the TEM1 β-lactamase. Although the presence of other β-lactamases in PA7 and/or potential bacterial lysis resulted in non-specific cleavage of the CCF2 substrate within host cells infected with the wild-type strain, significant levels of coumarin fluorescing cells following infection with a strain containing PumA-TEM1 (Appendix Fig S3B) suggest that PumA is translocated into host cells during infection.

PumA is associated with both TIRAP and MyD88 at the plasma membrane and intracellular compartments

To determine the mechanism by which PumA interferes with NF-κB activity, PumA was expressed in mammalian cells. We found PumA localized mostly at the plasma membrane, with some intracellular distribution, independently of the tag and in both immortal HeLa cells (Fig EV3A, top panel) and primary mouse embryonic fibroblasts (MEFs, Fig EV3B). As this localization was reminiscent of that of the TLR adaptor TIRAP (Fig EV3A and B), we co-transfected cells with PumA and TIRAP. We found extensive co-localization, in particular at the plasma membrane in both HeLa and MEFs (Fig 3A and B). We observed these results with any combination of tags (HA, Myc or GFP) for both proteins.

In contrast with TIRAP, MyD88 is mostly localized in intracellular structures that do not label the plasma membrane. We therefore co-expressed MyD88 with PumA. Surprisingly, we found enrichment of PumA in a proportion of MyD88-positive structures in both cell types although to a lesser extent than that observed with TIRAP (Fig 3A and B). These results were confirmed by structured illumination microscopy (SIM) to enable imaging at higher resolution (Fig 3C and D). PumA enrichment was observed with PumA tagged with Myc or HA and MyD88 fused to either HA, FLAG or Myc. Curiously, this phenotype was exacerbated when GFP-PumA, normally at the cell surface (Fig EV3) was co-expressed with MyD88, resulting in the majority of GFP-PumA being recruited to MyD88-positive compartments (Fig EV3C).

The TIR domain of PumA is responsible for interaction with both TIRAP and MyD88

We then investigated whether the TIR domain present in the first 136 amino acids of PumA was responsible for membrane targeting. $PumA_{1–136}$ was also efficiently targeted to the plasma membrane (Fig 4A). However, unlike TIRAP and another bacterial TIR protein BtpA/TcpB which are known to interact with specific phospholipids of the plasma membrane (Kagan & Medzhitov, 2006; Radhakrishnan *et al*, 2009), PumA and $PumA_{1–136}$ did not show any lipid binding properties when incubated with phosphoinositide phosphate strips (Fig 4B). We then tested whether PumA could interact with TIRAP, which could explain its membrane localization. We found that TIRAP-GFP and Myc-PumA co-immunoprecipitated (co-IP) suggesting TIRAP and PumA could be part of the same complex (Fig 4C). This association was confirmed using purified His-tagged PumA or $PumA_{1–136}$ immobilized on Ni-NTA resin, which both retained HA-TIRAP (Fig 4D).

As we had also observed enrichment of PumA in MyD88-positive compartments, we investigated whether PumA could interact with this adaptor protein. Although we did not observe and interaction between GFP-MyD88 and Myc-PumA (Fig 4C) nor HA-PumA and Myc-MyD88 (Appendix Fig S4A), using co-IP assays, His-PumA or $PumA_{1–136}$ were able to retain HA-Myd88 (Fig 5A), suggesting PumA is also able to interact with MyD88. To confirm these results, we took advantage of the strong enrichment in MyD88-positive compartments when Myd88 is co-expressed with the GFP-tagged version of PumA (Fig EV3C) and carried out co-IP in these conditions. Indeed, GFP-PumA and Myc-Myd88 could be co-immunoprecipitated as well as GFP-PumA and Myc-TIRAP (Fig 5B), suggesting that PumA can interact with MyD88. As a control for non-specific TIR–TIR interactions, we tested the ability of PumA to interact with TLR2, also by co-IP. Indeed, GFP-PumA could interact with FLAG-TIRAP but not FLAG-TLR2, suggesting some level of specificity in PumA targeting (Appendix Fig S4B and C).

Finally, we co-expressed in *E. coli* His-$PumA_{1–136}$ with His-MBP (Fig 5C), His-MBP-TIRAP (Fig 5D) or His-MBP-MyD88 (Fig 5E) and we could clearly see co-elution of both TIRAP and MyD88 in contrast to the His-MBP control (also see Appendix Fig S4D).

We next sought to determine whether the C-terminus of $PumA_{137–303}$ could also participate in these interactions. Lack of expression of His-$PumA_{137–303}$ in *E. coli* prevented us from purifying

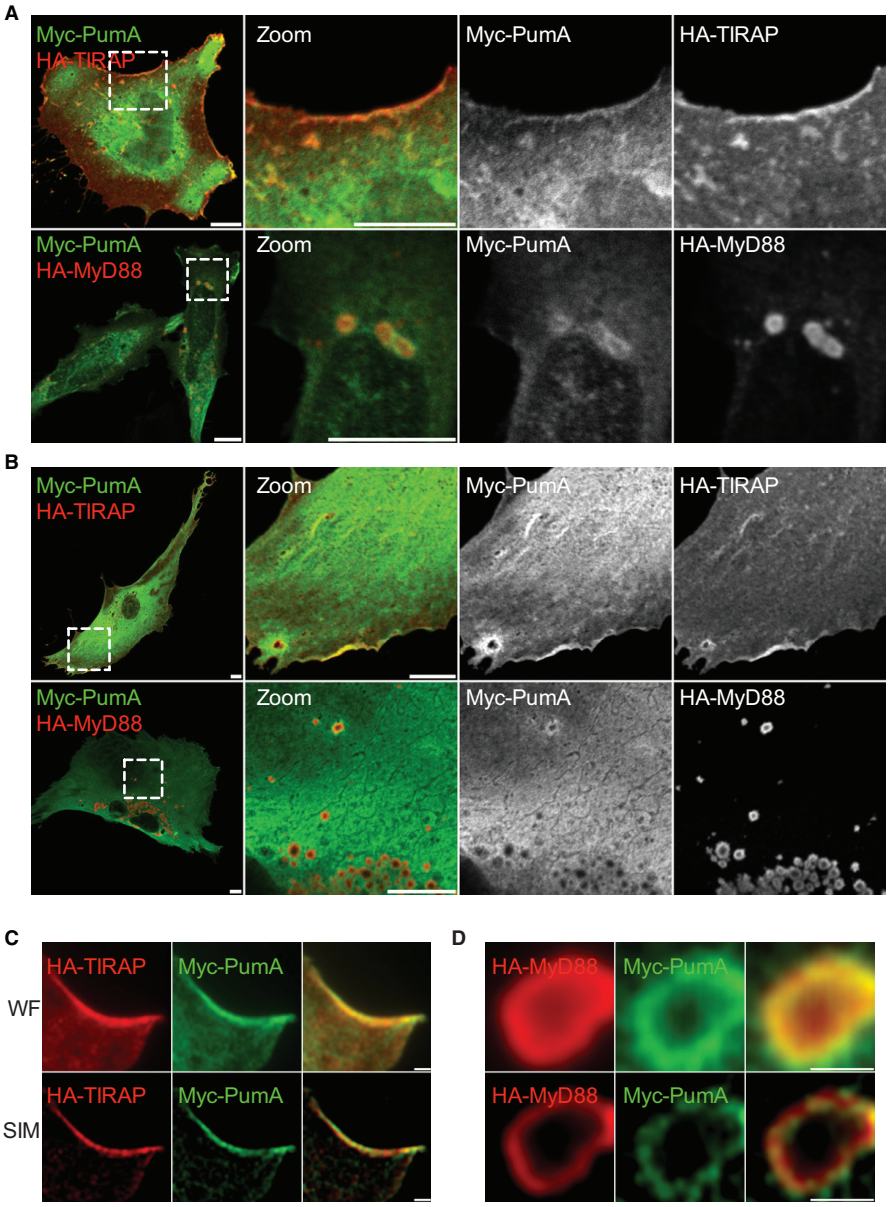

Figure 3. PumA co-localizes with TIRAP at the plasma membrane and to a lesser extent with intracellular MyD88, when ectopically expressed in host cells.

A, B Confocal microscopy of HeLa cells (A) and mouse embryonic fibroblast (MEFs) (B) co-expressing Myc-PumA and adaptor proteins HA-TIRAP (top panel) and HA-MyD88 (bottom panel). Cells were fixed after 10 h of transfection. Scale bars correspond to 10 μm.

C, D Representative micrographs obtained by super resolution structure illumination microscopy (SIM) of MEFs co-expressing (C) Myc-PumA and TIRAP and (D) Myc-PumA and HA-MyD88. Wide field (WF) is shown in top panels and structured illumination of wide field (SIM) in bottom panels. Scale bars correspond to 1 μm.

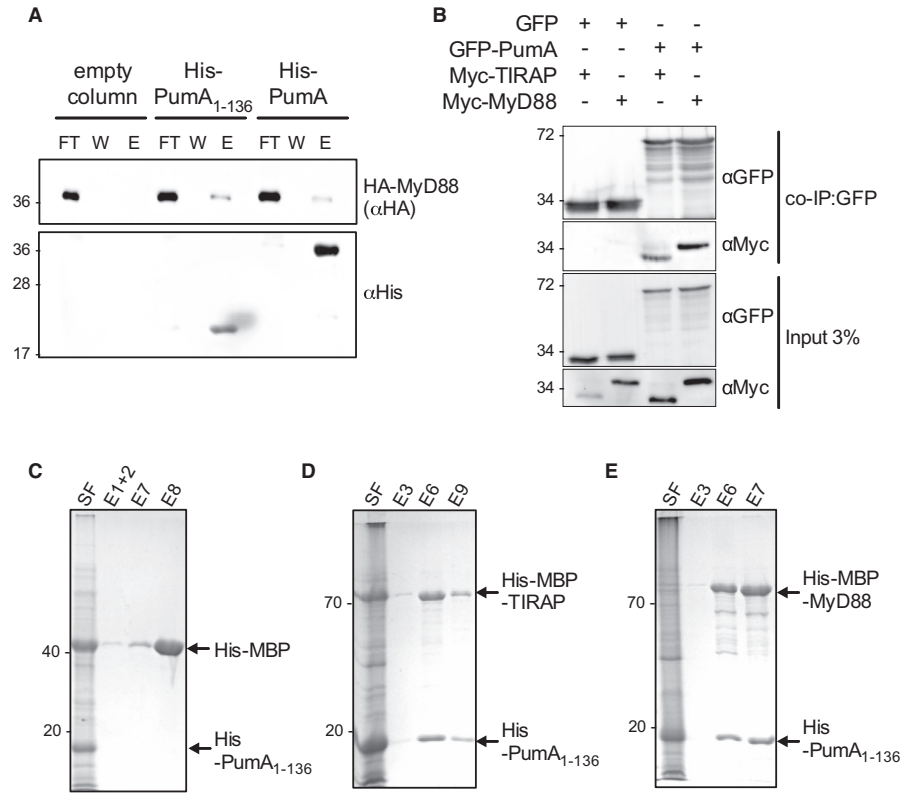

Figure 5. PumA is also capable of interacting with MyD88.

A Pull-down assay using extracts from cells expressing HA-MyD88 against His-PumA or His-PumA$_{1–136}$ immobilized on a Ni-NTA resin. Empty column was used as a control for non-specific binding. Interactions were visualized by Western blotting using anti-HA antibody, and column binding with anti-His (lower blot). Non-bound fraction (FT), last wash (W) and elution (E) are shown for each sample and the molecular weights indicated (kDa).

B Co-immunoprecipitation (co-IP) assay from cells expressing GFP-PumA and either Myc-TIRAP or Myc-MyD88. GFP was used as a control for non-specific binding. The co-IP was revealed using an anti-Myc antibody, the fraction bound to GFP-trapping beads using an anti-GFP antibody and the inputs (shown on the bottom two images) using both anti-Myc and anti-GFP antibodies.

C–E Co-purification of His-PumA$_{1–136}$ co-expressed in *E. coli* BL21 with either (C) His-MBP (control), (D) His-MBP-TIRAP or (E) His-MBP-MyD88. Interactions were visualized with coomassie blue stained gels. Soluble fraction (SF) and selected elutions (E) are shown for each sample and the molecular weights indicated (kDa).

Source data are available online for this figure.

this domain. We therefore carried out co-IP experiments with GFP-PumA$_{137–303}$ expressed in host cells. We could not detect any interaction between PumA$_{137–303}$ and TIRAP (Fig EV4A) nor between PumA$_{137–303}$ and MyD88 (Fig EV4B). However, it is important to note that expression of PumA$_{137–303}$ results in loss of plasma membrane localization. Instead, we observed formation of cellular aggregates that are positive for FK2 labelling (Fig EV4C), which recognizes mono- and poly-ubiquitinated proteins and could correspond to misfolded protein. For this reason, we cannot completely exclude a role of the C-terminus of PumA in these interactions. Nonetheless, our data identify TIRAP and MyD88 as host cell targets of PumA, which mediates interaction with these adaptor proteins via its TIR domain.

PumA interacts with the ESCRT-I component UBAP1

As PumA was able to interact with both TIRAP and MyD88, two key adaptors in TLR signalling, we hypothesized PumA's function was to block all immune pathways dependent on these adaptors. Using an *in vitro* luciferase assay, we tested key immune receptors implicated in *Pseudomonas* infection. Surprisingly, we found PumA could not only block TLR4, TLR5 and IL-1β but also the TNF receptor,

which is not dependent on TIR–TIR interactions (Fig EV5A). TNFR1 inhibition was specific to PumA as expression of the *Brucella* TIR domain-containing protein BtpA/TcpB did not have any significant effect (Fig EV5B). We therefore carried a yeast two-hybrid screen to identify an alternative target of PumA and found UBAP1, a key component of the ESCRT-I mediating trafficking and sorting of ubiquitinated cargo proteins on MVBs (Stefani *et al*, 2011; Agromayor *et al*, 2012). This interaction was confirmed by co-IP from cells co-expressing PumA and UBAP1 (Fig 6A and B) as well as by pull-down using purified PumA or $PumA_{1–136}$ and cell extracts with either streptavidin-tagged UBAP1 (Fig 6C) or Myc-UBAP1 (Appendix Fig S5A). These results were specific to PumA as the *Brucella* TIR protein BtpA/TcpB did not show any interaction (Fig 6C). Furthermore, $PumA_{137–303}$ could not co-IP UBAP1 (Fig EV4D) supporting a role of the TIR domain in targeting UBAP1. Not surprisingly, microscopy analysis of cells expressing both PumA and UBAP1 showed significant co-localization at the plasma membrane and intracellular compartments (Appendix Fig S5C).

We next investigated whether PumA is interacting with UBAP1 in the context of the ESCRT-I machinery. As over-expression of UBAP1 could result in its mislocalization, we carried out endogenous co-IP from cells expressing HA-PumA. Full-length PumA not only interacted very efficiently with endogenous UBAP1 but more importantly also co-immunoprecipitated TSG101 (Fig 6D), confirming PumA is targeting the ESCRT-I machinery. As expected, PumA also interacted with endogenous TIRAP (Fig 6D). The TIR domain of PumA only weakly interacted with endogenous UBAP1 and TIRAP (Fig 6E), whereas the C-terminus of PumA showed no interactions (Fig 6F).

While we were conducting this work, another study reported UBAP1 participates in control of TNFR1 and other cytokine receptor trafficking (Mamińska *et al*, 2016). Our data along with this recently published study thus suggest that PumA interaction with UBAP1 results in inhibition of the TNF receptor-mediated pathway. To determine whether PumA was targeting two different types of cellular compartments, one with UBAP1 controlling the TNFR pathway and another containing TLR adaptors, we analysed whether UBAP1 was excluded from TIRAP and MyD88 containing compartments. We first analysed their intracellular localization following transfection as we were not able to detect endogenous UBAP1 with currently available antibodies. Extensive co-localization was observed at the plasma membrane and intracellular structures when co-expressing UBAP1 and TIRAP (Fig 7A), with no visible impact on the normal distribution of TIRAP. However, in the case of MyD88, co-expression with UBAP1 resulted in accumulation of this adaptor at the plasma membrane, not seen in cells expressing MyD88 alone (Fig 7A, bottom panel and B). Quantification of membrane enrichment of MyD88 in cells expressing UBAP1 showed MyD88 membrane association was even more striking in the presence of UBAP1 (Fig 7C) than that observed when co-expressing TIRAP with MyD88 (Kagan & Medzhitov, 2006), suggesting UBAP1 could be participating in MyD88 intracellular sorting.

To determine whether UBAP1 could be interacting with these TLR adaptors, we carried out biochemical analysis of cells co-expressing UBAP1 and either TIRAP or MyD88. We could efficiently detect an interaction between UBAP1 and MyD88 by co-IP (Appendix Fig S5D and E) but not UBAP1 and membrin (Appendix Fig S5E), used as a control eukaryotic protein with the same tag. In the case of TIRAP, the co-IP was much less efficient (Appendix Fig S5D). These results suggest that UBAP1 may be associated with MyD88-containing compartments and to a lesser extent TIRAP, consistent with our microscopy observations. To confirm these results and ensure these interactions were taking place with UBAP1 in the context of the ESCRT-I, we determined whether MyD88 and TIRAP could interact with endogenous UBAP1 and TSG101. We found that HA-MyD88 co-immunoprecipitated both components of the ESCRT-I as well as endogenous TIRAP (Fig 7D), as expected. However, we did not observe an interaction between HA-TIRAP and endogenous UBAP1 nor TSG101 (Fig 7E), suggesting that only MyD88 can be found associated with the ESCRT-I.

Overall, these data suggest that PumA mediates interactions with UBAP1 in the context of ESCRT-I, which can itself associate with the TLR adaptor MyD88, also targeted by this *P. aeruginosa* effector protein.

Pseudomonas aeruginosa PA7 induces a decrease of TNFR1 in a PumA-dependent manner during infection *in vitro*

It is well described in the literature that inhibition of UBAP1 induces intracellular accumulation of EGFR, LTβR and TNFR1 (Stefani *et al*, 2011; Mamińska *et al*, 2016). To establish a link between PumA interaction with UBAP1 and the ability of PumA to reduce TNFα-dependent signalling (Fig EV5A), we analysed the levels of TNFR1 during infection. In wild-type PA7 infected A549 cells, we observed a decrease of TNFR1 compared to the negative control (Fig 7F). In contrast, the mutant lacking PumA was not able to reduce the levels of TNFR1 in infected cells and this phenotype could be fully restored by expression of PumA in the complemented strain. This is consistent with PumA targeting of UBAP1 and enhancing its activity during infection *in vitro*. Interestingly, we did not see any impact on the overall levels of TIRAP during infection (Fig 7F) suggesting that PumA is not inducing TIRAP degradation as was previously reported for BtpA (Sengupta *et al*, 2010).

Discussion

Many pathogens have developed sophisticated strategies to evade or modify host immune responses to their advantage. We have found that the TIR domain-containing protein PumA plays a major role in the virulence of multi-drug resistant *P. aeruginosa* PA7 strain. PumA ensures efficient inhibition of innate immune responses by interacting with MyD88 and TIRAP, key adaptor proteins for IL-1R and the main relevant TLRs in *Pseudomonas* infection (TLR4 and TLR5), as well as UBAP1 which regulates cytokine receptor pathways. These results identify UBAP1 as a novel cellular target for bacterial pathogens.

Pseudomonas aeruginosa is an important human pathogen associated with high level of mortality in nosocomial infections and cystic fibrosis patients. Most *P. aeruginosa* strains rely on a multitude of virulence factors to control host cellular pathways, including effectors delivered by the T3SS. However, in a cystic fibrosis context, colonizing strains modulate levels of expression of some of these virulence factors (Hauser *et al*, 2011), namely down-regulation of the T3SS (Jain *et al*, 2004) and undergo a remarkable accumulation of pathoadaptive mutations (Marvig *et al*, 2014). The

Published online: May 8, 2017
The EMBO Journal

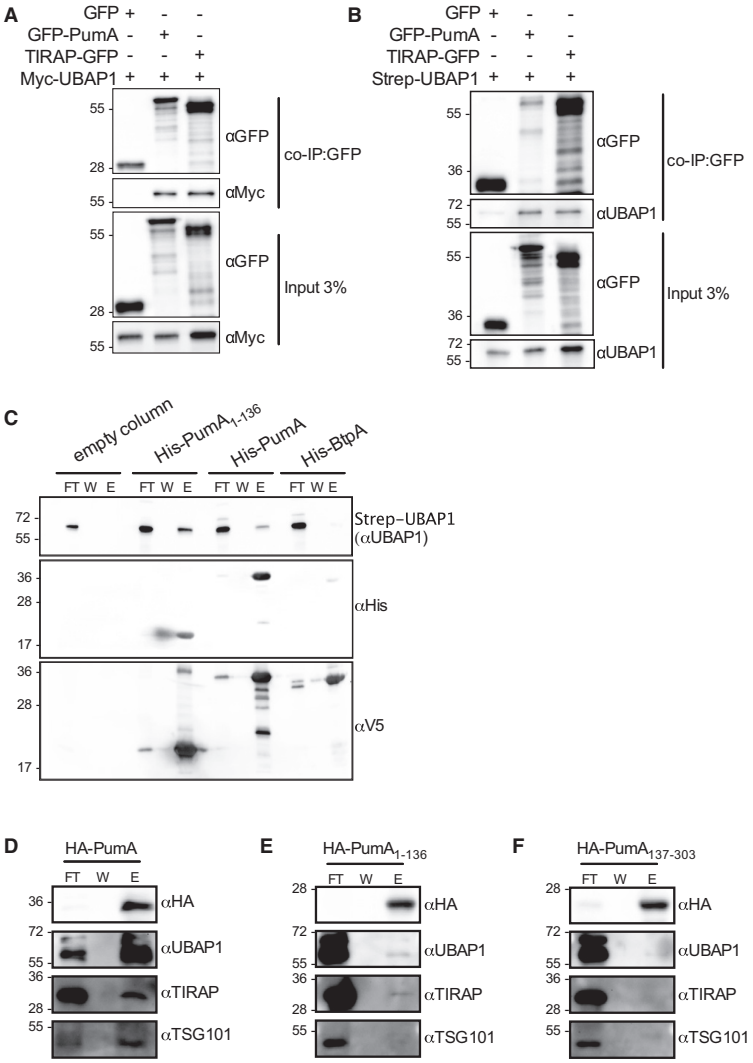

Figure 6. Identification of UBAP1 as a novel host protein targeted by the bacterial TIR domain of PumA.

A, B Co-immunoprecipitation (co-IP) assay from cells expressing Myc-UBAP1 (A) or Strep-UBAP1 (B) with either GFP, GFP-PumA or TIRAP-GFP. The co-IPs were revealed using an anti-Myc (A) or anti-UBAP1 (B) antibodies, the fractions bound to GFP-trapping beads using an anti-GFP antibody and the inputs using anti-Myc, anti-GFP or anti-UBPA1 antibodies as indicated.

C Pull-down assay using extracts from cells expressing Strep-UBAP1 against His-PumA or His-PumA$_{1–136}$ immobilized on a Ni-NTA resin. Empty column was used as a control for non-specific binding. Interactions were visualized by Western blotting using anti-UBAP1 antibody, and column binding with anti-His (middle blot), followed by anti-V5 (lower blot), necessary for detection of BtpA, which for reasons we do not understand cannot be easily detected with the anti-His antibody (Appendix Fig S5B).

D–F Endogenous co-IP from cells expressing (D) HA-PumA, (E) HA-PumA$_{1–136}$ and (F) HA-PumA$_{137–303}$. The fractions bound to HA-trapping beads were probed with anti-HA, anti-UBAP1, anti-TIRAP and anti-TSG101 antibodies. Non-bound fraction (FT), last wash (W) and elution (E) are shown for each sample and the molecular weights indicated (kDa).

Source data are available online for this figure.

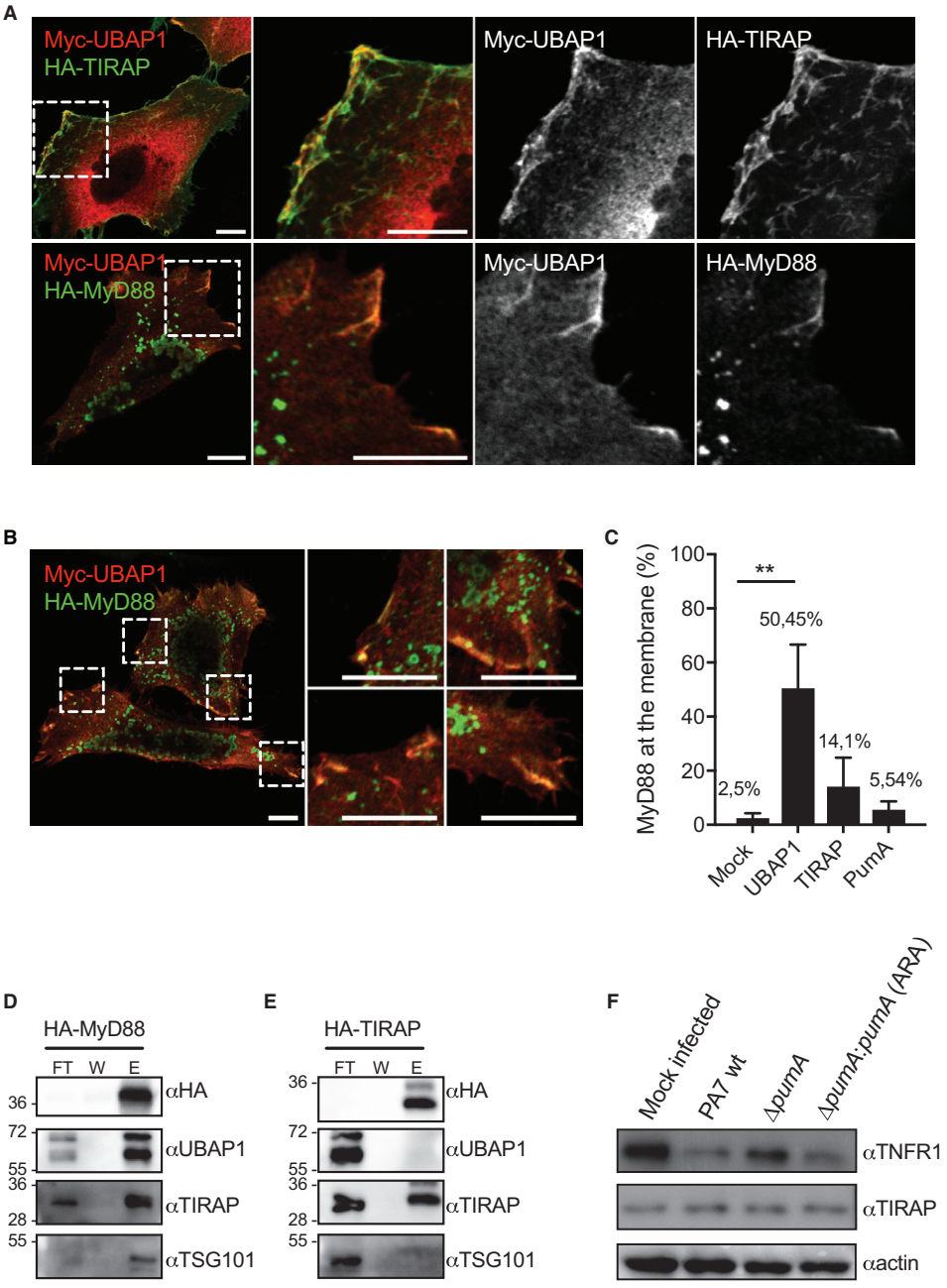

Figure 7.

Figure 7. Analysis of the impact of UBAP1 on TIRAP and MyD88.

A Representative micrographs obtained by confocal microscopy of HeLa cells co-expressing Myc-UBAP1 (red) and adaptor proteins HA-TIRAP (green, top panel) or HA-MyD88 (green, bottom panel). Cells were fixed after 10 h of transfection. Scale bars correspond to 10 μm.

B Different zoomed images showing HA-MyD88 (green) recruitment to the plasma membrane in the presence of Myc-UBAP1 (red). Scale bars correspond to 10 μm.

C Quantification of plasma membrane localization of MyD88 in cells expressing MyD88 alone or with either UBAP1, TIRAP or PumA. At least 200 cells were enumerated in three independent experiments, and membrane localization was defined under the strict criteria of clear line at the plasma membrane. Cells with MyD88-positive vesicles in close proximity to the plasma membrane were not counted as positive. Non-parametric one-way ANOVA Kruskal–Wallis test was performed, with Dunn's multiple comparisons test. $^{**}P < 0.01$.

D, E Endogenous co-IP from cells expressing (D) HA-MyD88 and (E) HA-TIRAP. The fractions bound to HA-trapping beads were probed with anti-HA, anti-UBAP1, anti-TIRAP and anti-TSG101 antibodies. Non-bound fraction (FT), last wash (W) and elution (E) are shown for each sample and the molecular weights indicated (kDa).

F Western blot of TNFR1 in A549 cells infected for 1 h with either *P. aeruginosa* PA7 wt, Δ*pumA* or Δ*pumA:pumA* (Ara) induced with 1% arabinose. A mock-infected sample was included as a negative control. The same blot was also probed for TIRAP and actin to control loading.

Source data are available online for this figure.

PA7-related *P. aeruginosa* strains lack the 20-Kb-long genomic region encoding the T3SS core components and all genes encoding secreted effectors but contains several additional genomic islands and potential novel virulence factors (Pirnay *et al*, 2009; Roy *et al*, 2010; Cadoret *et al*, 2014; Freschi *et al*, 2015). In some of these strains, such as CLJ1, an exolysin secreted by a two-partner secretion system is responsible for hypervirulence (Elsen *et al*, 2014). However, in PA7, this exolysin is detected at only low levels in the secretome and is not responsible for cytotoxicity (Reboud *et al*, 2016), suggesting an alternative pathogenicity mechanism. In this context, we hypothesize that PumA might be underlying an alternative pathogenicity mechanism to allow PA7 persistence within a host. Consistently, we observed a clear attenuation in virulence for a PA7 strain lacking *pumA* in both *C. elegans* and in a mouse lung infection model. Interestingly, no impact in the ability of the *pumA* mutant to disseminate systemically was observed suggesting a role in control of local pathology. This type of *P. aeruginosa* infection based on persistence and colonization rather than rapid cytotoxicity could be relevant in specific clinical contexts such as infection of wound and burn patients, aggravated by the high level of multi-drug resistance. It is interesting to note that other *Pseudomonas* contain a TIR domain protein, namely several strains pathogenic in plants. In this context, it will be interesting to analyse the role of the orthologous TIR protein in the plant pathogens *P. syringae* or *P. viridiflava* with over 90% identity to PumA in amino acid sequence for the TIR domain, regarding control of plant responses as these functions may be relevant across taxonomic kingdoms.

Pseudomonas is not the only bacterial pathogen to take advantage of the TIR domain to engage TIR–TIR interactions which are essential components of innate immune signalling. Bacterial targeting of TLRs has been best described for uropathogenic *E. coli* TcpC (Cirl *et al*, 2008) and *Brucella* BtpA, also known as TcpB (Cirl *et al*, 2008; Salcedo *et al*, 2008), even though their molecular mode of action remains elusive. *Brucella* relies on an additional TIR protein, BtpB to down-modulate inflammation during infection (Salcedo *et al*, 2013). TcpC was shown to interfere with MyD88-dependent and independent pathways to down-modulate TLR signalling and contribute to kidney pathology (Cirl *et al*, 2008; Yadav *et al*, 2010). In the case of *Brucella*, BtpA/TcpB has been described as a mimic of TIRAP, since it can directly bind specific phosphoinositides of the plasma membrane (Radhakrishnan *et al*, 2009). This is clearly distinct from PumA that shows no significant lipid binding properties. In addition, BtpA/TcpB was also shown to bind TIRAP, which results in its increased ubiquitination and degradation during infection (Sengupta *et al*, 2010), which also differs from PumA which despite TIRAP binding does not induce its degradation. Several studies have followed disputing the precise target of BtpA/TcpB with some proposing preferential binding to MyD88 (Chaudhary *et al*, 2011). One key question that remains unanswered is how these bacterial TIR proteins are entering host cells and where do they localize during infection? No direct imaging of bacterial TIR proteins has been described. In the case of TcpC, internalization into host cells was observed but the export mechanism was not identified (Cirl *et al*, 2008), whereas no data are available regarding *Salmonella*, *Yersinia*, *Staphyloccocus* and *Enterococcocus*. In the case of *Brucella*, depending on the fusion tags, translocation into host cells of BtpA/TcpB or BtpB was dependent or independent of the T4SS (Salcedo *et al*, 2013) whereas a separate group has proposed that BtpA/TcpB is cell permeable and may enter host cells in a passive manner (Radhakrishnan & Splitter, 2010). Unfortunately, PumA fusion with CyaA resulted in its cleavage preventing us from using this system. Using different fluorescent tags and the specific anti-PumA antibody, we were not able to confidently visualize it inside host cells during infection. We were however able to detect intracellular PumA using a TEM1 fusion. Further work needs to be carried out to confirm translocation of PumA into host cells and define the intracellular location of PumA during infection. PumA was also not found in the bacterial culture supernatant *in vitro*, suggesting that contact-dependent delivery is involved. How PumA is entering host cells will have to be further investigated, but since the T3SS is not present in PumA-encoding strains, it suggests that host cell delivery would need an alternative secretion pathway.

It is important to note that TIR domains are widespread in multicellular organisms, such as in plants (role in disease resistance) and amoebas (dual role in ingestion of bacteria and immune-like functions) as well as in numerous bacterial genera that include cyanobacteria and other non-pathogenic bacteria (Zhang *et al*, 2011). This suggests these domains have evolved as an essential protein–protein interaction platform that could have additional functions. Indeed, recently the TIR domain of TcpC has been shown to directly interact with the NACHT leucin-rich repeat PYD protein 3 (NLRP3) inflammasome and caspase-1, besides MyD88, to perturb inflammasome activation (Waldhuber *et al*, 2016). There are also additional potential targets yet to be identified for BtpA/TcpB since it interferes with microtubule dynamics (Radhakrishnan *et al*, 2011; Felix *et al*, 2014) and induces unfolded protein response (Smith *et al*, 2013).

This notion that bacterial TIR domains provide a broad interaction platform is supported by our observations. We found that in addition to directly interacting with TIRAP and MyD88, PumA also targets the ESCRT-I machinery by binding to UBAP1 as PumA could co-immunoprecipitate endogenous UBAP1 and TSG101. All these interactions seem to be mediated by the TIR domain of PumA, but endogenous co-IP experiments showed that the full-length PumA is required for efficient interactions to occur. It is likely that TIR–TIR interactions are taking place with TIRAP and MyD88. In the case of UBAP1, the PumA interacting domain remains to be identified. All yeast two-hybrid preys identified in our screen encoded for a region containing amino acid 45–164, present between two key functional domains: the N-terminal UBAP1-MVB12-associated (UMA) domain (residues 17–63) that binds the central stalk of ESCRT-I Vps37 and the central domain (residues 159–308), containing the recently identified key binding site for HDPTP which can act as a cargo adaptor (Gahloth *et al*, 2016). The C-terminal portion of UBAP1 includes a SOUBA domain (residues 381–502) known to bind ubiquitin (Agromayor *et al*, 2012). UBAP1 is a key component of ESCRT-I that enables sorting of ubiquitinated cargo on MVBs. PumA may be binding an intermediate region of UBAP1 that could partially overlap with that interacting with HDPTP. Further work is now necessary to confirm this hypothesis. In view of the recent work implicating UBAP1 in restriction of constitutive NF-κB signalling (Mamińska *et al*, 2016), PumA could be impacting the activation of TNFR pathway through UBAP1. Depletion of UBAP1 was shown to induce intracellular accumulation of the cytokine receptors in endosomal compartments (Mamińska *et al*, 2016), which leads to increase in constitutive levels of NF-κB, since UBAP1 cannot ensure proper steady-state cytokine receptor (such as LTβR and TNFR1) sorting and subsequent degradation. Since *in vitro* experiments suggest PumA is blocking TNF receptor-mediated pathway, PumA could be enhancing activity of UBAP1. This phenotype is specific of PumA since we observed no effect of another bacterial TIR domain-containing protein BtpA/TcpB which does not interact with UBAP1 and its ectopic expression does not result in inhibition of the TNF-induced pathway. Consistent with our hypothesis, wild-type PA7 decreases the levels of TNFR1 in A549 cells in a PumA-dependent manner suggesting targeting of UBAP1 is occurring during infection and could enhance its activity.

In an attempt to determine whether distinct intracellular locations were targeted by PumA to enable interaction with TLR adaptors and the ESCRT-I component UBAP1, we analysed whether UBAP1 was excluded from TIRAP or MyD88-enriched compartments. Surprisingly, co-IP experiments revealed endogenous UBAP1 itself and TSG101 could be found associated with MyD88 but not TIRAP, suggesting that the ESCRT-I machinery may be interacting with specific TLR adaptors. We therefore propose that additional crosstalk between these pathways may exist. MyD88 has been shown to interact with TLRs and with TIRAP via its TIR domain or the death domain. It remains to be demonstrated whether UBAP1 interacts directly with MyD88 but our data strongly suggest they can be found in the same complex, namely at the plasma membrane. Interestingly, co-expression of MyD88 and UBAP1 resulted in MyD88 enhanced plasma membrane targeting, to higher levels than that previously described for TIRAP (Kagan & Medzhitov, 2006). Further work is required to determine if UBAP1 interaction with MyD88 promotes activation of TLR signalling and whether PumA could disrupt this interaction. A few studies have suggested the implication of ESCRT-I or MVBs in the control of TLR pathways. In *Drosophila*, ESCRT-0 components modulate endosomal sorting of Toll (Husebye *et al*, 2006; Huang *et al*, 2010). ESCRT have been also shown to negatively regulate TLR7 and 9 to enable recycling of these receptors following ubiquitination (Chiang *et al*, 2012). More interestingly, inhibition of endosomal sorting via ESCRT-I increases LPS-induced signalling (Husebye *et al*, 2006), suggesting it is playing a role in sorting and degradation of activated receptor complexes.

In conclusion, our study describes a *P. aeruginosa* effector PumA that targets UBAP1 in the context of ESCRT-I and plays a major role in virulence. In addition, our data associate UBAP1 to MyD88, highlighting a potential larger role of endosomal sorting by ESCRT-I in regulation of TLR signalling.

Materials and Methods

Strains

Pseudomonas aeruginosa strains used in this study were wild-type PA7, PA14 or derived strains and were routinely cultured in liquid Luria Bertani (LB) medium. Antibiotics were added to *P. aeruginosa* cultures, when appropriate, at the following concentrations: 150 μg/ml tetracycline and 750 μg/ml carbenicillin. When indicated, arabinose at 1% or glucose at 0.5% was added to cultures. For *Escherichia coli* cultures, antibiotics were added when necessary at the following concentrations: 50 μg/ml kanamycin and 50 μg/ml ampicillin.

Construction of *Pseudomonas* Δ*pumA* mutant and complemented strains

The 500 base pairs upstream and 500 base pairs downstream of *pumA* gene (*PSPA7_2375;* NC_009656.1.) were amplified from *P. aeruginosa* PA7 genomic DNA to do overlapping PCR, using primers 5′-TTTGGGCCCAAGACGATCAGCGGCACC-3′, 5′-ATCGGCT CTGCCCTATGCCATCTTTTTAACTCCATCCTTGTAATTCC-3′, 5′-GG ATGGAGTTAAAAAGATGGCATAGGGCAGAGCCGAT-3′ and 5′-TT TTGATCACAACTACCCCGATGCGTT-3′, respectively. Then, the PCR product was sub-cloned into pGEM®-T Easy Vector (PROMEGA) and ligated into pKNG208 (Cadoret *et al*, 2014) following digestion with *SpeI* and *ApaI* to generate pKNG208-Δ*pumA*. This plasmid was introduced into *P. aeruginosa* PA7 by conjugation where it is incapable of autonomous replication. Homologous recombination events were primary selected using tetracyclin resistance (150 μg/ml) in *Pseudomonas* isolation agar (PIA) plates and secondary selected using sucrose 6% sensitivity in LB agar plates during 2–3 days at room temperate. PCR and sequencing analyses confirmed the *pumA* wild-type gene was deleted and Western blotting showed absence of PumA production of the PA7 Δ*pumA* strain (Appendix Fig S2B).

The mini-CTX-P_{BAD} plasmid was constructed by cloning the *SalI-AraC*-P_{BAD}-*Sac*I fragment from pJN105 vector (Newman & Fuqua, 1999) into the 6711 bp *SalI*/*Sac*I DNA fragment from miniCTX-lacZ vector (Hoang *et al*, 1998). *PSPA7_2375* gene was amplified with an artificial Shine-Dalgarno (AAGAAG) and cloned into mini-CTX-P_{BAD} digested by *Spe*I/*Sac*I using the SLIC method (Jeong *et al*, 2012).

Primers used were 5′-AGCCCGGGGGATCCACTAGTAGGAGGTGA GATATACAATGGCGGTCTTCATTAGTTA-3′ and 5′-ACCATCCAGT GCAGGAGCTCCTATGCGCGCGGCCACGGG-3′.

Construction of PA7 *pumA::bla1* strain

The 500 base pairs upstream and downstream of *pumA* stop codon from *P. aeruginosa* PA7 genomic DNA and *blaM* gene from pJC121 plasmid (Myeni *et al*, 2013) were PCR amplified using primers 5′-ATTACGCGTTAACCCGGGCCCAGGATGTTGACGGCTATC-3′, 5′-CAGCGTTTCTGGTGCGCCGCGGCCACGG-3′, 5′-CTGATTAAGTAGGG CAGAGCCGATCAGCTC-3′, 5′-ACACTGGCGGCCGTTACTAGTGCTG GACTGGCGCAACTA-3′, 5′-TGGCCGCGCGCACCAGAAACGCTGGT GAAA-3′ and 5′-ATCGGCTCTGCCCTACTTAATCAGTGAGGCACC T-3′ and used in overlapping PCR. DNA product was then cloned by the SLIC method (Jeong *et al*, 2012) into pKNG208 (Cadoret *et al*, 2014) digested by *Apa*I/*Spe*I to generate pKNG208-*pumA::bla1* vector.

Construction of eukaryotic expression vectors

The PumA constructs were obtained by cloning in the gateway pDONR™ (Life Technologies) and then cloned in the pENTRY Myc, HA or GFP vectors. The following primers were used 5′-GGGGA CAAGTTTGTACAAAAAAGCAGGCTTCGCGGTCTTCATTAGTTATT CCCACG-3′ and 5′-GGGGACCACTTTGTACAAGAAAGCTGGGTCC TATGCGCGCGGCCACGGGGTAGC-3′. $PumA_{1–136}$ was constructed with the following primers: 5′-GGGG ACAAGTTTGTACAAAAAA GCAGGCTTCATGGCGGTCTTCATTAGTTATTCC -3′; 5′-GGGGACCA CTTTGTACAAGAAAGCTGGGTCCTAACGGGACTGATCAGGATTAG AG-3′. $PumA_{137–303}$ with 5′-GGGGACAAGTTTGTACAAAAAAGCA GGCTTC ATTGAGGATGTTGACGGCTA-3′; 5′-GGGGACCACTTTG TACAAGAAAGCTGGGTC CTATGCGCGCGGCCACGGGGTAGC -3′.

Construction of prokaryotic expression vectors

The full-length *P. aeruginosa PA7 pumA* and its TIR domain (residues 1–136) were cloned into pET151/D-Topo (Invitrogen)—which carries the T7 promoter, N-terminal 6xHis and V5 tags, protease recognition site for tobacco etch virus (TEV) protease and ampicillin resistance gene. The following primers were used: 5′-CAC CATGGCGGTCTTCATTAGTTATTCC-3′ and 5′-TGATCGGCTCT GCCCTATGC-3′ for *pumA*; the same forward primer and 5′-CTAACGGGACTGATCAGGATTAGAG-3′ for *pumA* TIR domain. BtpA was cloned in this same vector. The HA-TIRAP and HA-Myd88 vector was used as a template to clone TIRAP and Myd88, respectively, into pRSF-MBP vector. This vector corresponds to pRSFDuet-1 (Novagen) but modified to insert 6xHis-MBP from pETM-41 vector (EMBL) behind the cloning multiple site.

Cell culture and transfections

HeLa, HEK 293T and A549 cells (all obtained from ATCC) were grown in DMEM supplemented with 10% of foetal calf serum (FCS). Mouse embryonic fibroblasts were prepared as described previously (Conner, 2001) and maintained in DMEM supplemented with 10% (FCS). All cells were transiently transfected using Fugene (Roche) for 24 h, according to manufacturer's instructions.

Pseudomonas infection of A549 cells

For adhesion assays and microscopy analysis of NF-κB, cells were first seeded into 24-well tissue culture plates at 2×10^5 cells/well (to obtain a monolayer) or 5×10^4 cells/well, respectively. Cells were infected with overnight cultures at a MOI of 10 or 100 of *P. aeruginosa* in 500 μl of complete medium per well. Plates were centrifuged at 400 × *g* for 5 min and then incubated for 1 h at 37°C with 5% CO_2 atmosphere. Cells were then washed five times with DMEM and either lysed or fixed. In the case of the cytotoxicity assays, cells were incubated for longer periods with complete media. When indicated, arabinose at 1% or glucose at 0.5% was added.

For NF-κB experiments, exponential phase cultures were also used, but no differences were detected. After 1 h, medium was removed and cells were washed two times with ice-cold PBS. Control samples were always performed by incubating cells with mock inocula and following the exact same procedure as for the infection.

For adhesion assays, cells were lysed with 500 μl of 0.1% Triton solution and pipetted vigorously several times. Lysed samples were harvest, and serial 10-fold dilutions in PBS were plated on LB agar to enumerate CFUs.

For Western blot analysis of TNFR1, cells were seeded in six-well plates at 2×10^5 cells/well and infected as described above. At 1 h post-infection, cells were washed with ice-cold PBS 2 times, were collected and lysed directly with loading buffer. For each sample, six wells were pooled.

Cell cytotoxicity exerted by bacteria was quantified with the cytotoxicity detection kit-LDH (Roche), which measures the activity of cellular lactate dehydrogenase released into the supernatants. The assays were performed according to the instructions of the manufacturer.

For propidium iodide staining, A549 cells were maintained in DMEM media supplemented with 10% FCS. Cells were seeded at 1×10^5 cells/ml in 96-well plate to achieve confluent monolayers. Cells were then infected with overnight cultures of *P. aeruginosa* or mutants supplemented with arabinose to a final concentration of 2% (as indicated) at a MOI of 100. The plates were centrifuged at 400 × *g* for 5 min and incubated for 1 h at 37°C. After 1 h of infection, cells were washed three times with PBS then incubated with complete media (without red phenol) containing propidium iodide and labelling measured during 6 h every 15 min with a Tecan Infinite M1000.

Immunofluorescence labelling and microscopy

Cells were fixed in Antigenfix (DiaPath), at room temperature for 10 min. Cells were then labelled at RT with primary antibody mix diluted in 0.1% saponin in PBS with 1% BSA and 10% horse serum for blocking. Primary antibody was incubated for 1 h followed by two washes in 0.1% saponin in PBS. Secondary antibodies were then mixed and incubated for a further 30 min, followed by two washes in 0.1% saponin in PBS, one wash in PBS and one wash in distilled water before mounting with Prolong Gold. Samples were examined on a Zeiss LSM710 or Zeiss LSM800 laser scanning confocal microscopes for image acquisition. Images of 1,024 × 1,024 pixels were then assembled using plugin FigureJ from ImageJ.

For immunofluorescence microscopy analysis of NF-κB, cells were permeabilized for 6 min with 0.1% Triton in PBS, followed by a blocking for 1 h with 2% BSA in PBS. Primary antibodies were

incubated for 1 h followed by two washes in 2% BSA in PBS, 30-min incubation for secondary antibodies, two washes in 2% BSA in PBS, one wash in PBS and one wash in water before mounting with Prolong Gold (Life Technologies). Samples were examined on a Zeiss LSM710 laser scanning confocal microscope for image acquisition. Images of 2,648 × 2,648 pixels were then passed through a specific plugin of ImageJ developed by L. Plantevin, based on a previous study (Noursadeghi *et al*, 2008); raw images were treated with a median filter and threshold moments, afterwards total NF-κB was subtracted from the Dapi channel to obtain cytoplasmic NF-κB. Total NF-κB was then subtracted from cytoplasmic NF-κB to obtain nuclear NF-κB (Fig EV1A). Quantification was always done by counting at least 200 cells per condition in minimum three independent experiments, for a total of at least 600 host cells analysed per condition.

Antibodies and reagents

Primary antibodies used were rabbit anti-p65 from Santa Cruz (clone C-20, ref. sc-372) at 1/250, mouse anti-myc9E10 (developed by Bishop, J.M. was obtained from the Developmental Studies Hybridoma Bank, created by the NICHD of the NIH and maintained at the University of Iowa), mouse anti-HA (Eurogentec, clone 16B12, ref. MMS-101R), rabbit anti-HA (Sigma, ref. H6908), rabbit anti-GFP (Amsbio, ref. TP401), rabbit anti-UBAP1 (Proteintech, ref. 12385-1-AP), mouse anti-His (Sigma, clone HIS-1, ref. H1029), mouse anti-FLAG (Sigma, clone M2, ref. F1804) all at 1/1000 and mouse anti-TNFR1 (Santa Cruz, clone H-5, ref. sc-8436) and rabbit anti-TSG101 (Atlas Antibodies, ref. HPA006161) both at 1/200. Rabbit polyclonal anti-PumA serum was obtained by repeated immunization of rabbits with purified PumA (Eurogentec) and was used at 1/1,000 for Western blot and for immunofluorescence microscopy. Purified BtpA was used to obtain chicken anti-BtpA (Eurogentec). Anti-EF-Tu antibody (kind gift from R. Voulhoux) was used at 1/10,000.

Secondary antibodies used were anti-rabbit, mouse, chicken or rat conjugated with Alexas-488, -555 or -647 all from Jackson ImmunoResearch. When necessary, phalloidin-568 (1/1,000) was used to label the actin cytoskeleton and DAPI nuclear dye (1/1,000) for the host cell nucleus. For Western blots, anti-mouse or rabbit-HRP antibodies were used at 1/5,000.

TEM translocation assay

HeLa cells were seeded in a 96-well plates at 1×10^4 cells/well overnight. Cells were then infected with an MOI of 100 by centrifugation at 4°C, 400 g for 5 min and 1 at 37°C 5% CO_2. Cells were washed with HBSS containing 2.5 mM probenecid. Then, 6 µl of CFF2 mix (as described by Life Technologies protocol) and 2.5 mM probenicid were added to each well, and incubated for 1.5 h at room temperature in the dark. Cells were finally washed with PBS, fixed using Antigenfix and analysed immediately by confocal microscopy (Zeiss LSM800) or flow cytometry (MACSQuant10 analyser).

Luciferase activity assay

HEK 293T cells were seeded in a 96-well plates at 2×10^4 cells/well overnight, and cells were transiently transfected with FuGENE® 6 (Promega) for 24 h for a total of 0.4 µg of DNA consisting of 50 ng TLR plasmids, 200 ng of pBIIXLuc reporter plasmid, 5 ng of control Renilla luciferase (pRL-null, Promega) and 50 ng of myc-PumA expression vector. The total amount of DNA was kept constant by adding empty vector. Where indicated, cells were treated with *E. coli* LPS (1 µg/ml) and Flagellin FLA-ST (1 µg/ml), all obtained from InvivoGen, for 6 h. In the case of IL-1β and TNFR, endogenous receptors were stimulated with IL-1β (100 ng/ml) and TNFα (100 ng/ml), respectively. Cells were then lysed and luciferase activity measured using Dual-Glo Luciferase Assay System (Promega).

Yeast two-hybrid screen

Full-length *pumA* cloned in pB27 (N-LexA-bait-C fusion) was used in a ULTImate screen against a human normal lung-RP1 library (Hybrigenics).

Protein expression and purification

Escherichia coli BL21 star (DE3) cells carrying pET151D topo-*pumA*, pET151D topo-$pumA_{1–136}$, or pRSFDuet-TIRAP or MyD88 plasmids were grown in 1 L Luria Bertani (LB) media containing ampicillin or kanamycin according to the plasmid at 37°C until an OD_{600} value of 0.5–0.8 was reached. Isopropyl-β-D-thiogalactopyranoside (IPTG) was added to final concentration of 1 mM, and culture was further grown overnight at 20°C. Cells were harvested by centrifugation at 6,000×*g* for 20 min at 4°C.

Bacterial pellets were lysed by sonication in cold lysis buffer (40 mM Tris–HCl pH8, 250 mM NaCl, 10% (v/v) glycerol, 1% (v/v) Triton X-100) supplemented with DNase-I, lysozyme and protease inhibitor tablets (Roche). Extracts were cleared at 16,000 × *g* for 20 min at 4°C and loaded onto a 5 ml His-Trap column or 5 ml MBP-Trap column (GE Healthcare) pre-equilibrated with buffer A (40 mM Tris [pH8], 250 mM NaCl, 5% glycerol). The column was washed successively with buffer A, 10% v/v buffer B (buffer A with 500 mM imidazole), 1M NaCl and eluted in a gradient of buffer B (His-Trap) or wash in buffer A and eluted in buffer A containing 20 mM maltose (MBP-Trap).

Proteins used for lipid binding assay were incubated with TEV protease, 1mM DTT and 0.5 mM EDTA, dialysed against buffer A at 4°C overnight. The untagged recombinant protein was purified through a second His-trap column. Pure fractions were pooled, concentrated and applied to size exclusion chromatography (Superdex 75 10/300; GE Healthcare).

Fractions were analysed by SDS–PAGE.

Pull-downs from cell extracts

Human embryonic kidney (HEK) 293T cells were seeded at 5×10^5 in 10-cm cell culture dish in Dulbecco's modified Eagle's medium (Life Technologies) supplemented with 10% foetal bovine serum. Cells were incubated overnight in a 37°C humidified atmosphere of 5% CO_2. Cells were transiently transfected with different plasmids (8 µg) using FuGENE 6 (Promega). 22 h after infection, cells were washed in ice-cold PBS, harvested and resuspended in 200 µl of RIPA buffer (Sigma) supplemented with phenylmethylsulfonyl fluoride (Sigma) and protease inhibitor

cocktail (Roche). Extracts were then centrifuged at 17,000 *g* at 4°C for 20 min. The supernatant was incubated with 50 μg of His tag recombinant protein during 2 h at 4°C, then incubated within gravity flow column (Agilent) containing 80 μl Ni-NTA agarose beads (Macherey-Nagel) during 1 h beforehand washed in water and pre-equilibrated in equilibrium buffer 20 mM Tris–HCl pH7.5, 250 mM NaCl. The column was washed successively three times in equilibrium buffer supplemented with 25 mM imidazole, three times in equilibrium buffer and eluted in equilibrium buffer supplemented with 500 mM imidazole. Proteins eluted were separated by SDS–PAGE, transferred to a PVDF membrane, incubated with specific primary antibodies for 1 h and detected with horseradish peroxidase (HRP)-conjugated secondary antibodies by using Clarity™ Western ECL Blotting Substrate (Bio-Rad).

Co-immunoprecipitations

HEK 293T cells were cultured in 100 mm × 20 mm cell culture dishes at 4×10^5 cells/dish overnight. Cells were transiently transfected with 14.7 μl of Torpedo ^{DNA} (Ibidi) for 24 h for a total of 5 μg of DNA/plate. On ice, after two washes with cold PBS, cells were collected by with a cell scraper and centrifuged at 80 g at 4°C during 5 min. Cell lysis and processing for co-immunoprecipitation were done as described by either GFP-Trap®_A kit (Chromotek) or with the PierceTM HA Epitope Antibody Agarose conjugate (Thermo scientific).

For endogenous co-IP, HeLa cells were cultured in 100 mm × 20 mm cell culture dishes at 1×10^6 cells/dish overnight. Cells were transiently transfected and collected as described above. Cell lysis and processing for co-immunoprecipitation were done following the manufacturers' instructions (PierceTM HA Epitope Antibody Agarose conjugate, Thermo scientific) but using 100 μl of beads and increasing the number of washes to 5.

Co-expression analysis

Escherichia coli BL21 star (DE3) cells harbouring both pET151D topo-$pumA_{1–136}$ and pRSF-Duet vector-TIRAP (or Myd88 or empty vector) plasmids were grown in LB media containing ampicillin and kanamycin at 37°C until an OD_{600} value of 0.5–0.8 and induced with 2 mM isopropyl-β-D-thiogalactopyranoside overnight at 20°C.

Cells were lysed and loaded onto a 5 ml MBP column as described in the protein expression and purification section. Fractions were analysed by SDS–PAGE.

Lipid binding assays

Lipid binding assays were performed as described previously (Marek & Kagan, 2012). Briefly, phosphoinositide phosphate (PIP) strips (Echelon Biosciences) were saturated in blocking buffer (10 mM Tris [pH8], 150 mM NaCl, 0.1% Tween 20, 0.1% Ovalbumin) for 1 h at room temperate under shacking. Strips were probed for 2 h at room temperate with each recombinant protein (2.5 μg) in the presence of the specific anti-protein antibody. PIP strips were then washed in blocking buffer three times for 10 min each and probed with an HRP-conjugated anti-rabbit IgG or anti-Hen IgY for 30 min in blocking buffer. Bound protein was detected using Clarity™ Western ECL Blotting Substrate.

Caenorhabditis elegans infection

The slow killing assay was performed as described previously (Garvis *et al*, 2009). Each independent assay consisted of three replicates. Briefly, five 60 mm NGM plates were inoculated with 60 μl of overnight culture of each bacterial strain and incubated at 37°C overnight. Plates were seeded with L4 stage hermaphrodite fer-15 worms (10 per plate). Plates were then incubated at 25°C and scored each day for live worms. A worm was considered dead when it no longer responded to touch. *Escherichia coli* was used as a control. Animal survival was plotted using GraphPad Prism version 6.0 for Mac, GraphPad Software, La Jolla, California, USA. Survival curves are considered significantly different from the control when *P*-values are < 0.05. Prism calculates survival fractions using the product limit (Kaplan–Meier) method. Prism compares survival curves by two methods: the log-rank test (also called the Mantel–Cox test) and the Gehan–Breslow–Wilcoxon test.

Mouse model of *Pseudomonas* acute infection

Wild-type C57BL6/J male mice, 8–10 weeks old, were purchased from Janvier laboratories. Mice were randomized before the experiments and infection were performed blindly. Following a light anaesthesia with isoflurane (Baxter), a pulmonary infection model was induced by intranasal instillation with 3×10^7 CFU of *P. aeruginosa* PA7 or PA7Δ*pumA* strains (except for survival studies conducted with lethal inocula of 4×10^7 CFU/mouse). All mice were sacrificed at 24 h or survival was monitored for 96 h.

To establish bacterial burden, mouse lungs and spleens were homogenized in sterile tubes with PBS. Lung and spleen homogenates were sequentially diluted and cultured on Lysogeny Broth agar plates for 24 h at 37°C to assess bacterial load. Bronchoalveolar lavage (BAL) was done as follows: lungs from each experimental group were washed with a total of 1.5 ml sterile phosphate-buffered saline (PBS). The recovered lavage fluid was centrifuged (200 g for 10 min), and red blood cells from the cellular pellet were lysed with 300 μl of ACK Lysis Buffer (Gibco). Cell counts were performed directly by optical microscopy.

Ethics statement

All experiments involving animals were carried out in compliance with French and European regulations on the care and protection of laboratory animals (European Commission Directive 86/609 and the French Act #2001–486, issued on June 6, 2001) and performed by certified personnel. The study and all experimental protocols associated were registered and approved by the French authorities (Ministère de l'Enseignement Supérieur et de la Recherche—Direction Générale pour la Recherche et l'Innovation—Secrétariat Autorisation de projet, registration number 00481.01). Animals were housed at the Lille University Animal Research Facility (Département Hospitalo-Universitaire de Recherche Expérimentale de Lille, France) accredited by the French Ministry of Agriculture for animal care and use in research (#B59–350009).

Fractionation of *Pseudomonas aeruginosa*

Pseudomonas aeruginosa strains were grown in LB for 4 h and adjusted to OD_{600} 20 in 1 ml cold 50 mM Tris–HCl pH 8.0 with 1 mM EDTA and protease inhibitors (Roche). All subsequent steps were conducted at 4°C. The cell samples were sonicated three times at 30-s intervals, with the resulting cellular debris pelleted by centrifugation three times at 4,000 *g* for 5 min, taking the uppermost supernatant for each spin. The total membrane fraction was separated from the soluble fraction by ultracentrifugation at 100,000 *g* for 1 h. After washing the membrane pellet thoroughly in sonication buffer, the inner membrane fraction was solubilized in 200 µl 50 mM Tris–HCl pH 7.6 with 2% (v/v) sodium lauroyl sarcosinate for 1 h with gentle agitation. The outer membrane fraction was pelleted by ultracentrifugation at 100,000 *g* for 1 h, washed and resuspended in sonication buffer. The preparation of supernatant samples separation by sodium dodecyl sulphate-polyacrylamide gel electrophoresis and subsequent immunoblotting has been described previously (Hachani *et al*, 2011). Immunodetection was conducted using monoclonal antibodies against RNA polymerase (NeoClone) and polyclonal antibodies against PilQ, XcpY (Michel *et al*, 1998) and LasB.

Expanded View for this article is available online.

Acknowledgements
This work was funded by the FINOVI foundation under a Young Researcher Starting Grant and the Cystic Fibrosis French Foundation Vaincre la Mucovicidose (VLM), grant RF20130500897. SS and SB are supported by INSERM and CNRS staff scientist contracts, respectively. SG and JBL are funded by the Région Rhônes-Alpes ARC1 Santé fellowships. PI and AL by the VLM and FINOVI grants. TW is supported by a Wellcome Trust PhD fellowship. We thank the following people: L. Plantevin for programming of ImageJ plugin; V. Gueguen-Chaignon and the Protein Science Facility (SFR Biosciences, France) for protein purification and plasma resonance experiments; R. Voulhoux (CNRS UMR7255, Aix-Marseille University, France) for anti-EF-Tu and LasB antibodies, PA7 strain and vectors pKNG208; G. Ball (CNRS UMR7255, Aix-Marseille University, France) for advice on genetics of PA7; S. Lory (Harvard Medical School, USA) for anti-PilQ antibody; pCMV-HA-MyD88 was a gift from B. Beutler (UT Southwestern Medical Center, USA; Addgene plasmid # 12287), FLAG-TLR5 from R. Medzhitov (Yale University, USA; Addgene plasmid # 13088), TIRAP-GFP and GFP-MyD88 from J. Kagan (Harvard Medical School, USA); HA-TIRAP from L. O'Neil (Trinity College Dublin, Ireland); Myc-TIRAP from A. Weber; L. Alexopolou (CIML, France) FLAG-TLR2 and FLAG-TLR4. We also thank the PLATIM of the SFR Biosciences for help with microscopy, T. Henry (CIRI, Lyon) for discussion and J. Kagan (Harvard Medical School, USA) for discussion and critical reading of the manuscript.

Author contributions
PRCI performed the majority of the experiments. AL carried out all purifications, pull-down and co-expression experiments. J-BL, TG, SB, SG, TEW, LW, SG, AB and SPS also performed experiments. PRCI, AL, SB, LT, AF, BG, PW, SPS conceived and designed experiments. All authors analysed data. SPS wrote the manuscript. All authors contributed to and corrected the manuscript.

Conflict of interest
The authors declare that they have no conflict of interest.

References

Agromayor M, Soler N, Caballe A, Kueck T, Freund SM, Allen MD, Bycroft M, Perisic O, Ye Y, McDonald B, Scheel H, Hofmann K, Neil SJD, Martin-Serrano J, Williams RL (2012) The UBAP1 subunit of ESCRT-I interacts with ubiquitin via a SOUBA domain. *Structure* 20: 414 – 428

Askarian F, van Sorge NM, Sangvik M, Beasley FC, Henriksen JR, Sollid JUE, van Strijp JAG, Nizet V, Johannessen M (2014) A *Staphylococcus aureus* TIR domain protein virulence factor blocks TLR2-mediated NF-κB signaling. *J Innate Immun* 6: 485 – 498

Bonham KS, Orzalli MH, Hayashi K, Wolf AI, Glanemann C, Weninger W, Iwasaki A, Knipe DM, Kagan JC (2014) A promiscuous lipid-binding protein diversifies the subcellular sites of toll-like receptor signal transduction. *Cell* 156: 705 – 716

Brubaker SW, Bonham KS, Zanoni I, Kagan JC (2015) Innate immune pattern recognition: a cell biological perspective. *Annu Rev Immunol* 33: 257 – 290

Cadoret F, Ball G, Douzi B, Voulhoux R (2014) Txc, a new type II secretion system of *Pseudomonas aeruginosa* strain PA7, is regulated by the TtsS/TtsR two-component system and directs specific secretion of the CbpE chitin-binding protein. *J Bacteriol* 196: 2376 – 2386

Chaudhary A, Ganguly K, Cabantous S, Waldo GS, Micheva-Viteva SN, Nag K, Hlavacek WS, Tung C-S (2011) The *Brucella* TIR-like protein TcpB interacts with the death domain of MyD88. *Biochem Biophys Res Commun* 417: 299 – 304

Chiang C-Y, Engel A, Opaluch AM, Ramos I, Maestre AM, Secundino I, De Jesus PD, Nguyen QT, Welch G, Bonamy GMC, Miraglia LJ, Orth AP, Nizet V, Fernandez-Sesma A, Zhou Y, Barton GM, Chanda SK (2012) Cofactors required for TLR7- and TLR9-dependent innate immune responses. *Cell Host Microbe* 11: 306 – 318

Choi YJ, Jung J, Chung HK, Im E, Rhee SH (2013) PTEN regulates TLR5-induced intestinal inflammation by controlling Mal/TIRAP recruitment. *FASEB J* 27: 243 – 254

Cirl C, Yadav M, Fischer H, Wagner H, Svanborg C, Miethke T (2008) Subversion of Toll-like receptor signaling by a unique family of bacterial Toll/interleukin-1 receptor domain-containing proteins. *Nat Med* 14: 399 – 406

Conner DA (2001) Mouse embryo fibroblast (MEF) feeder cell preparation. *Curr Protoc Mol Biol* Chapter 23: Unit 23.2–23.2.7

Elsen S, Huber P, Bouillot S, Couté Y, Fournier P, Dubois Y, Timsit JF, Maurin M, Attrée I (2014) A type III secretion negative clinical strain of *Pseudomonas aeruginosa* employs a two-partner secreted exolysin to induce hemorrhagic pneumonia. *Cell Host Microbe* 15: 164 – 176

Felix C, Kaplan-Türköz B, Ranaldi S, Koelblen T, Terradot L, O'callaghan D, Vergunst AC (2014) The Brucella TIR domain containing proteins BtpA and BtpB have a structural WxxxE motif important for protection against microtubule depolymerisation. *Cell Commun Signal* 12: 53.

Filloux A (2011) Protein secretion systems in *Pseudomonas aeruginosa*: an essay on diversity, evolution, and function. *Front Microbiol* 2: 155

Fitzgerald KA, Palsson-McDermott EM, Bowie AG, Jefferies CA, Mansell AS, Brady G, Brint E, Dunne A, Gray P, Harte MT, McMurray D, Smith DE, Sims JE, Bird TA, O'Neill LA (2001) Mal (MyD88-adapter-like) is required for toll-like receptor-4 signal transduction. *Nature* 413: 78 – 83

Freschi L, Jeukens J, Kukavica-Ibrulj I, Boyle B, Dupont M-J, Laroche J, Larose S, Maaroufi H, Fothergill JL, Moore M, Winsor GL, Aaron SD, Barbeau J, Bell SC, Burns JL, Cámara M, Cantin A, Charette SJ, Dewar K, Déziel É *et al* (2015) Clinical utilization of genomics data produced by the international *Pseudomonas aeruginos*a consortium. *Front Microbiol* 6: 1036

Gahloth D, Levy C, Heaven G, Stefani F, Wunderley L, Mould P, Cliff MJ, Bella J, Fielding AJ, Woodman P, Tabernero L (2016) Structural basis for selective interaction between the ESCRT regulator HD-PTP and UBAP1. *Structure* 24: 2115 – 2126

Garvis S, Munder A, Ball G, De Bentzmann S, Wiehlmann L, Ewbank JJ, Tümmler B, Filloux A (2009) *Caenorhabditis elegans* semi-automated liquid screen reveals a specialized role for the chemotaxis Gene cheB2 in *Pseudomonas aeruginosa* virulence. *PLoS Pathog* 5: e1000540

Hachani A, Lossi NS, Hamilton A, Jones C, Bleves S, Albesa-Jové D, Filloux A (2011) Type VI secretion system in *Pseudomonas aeruginosa*: secretion and multimerization of VgrG proteins. *J Biol Chem* 286: 12317 – 12327

Hauser AR, Jain M, Bar-Meir M, McColley SA (2011) Clinical significance of microbial infection and adaptation in cystic fibrosis. *Clin Microbiol Rev* 24: 29 – 70

Hoang TT, Karkhoff-Schweizer RR, Kutchma AJ, Schweizer HP (1998) A broad-host-range Flp-FRT recombination system for site-specific excision of chromosomally-located DNA sequences: application for isolation of unmarked *Pseudomonas aeruginosa* mutants. *Gene* 212: 77 – 86

Horng T, Barton GM, Medzhitov R (2001) TIRAP: an adapter molecule in the Toll signaling pathway. *Nat Immunol* 2: 835 – 841

Huang HR, Chen ZJ, Kunes S, Chang GD, Maniatis T (2010) Endocytic pathway is required for *Drosophila* Toll innate immune signaling. *Proc Natl Acad Sci USA* 107: 8322 – 8327

Husebye H, Halaas Ø, Stenmark H, Tunheim G, Sandanger Ø, Bogen B, Brech A, Latz E, Espevik T (2006) Endocytic pathways regulate Toll-like receptor 4 signaling and link innate and adaptive immunity. *EMBO J* 25: 683 – 692

Jain M, Ramirez D, Seshadri R, Cullina JF, Powers CA, Schulert GS, Bar-Meir M, Sullivan CL, McColley SA, Hauser AR (2004) Type III secretion phenotypes of *Pseudomonas aeruginosa* strains change during infection of individuals with cystic fibrosis. *J Clin Microbiol* 42: 5229 – 5237

Jeong J-Y, Yim H-S, Ryu J-Y, Lee HS, Lee J-H, Seen D-S, Kang SG (2012) One-step sequence- and ligation-independent cloning as a rapid and versatile cloning method for functional genomics studies. *Appl Environ Microbiol* 78: 5440 – 5443

Kagan JC, Medzhitov R (2006) Phosphoinositide-mediated adaptor recruitment controls Toll-like receptor signaling. *Cell* 125: 943 – 955

Kagan JC, Su T, Horng T, Chow A, Akira S, Medzhitov R (2008) TRAM couples endocytosis of Toll-like receptor 4 to the induction of interferon-beta. *Nat Immunol* 9: 361 – 368

Kearse M, Moir R, Wilson A, Stones-Havas S, Cheung M, Sturrock S, Buxton S, Cooper A, Markowitz S, Duran C, Thierer T, Ashton B, Meintjes P, Drummond A (2012) Geneious Basic: an integrated and extendable desktop software platform for the organization and analysis of sequence data. *Bioinformatics* 28: 1647 – 1649

Kharitidi D, Apaja PM, Manteghi S, Suzuki K, Malitskaya E, Roldan A, Gingras M-C, Takagi J, Lukacs GL, Pause A (2015) Interplay of endosomal pH and ligand occupancy in integrin a5b1 ubiquitination, endocytic sorting, and cell migration. *Cell Rep* 13: 599 – 609

Mamińska A, Bartosik A, Banach-Orłowska M, Pilecka I, Jastrzębski K, Zdżalik-Bielecka D, Castanon I, Poulain M, Neyen C, Wolińska-Nizioł L, Toruń A, Szymańska E, Kowalczyk A, Piwocka K, Simonsen A, Stenmark H, Fürthauer M, Gonzalez-Gaitan M, Miaczynska M (2016) ESCRT proteins restrict constitutive NF-κB signaling by trafficking cytokine receptors. *Sci Signal* 9: ra8

Marek LR, Kagan JC (2012) Phosphoinositide binding by the Toll adaptor dMyD88 controls antibacterial responses in *Drosophila*. *Immunity* 36: 612 – 622

Marvig RL, Sommer LM, Molin S, Johansen HK (2014) Convergent evolution and adaptation of *Pseudomonas aeruginosa* within patients with cystic fibrosis. *Nat Genet* 47: 57 – 64

Michel G, Bleves S, Ball G, Lazdunski A, Filloux A (1998) Mutual stabilization of the XcpZ and XcpY components of the secretory apparatus in *Pseudomonas aeruginosa*. *Microbiology* 144: 3379 – 3386

Myeni S, Child R, Ng TW, Kupko JJ, Wehrly TD, Porcella SF, Knodler LA, Celli J (2013) *Brucella* modulates secretory trafficking via multiple type IV secretion effector proteins. *PLoS Pathog* 9: e1003556

Nagpal K, Plantinga TS, Sirois CM, Monks BG, Latz E, Netea MG, Golenbock DT (2011) Natural loss-of-function mutation of myeloid differentiation protein 88 disrupts its ability to form myddosomes. *J Biol Chem* 286: 11875 – 11882

Newman JR, Fuqua C (1999) Broad-host-range expression vectors that carry the L-arabinose-inducible *Escherichia coli* araBAD promoter and the araC regulator. *Gene* 227: 197 – 203

Newman RM, Salunkhe P, Godzik A, Reed JC (2006) Identification and characterization of a novel bacterial virulence factor that shares homology with mammalian Toll/interleukin-1 receptor family proteins. *Infect Immun* 74: 594 – 601

Noursadeghi M, Tsang J, Haustein T, Miller RF, Chain BM, Katz DR (2008) Quantitative imaging assay for NF-kappaB nuclear translocation in primary human macrophages. *J Immunol Methods* 329: 194 – 200

Pirnay J-P, Bilocq F, Pot B, Cornelis P, Zizi M, Van Eldere J, Deschaght P, Vaneechoutte M, Jennes S, Pitt T, De Vos D (2009) *Pseudomonas aeruginosa* population structure revisited. *PLoS One* 4: e7740

Radhakrishnan GK, Yu Q, Harms JS, Splitter GA (2009) Brucella TIR domain-containing protein mimics properties of the toll-like receptor adaptor protein TIRAP. *J Biol Chem* 284: 9892 – 9898

Radhakrishnan GK, Splitter GA (2010) Biochemical and functional analysis of TIR domain containing protein from *Brucella melitensis*. *Biochem Biophys Res Commun* 397: 59 – 63

Radhakrishnan GK, Harms JS, Splitter GA (2011) Modulation of microtubule dynamics by a TIR domain protein from the intracellular pathogen *Brucella melitensis*. *Biochem J* 439: 79 – 83

Reboud E, Elsen S, Bouillot S, Golovkine G, Basso P, Jeannot K, Attrée I, Huber P (2016) Phenotype and toxicity of the recently discovered exlA-positive *Pseudomonas aeruginosa* strains collected worldwide. *Environ Microbiol* 18: 3425 – 3439

Rosadini CV, Kagan JC (2015) Microbial strategies for antagonizing Toll-like-receptor signal transduction. *Curr Opin Immunol* 32: 61 – 70

Roy PH, Tetu SG, Larouche A, Elbourne L, Tremblay S, Ren Q, Dodson R, Harkins D, Shay R, Watkins K, Mahamoud Y, Paulsen IT (2010) Complete genome sequence of the multiresistant taxonomic outlier *Pseudomonas aeruginosa* PA7. *PLoS One* 5: e8842

Salcedo SP, Marchesini MI, Lelouard H, Fugier E, Jolly G, Balor S, Muller A, Lapaque N, Demaria O, Alexopoulou L, Comerci DJ, Ugalde RA, Pierre P, Gorvel J-P (2008) *Brucella* control of dendritic cell maturation is dependent on the TIR-containing protein Btp1. *PLoS Pathog* 4: e21

Salcedo SP, Marchesini MI, Degos C, Terwagne M, Von Bargen K, Lepidi H, Herrmann CK, Santos Lacerda TL, Imbert PRC, Pierre P, Alexopoulou L, Letesson J-J, Comerci DJ, Gorvel J-P (2013) BtpB, a novel *Brucella* TIR-containing effector protein with immune modulatory functions. *Front Cell Infect Microbiol* 3: 28

Sengupta D, Koblansky A, Gaines J, Brown T, West AP, Zhang D, Nishikawa T, Park S-G, Roop RM, Ghosh S (2010) Subversion of innate immune responses by *Brucella* through the targeted degradation of the TLR signaling adapter, MAL. *J Immunol* 184: 956 – 964

Smith JA, Khan M, Magnani DD, Harms JS, Durward M, Radhakrishnan GK, Liu Y-P, Splitter GA (2013) Brucella induces an unfolded protein response via TcpB that supports intracellular replication in macrophages. *PLoS Pathog* 9: e1003785

Spear AM, Rana RR, Jenner DC, Flick-Smith HC, Oyston PCF, Simpson P, Matthews SJ, Byrne B, Atkins HS (2012) A Toll/interleukin (IL)-1 receptor domain protein from *Yersinia pestis* interacts with mammalian IL-1/Toll-like receptor pathways but does not play a central role in the virulence of *Y. pestis* in a mouse model of bubonic plague. *Microbiology* 158: 1593 – 1606

Stefani F, Zhang L, Taylor S, Donovan J, Rollinson S, Doyotte A, Brownhill K, Bennion J, Pickering-Brown S, Woodman P (2011) UBAP1 is a component of an endosome-specific ESCRT-I complex that is essential for MVB sorting. *Curr Biol* 21: 1245 – 1250

Waldhuber A, Snyder G, Römmler F, Cirl C, Müller T, Xiao T, Svanborg C, Miethke T (2016) A comparative analysis of the mechanism of toll-like receptor-disruption by TIR-containing protein C from uropathogenic *Escherichia coli*. *Pathogens* 5: 25

Wunderley L, Brownhill K, Stefani F, Tabernero L, Woodman P (2014) The molecular basis for selective assembly of the UBAP1-containing endosome-specific ESCRT-I complex. *J Cell Sci* 127: 663 – 672

Yadav M, Zhang J, Fischer H, Huang W, Lutay N, Cirl C, Lum J, Miethke T, Svanborg C (2010) Inhibition of TIR domain signaling by TcpC: MyD88-dependent and independent effects on *Escherichia coli* virulence. *PLoS Pathog* 6: e1001120

Yamamoto M, Sato S, Mori K, Hoshino K, Takeuchi O, Takeda K, Akira S (2002) Cutting edge: a novel Toll/IL-1 receptor domain-containing adapter that preferentially activates the IFN-beta promoter in the Toll-like receptor signaling. *J Immunol* 169: 6668 – 6672

Zhang Q, Zmasek CM, Cai X, Godzik A (2011) TIR domain-containing adaptor SARM is a late addition to the ongoing microbe-host dialog. *Dev Comp Immunol* 35: 461 – 468

Zou J, Baghdayan AS, Payne SJ, Shankar N (2014) A TIR domain protein from *E. faecalis* attenuates MyD88-Mediated signaling and NF-κB activation. *PLoS One* 9: e112010

References

1. Griffiths GWPQOM-C, Hoppeler H. Density of Newly Synthesized Plasma Membrane Proteins inIntracellularMembranes.I.StereologicalStudies. The Journal of Cell Biology. 1984;98: 1–9.

2. Borgese N, Francolini M, Snapp E. Endoplasmic reticulum architecture: structures in flux. Current Opinion in Cell Biology. 2006;18: 358–364. doi:10.1016/j.ceb.2006.06.008

3. Hayashi T, Rizzuto R, Hajnoczky G, Su T-P. MAM: more than just a housekeeper. Trends in Cell Biology. 2009;19: 81–88. doi:10.1016/j.tcb.2008.12.002

4. Pobre KFR, Poet GJ, Hendershot LM. The endoplasmic reticulum (ER) chaperone BiP is a master regulator of ER functions: Getting by with a little help from ERdj friends. J Biol Chem. American Society for Biochemistry and Molecular Biology; 2019;294: 2098–2108. doi:10.1074/jbc.REV118.002804

5. Feige MJ, Hendershot LM. Disulfide bonds in ER protein folding and homeostasis. Current Opinion in Cell Biology. Elsevier Ltd; 2011;23: 167–175. doi:10.1016/j.ceb.2010.10.012

6. Braakman I, Bulleid NJ. Protein Folding and Modification in the Mammalian Endoplasmic Reticulum. Annu Rev Biochem. 2011;80: 71–99. doi:10.1146/annurev-biochem-062209-093836

7. Bonifacino JS, Glick BS. The Mechanisms of Vesicle Budding and Fusion. 2004;116: 1–14.

8. Budnik A, Stephens DJ. ER exit sites – Localization and control of COPII vesicle formation. FEBS Letters. Federation of European Biochemical Societies; 2009;583: 3796–3803. doi:10.1016/j.febslet.2009.10.038

9. Gomez-Navarro N, Miller E. Protein sorting at the ER–Golgi interface. The Journal of Cell Biology. 2016;215: 769–778. doi:10.1083/jcb.201610031

10. Reynaud EG, Simpson JC. Navigating the secretory pathway. EMBO reports. 2013;3: 1–6.

11. Plate L, Wiseman RL. Regulating Secretory Proteostasis through the Unfolded Protein Response: From Function to Therapy. Trends in Cell Biology. 2017;27: 722–737. doi:10.1016/j.tcb.2017.05.006

12. Walter P, Ron D. The Unfolded Protein Response: From Stress Pathway to Homeostatic Regulation. 2011;: 1–7.

13. Hetz C, Papa FR. The Unfolded Protein Response and Cell Fate Control. Molecular Cell. Elsevier Inc; 2018;69: 169–181. doi:10.1016/j.molcel.2017.06.017

14. Heath-Engel HM, Chang NC, Shore GC. The endoplasmic reticulum in apoptosis and autophagy: role of the BCL-2 protein family. Oncogene. Nature Publishing Group; 2008;27: 6419–6433. doi:10.1038/onc.2008.309

15. Park HG, Han SI, Oh SY, Kang HS. Cellular responses to mild heat stress. CMLS, Cell Mol Life Sci. Birkhäuser-Verlag; 2005;62: 10–23. doi:10.1007/s00018-004-4208-7

16. Ritossa F. Discovery of the heat shock response. Cell Stress and Chaperones. 1996;1: 1–2.

17. Sylvie Blond-Elguindi SECWJDRJLSRSJFS, Gething M-JH. Affinity Panning of a Library of Peptides Displayed on Bacteriophages Reveals the Binding Specificity of BiP. Cell. 1993;75: 1–12.

18. Mayer MP, Kityk R. Insights into the molecular mechanism of allostery in Hsp70s. Front Mol Biosci. Frontiers; 2015;2: 4535–7. doi:10.3389/fmolb.2015.00058

19. Kampinga HH, Craig EA. The HSP70 chaperone machinery: J proteins as drivers of functional specificity. Nature Publishing Group; 2010;: 1–14. doi:10.1038/nrm2941

20. Cheetham ME, Caplan AJ. Structure, function and evolution of DnaJ: conservation and adptation of chaperone function. Cell Stress and Chaperones. 2001;: 1–9.

21. Misselwitz B, Staeck O, Rapoport TA. J Proteins Catalytically Activate Hsp70 Molecules to Trap a Wide Range of Peptide Sequences. Molecular Cell. 1998;: 1–11.

22. Kityk R, Kopp J, Mayer MP. Molecular Mechanism of J-Domain-Triggered ATP Hydrolysis by Hsp70 Chaperones. Molecular Cell. Elsevier Inc; 2018;69: 227–237.e4. doi:10.1016/j.molcel.2017.12.003

23. Jin Y, Awad W, Petrova K, Hendershot LM. Regulated release of ERdj3 from unfolded proteins by BiP. EMBO J. 2008;27: 2873–2882. doi:10.1038/emboj.2008.207

24. Behnke J, Feige MJ, Hendershot LM. BiP and Its Nucleotide Exchange Factors Grp170 and Sil1: Mechanisms of Action and Biological Functions. Journal of Molecular Biology. Elsevier Ltd; 2015;427: 1589–1608. doi:10.1016/j.jmb.2015.02.011

25. Sevier CS, Kaiser CA. Formation and transfer of disulphide bonds in living cells. Nat Rev Mol Cell Biol. 2002;3: 836–847. doi:10.1038/nrm954

26. Behnke J, Mann MJ, Scruggs F-L, Feige MJ, Hendershot LM. Members of the Hsp70 Family Recognize Distinct Types of Sequences to Execute ER Quality Control. Molecular Cell. Elsevier Inc; 2016;63: 739–752. doi:10.1016/j.molcel.2016.07.012

27. Oka OBV, Pringle MA, Schopp IM, Braakman I, Bulleid NJ. ERdj5 Is the ER Reductase that Catalyzes the Removal of Non-Native Disulfides and Correct Folding of the LDL Receptor. Molecular Cell. Elsevier; 2013;50: 793–804. doi:10.1016/j.molcel.2013.05.014

28. Mehrtash AB, Hochstrasser M. Ubiquitin-dependent protein degradation at the endoplasmic reticulum and nuclear envelope. Seminars in Cell and Developmental Biology. Elsevier; 2018;: 1–14. doi:10.1016/j.semcdb.2018.09.013

29. Smith DM, Benaroudj N, Goldberg A. Proteasomes and their associated ATPases: A destructive combination. Journal of Structural Biology. 2006;156: 72–83. doi:10.1016/j.jsb.2006.04.012

30. Taxis C, Hitt R, Park S-H, Deak PM, Kostova Z, Wolf DH. Use of modular substrates demonstrates mechanistic diversity and reveals differences in chaperone requirement of ERAD. J Biol Chem. American Society for Biochemistry and Molecular Biology; 2003;278: 35903–35913. doi:10.1074/jbc.M301080200

31. Ruggiano A, Carvalho P, Foresti O, Annamaria Ruggizno OF. ER-associated degradation: Protein quality control and beyond. The Journal of Cell Biology. 2014;: 1–11. doi:10.1083/jcb.201312042

32. Crowder JJ, Geigges M, Gibson RT, Fults ES, Buchanan BW, Sachs N, et al. Rkr1/Ltn1 Ubiquitin Ligase-mediated Degradation of Translationally Stalled Endoplasmic Reticulum Proteins. J Biol Chem. 2015;290: 1–14.

33. Bengtson MH, Joazeiro CAP. Role of a ribosome-associated E3 ubiquitin ligase in protein quality control. Nature. Nature Publishing Group; 2010;467: 470–473. doi:10.1038/nature09371

34. Malsburg von der K, Shao S, S R, Hedge. The ribosome quality control pathway can access nascent polypeptides stalled at the Sec61 translocon. Molecular Biology of the Cell. 2015;: 1–13. doi:10.1091/mbc.E15-01-0040)

35. Rubenstein EM, Kreft SG, Greenblatt W, Swanson R, Hochstrasser M. Aberrant substrate engagement of the ER translocon triggers degradation by the Hrd1 ubiquitin ligase. The Journal of Cell Biology. 2012;197: 761–773. doi:10.1083/jcb.201203061

36. Carvalho P, Goder V, Rapoport TA. Distinct Ubiquitin-Ligase Complexes Define Convergent Pathways for the Degradation of ER Proteins. Cell. 2006;126: 361–373. doi:10.1016/j.cell.2006.05.043

37. Plemper RK, Bordallo J, Deak PM, Taxis C, Hitt R, Wolf DH. Genetic interactions of Hrd3p and Der3p/Hrd1p with Sec61p suggest a retro-

translocation complex mediating protein transport for ER degradation. J Cell Sci. 1999;: 1–12.

38. Bhamidipati A, Denic V, Quan EM, Weissman JS. Exploration of the Topological Requirements of ERAD Identifies Yos9p as a Lectin Sensor of Misfolded Glycoproteins in the ER Lumen. Molecular Cell. 2005;19: 741–751. doi:10.1016/j.molcel.2005.07.027

39. Sato BK, Schulz D, Do PH, Hampton RY. Misfolded Membrane Proteins Are Specifically Recognized by the Transmembrane Domain of the Hrd1p Ubiquitin Ligase. Molecular Cell. Elsevier Ltd; 2009;34: 212–222. doi:10.1016/j.molcel.2009.03.010

40. Gauss R, Jarosch E, Sommer T, Hirsch C. A complex of Yos9p and the HRD ligase integrates endoplasmic reticulum quality control into the degradation machinery. Nat Cell Biol. 2006;8: 849–854. doi:10.1038/ncb1445

41. Mohorko E, Glockshuber R, Aebi M. Oligosaccharyltransferase: the central enzyme of N-linked protein glycosylation. J Inherit Metab Dis. John Wiley & Sons, Ltd; 2011;34: 869–878. doi:10.1007/s10545-011-9337-1

42. Aebi M, Bernasconi R, Clerc S, Molinari M. N-glycan structures: recognition and processing in the ER. Trends in Biochemical Sciences. Elsevier Ltd; 2010;35: 74–82. doi:10.1016/j.tibs.2009.10.001

43. Liu Y-C, Fujimori DG, Weissman JS. Htm1p–Pdi1p is a folding-sensitive mannosidase that marks N-glycoproteins for ER-associated protein degradation. Proc Natl Acad Sci USA. 2016;113: E4015–E4024. doi:10.1073/pnas.1608795113

44. Xie W, Ng DTW. ERAD substrate recognition in budding yeast. Seminars in Cell and Developmental Biology. Elsevier Ltd; 2010;21: 533–539. doi:10.1016/j.semcdb.2010.02.007

45. Pfeiffer A, Stephanowitz H, Krause E, Volkwein C, Hirsch C, Jarosch E, et al. A Complex of Htm1 and the Oxidoreductase Pdi1 Accelerates Degradation of Misfolded Glycoproteins. J Biol Chem. 2016;291: 12195–12207. doi:10.1074/jbc.M115.703256

46. Denic V, Quan EM, Weissman JS. A Luminal Surveillance Complex that Selects Misfolded Glycoproteins for ER-Associated Degradation. Cell. 2006;126: 349–359. doi:10.1016/j.cell.2006.05.045

47. Yamaguchi D, Hu D, Matsumoto N, Yamamoto K. Human XTP3-B binds to 1-antitrypsin variant nullHong Kong via the C-terminal MRH domain in a glycan-dependent manner. Glycobiology. 2010;20: 348–355. doi:10.1093/glycob/cwp182

48. Vabulas RM, Hartl U. Protein Synthesis upon Acute Nutrient Restriction Relies on Proteasome Function. Science. American Association for the Advancement of Science; 2005;310: 1957–1960. doi:10.1126/science.1117637

49. Swanson R, Locher M, Hochstrasser M. A conserved ubiquitin ligase of the nuclear envelope/endoplasmic reticulum that functions in both ER-associated and Mat. Genes Development. 2001;: 1–16.

50. Habeck G, Ebner FA, Shimada-Kreft H, Kreft SG. The yeast ERAD-C ubiquitin ligase Doa10 recognizes an intramembrane degron. The Journal of Cell Biology. 2015;209: 261–273. doi:10.1083/jcb.201408088

51. Ruggiano A, Mora G, Buxó L, Carvalho P. Spatial control of lipid droplet proteins by the ERAD ubiquitin ligase Doa10. EMBO J. 2016;35: 1644–1655. doi:10.15252/embj.201593106

52. Kreft SG, Hochstrasser M. An Unusual Transmembrane Helix in the Endoplasmic Reticulum Ubiquitin Ligase Doa10 Modulates Degradation of Its Cognate E2 Enzyme. J Biol Chem. 2011;: 1–13.

53. Walter J, Volkwein C, Sommer T. Sec61p-independent degradation of the tail-anchored ER membrane protein Ubc6p. EMBO J. 2013;: 1–8.

54. Schoebel S, Mi W, Stein A, Ovchinnikov S, Pavlovicz R, DiMaio F, et al. Cryo-EM structure of the protein-conducting ERAD channel Hrd1 in complex with Hrd3. Nature. Nature Publishing Group; 2017;548: 352–355. doi:10.1038/nature23314

55. Zattas D, Berk JM, Kreft SG, Hochstrasser M. A Conserved C-terminal Element in the Yeast Doa10 and Human MARCH6 Ubiquitin Ligases Required for Selective Substrate Degradation. J Biol Chem. 2016;291: 12105–12118. doi:10.1074/jbc.M116.726877

56. Huyer G, Piluek WF, Fansler Z, Kreft SG, Hochstrasser M, Brodsky JL, et al. Distinct Machinery Is Required in Saccharomyces cerevisiaefor the Endoplasmic Reticulum-associated Degradation of a Multispanning Membrane Protein and a Soluble Luminal Protein. J Biol Chem. 2004;279: 38369–38378. doi:10.1074/jbc.M402468200

57. Shiber A, Breuer W, Brandeis M, Ravid T. Ubiquitin conjugation triggers misfolded protein sequestration into quality control foci when Hsp70 chaperone levels are limiting. Molecular Biology of the Cell. 2013;: 1–12. doi:10.1091/mbc.E13-01-0010)

58. Rapoport TA. Protein transport across the endoplasmic reticulum membrane. FEBS Journal. John Wiley & Sons, Ltd (10.1111); 2008;275: 4471–4478. doi:10.1111/j.1742-4658.2008.06588.x

59. Tsai B, Ye Y, Rapoport TA. Retro-translocation of proteins from the endoplasmic reticulum into the cytosol. Nat Rev Mol Cell Biol. 2002;3: 246–255. doi:10.1038/nrm780

60. Dupont S, Mamidi A, Cordenonsi M, Montagner M, Zacchigna L, Adorno M, et al. FAM/USP9x, a Deubiquitinating Enzyme Essential for TGFβ Signaling, Controls Smad4 Monoubiquitination. Cell. Elsevier Inc; 2009;136: 123–135. doi:10.1016/j.cell.2008.10.051

61. Yau R, Rape M. The increasing complexity of the ubiquitin code. Nature Publishing Group. Nature Publishing Group; 2016;18: 579–586. doi:10.1038/ncb3358

62. Suresh B, Lee J, Kim K-S, Ramakrishna S. Review Article The Importance of Ubiquitination and Deubiquitination in Cellular Reprogramming. Stem Cells International. Hindawi Publishing Corporation; 2016;: 1–14. doi:10.1155/2016/6705927

63. Deshaies RJ, Joazeiro CAP. RING Domain E3 Ubiquitin Ligases. Annu Rev Biochem. 2009;78: 399–434. doi:10.1146/annurev.biochem.78.101807.093809

64. Kostova Z, Mariano J, Scholz S, Koenig C, Weissman AM. A Ubc7p-binding domain in Cue1p activates ER-associated protein degradation. J Cell Sci. 2009;122: 1374–1381. doi:10.1242/jcs.044255

65. Xu P, Duong DM, Seyfried NT, Cheng D, Xie Y, Robert J, et al. Quantitative Proteomics Reveals the Function of Unconventional Ubiquitin Chains in Proteasomal Degradation. Cell. 2009;137: 133–145. doi:10.1016/j.cell.2009.01.041

66. Bagola K, Delbrück von M, Dittmar G, Scheffner M, Ziv I, Glickman MH, et al. Ubiquitin Binding by a CUE Domain Regulates Ubiquitin Chain Formation by ERAD E3 Ligases. Molecular Cell. Elsevier Inc; 2013;50: 528–539. doi:10.1016/j.molcel.2013.04.005

67. Foresti O, Rodriguez-Vaello V, Funaya C, Carvalho P. Quality control of inner nuclear membrane proteins by the Asi complex. Science. 2014;346: 748–751. doi:10.1126/science.1257522

68. Xia D, Tang WK, Ye Y. Structure and function of the AAA+ ATPase p97/Cdc48p. Gene. 2016;583: 64–77. doi:10.1016/j.gene.2016.02.042

69. Neuber O, Jarosch E, Volkwein C, Walter J, Sommer T. Ubx2 links the Cdc48 complex to ER-associated protein degradation. Nat Cell Biol. 2005;7: 993–998. doi:10.1038/ncb1298

70. Ye Y, Meyer HH, Rapoport TA. Function of the p97–Ufd1–Npl4 complex in retrotranslocation from the ER to the cytosol. The Journal of Cell Biology. 2003;162: 71–84. doi:10.1083/jcb.200302169

71. Bodnar N, Rapoport T. Toward an understanding of the Cdc48/p97 ATPase. F1000Res. 2017;6: 1318–10. doi:10.12688/f1000research.11683.1

72. Bodnar NO, Rapoport TA. Molecular Mechanism of Substrate Processing by the Cdc48 ATPase Complex. Cell. Elsevier Inc; 2017;169: 722–730.e9. doi:10.1016/j.cell.2017.04.020

73. DeMartino GN, Slaughter CA. The Proteasome, a Novel Protease Regulated by Multiple Mechanisms. J Biol Chem. 1999;: 1–5.

74. Thibaudeau TA, Smith DM. A Practical Review of Proteasome Pharmacology. Ma Q, editor. Pharmacol Rev. American Society for Pharmacology and Experimental Therapeutics; 2019;71: 170–197. doi:10.1124/pr.117.015370

75. Finley D, Chen X, Walters KJ. Gates, Channels, and Switches: Elements of the Proteasome Machine. Trends in Biochemical Sciences. 2016;41: 77–93. doi:10.1016/j.tibs.2015.10.009

76. Beck F, Unverdorben P, Bohn S, Schweitzer A, Pfeifer G, Sakata E, et al. Near-atomic resolution structural model of the yeast 26S proteasome. PNAS. 2012;: 1–6. doi:10.1073/pnas.1213333109/-/DCSupplemental

77. de Poot SAH, Tian G, Finley D. Meddling with Fate: The Proteasomal Deubiquitinating Enzymes. Journal of Molecular Biology. 2017;429: 3525–3545. doi:10.1016/j.jmb.2017.09.015

78. Collins GA, Goldberg AL. The Logic of the 26S Proteasome. Cell. Elsevier Inc; 2017;169: 792–806. doi:10.1016/j.cell.2017.04.023

79. Bashore C, Dambacher CM, Goodall EA, Matyskiela ME, Lander GC, Martin A. Ubp6 deubiquitinase controls conformational dynamics and substrate degradation of the 26S proteasome. Nat Struct Mol Biol. Nature Publishing Group; 2015;22: 712–719. doi:10.1038/nsmb.3075

80. Peth A, Kukushkin N, Bossé M, Goldberg AL. Ubiquitinated Proteins Activate the Proteasomal ATPases by Binding to Usp14 or Uch37 Homologs. J Biol Chem. 2013;288: 7781–7790. doi:10.1074/jbc.M112.441907

81. Peth A, Uchiki T, Goldberg AL. ATP-Dependent Steps in the Binding of Ubiquitin Conjugates to the 26S Proteasome that Commit to Degradation. Molecular Cell. Elsevier Inc; 2010;40: 671–681. doi:10.1016/j.molcel.2010.11.002

82. Rabl J, Smith DM, Yu Y, Chang S-C, Goldberg AL, Cheng Y. Mechanism of Gate Opening in the 20S Proteasome by the Proteasomal ATPases. Molecular Cell. 2008;30: 360–368. doi:10.1016/j.molcel.2008.03.004

83. Khor B, Bredemeyer AL, Huang C-Y, Turnbull IR, Evans R, Maggi LB, et al. Proteasome activator PA200 is required for normal spermatogenesis. Molecular and Cellular Biology. American Society for Microbiology Journals; 2006;26: 2999–3007. doi:10.1128/MCB.26.8.2999-3007.2006

84. Qian M-X, Pang Y, Liu CH, Haratake K, Du B-Y, Ji D-Y, et al. Acetylation-Mediated Proteasomal Degradation of Core Histones during DNA Repair and Spermatogenesis. Cell. Elsevier Inc; 2013;153: 1012–1024. doi:10.1016/j.cell.2013.04.032

85. Cyr DM, Hebert DN. Protein quality control—linking the unfolded protein response to disease. EMBO reports. 2009;10: 1206–1210. doi:10.1038/embor.2009.224

86. Carrara M, Prischi F, Ali M. UPR Signal Activation by Luminal Sensor Domains. IJMS. 2013;14: 6454–6466. doi:10.3390/ijms14036454

87. Wang M, Kaufman RJ. Protein misfolding in the endoplasmic reticulum as a conduit to human disease. Nature. 2016;529: 326–335. doi:10.1038/nature17041

88. Carrara M, Prischi F, Nowak PR, Kopp MC, Ali M. Noncanonical binding of BiP ATPase domain to Ire1 and Perk is dissociated by unfolded protein C. eLIFE. 2015;: 1–16. doi:10.7554/eLife.03522.001

89. Maurel M, McGrath EP, Mnich K, Healy S, Chevet E, Samali A. Controlling the unfolded protein response-mediated life and death decisions in cancer. Seminars in Cancer Biology. Elsevier Ltd; 2015;33: 57–66. doi:10.1016/j.semcancer.2015.03.003

90. Wang M, Law ME, Castellano RK, Law BK. The unfolded protein response as a target for anticancer therapeutics. Critical Reviews in Oncology / Hematology. Elsevier; 2018;127: 66–79. doi:10.1016/j.critrevonc.2018.05.003

91. Kozutsumi Y, Segal M, Normington K, Gething M-J, Sambrook J. The presence of malfolded proteins in the endoplasmic reticulum signals the induction of glucose-regulated proteins. Nature. 1988;: 1–3.

92. Calfon M, Zeng H, Urano F, Till JH, Hubbard SR, Harding HP, et al. IRE1 coupkes endoplasmic reticulum load to secretory capacity by processing the XBP-1 mRNA. Nature. 2002;415: 1–6.

93. Yoshida H, Matsui T, Yamamoto A, Okada T, Mori K. XBP1 mRNA Is Induced by ATF6 and Spliced by IRE1 in Response to ER Stress to Produce a Highly Active Transcription Factor. Cell. 2001;: 1–11.

94. Acosta-Alvear D, Zhou Y, Blais A, Tsikitis M, Lents NH, Arias C, et al. XBP1 Controls Diverse Cell Type- and Condition-Specific Transcriptional Regulatory Networks. Molecular Cell. 2007;27: 53–66. doi:10.1016/j.molcel.2007.06.011

95. Kanda S, Yanagitani K, Yokota Y, Esaki Y, Kohno K. Autonomous translational pausing is required for XBP1umRNA recruitment to the ER via the SRP pathway. Proc Natl Acad Sci USA. 2016;113: E5886–E5895. doi:10.1073/pnas.1604435113

96. Yanagitani K, Kimata Y, Kohno K. Translational Pausing Ensures Membrane Targeting and Cytoplasmic Splicing of XBP1u mRNA. Science. 2011;: 1–5.

97. Plumb R, Zhang Z-R, Appathurai S, Mariappan M. A functional link between the co-translational protein translocation pathway and the UPR. 2015;: 1–18. doi:10.7554/eLife.07426.001

98. Kosmaczewski SG, Edwards TJ, Han SM, Eckwahl MJ, Meyer BI, Peach S, et al. The RtcB RNA ligase is an essential component of the metazoan unfolded protein response. EMBO reports. 2014;15: 1278–1285. doi:10.15252/embr.201439531

99. Coupling of Stress in the ER to Activation of JNK Protein Kinases by Transmembrane Protein Kinase IRE1. 2000;: 1–4.

100. Harding HP, Zhang Y, Bertolotti A, Zeng H, Ron D. Perk is Essential for Translational Regulation and Cell Survival during the Unfolded Protein Response. Molecular Cell. 2000;: 1–8.

101. Cabrera E, Hernández-Pérez S, Koundrioukoff S, Debatisse M, Kim D, Smolka MB, et al. PERK inhibits DNA replication during the Unfolded Protein Response via Claspin and Chk1. Nature Publishing Group. Nature Publishing Group; 2016;36: 678–686. doi:10.1038/onc.2016.239

102. Haze K, Yoshida H, Yanagi H, Yura T, Mori K. Mammalian Transcription Factor ATF6 Is Synthesized as a Transmembrane Protein and Activated by Proteolysis in Response to Endoplasmic Reticulum Stress. Molecular Biology of the Cell. 1999;: 1–13.

103. Yamamoto K, Sato T, Matsui T, Sato M, Okada T, Yoshida H, et al. Transcriptional Induction of Mammalian ER Quality Control Proteins Is Mediated by Single or Combined Action of ATF6α and XBP1. Developmental Cell. 2007;13: 365–376. doi:10.1016/j.devcel.2007.07.018

104. Thuerauf DK, Marcinko M, Belmont PJ, Glembotski CC. Effects of the Isoform-specific Characteristics of ATF6□ and ATF6□ on Endoplasmic Reticulum Stress Response Gene Expression and Cell Viability. 2007;: 1–15.

105. Shoulders MD, Ryno LM, Genereux JC, Moresco JJ, Tu PG, Wu C, et al. Stress-Independent Activation of XBP1s and/or ATF6 Reveals Three Functionally Diverse ER Proteostasis Environments. Cell Reports. 2013;3: 1279–1292. doi:10.1016/j.celrep.2013.03.024

106. Sisinni L, Pietrafesa M, Lepore S, Maddalena F, Condelli V, Esposito F, et al. Endoplasmic Reticulum Stress and Unfolded Protein Response in Breast Cancer: The Balance between Apoptosis and Autophagy and Its Role in Drug Resistance. IJMS. Multidisciplinary Digital Publishing Institute; 2019;20: 857–18. doi:10.3390/ijms20040857

107. Shore GC, Papa FR, Oakes SA. Signaling cell death from the endoplasmic reticulum stress response. Current Opinion in Cell Biology. 2011;23: 143–149. doi:10.1016/j.ceb.2010.11.003

108. Urra H, Dufey E, Lisbona F, Rojas-Rivera D, Hetz C. When ER stress reaches a dead end. Biochimica et Biophysica Acta (BBA) - Molecular Cell Research. Elsevier B.V; 2013;1833: 3507–3517. doi:10.1016/j.bbamcr.2013.07.024

109. Hollien J, Weissman JS. Decay of Endoplasmic Reticulum-Localized mRNAs During the Unfolded Protein Response. Science. 2017;313: 101–104. doi:10.1126/science.1126121

110. Maurel M, Chevet E, Tavernier J, Gerlo S. Getting RIDD of RNA: IRE1 in cell fate regulation. Trends in Biochemical Sciences. Elsevier Ltd; 2014;39: 245–254. doi:10.1016/j.tibs.2014.02.008

111. Papa AGLJ-PUPVKPRGYNAISSVNBBMHNHPGSHQTATSOF, Upton J-P, Praveen PVK, Ghosh R, Nakagawa Y, Igbaria A, et al. IRE1alpha; Induces Thioredoxin-Interacting Protein to Activate the NLRP3 Inflammasome and Promote Programmed Cell Death under Irremediable ER Stress. Cell Metabolism. Elsevier Inc; 2012;16: 250–264. doi:10.1016/j.cmet.2012.07.007

112. Nishitoh H, Matsuzawa A, Tobiume K, Saegusa K, Takeda K, Inoue K, et al. ASK1 is essential for endoplasmic reticulum stress-induced neuronal cell death triggered by expanded polyglutamine repeats. Genes Development. 2002;: 1–12.

113. Urano F, Wang X, Bertolotti A, Zhang Y, Chung P, Harding HP, et al. Coupling of Stress in the ER to Activation of JNK Protein Kinases by Transmembrane Protein Kinase IRE1. Science. 2000;: 1–4.

114. Castillo K, Rojas-Rivera D, Lisbona F, Caballero B, Nassif M, Court FA, et al. BAX inhibitor-1 regulates autophagy by controlling the IRE1α branch of the unfolded protein response. EMBO J. 2017;36: 1640–1640. doi:10.15252/embj.201797020

115. Nguyen DT, Chevet E. Nck-dependent Activation of Extracellular Signal-regulated Kinase-1 and Regulation of Cell Survival during Endoplasmic Reticulum Stress. 2004;: 1–13. doi:10.1091/mbc.E03–11

116. Morita S, Villalta SA, Feldman HC, Register AC, Rosenthal W, Hoffmann-Petersen IT, et al. Targeting ABL-IRE1α Signaling Spares ER-Stressed Pancreatic β Cells to Reverse Autoimmune Diabetes. Cell Metabolism. Elsevier; 2017;25: 883–897.e8. doi:10.1016/j.cmet.2017.03.018

117. Hetz C, Korsmeyer SJ. Proapoptotic BAX and BAK Modulate the Unfolded Protein Rrsponse by a Direct Interaction with IRE1a. Science. 2006;312: 570–572. doi:10.1126/science.1122033

118. Rodriguez DA, Zamorano S, Lisbona F, Rojas-Rivera D, Urra H, Cubillos-Ruiz JR, et al. BH3-only proteins are part of a regulatory network that control the sustained signalling of the unfolded protein response sensor IRE1&alpha. EMBO J. Nature Publishing Group; 2012;31: 2322–2335. doi:10.1038/emboj.2012.84

119. Lisbona F, Rojas-Rivera D, Thielen P, Zamorano S, Todd D, Martinon F, et al. BAX Inhibitor-1 Is a Negative Regulator of the ER Stress Sensor IRE1&alpha. Molecular Cell. Elsevier Ltd; 2009;33: 679–691. doi:10.1016/j.molcel.2009.02.017

120. Pinkaew D, Chattopadhyay A, King MD, Chunhacha P, Liu Z, Stevenson HL, et al. Fortilin binds IRE1Î± and prevents ER stress from signaling apoptotic cell death. Nature Communications. Springer US; 2017;: 1–15. doi:10.1038/s41467-017-00029-1

121. Sun S, Shi G, Sha H, Ji Y, Han X, Shu X, et al. IRE1α is an endogenous substrate of endoplasmic-reticulum-associated degradation. Nat Cell Biol. 2015;17: 1546–1555. doi:10.1038/ncb3266

122. Ma Y, Brewer JW, Alan Diehl J, Hendershot LM. Two Distinct Stress Signaling Pathways Converge Upon the CHOP Promoter During the Mammalian Unfolded Protein Response. Journal of Molecular Biology. 2002;318: 1351–1365. doi:10.1016/S0022-2836(02)00234-6

123. Ma Y, Hendershot LM. Herp Is Dually Regulated by Both the Endoplasmic Reticulum Stress-specific Branch of the Unfolded Protein Response and a Branch That Is Shared with Other Cellular Stress Pathways. J Biol Chem. 2004;279: 13792–13799. doi:10.1074/jbc.M313724200

124. Yang Y, Liu L, Naik I, Braunstein Z, Zhong J, Ren B. Transcription Factor C/EBP Homologous Protein in Health and Diseases. Front Immunol. 2017;8: 381–18. doi:10.3389/fimmu.2017.01612

125. Kseniya Petrova SOLMH, Ron D. Regulated association of misfolded endoplasmic reticulum lumenal proteins with P58/DNAJc3. EMBO J. 2008;: 1–11.

126. Kim C, Kim B. Anti-Cancer Natural Products and Their Bioactive Compounds Inducing ER Stress-Mediated Apoptosis: A Review. Nutrients. 2018;10: 1021–29. doi:10.3390/nu10081021

127. Yamaguchi H, Wang H-G. CHOP Is Involved in Endoplasmic Reticulum Stress-induced Apoptosis by Enhancing DR5 Expression in Human Carcinoma Cells. J Biol Chem. 2004;279: 45495–45502. doi:10.1074/jbc.M406933200

128. Puthalakath H, O'Reilly LA, Gunn P, Lee L, Kelly PN, Huntington ND, et al. ER Stress Triggers Apoptosis by Activating BH3-Only Protein Bim. Cell. 2007;129: 1337–1349. doi:10.1016/j.cell.2007.04.027

129. Eletto D, Eletto D, Dersh D, Gidalevitz T, Argon Y. Protein Disulfide Isomerase A6 Controls the Decay of IRE1α Signaling via Disulfide-Dependent Association. Molecular Cell. 2014;53: 562–576. doi:10.1016/j.molcel.2014.01.004

130. Higa A, Taouji S, Lhomond S, Jensen D, Fernandez-Zapico ME, Simpson JC, et al. Endoplasmic Reticulum Stress-Activated Transcription Factor ATF6 Requires the Disulfide Isomerase PDIA5 To Modulate Chemoresistance. Molecular and Cellular Biology. 2014;34: 1839–1849. doi:10.1128/MCB.01484-13

131. Hetz C. The unfolded protein response: controlling cell fate decisions under ER stress and beyond. Nat Rev Mol Cell Biol. 2012;13: 89–102. doi:10.1038/nrm3270

132. Lin W, Popko B. Endoplasmic reticulum stress in disorders of myelinating cells. Nat Neurosci. 2009;12: 379–385. doi:10.1038/nn.2273

133. Ghosh R, Wang L, Wang ES, Perera BGK, Igbaria A, Morita S, et al. Allosteric Inhibition of the IRE1α RNase Preserves Cell Viability and Function during Endoplasmic Reticulum Stress. Cell. Elsevier Inc; 2014;158: 534–548. doi:10.1016/j.cell.2014.07.002

134. Yan W, Frank CL, Korth MJ, Sopher BL, Novoa I, Ron D, et al. Control of PERK eIF2□ kinase activity by the endoplasmic reticulum stress-induced molecular chaperone P58. PNAS. 2002;: 1–6.

135. Lencer WI, DeLuca H, Grey MJ, Cho JA. Innate immunity at mucosal surfaces: the IRE1-RIDD-RIG-I pathway. Trends in Immunology. Elsevier Ltd; 2015;36: 401–409. doi:10.1016/j.it.2015.05.006

136. Kawai T, Akira S. The role of pattern-recognition receptors in innate immunity: update on Toll-like receptors. Nature Publishing Group. Nature Publishing Group; 2010;11: 373–384. doi:10.1038/ni.1863

137. Martinon F, Chen X, Lee A-H, Glimcher LH. TLR activation of the transcription factor XBP1 regulates innate immune responses in macrophages. Nature Publishing Group. Nature Publishing Group; 2010;11: 411–418. doi:10.1038/ni.1857

138. Keestra-Gounder AM, Byndloss MX, Seyffert N, Young BM, Chávez-Arroyo A, Tsai AY, et al. NOD1 and NOD2 signalling links ER stress with inflammation. Nature. Nature Publishing Group; 2016;532: 394–397. doi:10.1038/nature17631

139. Zhang K, Kaufman RJ. From endoplasmic-reticulum stress to the inflammatory response. Nature. 2008;454: 455–462. doi:10.1038/nature07203

140. Kitamura M. Control of NF-κB and Inflammation by the Unfolded Protein Response. International Reviews of Immunology. 2011;30: 4–15. doi:10.3109/08830185.2010.522281

141. Parzych KR, Klionsky DJ. An Overview of Autophagy: Morphology, Mechanism, and Regulation. Antioxidants & Redox Signaling. 2014;20: 460–473. doi:10.1089/ars.2013.5371

142. Lamb CA, Yoshimori T, Tooze SA. The autophagosome: origins unknown, biogenesis complex. Nature Publishing Group. Nature Publishing Group; 2013;14: 759–774. doi:10.1038/nrm3696

143. Rogov VV, Stolz A, Ravichandran AC, Rios Szwed DO, Suzuki H, Kniss A, et al. Structural and functional analysis of the GABARAP interaction motif (GIM). EMBO reports. 2017;18: 1382–1396. doi:10.15252/embr.201643587

144. Sahu R, Kaushik S, Clement CC, Cannizzo ES, Scharf B, Follenzi A, et al. Microautophagy of Cytosolic Proteins by Late Endosomes. DEVCEL. Elsevier; 2011;20: 131–139. doi:10.1016/j.devcel.2010.12.003

145. Orenstein SJ, Cuervo AM. Chaperone-mediated autophagy: Molecular mechanisms and physiological relevance. Seminars in Cell and Developmental Biology. 2010;21: 719–726. doi:10.1016/j.semcdb.2010.02.005

146. Birgisdottir AB, Lamark T, Johansen T. Alternative fates of newly formed PrPSc upon prion conversion on the plasma membrane. J Cell Sci. 2013;: 1–11. doi:10.1242/jcs.126128

147. Gatica D, Lahiri V, Klionsky DJ. Cargo recognition and degradation by selective autophagy. Nat Cell Biol. Springer US; 2018;: 1–10. doi:10.1038/s41556-018-0037-z

148. Khaminets A, Heinrich T, Mari M, Grumati P, Huebner AK, Akutsu M, et al. Regulation of endoplasmic reticulum turnover by selective autophagy. Nature. 2015;522: 354–358. doi:10.1038/nature14498

149. Mizushima N, Komatsu M. Autophagy: Renovation of Cells and Tissues. Cell. Elsevier Inc; 2011;147: 728–741. doi:10.1016/j.cell.2011.10.026

150. Bernales S, McDonald KL, Walter P. Autophagy Counterbalances Endoplasmic Reticulum Expansion during the Unfolded Protein Response. Ploegh H, editor. PLoS Biol. 2006;4: e423–14. doi:10.1371/journal.pbio.0040423

151. Schuck S, Gallagher CM, Walter P. ER-phagy mediates selective degradation of endoplasmic reticulum independently of the core autophagy machinery. J Cell Sci. 2014;127: 4078–4088. doi:10.1242/jcs.154716

152. Cebollero E, Reggiori F, Kraft C. Reticulophagy and Ribophagy: Regulated Degradation of Protein Production Factories. International Journal of Cell Biology. 2012;2012: 1–9. doi:10.1155/2012/182834

153. Mochida K, Oikawa Y, Kimura Y, Kirisako H, Hirano H, Ohsumi Y, et al. Receptor-mediated selective autophagy degrades the endoplasmic reticulum and the nucleus. Nature. 2015;522: 359–362. doi:10.1038/nature14506

154. Fujita E, Kouroku Y, Isoai A, Kumagai H, Misutani A, Matsuda C, et al. Two endoplasmic reticulum-associated degradation (ERAD) systems for the novel variant of the mutant dysferlin: ubiquitin/proteasome ERAD(I) and autophagy/lysosome ERAD(II). Human Molecular Genetics. 2007;16: 618–629. doi:10.1093/hmg/ddm002

155. Hidvegi T, Perlmutter DH. An Autophagy-Enhancing Drug Promotes Degradation of Mutant alpha1-Antitrpsin Z and Reduces Hepatic Fibrosis. Science. American Association for the Advancement of Science; 2010;329: 226–229. doi:10.1126/science.1188954

156. Houck SA, Ren HY, Madden VJ, Bonner JN, Conlin MP, Janovick JA, et al. Quality Control Autophagy Degrades Soluble ERAD-Resistant Conformers of the Misfolded Membrane Protein GnRHR. Molecular Cell. Elsevier Inc; 2014;54: 166–179. doi:10.1016/j.molcel.2014.02.025

157. Kurth I, Pamminger T, Hennings JC, Soehendra D, Huebner AK, Rotthier A, et al. Mutations in FAM134B, encoding a newly identified Golgi protein, cause severe sensory and autonomic neuropathy. Nature Genetics. Nature Publishing Group; 2009;41: 1179–1181. doi:10.1038/ng.464

158. Grumati P, Dikic I, Stolz A. ER-phagy at a glance. J Cell Sci. 2018;131: jcs217364–6. doi:10.1242/jcs.217364

159. Smith MD, Harley ME, Kemp AJ, Wills J, Lee M, Arends M, et al. CCPG1 Is a Non-canonical Autophagy Cargo Receptor Essential for ER-Phagy and Pancreatic ER Proteostasis. DEVCEL. Elsevier Inc; 2018;44: 217–232.e11. doi:10.1016/j.devcel.2017.11.024

160. Fumagalli F, Noack J, Bergmann TJ, Cebollero E, Pisoni GB, Fasana E, et al. Translocon component Sec62 acts in endoplasmic reticulum turnover during stress recovery. Nat Cell Biol. 2016;18: 1173–1184. doi:10.1038/ncb3423

161. Smith JA, Khan M, Magnani DD, Harms JS, Durward M, Radhakrishnan GK, et al. Brucella Induces an Unfolded Protein Response via TcpB That Supports Intracellular Replication in Macrophages. Roy CR, editor. PLoS Pathog. 2013;9: e1003785–12. doi:10.1371/journal.ppat.1003785

162. Chino H, Hatta T, Natsume T, Mizushima N. Intrinsically Disordered Protein TEX264 Mediates ER-phagy. Molecular Cell. Elsevier Inc; 2019;: 1–20. doi:10.1016/j.molcel.2019.03.033

163. Chen Q, Xiao Y, Chai P, Zheng P, Teng J, Chen J. ATL3 Is a Tubular ER-Phagy Receptor for GABARAP- Mediated Selective Autophagy. Current Biology. Elsevier Ltd; 2019;29: 846–855.e6. doi:10.1016/j.cub.2019.01.041

164. Dikic I. Open questions: why should we care about ER-phagy and ER remodelling? BMC Biol. 2018;16: jcs217364–6. doi:10.1186/s12915-018-0603-7

165. Leitman J, Shenkman M, Gofman Y, Shtern NO, Ben-Tal N, Hendershot LM, et al. Herp coordinates compartmentalization and recruitment of HRD1 and misfolded proteins for ERAD. Molecular Biology of the Cell. 2014;25: 1–11. doi:10.1091/mbc.E13-06-0350)

166. Huang C-H, Chu Y-R, Ye Y, Chen X. Role of HERP and a HERP-related Protein in HRD1-dependent Protein Degradation at the Endoplasmic Reticulum. The Journal of Biological Chemistry. 2014;287: 1–11.

167. Schröder M. Endoplasmic reticulum stress responses. CMLS, Cell Mol Life Sci. 2007;65: 862–894. doi:10.1007/s00018-007-7383-5

168. Kokame K, Agarwala KL, Kato H, Miyata T. Herp, a New Ubiquitin-like Membrane Protein Induced by Endoplasmic Reticulum Stress. J Biol Chem. 2000;275: 32846–32853. doi:10.1074/jbc.M002063200

169. Schulze A, Standera S, Buerger E, Kikkert M, van Voorden S, Wiertz E, et al. The Ubiquitin-domain Protein HERP forms a Complex with Components of the Endoplasmic Reticulum Associated Degradation Pathway. Journal of Molecular Biology. 2005;354: 1021–1027. doi:10.1016/j.jmb.2005.10.020

170. Chan SL, Fu W, Zhang P, Cheng A, Lee J, Kokame K, et al. Herp stabilizes neuronal Ca2+ homeostasis and mitochondrial function during endoplasmic reticulum stress. J Biol Chem. American Society for Biochemistry and Molecular Biology; 2004;279: 28733–28743. doi:10.1074/jbc.M404272200

171. Tuvia S, Taglicht D, Erez O, Alroy I, Alchanati I, Bicoviski V, et al. The ubiquitin E3 ligase POSH regulates calcium homeostasis through spatial control of Herp. The Journal of Cell Biology. 2007;177: 51–61. doi:10.1083/jcb.200611036

172. Ma Y, Hendershot LM. Herp Is Dually Regulated by Both the Endoplasmic Reticulum Stress-specific Branch of the Unfolded Protein Response and a Branch That Is Shared with Other Cellular Stress Pathways. J Biol Chem. 2004;279: 13792–13799. doi:10.1074/jbc.M313724200

173. Okuda-Shimizu Y, Hendershot LM. Characterization of an ERAD Pathway for Nonglycosylated BiP Substrates, which Require Herp. Molecular Cell. 2007;28: 544–554. doi:10.1016/j.molcel.2007.09.012

174. Hori O, Ichinoda F, Yamaguchi A, Tamatani T, Taniguchi M, Koyama Y, et al. Role of Herp in the endoplasmic reticulum stress response. Genes to Cells. 2004;9: 457–469. doi:10.1111/j.1356-9597.2004.00735.x

175. Jarosch E, Taxis C, Volkwein C, Bordallo J, Finley D, Wolf DH, et al. Protein dislocation from the ER requires polyubiquitination and the AAA-ATPase Cdc48. Nat Cell Biol. 2002;4: 134–139. doi:10.1038/ncb746

176. Kny M, Standera S, Hartmann-Petersen R, Kloetzel P-M, Seeger M. Herp Regulates Hrd1-mediated Ubiquitylation in a Ubiquitin- like Domain-dependent Manner. The Journal of Biological Chemistry. 2011;286: 1–6.

177. Li W, TU D, Li L, Wollert T, Ghirlando R, Brunger AT, et al. Mechanistic insights into active site-associated polyubiquitination by the ubiquitin-conjugating enzyme Ube2g2. PNAS. 2009;: 1–6.

178. Yan L, Liu W, Zhang H, Liu C, Shang Y, Ye Y, et al. Ube2g2-gp78-mediated HERP polyubiquitylation is involved in ER stress recovery. J Cell Sci. 2014;127: 1417–1427. doi:10.1242/jcs.135293

179. Kim T-Y, Kim E, Yoon SK, Yoon J-B. Herp enhances ER-associated protein degradation by recruiting ubiquilins. Biochemical and Biophysical Research Communications. 2008;369: 741–746. doi:10.1016/j.bbrc.2008.02.086

180. He B. Viruses, endoplasmic reticulum stress, and interferon responses. Cell Death Differ. 2006;13: 393–403. doi:10.1038/sj.cdd.4401833

181. He K, Ravindran MS, Tsai B. A bacterial toxin and a nonenveloped virus hijack ER-to-cytosol membrane translocation pathways to cause disease. Critical Reviews in Biochemistry and Molecular Biology. 2015;50: 477–488. doi:10.3109/10409238.2015.1085826

182. Fogel N. Tuberculosis: A disease without boundaries. Tuberculosis. Elsevier Ltd; 2015;95: 527–531. doi:10.1016/j.tube.2015.05.017

183. Schön T, Miotto P, Köser CU, Viveiros M, Böttger E, Cambau E. Mycobacterium tuberculosis drug-resistance testing: challenges, recent

developments and perspectives. Clinical Microbiology and Infection. Elsevier Ltd; 2017;23: 154–160. doi:10.1016/j.cmi.2016.10.022

184. Keshavjee S, Farmer PE. Tuberculosis, Drug Resistance, and the History of Modern Medicine. N Engl J Med. 2012;367: 931–936. doi:10.1056/NEJMra1205429

185. Choi H-H, Shin D-M, Kang G, Kim K-H, Park JB, Hur GM, et al. Endoplasmic reticulum stress response is involved in Mycobacterium tuberculosis protein ESAT-6-mediated apoptosis. FEBS Letters. Federation of European Biochemical Societies; 2010;584: 2445–2454. doi:10.1016/j.febslet.2010.04.050

186. Choi J-A, Lim Y-J, Cho S-N, Lee J-H, Jeong JA, Kim EJ, et al. Mycobacterial HBHA induces endoplasmic reticulum stress-mediated apoptosis through the generation of reactive oxygen species and cytosolic Ca2+ in murine macrophage RAW 264.7 cells. Cell Death and Disease. Nature Publishing Group; 2013;4: e957–11. doi:10.1038/cddis.2013.489

187. Lim Y-J, Choi J-A, Choi H-H, Cho S-N, Kim H-J, Jo E-K, et al. Endoplasmic Reticulum Stress Pathway-Mediated Apoptosis in Macrophages Contributes to the Survival of Mycobacterium tuberculosis. Shea BJ, editor. PLoS ONE. 2011;6: e28531–10. doi:10.1371/journal.pone.0028531

188. Pagliano P, Arsian F, Ascione T. Epidemiology and treatment of the commonest form of listeriosis: meningitis and bacteraemia. Le Infezioni in Medicina. 2017;: 1–7.

189. Pillich H, Loose M, Zimmer K-P, Chakraborty T. Activation of the unfolded protein response by Listeria monocytogenes. Cellular Microbiology. 2012;14: 949–964. doi:10.1111/j.1462-5822.2012.01769.x

190. Schnupf P, Portnoy DA. Listeriolysin O: a phagosome-specific lysin. Microbes and Infection. 2007;9: 1176–1187. doi:10.1016/j.micinf.2007.05.005

191. Kamimura D, Bevan MJ. NIH Public Access. Journal of Immunology. 2009;181: 1–20.

192. Willhite DC, Blanke SR. Helicobacter pylorivacuolating cytotoxin enters cells, localizes to the mitochondria, and induces mitochondrial membrane permeability changes correlated to toxin channel activity. Cellular Microbiology. 2004;6: 143–154. doi:10.1046/j.1462-5822.2003.00347.x

193. Halder P, Datta C, Kumar R, Sharma AK, Basu J, Kundu M. The secreted antigen, HP0175, of Helicobacter pylorilinks the unfolded protein response (UPR) to autophagy in gastric epithelial cells. Cellular Microbiology. John Wiley & Sons, Ltd (10.1111); 2015;17: 714–729. doi:10.1111/cmi.12396

194. Basu S, Pathak SK, Chatterjee G, Pathak S, Basu J, Kundu M. Helicobacter pyloriProtein HP0175 Transactivates Epidermal Growth Factor Receptor through TLR4 in Gastric Epithelial Cells. J Biol Chem. 2008;283: 32369–32376. doi:10.1074/jbc.M805053200

195. McBride JW, Walker DH. Molecular and cellular pathobiology of Ehrlichia infection: targets for new therapeutics and immunomodulation strategies. Expert Rev Mol Med. Cambridge University Press; 2011;13: 4804–24. doi:10.1017/S1462399410001730

196. Walker DH, Paris DH, Day NP, Shelite TR. Unresolved Problems Related to Scrub Typhus: A Seriously Neglected Life-Threatening Disease. The American Journal of Tropical Medicine and Hygiene. 2013;89: 301–307. doi:10.4269/ajtmh.13-0064

197. Rodino KG, VieBrock L, Evans SM, Ge H, Richards AL, Carlyon JA. Orientia tsutsugamushi Modulates Endoplasmic Reticulum-Associated Degradation To Benefit Its Growth. Palmer GH, editor. Infect Immun. American Society for Microbiology Journals; 2018;86: 301–16. doi:10.1128/IAI.00596-17

198. Ko Y, Choi J-H, Ha N-Y, Kim I-S, Cho N-H, Choi M-S. Active escape of Orientia tsutsugamushi from cellular autophagy. Bäumler AJ, editor. Infect Immun. American Society for Microbiology Journals; 2013;81: 552–559. doi:10.1128/IAI.00861-12

199. Niu H, Xiong Q, Yamamoto A, Hayashi-Nishino M, Rikihisa Y. Autophagosomes induced by a bacterial Beclin 1 binding protein facilitate obligatory intracellular infection. PNAS. 2012;109: 1–8. doi:10.1073/pnas.1218674109/-/DCSupplemental

200. Lin M, Liu H, Xiong Q, Niu H, Cheng Z, Yamamoto A, et al. Ehrlichia secretes Etf-1 to induce autophagy and capture nutrients for its growth through RAB5 and class III phosphatidylinositol 3-kinase. Autophagy. Taylor & Francis; 2016;12: 2145–2166. doi:10.1080/15548627.2016.1217369

201. Mehlitz A, Karunakaran K, Herweg J-A, Krohne G, van de Linde S, Rieck E, et al. The chlamydial organism Simkania negevensisforms ER vacuole contact sites and inhibits ER-stress. Cellular Microbiology. 2014;16: 1224–1243. doi:10.1111/cmi.12278

202. Stephens RS, Myers G, Eppinger M, Bavoil PM. Divergence without difference: phylogenetics and taxonomy of Chlamydiaresolved. FEMS Immunology & Medical Microbiology. 2009;55: 115–119. doi:10.1111/j.1574-695X.2008.00516.x

203. Kuo C-C, Jackson LA, Campbell LA, Grayston JT. Chlamydia pneumoniae. Clinical Microbiology Reviews. 1995;8: 1–11.

204. Derré I. Chlamydiaeinteraction with the endoplasmic reticulum: contact, function and consequences. Cellular Microbiology. John Wiley & Sons, Ltd (10.1111); 2015;17: 959–966. doi:10.1111/cmi.12455

205. Shima K, Klinger M, Schütze S, Kaufhold I, Solbach W, Reiling N, et al. The role of endoplasmic reticulum-related BiP/GRP78 in interferon gamma-induced persistent Chlamydia pneumoniaeinfection. Cellular Microbiology. 2015;17: 923–934. doi:10.1111/cmi.12416

206. Siegmund D, Wicovsky A, Schmitz I, Schulze-Osthoff K, Kreuz S, Leverkus M, et al. Death receptor-induced signaling pathways are differentially regulated by gamma interferon upstream of caspase 8 processing. Molecular and Cellular Biology. American Society for Microbiology Journals; 2005;25: 6363–6379. doi:10.1128/MCB.25.15.6363-6379.2005

207. Li X, McKinstry KK, Swain SL, Dalton DK. IFN-gamma acts directly on activated CD4+ T cells during mycobacterial infection to promote apoptosis by inducing components of the intracellular apoptosis machinery and by inducing extracellular proapoptotic signals. The Journal of Immunology. American Association of Immunologists; 2007;179: 939–949. doi:10.4049/jimmunol.179.2.939

208. MD PBAC, MD AB, MD PEB. Legionnaires' disease. The Lancet. Elsevier Ltd; 2016;387: 376–385. doi:10.1016/S0140-6736(15)60078-2

209. Treacy-Abarca S, Mukherjee S. Legionella suppresses the host unfolded protein response via multiple mechanisms. Nature Communications. Nature Publishing Group; 2015;6: 1–10. doi:10.1038/ncomms8887

210. Belyi Y, Niggeweg R, Opitz B, Vogelsesang M, Hippenstiel S, Wilm M, et al. Legionella pneumophila glucosyltransferase inhibits host elongation factor 1A. PNAS. 2006;104: 1–6.

211. Hempstead AD, Isberg RR. Inhibition of host cell translation elongation by Legionella pneumophila blocks the host cell unfolded protein response. Proc Natl Acad Sci USA. National Academy of Sciences; 2015;112: E6790–7. doi:10.1073/pnas.1508716112

212. Ivanov SS, Roy CR. Pathogen signatures activate a ubiquitination pathway that modulates the function of the metabolic checkpoint kinase mTOR. Nature Publishing Group. Nature Publishing Group; 2013;14: 1219–1228. doi:10.1038/ni.2740

213. Fontana MF, Banga S, Barry KC, Shen X, Tan Y, Luo Z-Q, et al. Secreted Bacterial Effectors That Inhibit Host Protein Synthesis Are Critical for Induction of the Innate Immune Response to Virulent Legionella pneumophila. Roy CR, editor. PLoS Pathog. Public Library of Science; 2011;7: e1001289–15. doi:10.1371/journal.ppat.1001289

214. Barel M, Harduin-Lepers A, Portier L, Slomianny M-C, Charbit A. Host glycosylation pathways and the unfolded protein response contribute to the infection by Francisella. Cellular Microbiology. 2nd ed. 2016;18: 1763–1781. doi:10.1111/cmi.12614

215. Qin Q-M, Pei J, Ancona V, Shaw BD, Ficht TA, de Figueiredo P. RNAi Screen of Endoplasmic Reticulum–Associated Host Factors Reveals a Role for IRE1α in Supporting Brucella Replication. Schneider DS, editor. PLoS Pathog. 2008;4: e1000110–16. doi:10.1371/journal.ppat.1000110

216. Wai T, Langer T. Mitochondrial Dynamics and Metabolic Regulation. Trends in Endocrinology & Metabolism. Elsevier Ltd; 2016;27: 105–117. doi:10.1016/j.tem.2015.12.001

217. Zemirli N, Morel E, Molino D. Mitochondrial Dynamics in Basal and Stressful Conditions. IJMS. Multidisciplinary Digital Publishing Institute; 2018;19: 564–19. doi:10.3390/ijms19020564

218. Pernas L, Scorrano L. Mito-Morphosis: Mitochondrial Fusion, Fission, and Cristae Remodeling as Key Mediators of Cellular Function. Annu Rev Physiol. 2016;78: 505–531. doi:10.1146/annurev-physiol-021115-105011

219. Wang Z, Wu M. An integrated phylogenomic approach toward pinpointing the origin of mitochondria. Sci Rep. 2015;5: 320–12. doi:10.1038/srep07949

220. Vogel F, Bornhövd C, Neupert W, Reichert AS. Dynamic subcompartmentalization of the mitochondrial inner membrane. The Journal of Cell Biology. 2006;175: 237–247. doi:10.1083/jcb.200605138

221. John GB, Zha J. The Mitochondrial Inner Membrane Protein Mitofilin Controls Cristae Morphology. Molecular Biology of the Cell. 2005;: 1–12. doi:10.1091/mbc.E04

222. Bartolák-Suki E, Imsirovic J, Nishibori Y, Krishnan R, Suki B. Regulation of Mitochondrial Structure and Dynamics by the Cytoskeleton and Mechanical Factors. IJMS. Multidisciplinary Digital Publishing Institute; 2017;18: 1812–17. doi:10.3390/ijms18081812

223. Liesa M, Palacín M, Zorzano A. Mitochondrial Dynamics in Mammalian Health and Disease. Physiological Reviews. 2009;89: 799–845. doi:10.1152/physrev.00030.2008

224. Lackner LL. Shaping the dynamic mitochondrial network. 2014;12: 1–10. doi:10.1186/1741-7007-12-35

225. Olichon A, Guillou E, Delettre C, Landes T, Arnauné-Pelloquin L, Emorine LJ, et al. Mitochondrial dynamics and disease, OPA1. Biochimica et Biophysica Acta (BBA) - Molecular Cell Research. 2006;1763: 500–509. doi:10.1016/j.bbamcr.2006.04.003

226. Kijima K, Numakura C, Izumino H, Umetsu K, Nezu A, Shiiki T, et al. Mitochondrial GTPase mitofusin 2 mutation in Charcot?Marie?Tooth neuropathy type 2A. Hum Genet. 2004;116: 23–27. doi:10.1007/s00439-004-1199-2

227. Züchner S, Noureddine M, Kennerson M, Verhoeven K, Claeys K, Jonghe PD, et al. Mutations in the pleckstrin homology domain of dynamin 2 cause dominant intermediate Charcot-Marie-Tooth disease. Nature Genetics. Nature Publishing Group; 2005;37: 289–294. doi:10.1038/ng1514

228. Legros F, Lombès A, Frachon P, Rojo M. Mitochondrial Fusion in Human Cells Is Efficient, Requires the Inner Membrane Potential, and Is Mediated by Mitofusins. Molecular Biology of the Cell. 2002;13: 1–12. doi:10.1091/mbc.E02

229. Eura Y. Two Mitofusin Proteins, Mammalian Homologues of FZO, with Distinct Functions Are Both Required for Mitochondrial Fusion. Journal of Biochemistry. 2003;134: 333–344. doi:10.1093/jb/mvg150

230. Mishra P, Carelli V, Manfredi G, Chan DC. Proteolytic Cleavage of Opa1 Stimulates Mitochondrial Inner Membrane Fusion and Couples Fusion to Oxidative Phosphorylation. Cell Metabolism. 2014;19: 630–641. doi:10.1016/j.cmet.2014.03.011

231. Tondera D, Grandemange SEP, Jourdain A, Karbowski M, Mattenberger Y, Herzig SEB, et al. SLP-2 is required for stress-induced mitochondrial hyperfusion. EMBO J. Nature Publishing Group; 2009;28: 1589–1600. doi:10.1038/emboj.2009.89

232. Friedman JR, Lackner LL, West M, DiBenedetto JR, Nunnari J, Voeltz GK. ER tubules mark sites of mitochondrial division. Science. American Association for the Advancement of Science; 2011;334: 358–362. doi:10.1126/science.1207385

233. Kraus F, Ryan MT. The constriction and scission machineries involved in mitochondrial fission. J Cell Sci. The Company of Biologists Ltd; 2017;130: 2953–2960. doi:10.1242/jcs.199562

234. Hoppins S, Lackner L, Nunnari J. The Machines that Divide and Fuse Mitochondria. Annu Rev Biochem. 2007;76: 751–780. doi:10.1146/annurev.biochem.76.071905.090048

235. Arasaki K, Shimizu H, Mogari H, Nishida N, Hirota N, Furuno A, et al. A Role for the Ancient SNARE Syntaxin 17 in Regulating Mitochondrial Division. DEVCEL. Elsevier Inc; 2015;32: 304–317. doi:10.1016/j.devcel.2014.12.011

236. Yaffe MP. The Machinery of Mitochondrial Inheritance and Behavior. Science. 1999;: 1–6.

237. Bach D, Pich S, Soriano FX, Vega N, Baumgartner B, Oriola J, et al. Mitofusin-2 determines mitochondrial network architecture and mitochondrial metabolism. A novel regulatory mechanism altered in obesity. J Biol Chem. American Society for Biochemistry and Molecular Biology; 2003;278: 17190–17197. doi:10.1074/jbc.M212754200

238. Huang P, Galloway CA, Yoon Y. Control of Mitochondrial Morphology Through Differential Interactions of Mitochondrial Fusion and Fission Proteins. Jackson CL, editor. PLoS ONE. Public Library of Science; 2011;6: e20655–14. doi:10.1371/journal.pone.0020655

239. Anand R, Wai T, Baker MJ, Kladt N, Schauss AC, Rugarli E, et al. The i-AAA protease YME1L and OMA1 cleave OPA1 to balance mitochondrial fusion and fission. The Journal of Cell Biology. Rockefeller University Press; 2014;204: 919–929. doi:10.1083/jcb.201308006

240. Arnoult D. Mitochondrial fragmentation in apoptosis. Trends in Cell Biology. 2007;17: 6–12. doi:10.1016/j.tcb.2006.11.001

241. Otera H, Ishihara N, Mihara K. New insights into the function and regulation of mitochondrial fission. BBAMCR. Elsevier B.V; 2013;1833: 1256–1268. doi:10.1016/j.bbamcr.2013.02.002

242. Yu T, Wang L, Yoon Y. HHS Public Access. Frontiers in Biosciences. 2015;: 1–22.

243. Pickles S, Vigié P, Youle RJ. Mitophagy and Quality Control Mechanisms in Mitochondrial Maintenance. Current Biology. Elsevier Ltd; 2018;28: R170–R185. doi:10.1016/j.cub.2018.01.004

244. Hagenbuchner J, Kuznetsov AV, Obexer P, Ausserlechner MJ. BIRC5/Survivin enhances aerobic glycolysis and drug resistance by altered regulation of the mitochondrial fusion/fission machinery. Nature Publishing Group; 2012;32: 4748–4757. doi:10.1038/onc.2012.500

245. Mishra P, Chan DC. Metabolic regulation of mitochondrial dynamics. The Journal of Cell Biology. Rockefeller University Press; 2016;212: 379–387. doi:10.1083/jcb.201511036

246. Rambold AS, Kostelecky B, Elia N, Lippincott-Schwartz J. Tubular network formation protects mitochondria from autophagosomal degradation during nutrient starvation. PNAS. 2011;108: 1–6. doi:10.1073/pnas.1107402108/-/DCSupplemental

247. Mitra K, Wunder C, Roysam B, Lin G, Lippincott-Schwartz J. A hyperfused mitochondrial state achieved at G. PNAS. 2009;106: 1–6.

248. Ueda E, Ishihara N. Mitochondrial hyperfusion causes neuropathy in a fly model of CMT2A. EMBO reports. EMBO Press; 2018;19: e46502–2. doi:10.15252/embr.201846502

249. Copeland DE, Dalton AJ. An Association between Mitochondira and the Endoplasmic Reticulum in Cells of the Pseudobranch Gland of a Teleost. J Biophysic and Biochem Cytol. 1959;5: 1–7.

250. Szabadkai G, Simoni AM, Rizzuto R. Mitochondrial Ca2+ uptake requires sustained Ca2+ release from the endoplasmic reticulum. J Biol Chem. American Society for Biochemistry and Molecular Biology; 2003;278: 15153–15161. doi:10.1074/jbc.M300180200

251. Study of the transfer of phospholipids from the endoplasmic reticulum to the outer. 2002;: 1–5.

252. Verfaillie T, Rubio N, Garg AD, Bultynck G, Rizzuto R, Decuypere J-P, et al. PERK is required at the ER-mitochondrial contact sites to convey apoptosis after ROS-based ER stress. Nature Publishing Group; 2012;19: 1880–1891. doi:10.1038/cdd.2012.74

253. Hamasaki M, Furuta N, Matsuda A, Nezu A, Yamamoto A, Fujita N, et al. Autophagosomes form at ER-mitochondria contact sites. Nature. Nature Publishing Group; 2013;495: 389–393. doi:10.1038/nature11910

254. Rusinol A, Cui Z, Chen MH, VAnce JE. Unique Mitochondria-associated MembranFeractionfrom Rat Liver Has a High Capacity. The Journal of Biological Chemistry. 2001;: 1–9.

255. Boehning D, Patterson RL, Sedaghat L, Glebova NO, Kurosaki T, Snyder SH. Cytochrome c binds to inositol (1,4,5) trisphosphate receptors, amplifying calcium-dependent apoptosis. Nat Cell Biol. Nature Publishing Group; 2003;5: 1051–1061. doi:10.1038/ncb1063

256. Cárdenas C, Miller RA, Smith I, Bui T, Molgó J, Müller M, et al. Essential Regulation of Cell Bioenergetics by Constitutive InsP3 Receptor Ca2+ Transfer to Mitochondria. Cell. 2010;142: 270–283. doi:10.1016/j.cell.2010.06.007

257. Gellerich FN, Gizatullina Z, Trumbeckaite S, Nguyen HP, Pallas T, Arandarcikaite O, et al. The regulation of OXPHOS by extramitochondrial calcium. BBA - Bioenergetics. Elsevier B.V; 2010;1797: 1018–1027. doi:10.1016/j.bbabio.2010.02.005

258. Giorgi C, Marchi S, Pinton P. The machineries, regulation and cellular functions of mitochondrial calcium. Nature Publishing Group. Springer US; 2018;: 1–18. doi:10.1038/s41580-018-0052-8

259. Rizzuto R, De Stefani D, Raffaello A, Mammucari C. Mitochondria as sensors and regulators of calcium signalling. Nature Publishing Group. Nature Publishing Group; 2012;13: 566–578. doi:10.1038/nrm3412

260. de Brito OM, Scorrano L. Mitofusin 2 tethers endoplasmic reticulum to mitochondria. Nature. 2008;456: 605–610. doi:10.1038/nature07534

261. Simmen T, Aslan JE, Blagoveshschenskaya AD, Feliciangeli SF, Hung C-H, Crump CM, et al. PACS-2 controls endoplasmic reticulum– mitochondria communication and Bid-mediated apoptosis. EMBO J. 2005;: 1–13.

262. Myhill N, Lynes EM, Nanji JA, Blagoveshschenskaya AD, Banach-Ortowska M, Fei H, et al. The Subcellular Distribution of Calnexin Is Mediated by PACS-2. Molecular Biology of the Cell. 2008;: 1–12. doi:10.1091/mbc.E07–10

263. Michalak M, Parker JMR, Opas M. signaling and calcium binding chaperones of the endoplasmic reticulum. Cell Calcium. 2003;: 1–10. doi:10.1016/S0143-4160(02)00188-4

264. Hayashi T, Su T-P. Sigma-1 Receptor Chaperones at the ER- Mitochondrion Interface Regulate Ca2+ Signaling and Cell Survival. Cell. 2007;131: 596–610. doi:10.1016/j.cell.2007.08.036

265. Kornmann B, Currie E, Collins SR, Schuldiner M, Nunnari J, Weissman JS, et al. An ER-mitochondria tethering complex revealed by a synthetic biology screen. Science. American Association for the Advancement of Science; 2009;325: 477–481. doi:10.1126/science.1175088

266. Murley A, Lackner LL, Osman C, West M, Voeltz GK, Walter P, et al. ER-associated mitochondrial division links the distribution of mitochondria and mitochondrial DNA in yeast. eLIFE. 2013;2: 1371–16. doi:10.7554/eLife.00422

267. Carreras-Sureda A, a FXNJX, Urra H, Durand S, Mortenson DE, Sagredo A, et al. Non-canonical function of IRE1α determines mitochondria-associated endoplasmic reticulum composition to control calcium transfer and bioenergetics. Nat Cell Biol. Springer US; 2019;: 1–23. doi:10.1038/s41556-019-0329-y

268. Um J-H, Yun J. Emerging role of mitophagy in human diseases and physiology. BMB Rep. 2017;50: 299–307. doi:10.5483/BMBRep.2017.50.6.056

269. Lamb CA, Yoshimori T, Tooze SA. The autophagosome: origins unknown, biogenesis complex. Nature Publishing Group. Nature Publishing Group; 2013;14: 759–774. doi:10.1038/nrm3696

270. Lebeau J, Saunders JM, Moraes VWR, Madhavan A, Madrazo N, Anthony MC, et al. The PERK Arm of the Unfolded Protein Response Regulates Mitochondrial Morphology during Acute Endoplasmic Reticulum Stress. Cell Reports. 2018;22: 2827–2836. doi:10.1016/j.celrep.2018.02.055

271. Bravo R, Vicencio JM, Parra V, Troncoso R, Munoz JP, Bui M, et al. Increased ER-mitochondrial coupling promotes mitochondrial respiration and bioenergetics during early phases of ER stress. J Cell Sci. The Company of Biologists Ltd; 2011;124: 2511–2511. doi:10.1242/jcs.095455

272. oz JPMN, Ivanova SSK, nchez-Wandelmer JSA, bal PMIN-CO, Noguera E, Sancho A, et al. Mfn2 modulates the UPR and mitochondrial function via repression of PERK. EMBO J. Nature Publishing Group; 2013;32: 2348–2361. doi:10.1038/emboj.2013.168

273. Mori T, Hayashi T, Hayashi E, Su T-P. Sigma-1 Receptor Chaperone at the ER-Mitochondrion Interface Mediates the Mitochondrion-ER-Nucleus Signaling for Cellular Survival. Okamoto S-I, editor. PLoS ONE. Public Library of Science; 2013;8: e76941–13. doi:10.1371/journal.pone.0076941

274. Mihaylova MM, Shaw RJ. The AMPK signalling pathway coordinates cell growth, autophagy and metabolism. Nat Cell Biol. Nature Publishing Group; 2011;13: 1016–1023. doi:10.1038/ncb2329

275. Biala AK, Kirshenbaum LA. The interplay between cell death signaling pathways in the heart. Trends in Cardiovascular Medicine. Elsevier; 2014;24: 325–331. doi:10.1016/j.tcm.2014.08.002

276. Green DR. At the gates of death. Cancer Cell. 2006;9: 328–330. doi:10.1016/j.ccr.2006.05.004

277. Denecker G, Vercammen D, Steemans M, Berghe TV, Brouckaert G, Van Loo G, et al. Death receptor-induced apoptotic and necrotic cell death: differential role of caspases and mitochondria. Cell Death Differ. 2001;: 1–12.

278. Bononi A, Bonora M, Marchi S, Missiroli S, Poletti F, Giorgi C, et al. Identification of PTEN at the ER and MAMs and its regulation of Ca2+ signaling and apoptosis in a protein phosphatase-dependent manner. Cell Death Differ. Nature Publishing Group; 2013;20: 1631–1643. doi:10.1038/cdd.2013.77

279. Escoll P, Buchrieser C. Metabolic reprogramming of host cells upon bacterial infection: Why shift to a Warburg-likemetabolism? FEBS J. John Wiley & Sons, Ltd (10.1111); 2018;285: 2146–2160. doi:10.1111/febs.14446

280. O'Neill LAJ, Kishton RJ, Rathmell J. A guide to immunometabolism for immunologists. Nat Rev Immunol. Nature Publishing Group; 2016;16: 553–565. doi:10.1038/nri.2016.70

281. Vander Heiden MG, Cantley LC, Thompson CB. Understanding the Warburg effect: the metabolic requirements of cell proliferation. Science. American Association for the Advancement of Science; 2009;324: 1029–1033. doi:10.1126/science.1160809

282. Liberti MV, Locasale JW. The Warburg Effect: How Does it Benefit Cancer Cells? Trends in Biochemical Sciences. 2016;41: 211–218. doi:10.1016/j.tibs.2015.12.001

283. Michalek RD, Gerriets VA, Jacobs SR, Macintyre AN, MacIver NJ, Mason EF, et al. Cutting edge: distinct glycolytic and lipid oxidative metabolic programs are essential for effector and regulatory CD4+ T cell subsets. J Immunol. American Association of Immunologists; 2011;186: 3299–3303. doi:10.4049/jimmunol.1003613

284. Peng M, Li MO. Aerobic glycolysis promotes T helper 1 cell differentiation through an epigenetic mechanism. Science. American Association for the Advancement of Science; 2016;354: 477–481. doi:10.1126/science.aag2602

285. Araujo L, Khim P, Mkhikian H, Mortales C-L, Demetriou M. Glycolysis and glutaminolysis cooperatively control T cell function by limiting metabolite supply to N-glycosylation. eLIFE. 2017;: 1–16. doi:10.7554/eLife.21330.001

286. Palsson-McDermott EM, Curtis AM, Goel G, Lauterbach MAR, Sheedy FJ, Gleeson LE, et al. Pyruvate Kinase M2 Regulates Hif-1α Activity and IL-1β Induction and Is a Critical Determinant of the Warburg Effect in LPS-Activated Macrophages. Cell Metabolism. 2015;21: 65–80. doi:10.1016/j.cmet.2014.12.005

287. O'Neill LAJ, Pearce EJ. Immunometabolism governs dendritic cell and macrophage function. J Exp Med. Rockefeller University Press; 2016;213: 15–23. doi:10.1084/jem.20151570

288. Doughty CA, Bleiman BF, Wagner DJ, Dufort FJ, Mataraza JM, Roberts MF, et al. Antigen receptor-mediated changes in glucose metabolism in B lymphocytes: role of phosphatidylinositol 3-kinase signaling in the glycolytic control of growth. Blood. American Society of Hematology; 2006;107: 4458–4465. doi:10.1182/blood-2005-12-4788

289. Gardiner CM, Finlay DK. What Fuels Natural Killers? Metabolism and NK Cell Responses. Front Immunol. 2017;8: 536–8. doi:10.3389/fimmu.2017.00367

290. Fox CJ, Hammerman PS, Thompson CB. Fuel feeds function: energy metabolism and the T-cell response. Nat Rev Immunol. 2005;5: 844–852. doi:10.1038/nri1710

291. Tannahill GM, Curtis AM, Adamik J, Palsson-McDermott EM, McGettrick AF, Goel G, et al. Succinate is an inflammatory signal that induces IL-1β through HIF-1α. Nature. Nature Publishing Group; 2013;496: 238–242. doi:10.1038/nature11986

292. Shi LZ, Wang R, Huang G, Vogel P, Neale G, Green DR, et al. HIF1alpha-dependent glycolytic pathway orchestrates a metabolic checkpoint for the differentiation of TH17 and Treg cells. J Exp Med. Rockefeller University Press; 2011;208: 1367–1376. doi:10.1084/jem.20110278

293. Pearce EL, Pearce EJ. Metabolic Pathways in Immune Cell Activation and Quiescence. Immunity. 2013;38: 633–643. doi:10.1016/j.immuni.2013.04.005

294. Siegl C, Prusty BK, Karunakaran K, Wischhusen J, Rudel T. Tumor Suppressor p53 Alters Host Cell Metabolism to Limit Chlamydia trachomatis Infection. CellReports. The Authors; 2014;9: 918–929. doi:10.1016/j.celrep.2014.10.004

295. Escoll P, Song O-R, Viana F, Steiner B, Lagache T, Olivo-Marin J-C, et al. Legionella pneumophila Modulates Mitochondrial Dynamics to Trigger Metabolic Repurposing of Infected Macrophages. Cell Host and Microbe. Elsevier Inc; 2017;22: 302–316.e7. doi:10.1016/j.chom.2017.07.020

296. Shi L, Salamon H, Eugenin EA, Pine R, Cooper A, Gennaro ML. Infection with Mycobacterium tuberculosis induces the Warburg effect in mouse lungs. Sci Rep. Nature Publishing Group; 2015;: 1–13. doi:10.1038/srep18176

297. Roop RM II, Caswell CC. Bacterial Persistence: Finding the ``Sweet Spot''. Cell Host and Microbe. Elsevier Inc; 2013;14: 119–120. doi:10.1016/j.chom.2013.07.016

298. Xavier MN, Winter MG, Spees AM, Hartigh den AB, Nguyen K, Roux CM, et al. PPARγ-Mediated Increase in Glucose Availability Sustains Chronic Brucella abortus Infection in Alternatively Activated Macrophages. Cell Host and Microbe. 2013;14: 159–170. doi:10.1016/j.chom.2013.07.009

299. Stavru F, Bouillaud F, Sartori A, Ricquier D, Cossart P. Listeria monocytogenes transiently alters mitochondrial dynamics during infection. PNAS. 2011;108: 1–6. doi:10.1073/pnas.1100126108/-/DCSupplemental/pnas.201100126SI.pdf

300. Zhang Y, Yao Y, Qiu X, Wang G, Hu Z, Chen S, et al. Listeria hijacks host mitophagy through a novel mitophagy receptor to evade killing. Nature Immunology. Springer US; 2019;: 1–19. doi:10.1038/s41590-019-0324-2

301. Madariaga MG, Rezai K, Trenholme GM, Weinstein RA. Q fever: a biological weapon in your backyard. The Lancet Infectious Diseases. 2003;3: 709–721. doi:10.1016/S1473-3099(03)00804-1

302. Rotz LD, Khan AS, Lillibridge SR, Ostroff SM, Hughes JM. Public Health Assessment of Potential Biological Terrorism Agents. Emerging Infectious Diseases. 2002;8: 1–6.

303. Larson CL, Beare PA, Voth DE, Howe D, Cockrell DC, Bastidas RJ, et al. Coxiella burnetii effector proteins that localize to the parasitophorous vacuole membrane promote intracellular replication. Roy CR, editor. Infect Immun. American Society for Microbiology Journals; 2015;83: 661–670. doi:10.1128/IAI.02763-14

304. Carey KL, Newton HJ, Lührmann A, Roy CR. The Coxiella burnetii Dot/Icm System Delivers a Unique Repertoire of Type IV Effectors into Host Cells and Is Required for Intracellular Replication. Christie P, editor. PLoS Pathog. Public Library of Science; 2011;7: e1002056–18. doi:10.1371/journal.ppat.1002056

305. Weber MM, Chen C, Rowin K, Mertens K, Galvan G, Zhi H, et al. Identification of Coxiella burnetii type IV secretion substrates required for intracellular replication and Coxiella-containing vacuole formation. Journal of Bacteriology. American Society for Microbiology Journals; 2013;195: 3914–3924. doi:10.1128/JB.00071-13

306. Voth DE, Howe D, Beare PA, Vogel JP, Unsworth N, Samuel JE, et al. The Coxiella burnetii ankyrin repeat domain-containing protein family is heterogeneous, with C-terminal truncations that influence Dot/Icm-mediated secretion. Journal of Bacteriology. American Society for Microbiology Journals; 2009;191: 4232–4242. doi:10.1128/JB.01656-08

307. Lührmann A, Nogueira CV, Carey KL, Roy CR. Inhibition of pathogen-induced apoptosis by a Coxiella burnetii type IV effector protein. PNAS. 2010;107: 1–5. doi:10.1073/pnas.1004380107/-/DCSupplemental

308. Schäfer W, Eckart RA, Schmid B, Cagköylü H, Hof K, Muller YA, et al. Nuclear trafficking of the anti-apoptotic Coxiella burnetiieffector protein AnkG requires binding to p32 and Importin-α1. Cellular Microbiology. 2016;19: e12634–14. doi:10.1111/cmi.12634

309. Schäfer W, Eckart RA, Schmid B, Cagköylü H, Hof K, Muller YA, et al. Nuclear trafficking of the anti-apoptotic Coxiella burnetiieffector protein AnkG requires binding to p32 and Importin-α1. Cellular Microbiology. John Wiley & Sons, Ltd (10.1111); 2016;19: e12634–14. doi:10.1111/cmi.12634

310. Fielden LF, Moffatt JH, Kang Y, Baker MJ, Khoo CA, Roy CR, et al. A Farnesylated Coxiella burnetii Effector Forms a Multimeric Complex at the Mitochondrial Outer Membrane during Infection. Palmer GH, editor. Infect Immun. American Society for Microbiology Journals; 2017;85: 225–15. doi:10.1128/IAI.01046-16

311. Willhite DC, Cover TL, Blanke SR. Cellular vacuolation and mitochondrial cytochrome c release are independent outcomes of Helicobacter pylori vacuolating cytotoxin activity that are each dependent on membrane channel formation. J Biol Chem. American Society for Biochemistry and Molecular Biology; 2003;278: 48204–48209. doi:10.1074/jbc.M304131200

312. Lina TT, Farris T, Luo T, Mitra S, Zhu B, McBride JW. Hacker within! Ehrlichia chaffeensis Effector Driven Phagocyte Reprogramming Strategy. Frontiers in cellular and infection microbiology. Frontiers; 2016;6: 507–17. doi:10.3389/fcimb.2016.00058

313. Rikihisa Y. Molecular Pathogenesis of Ehrlichia chaffeensisInfection. Annu Rev Microbiol. 2015;69: 283–304. doi:10.1146/annurev-micro-091014-104411

314. Liu H, Bao W, Lin M, Niu H, Rikihisa Y. Ehrlichia type IV secretion effector ECH0825 is translocated to mitochondria and curbs ROS and apoptosis by upregulating host MnSOD. Cellular Microbiology. John Wiley & Sons, Ltd (10.1111); 2012;14: 1037–1050. doi:10.1111/j.1462-5822.2012.01775.x

315. Anderson M, Sansonetti PJ, Marteyn BS. Shigella Diversity and Changing Landscape: Insights for the Twenty-First Century. Frontiers in cellular and infection microbiology. Frontiers; 2016;6: a014159–9. doi:10.3389/fcimb.2016.00045

316. Ray K, Marteyn B, Sansonetti PJ, Tang CM. Life on the inside: the intracellular lifestyle of cytosolic bacteria. Nat Rev Microbiol. Nature Publishing Group; 2009;7: 333–340. doi:10.1038/nrmicro2112

317. Helle SCJ, Feng Q, Aebersold MJ, Hirt L, Grüter RR, Vahid A, et al. Mechanical force induces mitochondrial fission. eLIFE. 2017;: 1–26. doi:10.7554/eLife.30292.001

318. Escoll P, Buchrieser C. Metabolic reprogramming of host cells upon bacterial infection: Why shift to a Warburg-likemetabolism? FEBS J. 2018;285: 2146–2160. doi:10.1111/febs.14446

319. Rolando M, Escoll P, Nora T, Botti J, Boitez V, Bedia C, et al. Legionella pneumophila S1P-lyase targets host sphingolipid metabolism and restrains autophagy. Proc Natl Acad Sci USA. National Academy of Sciences; 2016;113: 1901–1906. doi:10.1073/pnas.1522067113

320. Degtyar E, Zusman T, Ehrlich M, Segal G. A Legionellaeffector acquired from protozoa is involved in sphingolipids metabolism and is targeted to the host cell mitochondria. Cellular Microbiology. John Wiley & Sons, Ltd (10.1111); 2009;11: 1219–1235. doi:10.1111/j.1462-5822.2009.01328.x

321. Spiegel S, Milstien S. Sphingosine-1-phosphate: an enigmatic signalling lipid. Nat Rev Mol Cell Biol. Nature Publishing Group; 2003;4: 397–407. doi:10.1038/nrm1103

322. Stiban J, Caputo L, Colombini M. Ceramide synthesis in the endoplasmic reticulum can permeabilize mitochondria to proapoptotic proteins. J Lipid Res. American Society for Biochemistry and Molecular Biology; 2008;49: 625–634. doi:10.1194/jlr.M700480-JLR200

323. Young MM, Kester M, Wang H-G. Sphingolipids: regulators of crosstalk between apoptosis and autophagy. J Lipid Res. American Society for Biochemistry and Molecular Biology; 2013;54: 5–19. doi:10.1194/jlr.R031278

324. Abu Khweek A, Kanneganti A, C Guttridge D D, Amer AO. The Sphingosine-1-Phosphate Lyase (LegS2) Contributes to the Restriction of Legionella pneumophila in Murine Macrophages. BenMohamed L, editor. PLoS ONE. Public Library of Science; 2016;11: e0146410–16. doi:10.1371/journal.pone.0146410

325. Dunning Hotopp JC, Lin M, Madupu R, Crabtree J, Angiuoli SV, Eisen J, et al. Comparative Genomics of Emerging Human Ehrlichiosis Agents. PLoS Genet. Public Library of Science; 2006;2: e21–16. doi:10.1371/journal.pgen.0020021

326. Franco MP, Mulder M, Gilman RH, Smits HL. Human brucellosis. The Lancet Infectious Diseases. 2007;7: 775–786. doi:10.1016/S1473-3099(07)70286-4

327. Pappas G, Papadimitriou P, Akritidis N, Christou L, Tsianos EV. The new global map of human brucellosis. The Lancet Infectious Diseases. 2006;6: 91–99. doi:10.1016/S1473-3099(06)70382-6

328. Galinska EM, Zagorski J. Brucellosis in humans – etiology, diagnostics, clinical forms. Annals of Agricultural and Environmental Medicine. 2013;: 1–6.

329. Ducrotoy M, Bertu WJ, Matope G, Cadmus S, Conde-Álvarez R, Gusi AM, et al. Brucellosis in Sub-Saharan Africa: Current challenges for management, diagnosis and control. Acta Tropica. Elsevier B.V; 2017;165: 179–193. doi:10.1016/j.actatropica.2015.10.023

330. Elberg SS, JR KF. Immunization against Brucella Infection. Journal of Bacteriology. 1956;: 1–7.

331. Chen TH, Elberg SS. Immunization against *Brucella* Infections: Immune Response of Mice, Guinea pigs, and *Cynomolgus philipinensis* to Live and Killed *Brucella melitensis* Strain Rev. I Administered by Various Methods

. The Journal of Infectious Diseases. 1970;122: 1–12.

332. Dorneles EM, Sriranganathan N, Lage AP. Recent advances in Brucella abortus vaccines. Veterinary Research. Veterinary Research; 2015;: 1–10. doi:10.1186/s13567-015-0199-7

333. Jia P. Human brucellosis occurrences in inner mongolia, China: a spatio-temporal distribution and ecological niche modeling approach. 2015;: 1–16. doi:10.1186/s12879-015-0763-9

334. Hull NC, Schumaker BA. Comparisons of brucellosis between human and veterinary medicine. Infection Ecology & Epidemiology. Taylor & Francis; 2018;8: 1–12. doi:10.1080/20008686.2018.1500846

335. Anderson ML. Infectious causes of bovine abortion during mid- to late-gestation. Theriogenology. 2007;68: 474–486. doi:10.1016/j.theriogenology.2007.04.001

336. Guzman-Verri C, Gonzalez-Barrientos R, Hernandez-Mora G, Morales J-A, Baquero-Calvo E, Chaves-Olarte E, et al. Brucella ceti and brucellosis in cetaceans. Frontiers in cellular and infection microbiology. 2012;: 1–22. doi:10.3389/fcimb.2012.00003/abstract

337. Nymo IH, Tryland M, Godfroid J. A review of Brucella infection in marine mammals, with special emphasis on Brucella pinnipedialis in the hooded seal (Cystophora cristata). Veterinary Research. BioMed Central Ltd; 2011;42: 93. doi:10.1186/1297-9716-42-93

338. Buzgan T, Karahocagil MK, Irmak H, Baran AI, Karsen H, Evirgen O, et al. Clinical manifestations and complications in 1028 cases of brucellosis: a retrospective evaluation and review of the literature. International Journal of Infectious Diseases. International Society for Infectious Diseases; 2010;14: e469–e478. doi:10.1016/j.ijid.2009.06.031

339. Dean AS, Crump L, Greter H, Hattendorf J, Schelling E, Zinsstag J. Clinical Manifestations of Human Brucellosis: A Systematic Review and Meta-Analysis. Carabin H, editor. PLoS Negl Trop Dis. 2012;6: e1929–9. doi:10.1371/journal.pntd.0001929

340. Gul HC, Erdem H, Bek S. Overview of neurobrucellosis: a pooled analysis of 187 cases. International Journal of Infectious Diseases. 2009;13: e339–e343. doi:10.1016/j.ijid.2009.02.015

341. Aparicio ED.

Epidemiology of brucellosis in domestic animals caused by *Brucella melitensis, Brucella suis* and *Brucella abortus*

. 2013;32: 1–9.

342. Atluri VL, Xavier MN, de Jong MF, Hartigh den AB, Tsolis RM. Interactions of the Human Pathogenic BrucellaSpecies with Their Hosts. Annu Rev Microbiol. 2011;65: 523–541. doi:10.1146/annurev-micro-090110-102905

343. Celli J. Surviving inside a macrophage: The many ways of Brucella. Research in Microbiology. 2006;157: 93–98. doi:10.1016/j.resmic.2005.10.002

344. Salcedo SP, Marchesini MI, Lelouard H, Fugier E, Jolly G, Balor S, et al. Brucella Control of Dendritic Cell Maturation Is Dependent on the TIR-Containing Protein Btp1. PLoS Pathog. 2008;4: e21–16. doi:10.1371/journal.ppat.0040021

345. Ferrero MC, Fossati CA, Baldi PC. Smooth Brucella strains invade and replicate in human lung epithelial cells without inducing cell death. Microbes and Infection. Elsevier Masson SAS; 2009;11: 476–483. doi:10.1016/j.micinf.2009.01.010

346. Pizarro-Cerda J, Méresse S, Parton RG, van der Goot G, Sola-Landa A, Lopez-Goni I, et al. Brucella abortus. Infect Immun. 1998;66: 1–14.

347. Riley LK, Robertson DC. Ingestion and Intracellular Survival of Brucella abortus in Human and Bovine Polymorphonuclear Leukocytes. Infect Immun. 2005;: 1–7.

348. Delpino MV, Fossati CA, Baldi PC. Proinflammatory response of human osteoblastic cell lines and osteoblast-monocyte interaction upon infection with Brucella spp. Infect Immun. American Society for Microbiology Journals; 2009;77: 984–995. doi:10.1128/IAI.01259-08

349. Anderson TD, CHeville NF.

UltrastructuralMorphometricAnalysis of Brucellaabortus-Infected Trophoblastsin Experimental Placentitis

. American Journal of Pathology. 1986;: 1–12.

350. Martirosyan A, Moreno E, Gorvel J-P. An evolutionary strategy for a stealthy intracellular Brucella pathogen. immunological Reviews. 2011;: 1–24.

351. Andersen-Nissen E, Smith KD, Strobe KL, Barrett SLR, Cookson BT, Logan SM, et al. Evasion of Toll-like receptor 5 by flagellated bacteria. PNAS. 2005;102: 9247–9252.

352. Terwagne M, Ferooz J, Rolán HG, Sun Y-H, Atluri V, Xavier MN, et al. Innate immune recognition of flagellin limits systemic persistence of Brucella. Cellular Microbiology. 2013;15: 942–960. doi:10.1111/cmi.12088

353. Mancilla M. Smooth to Rough Dissociation in Brucella: The Missing Link to Virulence. Frontiers in cellular and infection microbiology. Frontiers; 2016;5: 4913–7. doi:10.3389/fcimb.2015.00098

354. Hoffmann EM, Houle JJ. Failure of Brucella abortus Lipopolysaccharide (LPS) to activate the alternative pathway of complement. Veterinary Immunology and Immunopathology. 1983;: 1–12.

355. Forestier C, Deleuil F, Lapaque N, Moreno E, Gorvel JP. Brucella abortus Lipopolysaccharide in Murine Peritoneal Macrophages Acts as a Down-Regulator of T Cell Activation. The Journal of Immunology. 2000;165: 5202–5210. doi:10.4049/jimmunol.165.9.5202

356. Green ER, Mecsas J. Bacterial Secretion Systems: An Overview. American Society of Microbiology; 2016;4: 215–239. doi:10.1128/microbiolspec.VMBF-0012-2015

357. Sankarasubramanian J, Vishnu US, Dinakaran V, Sridhar J, Gunasekaran P, Rajendhran J. Computational prediction of secretion systems and secretomes of Brucella: identification of novel type IV effectors and their interaction with the host. Mol BioSyst. Royal Society of Chemistry; 2016;12: 178–190. doi:10.1039/C5MB00607D

358. Gonzalez-Rivera C, Bhatty M, Christie PJ. Mechanism and Function of Type IV Secretion During Infection of the Human Host. Virulence Mechanisms of Bacterial Pathogens, Fifth Edition. American Society of Microbiology; 2016. pp. 265–303. doi:10.1128/microbiolspec.VMBF-0024-2015

359. Li YG, Hu B, Christie PJ. Biological and Structural Diversity of Type IV Secretion Systems. Microbiology Spectrum. 2019;7: 1–15. doi:10.1128/microbiolspec.PSIB-0012-2018

360. Nora T, Lomma M, Gomez-Valero L, Buchrieser C. Molecular mimicry: an important virulence strategy employed by Legionella pneumophilato subvert host functions. Future Microbiology. 2009;4: 691–701. doi:10.2217/fmb.09.47

361. Celli J, de Chastellier C, Franchini D-M, Pizarro-Cerda J, Moreno E, Gorvel J-P. BrucellaEvades Macrophage Killing via VirB-dependent Sustained Interactions with the Endoplasmic Reticulum. J Exp Med. 2003;198: 545–556. doi:10.1084/jem.20030088

362. de Jong MF, Starr T, Winter MG, Hartigh den AB, Child R, Knodler LA, et al. Sensing of bacterial type IV secretion via the unfolded protein response. Roy C, Rikihisa Y, editors. mBio. American Society for Microbiology; 2013;4: e00418–12. doi:10.1128/mBio.00418-12

363. Sieira R, Comerci DJ, Ugalde RA. A Homologue of an Operon Required for DNA Transfer in. Journal of Bacteriology. 2000;: 1–7.

364. Comerci DJ, Martinez-Lorenzo MJ, Ugalde RA. Essential role of the VirB machinery in the maturation of the Brucella abortus-containing vacuole. Cellular Microbiology. 2001;: 1–10.

365. Hong P, Tsolis RM, Ficht TA. Identification of Genes Required for Chronic Persistence of. Infect Immun. 2000;: 1–6.

366. Hartigh den AB, Rolán HG, de Jong MF, Tsolis RM. VirB3 to VirB6 and VirB8 to VirB11, but not VirB7, are essential for mediating persistence of Brucella in the reticuloendothelial system. Journal of Bacteriology. American Society for Microbiology Journals; 2008;190: 4427–4436. doi:10.1128/JB.00406-08

367. Lestrate P, Delrue RM, Danese I, Didembourg C, Taminiau B, Mertens P, et al. Identification and characterization of in vivo attenuated mutants of Brucella melitensis. Molecular Microbiology. 2000;38: 543–551.

368. Delrue R-M, Lestrate P, Tibor A, Letesson J-J, Bolle X. Brucellapathogenesis, genes identified from random large-scale screens. FEMS Microbiology Letters. 2004;231: 1–12. doi:10.1016/S0378-1097(03)00963-7

369. Roux CM, Rolán HG, Santos RL, Beremand PD, Thomas TL, Adams LG, et al. Brucella requires a functional Type IV secretion system to elicit innate immune responses in mice. Cellular Microbiology. 2007;9: 1851–1869. doi:10.1111/j.1462-5822.2007.00922.x

370. Copin R, Vitry M-A, Hanot Mambres D, Machelart A, De Trez C, Vanderwinden J-M, et al. In Situ Microscopy Analysis Reveals Local Innate Immune Response Developed around Brucella Infected Cells in Resistant and Susceptible Mice. Roy CR, editor. PLoS Pathog. Public Library of Science; 2012;8: e1002575–18. doi:10.1371/journal.ppat.1002575

371. Vitry M-A, De Trez C, Goriely S, Dumoutier L, Akira S, Ryffel B, et al. Crucial role of gamma interferon-producing CD4+ Th1 cells but dispensable function of CD8+ T cell, B cell, Th2, and Th17 responses in the control of Brucella melitensis infection in mice. Morrison RP, editor. Infect Immun. American Society for Microbiology Journals; 2012;80: 4271–4280. doi:10.1128/IAI.00761-12

372. Xavier MN, Winter MG, Spees AM, Nguyen K, Atluri VL, Silva TMA, et al. CD4+ T Cell-derived IL-10 Promotes Brucella abortus Persistence via Modulation of Macrophage Function. Roy CR, editor. PLoS Pathog. Public Library of Science; 2013;9: e1003454–17. doi:10.1371/journal.ppat.1003454

373. Hunt AC, Bothwell PW. Histological findings in human brucellosis. Journal of Clinical Pathology. 2004;: 1–6.

374. Radhakrishnan GK, Splitter GA. Brucella TIR Domain-containing Protein Mimics Properties of the Toll-like Receptor Adaptor Protein TIRAP. The Journal of Biological Chemistry. 2009;284: 1–7.

375. Barrionuevo P, Delpino MV, Pozner RG, Velásquez LN, Cassataro J, Giambartolomei GH. Brucella abortusinduces intracellular retention of MHC-I molecules in human macrophages down-modulating cytotoxic CD8 +T cell responses. Cellular Microbiology. 2012;15: 487–502. doi:10.1111/cmi.12058

376. Naroeni A, Porte F. Role of cholesterol and the ganglioside GM(1) in entry and short-term survival of Brucella suis in murine macrophages. Infect Immun. American Society for Microbiology Journals; 2002;70: 1640–1644. doi:10.1128/iai.70.3.1640-1644.2002

377. Kim S, Watarai M, Suzuki H, Makino S-I, Kodama T, Shirahata T. Lipid raft microdomains mediate class A scavenger receptor-dependent infection of Brucella abortus. Microbial Pathogenesis. 2004;37: 11–19. doi:10.1016/j.micpath.2004.04.002

378. Porte F, Naroeni A, Ouahrani-Bettache S, Liautard J-P. Role of the Brucella suis lipopolysaccharide O antigen in phagosomal genesis and in inhibition of phagosome-lysosome fusion in murine macrophages. Infect Immun. American Society for Microbiology Journals; 2003;71: 1481–1490. doi:10.1128/iai.71.3.1481-1490.2003

379. Archambaud C, Salcedo SP, Lelouard H, Devilard E, de Bovis B, Van Rooijen N, et al. Contrasting roles of macrophages and dendritic cells in controlling initial pulmonary Brucella infection. Eur J Immunol. John Wiley & Sons, Ltd; 2010;40: 3458–3471. doi:10.1002/eji.201040497

380. Bellaire BH, Roop RM, Cardelli JA. Opsonized virulent Brucella abortus replicates within nonacidic, endoplasmic reticulum-negative, LAMP-1-positive phagosomes in human monocytes. Infect Immun. American Society for Microbiology Journals; 2005;73: 3702–3713. doi:10.1128/IAI.73.6.3702-3713.2005

381. Billard E, Cazevieille C, Dornand J, Gross A. High Susceptibility of Human Dendritic Cells to Invasion by the Intracellular Pathogens Brucella suis, B. abortus, and B. melitensis. Infect Immun. 2005;73: 8418–8424. doi:10.1128/IAI.73.12.8418-8424.2005

382. Starr T, Ng TW, Wehrly TD, Knodler LA, Celli J. Brucella Intracellular Replication Requires Trafficking Through the Late Endosomal/Lysosomal Compartment. Traffic. 2008;9: 678–694. doi:10.1111/j.1600-0854.2008.00718.x

383. Porte F, Liautard J-P, Köhler S. Early Acidification of Phagosomes Containing. Infect Immun. 1999;67: 1–7.

384. Boschiroli ML, Ouahrani-Bettache S, Foulongne V, Michaux-Charachon S, Bourg G, Allardet-Servent A, et al. The Brucella suis virB operon is induced intracellularly in macrophages. PNAS. 2002;: 1–6.

385. Drecktrah D, Knodler LA, Howe D, Steele-Mortimer O. Salmonella Trafficking is Defined by Continuous Dynamic Interactions with the Endolysosomal System. Traffic. John Wiley & Sons, Ltd (10.1111); 2006;8: 212–225. doi:10.1111/j.1600-0854.2006.00529.x

386. Deghelt MEL, Mullier C, Sternon JFCO, Francis N, Laloux GER, Dotreppe D, et al. G1-arrested newborn cells are the predominant infectious form of the pathogen Brucella abortus. Nature Communications. Nature Publishing Group; 1AD;5: 1–12. doi:10.1038/ncomms5366

387. Sedzicki J, Tschon T, Low SH, Willemart K, Goldie KN, Letesson J-J, et al. 3D correlative electron microscopy reveals continuity of Brucella-containing vacuoles with the endoplasmic reticulum. J Cell Sci. The Company of Biologists Ltd; 2018;131: jcs210799–11. doi:10.1242/jcs.210799

388. Celli J, Salcedo SP, Gorvel J-P. Brucella coopts the small GTPase Sar1 for intracellular replication. PNAS. 2005;: 1–6.

389. Tisdale EJ, Bourne JR, Khosravi-Far R, Der CJ, Balch WE. GTP-Binding Mutants of Rabl and Rab2 are Potent Inhibitors of Vesicular Transport from the Endoplasmic Reticulum to the Golgi Complex. The Journal of Cell Biology. 1992;: 1–13.

390. Bhuin T, Roy JK. Rab proteins_ The key regulators of intracellular vesicle transport. Experimental Cell Research. Elsevier; 2014;328: 1–19. doi:10.1016/j.yexcr.2014.07.027

391. Fugier E, Salcedo SP, de Chastellier C, Pophillat M, Muller A, Arce-Gorvel V, et al. The Glyceraldehyde-3-Phosphate Dehydrogenase and the Small GTPase Rab 2 Are Crucial for Brucella Replication. Ausubel FM, editor. PLoS Pathog. 2009;5: e1000487–13. doi:10.1371/journal.ppat.1000487

392. Miller CN, Smith EP, Cundiff JA, Knodler LA, Bailey Blackburn J, Lupashin V, et al. A Brucella Type IV Effector Targets the COG Tethering Complex to Remodel Host Secretory Traffic and Promote Intracellular Replication. Cell Host and Microbe. 2017;22: 317–329.e7. doi:10.1016/j.chom.2017.07.017

393. Taguchi Y, Imaoka K, Kataoka M, Uda A, Nakatsu D, Horii-Okazaki S, et al. Yip1A, a Novel Host Factor for the Activation of the IRE1 Pathway of the Unfolded Protein Response during Brucella Infection. Tsolis RM, editor. PLoS Pathog. Public Library of Science; 2015;11: e1004747–28. doi:10.1371/journal.ppat.1004747

394. Starr T, Child R, Wehrly TD, Hansen B, Hwang S, López-Otin C, et al. Selective Subversion of Autophagy Complexes Facilitates Completion of the Brucella Intracellular Cycle. Cell Host and Microbe. Elsevier Inc; 2012;11: 33–45. doi:10.1016/j.chom.2011.12.002

395. Celli J. The Intracellular Life Cycle of Brucella spp. Microbiology Spectrum. 2019;7: 1–17. doi:10.1128/microbiolspec.BAI-0006-2019

396. Salcedo SP, Chevrier N, Lacerda TLS, Ben Amara A, Gerart S, Gorvel VA, et al. Pathogenic Brucellae Replicate in Human Trophoblasts. The Journal of Infectious Diseases. 2013;207: 1075–1083. doi:10.1093/infdis/jit007

397. García Méndez KB, Hielpos SM, Soler Llorens PF, Arce-Gorvel V, Hale C, Gorvel J-P, et al. Infection by Brucella melitensisor Brucella papionismodifies essential physiological functions of human trophoblasts. Cellular Microbiology. John Wiley & Sons, Ltd (10.1111); 2019;21: e13019–13. doi:10.1111/cmi.13019

398. Döhmer PH, Valguarnera E, Czibener C, Ugalde JE. Identification of a type IV secretion substrate of Brucella abortusthat participates in the early stages of intracellular survival. Cellular Microbiology. 2013;16: 396–410. doi:10.1111/cmi.12224

399. de Barsy M, Jamet A, Filopon D, Nicolas C, Laloux G, Rual J-F, et al. Identification of a Brucella spp. secreted effector specifically interacting with human small GTPase Rab2. Cellular Microbiology. 2011;13: 1044–1058. doi:10.1111/j.1462-5822.2011.01601.x

400. Myeni S, Child R, Ng TW, Kupko JJ, Wehrly TD, Porcella SF, et al. Brucella Modulates Secretory Trafficking via Multiple Type IV Secretion Effector Proteins. Valdivia RH, editor. PLoS Pathog. Public Library of Science; 2013;9: e1003556–18. doi:10.1371/journal.ppat.1003556

401. Willett R, Blackburn JB, Climer L, Pokrovskaya I, Kudlyk T, Wang W, et al. COG lobe B sub-complex engages v-SNARE GS15 and functions via regulated interaction with lobe A sub-complex. Nature Publishing Group. Nature Publishing Group; 2016;: 1–19. doi:10.1038/srep29139

402. de Jong MF, Sun Y-H, Hartigh den AB, van Dijl JM, Tsolis RM. Identification of VceA and VceC, two members of the VjbR regulon that are translocated into macrophages by the Brucellatype IV secretion system. Molecular Microbiology. John Wiley & Sons, Ltd (10.1111); 2008;70: 1378–1396. doi:10.1111/j.1365-2958.2008.06487.x

403. Sengupta D, Koblansky A, Gaines J, Brown T, West AP, Zhang D, et al. Subversion of innate immune responses by Brucella through the targeted degradation of the TLR signaling adapter, MAL. J Immunol. American Association of Immunologists; 2010;184: 956–964. doi:10.4049/jimmunol.0902008

404. Chaudhary A, Ganguly K, Cabantous S, Waldo GS, Micheva-Viteva SN, Nag K, et al. The Brucella TIR-like protein TcpB interacts with the death domain of MyD88. Biochemical and Biophysical Research Communications. 2012;417: 299–304. doi:10.1016/j.bbrc.2011.11.104

405. Gorvel J-P, Salcedo SP. BtpB, a novel Brucella TIR-containing effector protein with immune modulatory functions. Frontiers in cellular and infection microbiology. 2013;: 1–13. doi:10.3389/fcimb.2013.00028/abstract

406. Spera JM, Herrmann CK, Roset MS, Comerci DJ, Ugalde JE. A Brucella virulence factor targets macrophages to trigger B-cell proliferation. J Biol Chem. American Society for Biochemistry and Molecular Biology; 2013;288: 20208–20216. doi:10.1074/jbc.M113.453282

407. Spera JM, Ugalde JE, Mucci J, Comerci DJ, Ugalde RA. A B lymphocyte mitogen is a Brucella abortus virulence factor required for persistent infection. 2006;: 1–6.

408. Abu Kwaik Y, Bumann D. Host Delivery of Favorite Meals for Intracellular Pathogens. Miller VL, editor. PLoS Pathog. Public Library of Science; 2015;11: e1004866–8. doi:10.1371/journal.ppat.1004866

409. Biswas SK, Mantovani A. Orchestration of Metabolism by Macrophages. Cell Metabolism. Elsevier Inc; 2012;15: 432–437. doi:10.1016/j.cmet.2011.11.013

410. Odegaard JI, Chawla A. Alternative Macrophage Activation and Metabolism. Annu Rev Pathol Mech Dis. 2011;6: 275–297. doi:10.1146/annurev-pathol-011110-130138

411. Czyż DM, Willett JW, Crosson S. Brucella abortus Induces a Warburg Shift in Host Metabolism That Is Linked to Enhanced Intracellular Survival of the Pathogen. O'Toole G, editor. Journal of Bacteriology. American Society for Microbiology Journals; 2017;199: 420–14. doi:10.1128/JB.00227-17

412. Lobet E, Willemart K, Ninane NXL, Demazy C, Sedzicki J, Lelubre C, et al. Mitochondrial fragmentation affects neither the sensitivity to TNFα-induced apoptosis of Brucella-infected cells nor the intracellular replication of the bacteria. Nature Publishing Group. Springer US; 2018;: 1–17. doi:10.1038/s41598-018-23483-3

413. Vannuvel K, Renard P, Raes M, Arnould T. Functional and morphological impact of ER stress on mitochondria. J Cell Physiol. John Wiley & Sons, Ltd; 2013;228: 1802–1818. doi:10.1002/jcp.24360

414. De Vos KJ, Sheetz MP. Visualization and Quantification of Mitochondrial Dynamics in Living Animal Cells. Mitochondria, 2nd Edition. Elsevier; 2007. pp. 627–682. doi:10.1016/S0091-679X(06)80030-0

415. Kittinger C, Kirschner A, Lipp M, Baumert R, Mascher F, Farnleitner A, et al. Antibiotic Resistance of Acinetobacter spp. Isolates from the River Danube: Susceptibility Stays High. IJERPH. 2018;15: 52–8. doi:10.3390/ijerph15010052

416. Torfs E, Piller T, Cos P, Cappoen D. Opportunities for Overcoming Mycobacterium tuberculosis Drug Resistance: Emerging Mycobacterial Targets and Host-Directed Therapy. IJMS. Multidisciplinary Digital Publishing Institute; 2019;20: 2868–23. doi:10.3390/ijms20122868

417. Gr xe1 cio AJDS, Gr xe1 cio MAXLA. Review Article Plague: A Millenary Infectious Disease Reemerging in the XXI Century. BioMed Research International. Hindawi; 2017;: 1–8. doi:10.1155/2017/5696542

418. Mick V, Le Carrou G, Corde Y, Game Y, Jay M, Garin-Bastuji B. Brucella melitensis in France: Persistence in Wildlife and Probable Spillover from Alpine Ibex to Domestic Animals. Roop RM, editor. PLoS ONE. Public Library of Science; 2014;9: e94168–9. doi:10.1371/journal.pone.0094168

419. Hofer E, Hammerl JA, Zygmunt MS, Cloeckaert A, Koylass M, Whatmore AM, et al. Brucella vulpis sp. nov., a novel Brucella species isolated from mandibular lymph nodes of red foxes (Vulpes vulpes) in Austria. International Journal of Systematic and Evolutionary Microbiology. 2016;: 1–9. doi:10.1099/ijsem.0.000998

420. Escoll P, Song O-R, Viana F, Steiner B, Lagache T, Olivo-Marin J-C, et al. Legionella pneumophila Modulates Mitochondrial Dynamics to Trigger Metabolic Repurposing of Infected Macrophages. Cell Host and Microbe. Elsevier Inc; 2017;22: 302–316.e7. doi:10.1016/j.chom.2017.07.020

421. Serrat R, López-Doménech G, Mirra S, Quevedo M, Garcia-Fernàndez J, Ulloa F, et al. The Non-Canonical Wnt/PKC Pathway Regulates Mitochondrial Dynamics through Degradation of the Arm-Like Domain-Containing Protein Alex3. Gottardi C, editor. PLoS ONE. Public Library of Science; 2013;8: e67773–13. doi:10.1371/journal.pone.0067773

422. Csordás G, Várnai P, Golenár T, Roy S, Purkins G, Schneider TG, et al. Imaging Interorganelle Contacts and Local Calcium Dynamics at the ER-Mitochondrial

Interface. Molecular Cell. Elsevier Ltd; 2010;39: 121–132. doi:10.1016/j.molcel.2010.06.029

423. Al-Quadan T, Kwaik YA. Molecular Characterization of Exploitation of the Polyubiquitination and Farnesylation Machineries of Dictyostelium Discoideum by the AnkB F-Box Effector of Legionella Pneumophila. Front Microbiol. 2011;2: 1–10. doi:10.3389/fmicb.2011.00023

424. Méresse S. Is host lipidation of pathogen effector proteins a general virulence mechanism? 2011;: 1–3. doi:10.3389/fmicb.2011.00073/full

425. Boucrot E, Beuzón CR, Holden DW, Gorvel J-P, Méresse S. Salmonella typhimurium SifA effector protein requires its membrane-anchoring C-terminal hexapeptide for its biological function. J Biol Chem. American Society for Biochemistry and Molecular Biology; 2003;278: 14196–14202. doi:10.1074/jbc.M207901200

426. Price CTD, Al-Quadan T, Santic M, Jones SC, Abu Kwaik Y. Exploitation of conserved eukaryotic host cell farnesylation machinery by an F-box effector of Legionella pneumophila. J Exp Med. Rockefeller University Press; 2010;207: 1713–1726. doi:10.1084/jem.20100771

427. Price CTD, Jones SC, Amundson KE, Kwaik YA. Host-Mediated Post-Translational Prenylation of Novel Dot/Icm-Translocated Effectors of Legionella Pneumophila. Front Microbiol. Frontiers; 2010;1: 1–9. doi:10.3389/fmicb.2010.00131

428. Lynes EM, Raturi A, Shenkman M, Ortiz-Sandoval C, Yap MC, Wu J, et al. Palmitoylation is the switch that assigns calnexin to quality control or ER Ca2+ signaling. J Cell Sci. The Company of Biologists Ltd; 2013;126: 3893–3903. doi:10.1242/jcs.125856

429. Arriola Benitez PC, Rey Serantes D, Herrmann CK, Pesce Viglietti AI, Vanzulli S, Giambartolomei GH, et al. The Effector Protein BPE005 from Brucella abortus Induces Collagen Deposition and Matrix Metalloproteinase 9 Downmodulation via Transforming Growth Factor β1 in Hepatic Stellate Cells. Young VB, editor. Infect Immun. 2nd ed. 2016;84: 598–606. doi:10.1128/IAI.01227-15

430. Elkington PTG, O'Kane CM, Friedland JS. The paradox of matrix metalloproteinases in infectious disease. Clin Exp Immunol. John Wiley & Sons, Ltd (10.1111); 2005;142: 12–20. doi:10.1111/j.1365-2249.2005.02840.x

431. Marchesini MI, Morrone Seijo SM, Guaimas FF, Comerci DJ. A T4SS Effector Targets Host Cell Alpha-Enolase Contributing to Brucella abortus Intracellular Lifestyle. Frontiers in cellular and infection microbiology. Frontiers; 2016;6: 553–14. doi:10.3389/fcimb.2016.00153

432. Giallongo A, Feo S, Moore R, Croce CM, Showe LC. Molecular cloning and nucleotide sequence. PNAS. 1983;83: 1–5.

433. Scharte M, Han X, Bertges DJ, Fink MP, Delude RL. Cytokines induce HIF-1 DNA binding and the expression of HIF-1-dependent genes in cultured rat enterocytes. American Journal of Physiology-Gastrointestinal and Liver Physiology. 2003;284: G373–G384. doi:10.1152/ajpgi.00076.2002

434. Cui G, Wei P, Zhao Y, Guan Z, Yang L, Sun W, et al. Brucella infection inhibits macrophages apoptosis via Nedd4-dependent degradation of calpain2. Veterinary Microbiology. Elsevier B.V; 2014;174: 195–205. doi:10.1016/j.vetmic.2014.08.033

435. Gross A, Dornand J. in vitro *brucella suis* infection prevents the programmed cell death of human monocytic cells

. Infect Immun. 1999;: 1–10.

436. He Y, Reichow S, Ramamoorthy S, Ding X, Lathigra R, Craig JC, et al. Brucella melitensis triggers time-dependent modulation of apoptosis and down-regulation of mitochondrion-associated gene expression in mouse macrophages. Infect Immun. American Society for Microbiology Journals; 2006;74: 5035–5046. doi:10.1128/IAI.01998-05

437. Peleg AY, Seifert H, Paterson DL. Acinetobacter baumannii: emergence of a successful pathogen. Clinical Microbiology Reviews. American Society for Microbiology Journals; 2008;21: 538–582. doi:10.1128/CMR.00058-07

438. Wisplinghoff H, Bischoff T, TAllent SM, Seifert H, Wenzel RP, Edmond MB. Nosocomial Bloodstream Infections in US Hospitals: Analysis of 24,179 Cases from a Prospective Nationwide Surveillance Study. Clinical Infectious Diseases. 2004;: 1–9.

439. Pereira SG, Domingues VS, Theriága J, Chasqueira M de J, Paixão P. Non-Antimicrobial Drugs: Etodolac as a Possible Antimicrobial or Adjuvant Agent Against ESKAPE Pathogens. TOMICROJ. 2018;12: 288–296. doi:10.2174/1874285801812010288

440. Bhargava N, Sharma P, Capalash N. Quorum sensing in Acinetobacter: an emerging pathogen. Critical Reviews in Microbiology. 2010;36: 349–360. doi:10.3109/1040841X.2010.512269

441. Oh MH, Choi CH. Role of LuxIR Homologue AnoIR in Acinetobacter nosocomialis and the Effect of Virstatin on the Expression of anoR Gene. Journal of Microbiology and Biotechnology. 2015;25: 1390–1400. doi:10.4014/jmb.1504.04069

442. Churchill MEA, Chen L. Structural Basis of Acyl-homoserine Lactone-Dependent Signaling. Chem Rev. 2011;111: 68–85. doi:10.1021/cr1000817

443. Rosadini CV, Kagan JC. Microbial strategies for antagonizing Toll-like-receptor signal transduction. Current Opinion in Immunology. 2015;32: 61–70. doi:10.1016/j.coi.2014.12.011

444. Wunderley L, Brownhill K, Stefani F, Tabernero L, Woodman P. The molecular basis for selective assembly of the UBAP1-containing endosome-specific ESCRT-I complex. J Cell Sci. The Company of Biologists Ltd; 2014;127: 663–672. doi:10.1242/jcs.140673

445. Maminska A, Bartosik A, Banach-Ortowska M, Pilecka I, Jastrzebski K, Zdzalik-Bielecka D, et al. ESCRT proteins restrict constitutive NF-kB signaling by trafficking cytokine receptors. Science Signaling. 2016;9: 1–14.